The Large Hadron Collider

Philippe Lebrun

CERN, Geneva, Switzerland

65th Scottish Universities Summer School in Physics

St Andrews, 16-29 August 2009

Contents

- The LHC in a nutshell
- Performance
  - Energy
  - Luminosity
  - Collective effects
  - Dynamic aperture
- Technology
  - Superconducting magnets
  - Powering and protection
  - Cryogenics
  - Vacuum
- Project management

The largest scientific instrument in the world

Colliding counter-rotating beams of hadrons

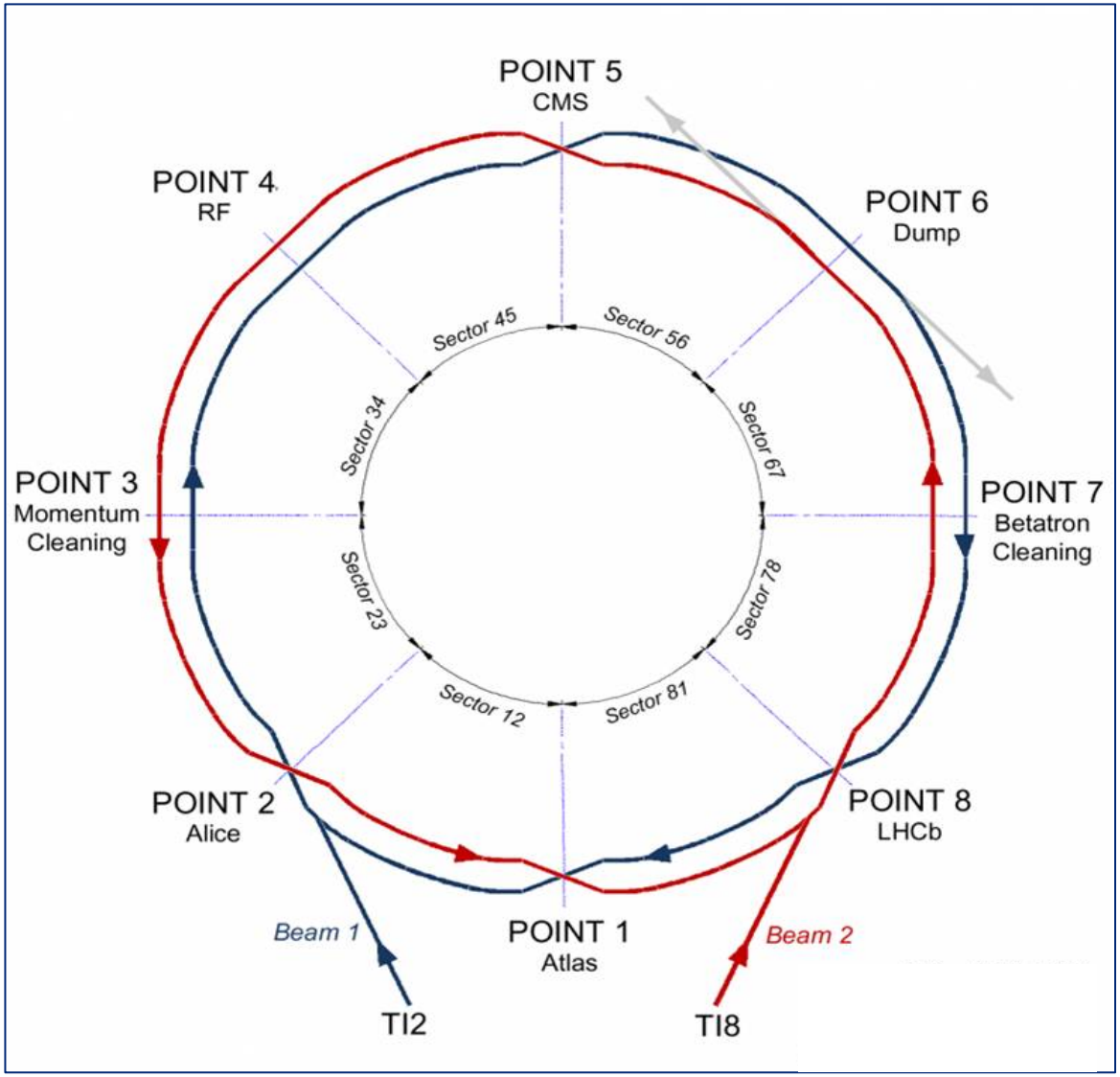

A new territory in energy and luminosity

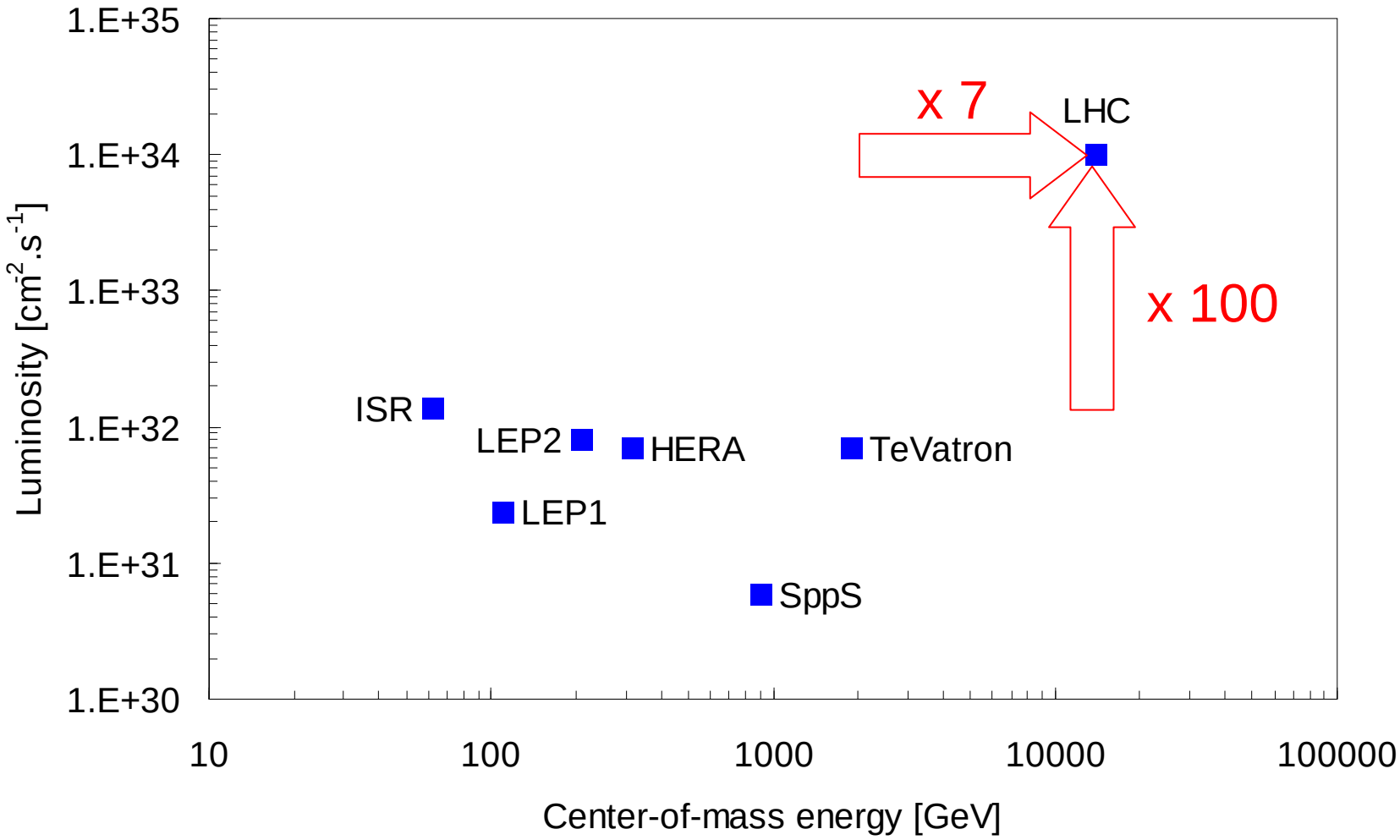

Advanced technology at work

23 km of superconducting magnets cooled in superfluid helium at 1.9 K

A global project serving the world community of particle physicists

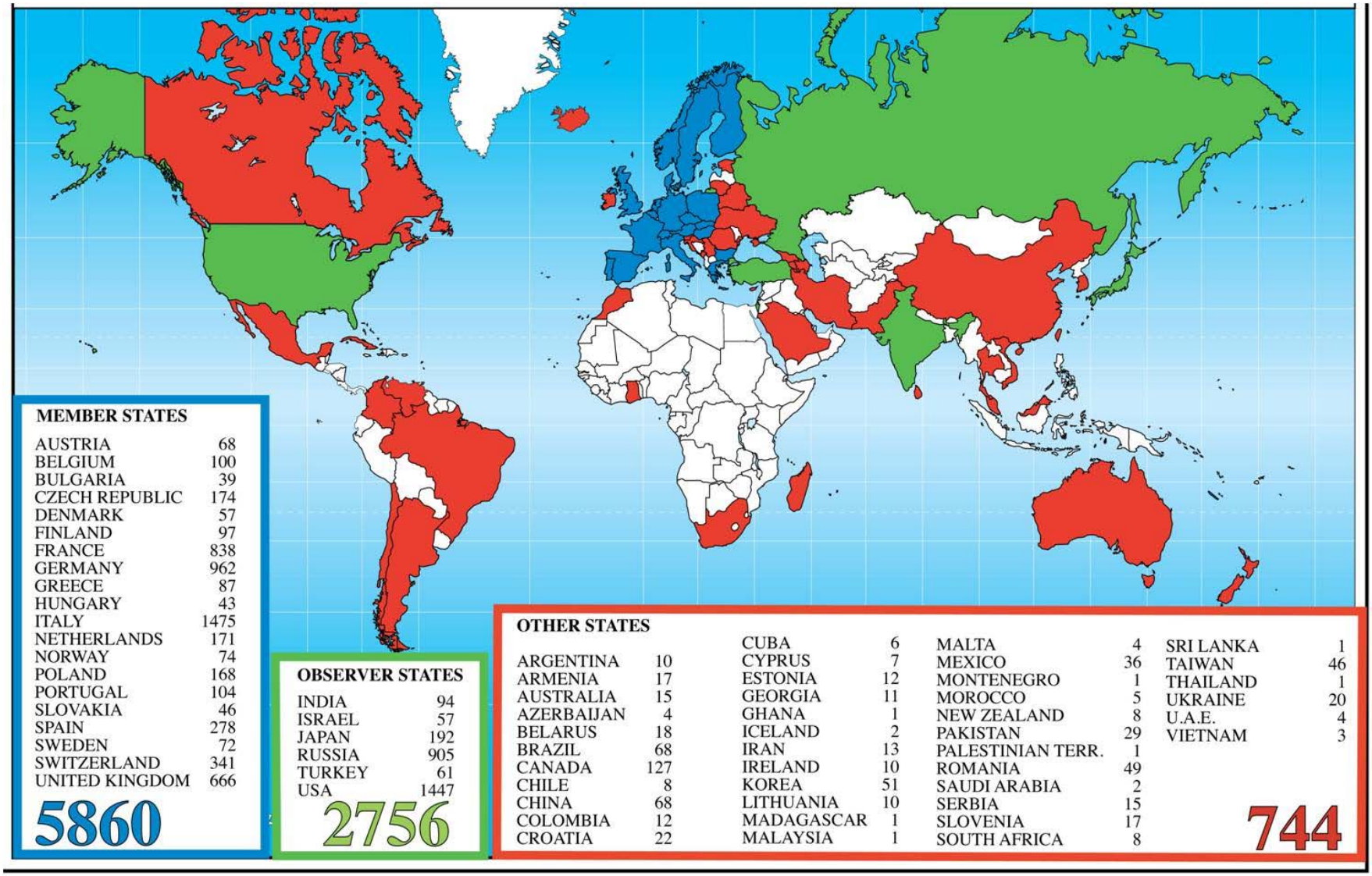

Making best use of CERN's infrastructure

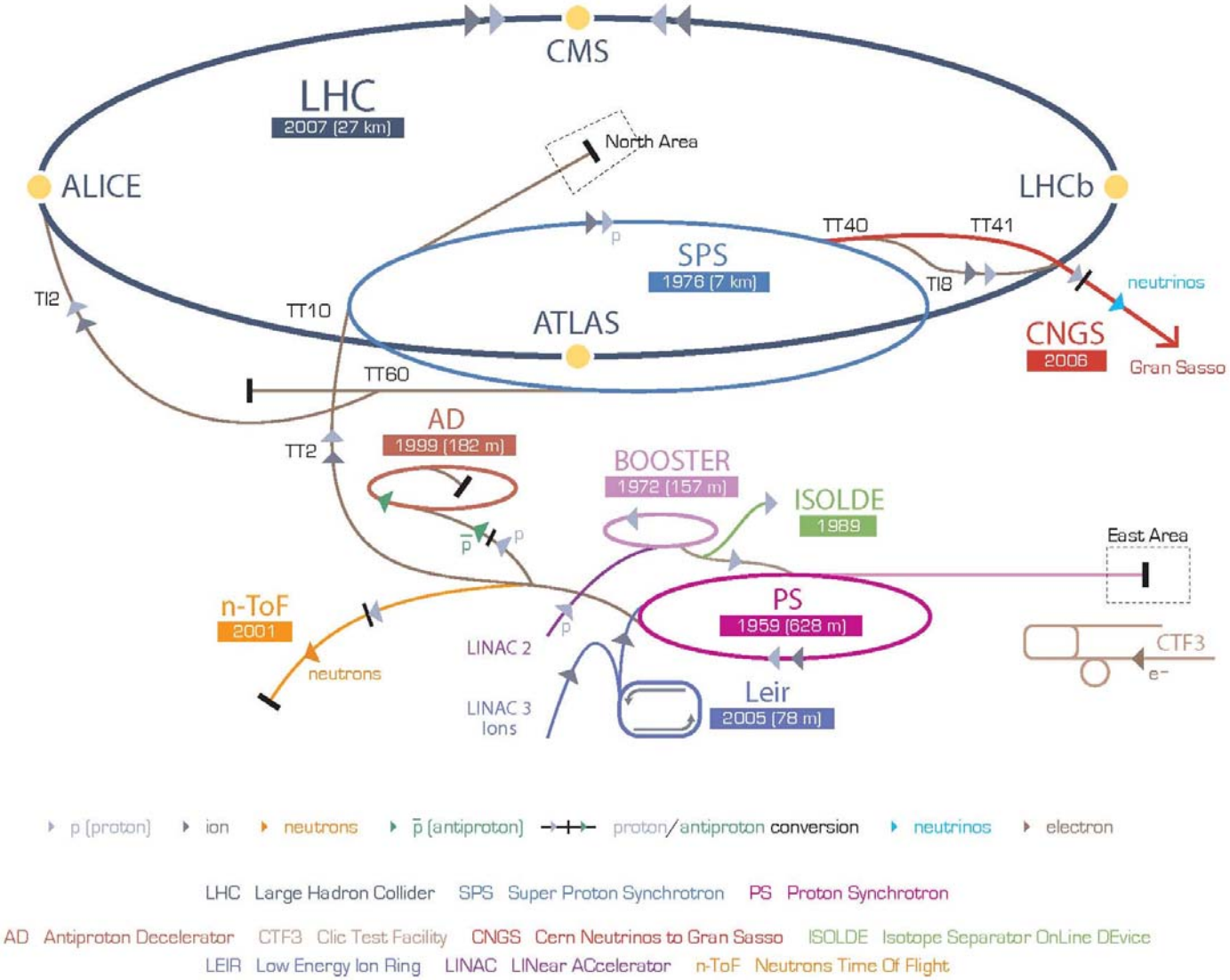

Overall layout of LHC and its detectors

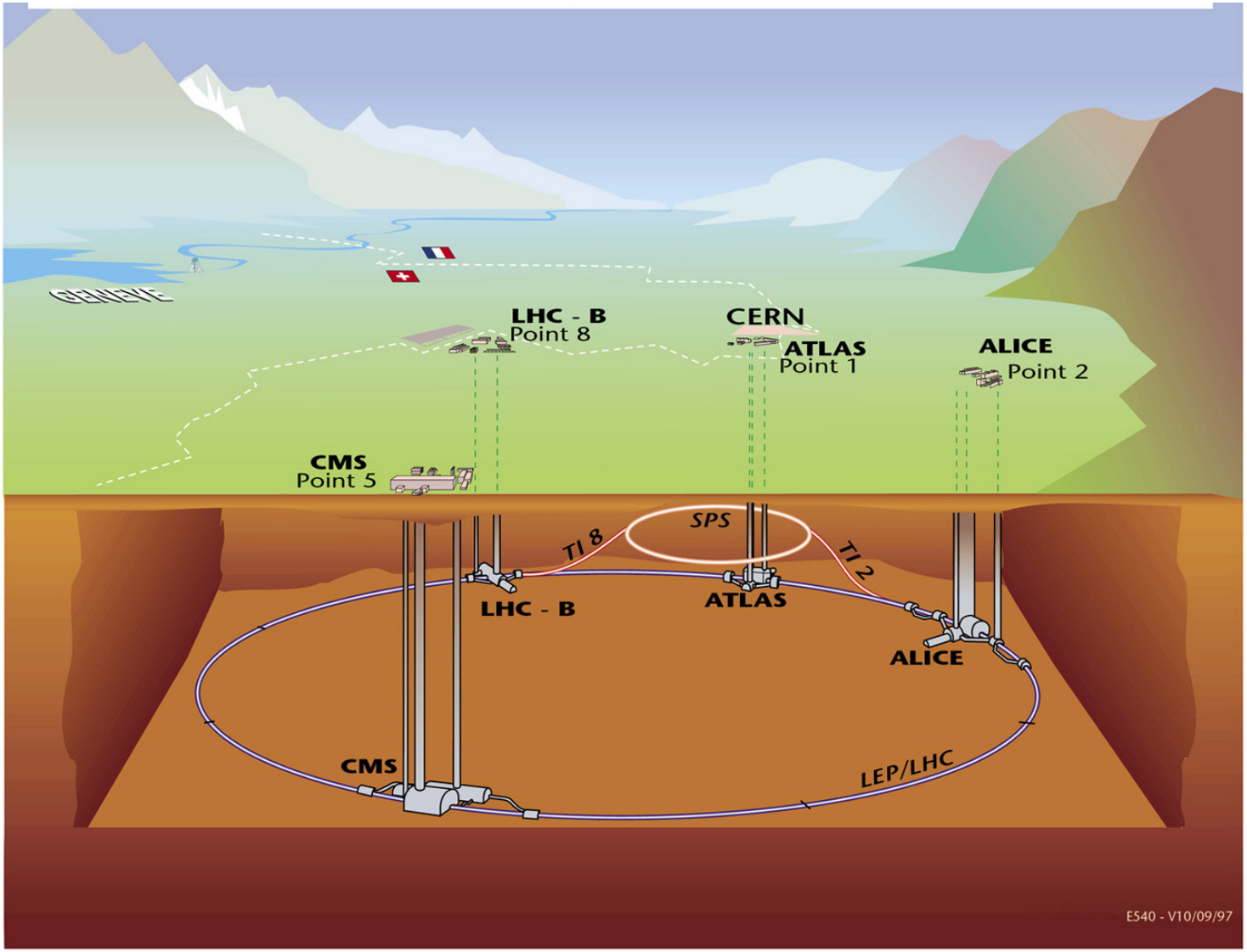

Main parameters of LHC (p-p)

• Circumference	26.7	km
• Beam energy at collision	7	TeV
• Beam energy at injection	0.45	TeV
• Dipole field at 7 TeV	8.33	T
• Luminosity	10^{34}	$cm^{-2}.s^{-1}$
• Beam current	0.58	A
• Protons per bunch	1.15×10^{11}	
• Number of bunches	2808	
• Nominal bunch spacing	24.95	ns
• Normalized emittance	3.75	μm.rad
• Total crossing angle	285	μrad
• Energy loss per turn	6.7	keV
• Critical synchrotron energy	44.1	eV
• Radiated power per beam	3.6	kW
• Stored energy per beam	362	MJ
• Stored energy in magnets	11	GJ
• Operating temperature	1.9	K

Contents

- The LHC in a nutshell
- Performance
  - Energy
  - Luminosity
  - Collective effects
  - Dynamic aperture
- Technology
  - Superconducting magnets
  - Powering and protection
  - Cryogenics
  - Vacuum
- Project management

The first circular accelerator
Lawrence and Livingston's 80 keV cyclotron (1930)

Ernest O. Lawrence

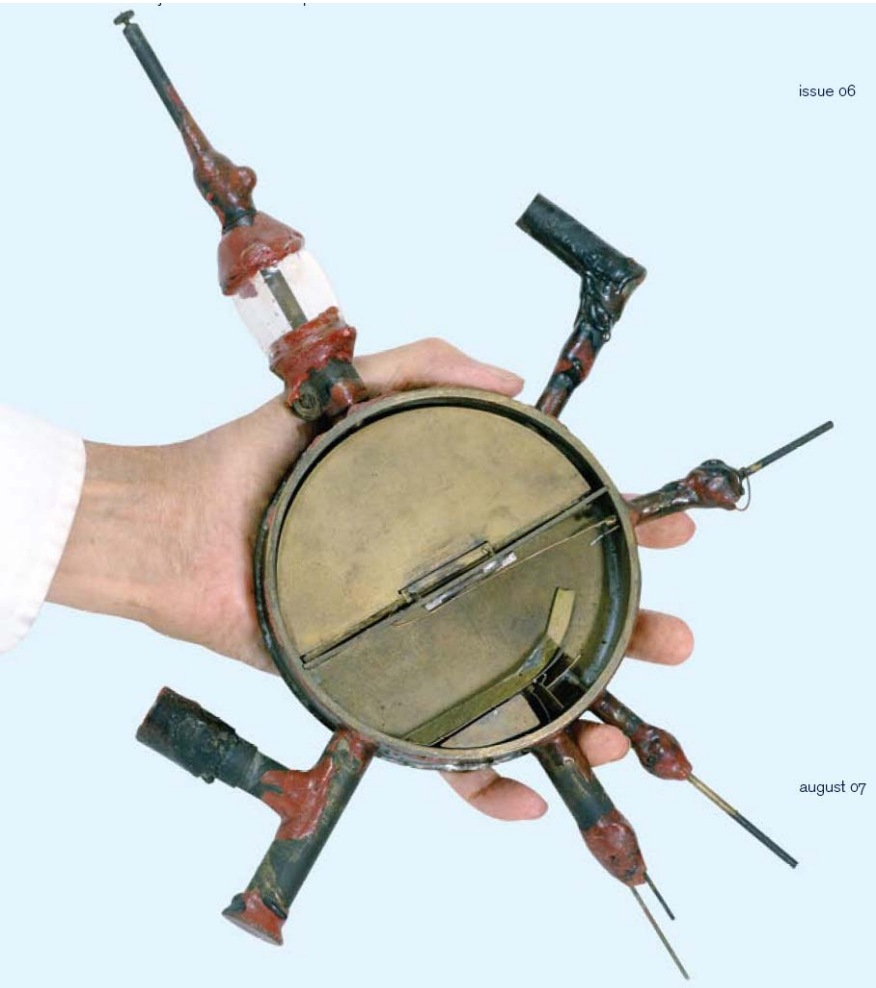

- sustained exponential development for more than 70 years
- progress achieved through repeated jumps from saturating to emerging technologies
- superconductivity, key technology of high-energy machines since the 1980s

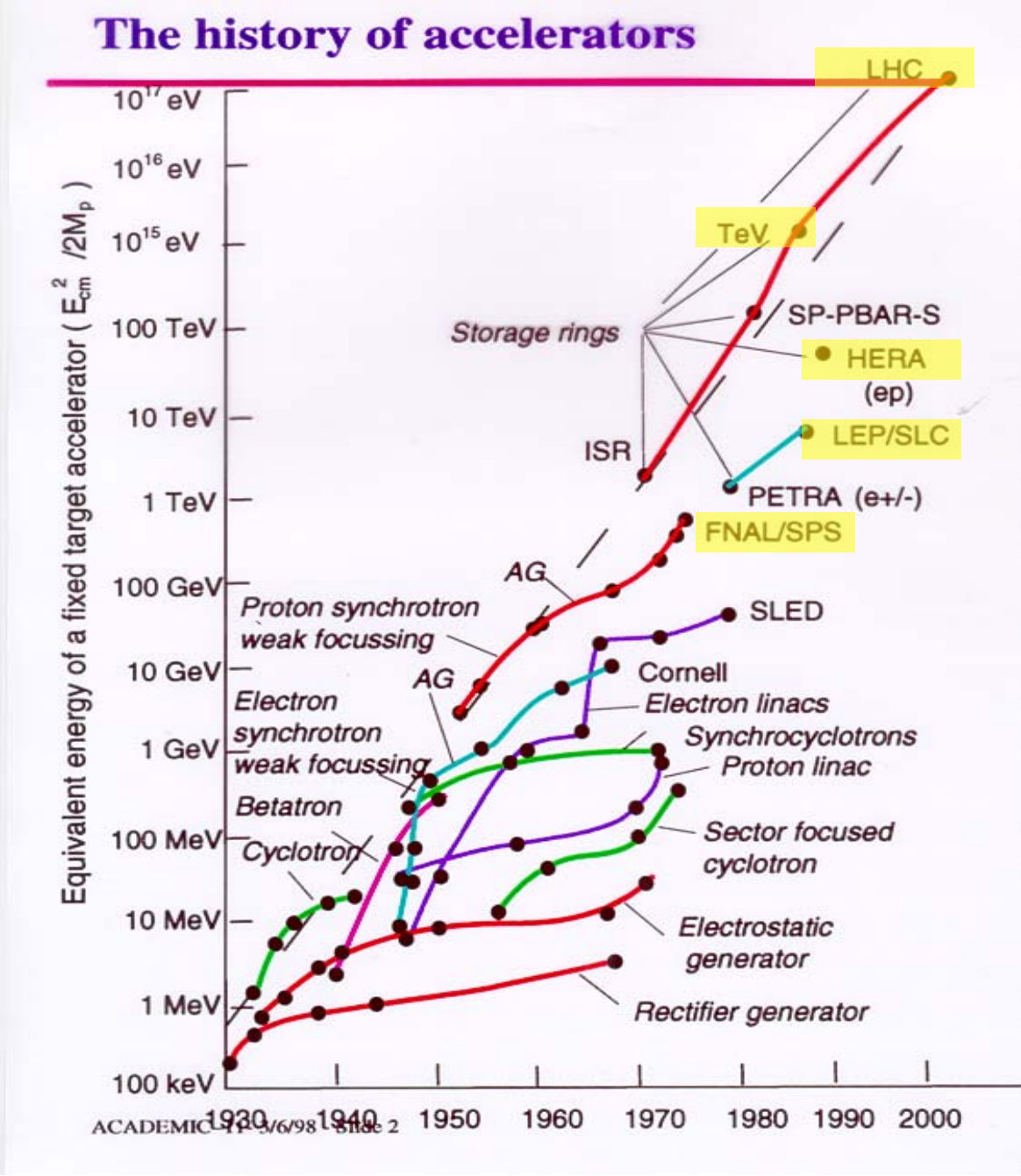

Beam energy and bending field

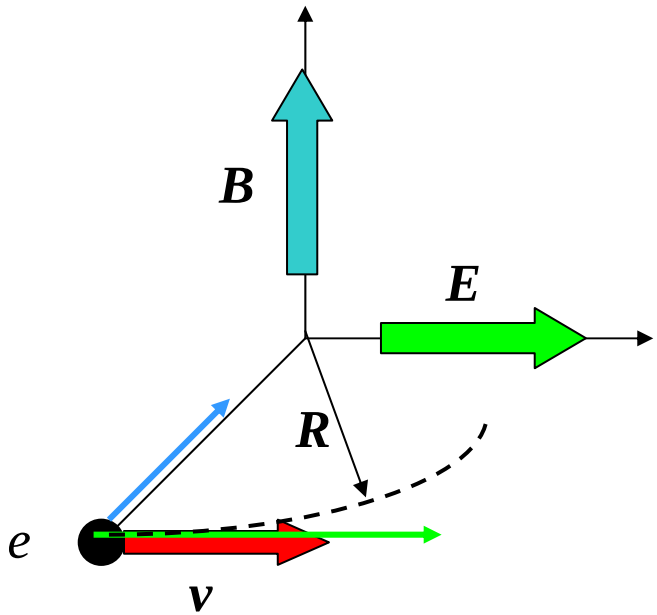

Lorentz force on charged particle

$$\vec{F} = e\left(\vec{E} + \vec{v} \wedge \vec{B}\right)$$

Charge

Electric field

Velocity

Magnetic field

In a circular accelerator

Particle momentum → $p = e\,B\,R$ ← Radius of curvature

$$p\,[GeV/c] \approx 0.3\,B\,[T]\,R[m]$$

The LHC needs a field of 8.33 T to bend 7 TeV beams along the curvature of the tunnel, with a radius of 2804 m

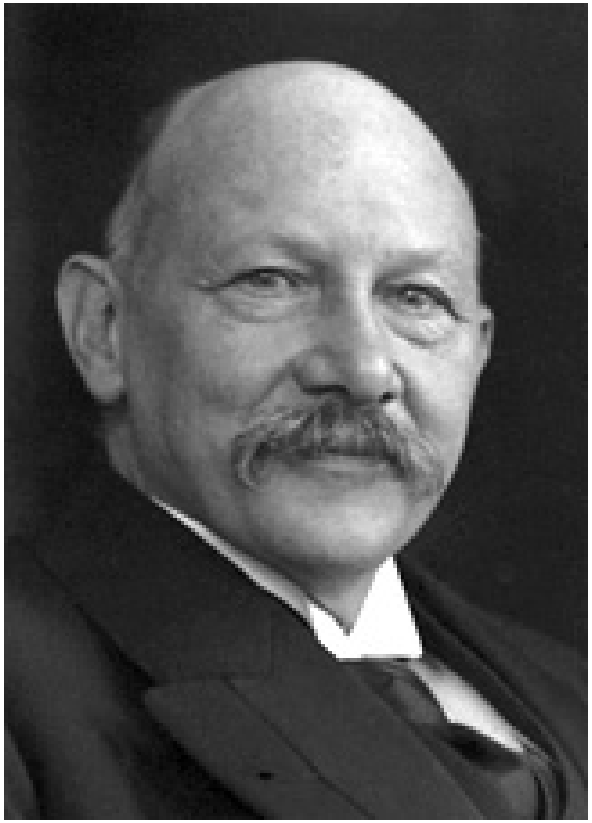

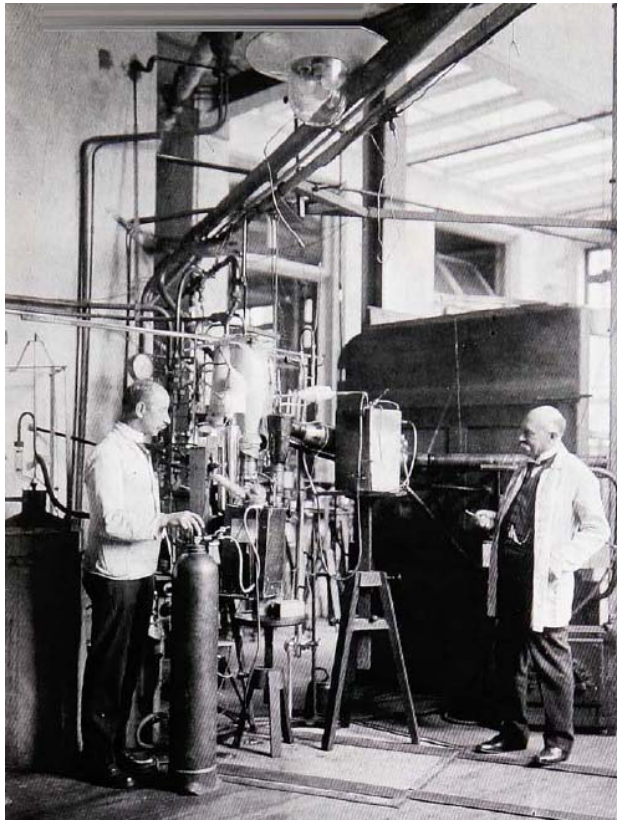

HEIKE KAMERLINGH ONNES

Investigations into the properties of substances at low temperatures, which have led, amongst other things, to the preparation of liquid helium

Nobel Lecture, December 11, 1913

First liquefaction of helium (1908)

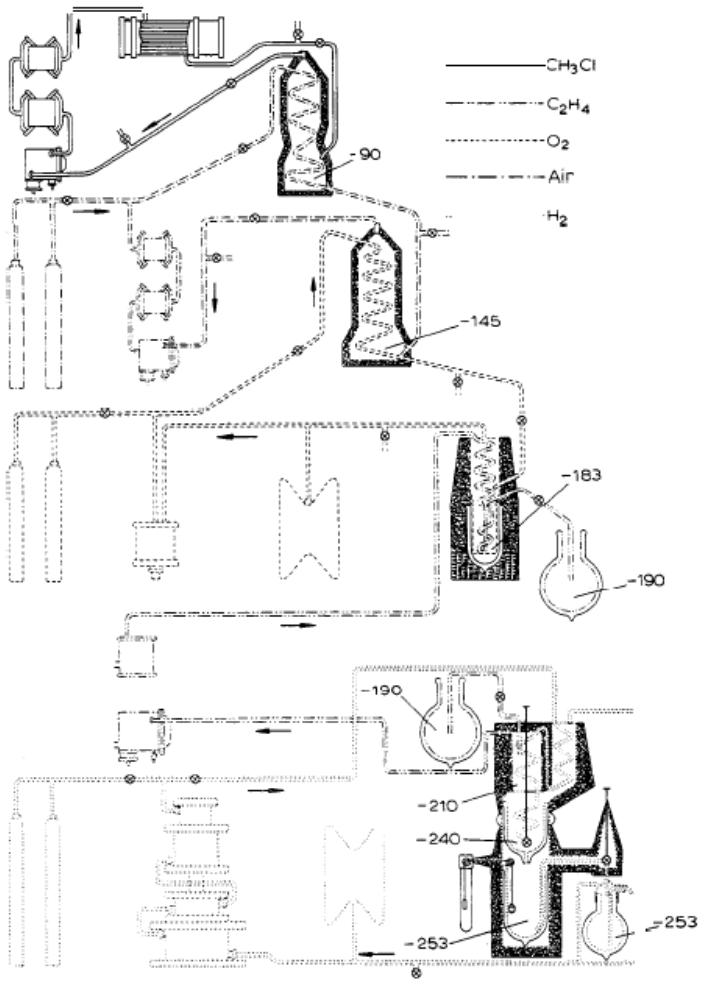

Leiden « cascade » to produce liquid hydrogen

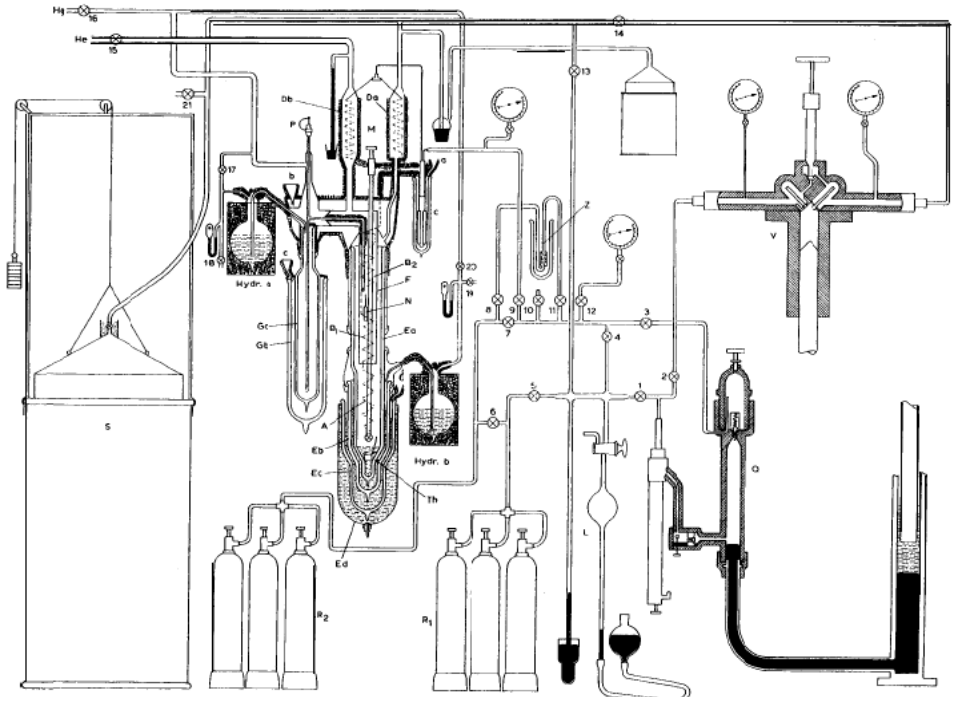

Helium liquefaction stage

Discovery of superconductivity (1911)

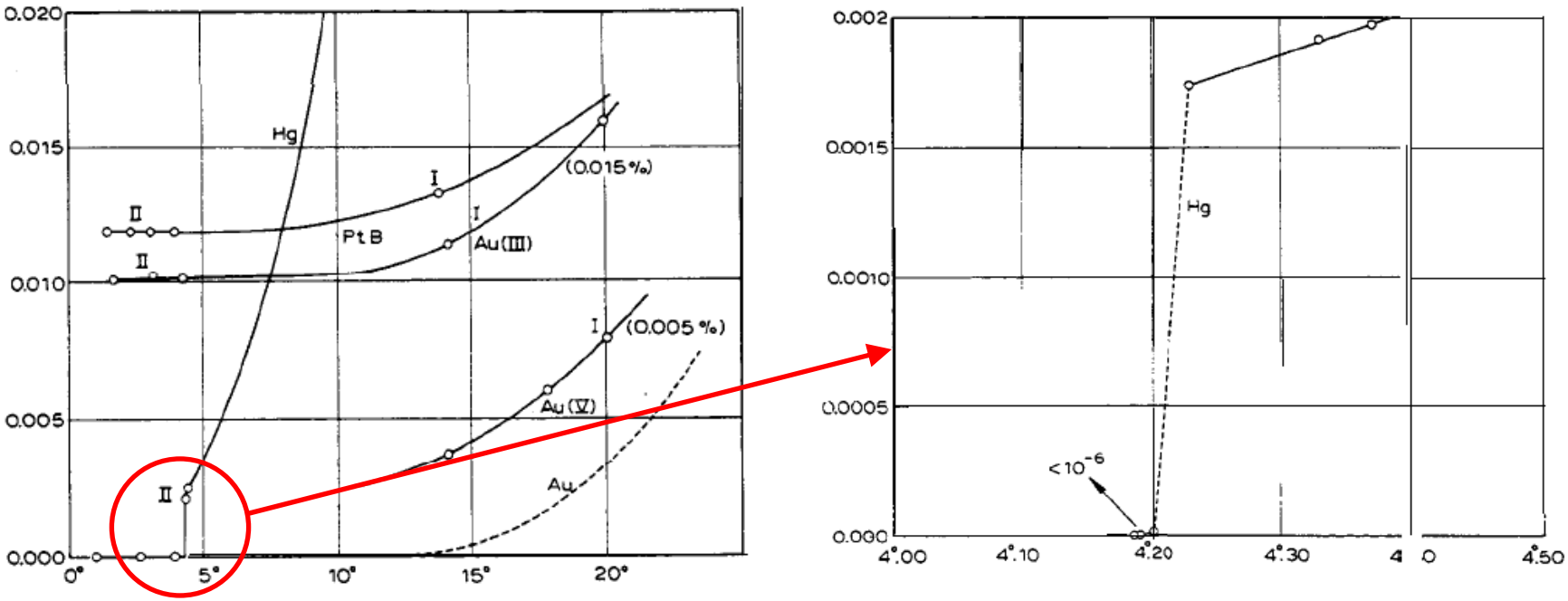

Thus the mercury at 4.2°K has entered a new state, which, owing to its particular electrical properties, can be called the state of superconductivity.

First idea of superconducting magnets (H. K. Onnes 1913)

dendum 2.) There is also the question as to whether the absence of Joule heat makes feasible the production of strong magnetic fields using coils without iron,* for a current of very great density can be sent through very fine, closely wound wire spirals. Thus we were successful in sending a current of 0.8 amperes, i.e. of 56 amperes per square millimetre, through a coil, which contained 1,000 turns of a diameter of 1/70 square mm per square centimetre at right angles to the turns.

critical field of superconductors!

after this lecture was given and produced surprising results. In fields below a threshold value (for lead at the boiling point of helium 600 Gauss), which was not reached during the experiment with the small coil mentioned in the text, there is no magnetic resistance at all. In fields above this threshold value a relatively large resistance arises at once, and grows considerably with the field. Thus in an unexpected way a difficulty in the production of intensive magnetic fields with coils without iron faced us. The discovery of the

Vortex lattice of type-II superconductors (1954)

Alexei Abrikosov

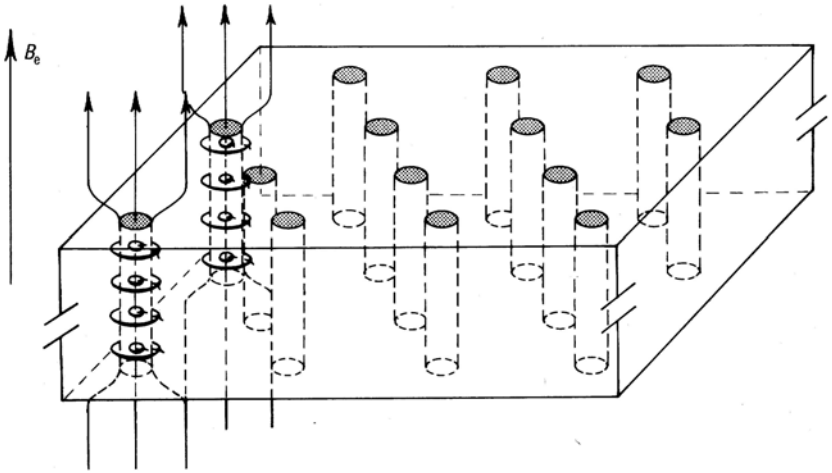

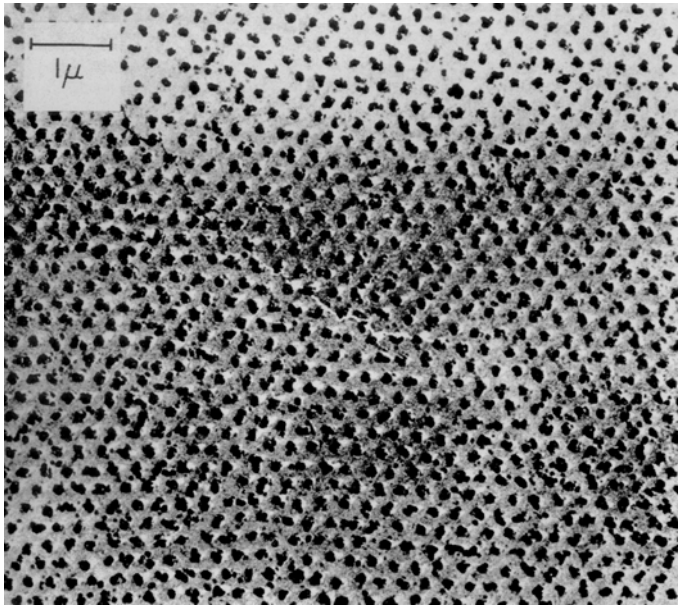

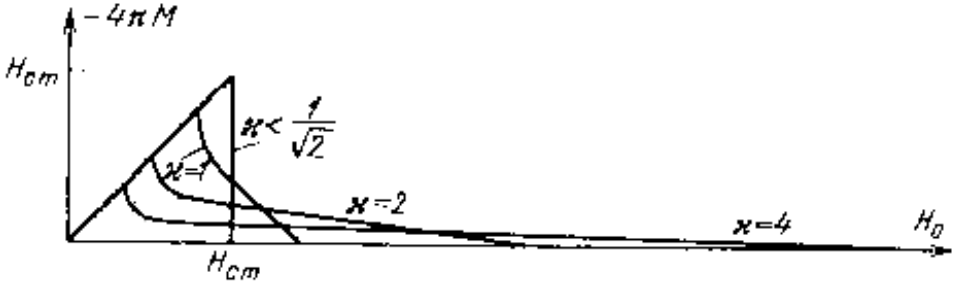

Critical field of superconductors

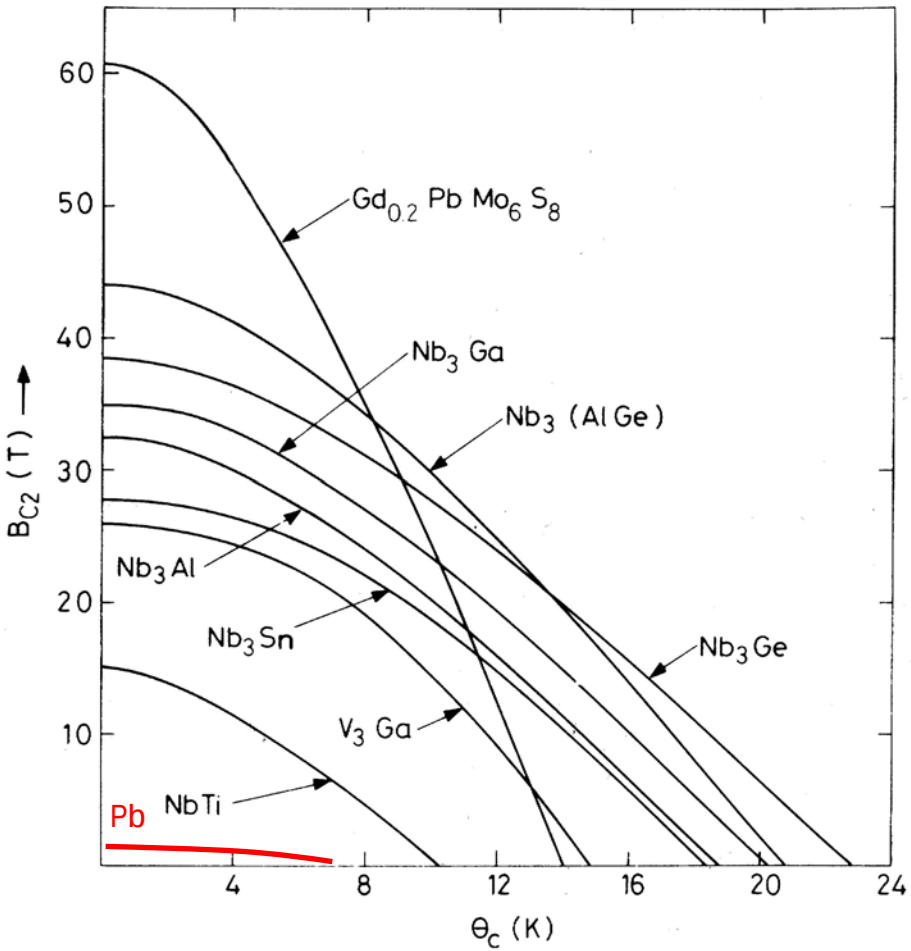

BCS theory of superconductivity (1957)

PHYSICAL REVIEW VOLUME 108, NUMBER 5 DECEMBER 1, 1957

Theory of Superconductivity*

J. Bardeen, L. N. Cooper,† and J. R. Schrieffer‡
Department of Physics, University of Illinois, Urbana, Illinois

(Received July 8, 1957)

A theory of superconductivity is presented, based on the fact that the interaction between electrons resulting from virtual exchange of
between the
energy, $\hbar\omega$. I
this attracti
Coulomb inte
individual-pa
formed from
in which elec
and moment
amount prop
isotope effec
the energ
less than
conducting
he repulsi
described l
te of a sup
nal state co
pairs of c
n the norm
)², consiste
et of excit
one-to-one correspondence with those of the normal phase is obtained by specifying occupation of certain Bloch states and by
t to form a
he theory y
ffect in the
cific heats a
n are in go
o for indivi
.5kT_c at T
single-parti
ing wave f
culations of
al pair con-
nsition and
Calculated
heir temper-
nt. There is
h decreases
s of matrix
xcited-state
tion expan-
given.

John Bardeen

Leon Neil Cooper

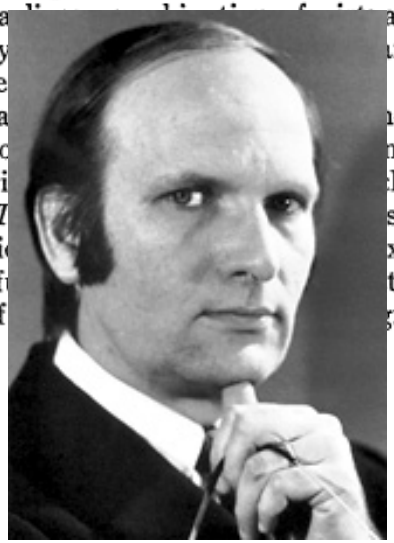

John Robert Schrieffer

First « high-field » superconducting magnet

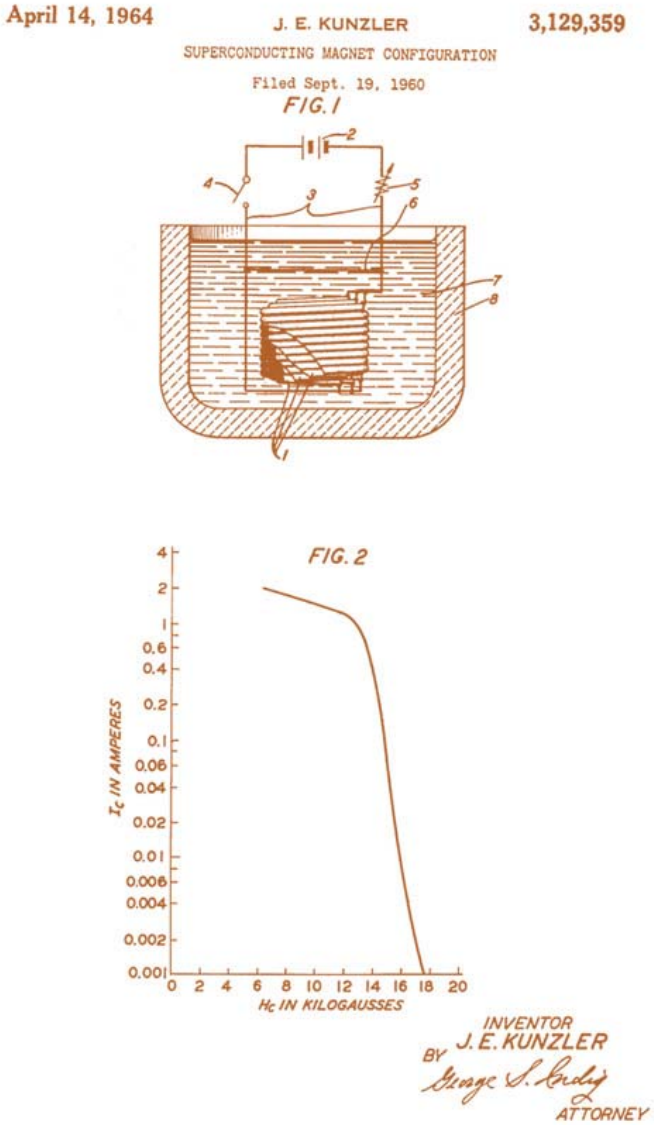

Patent filed in 1960 by J. Kunzler, of Bell Laboratories (registered in 1964)

1.5 T reached with magnet wound from molybdenium-rhenium alloy wire

Discovery of Nb-Ti alloys (1961)

PHYSICAL REVIEW VOLUME 123, NUMBER 5 SEPTEMBER 1, 1961

Superconducting Solid Solution Alloys of the Transition Elements

J. K. HULM AND R. D. BLAUGHER
Westinghouse Research Laboratories, Pittsburgh, Pennsylvania
(Received April 19, 1961)

The solid solution alloys formed by the incomplete *d*-shell metals in groups 4, 5, 6, and 7 have been tested for superconductivity down to 1°K. For alloys formed between neighboring elements in a given *row* of the periodic table, two transi
proximately equal to 4.7 and 6.4, resp
upper maximum is absent. Similar ma
rows of the periodic table, thus confir
normal density-of-states function, $N(0$
these peaks lying at about the same com
ent work. The relationship of T_c to $N($
data are also presented for alloys comp
In this case, the form of the relationsh

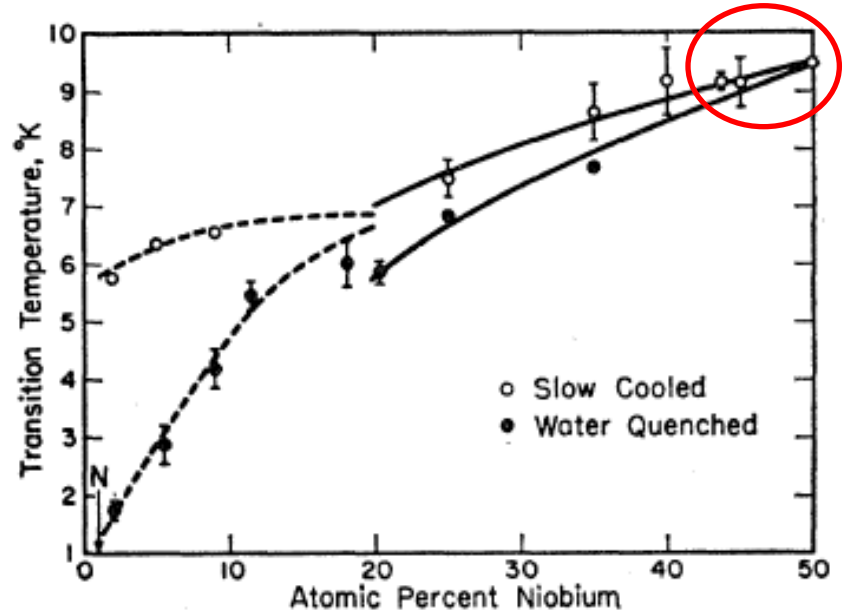

FIG. 6. Transition temperature versus composition for titanium-niobium alloys prepared by different types of heat treatment.

High-luminosity insertion at the CERN ISR (1979)

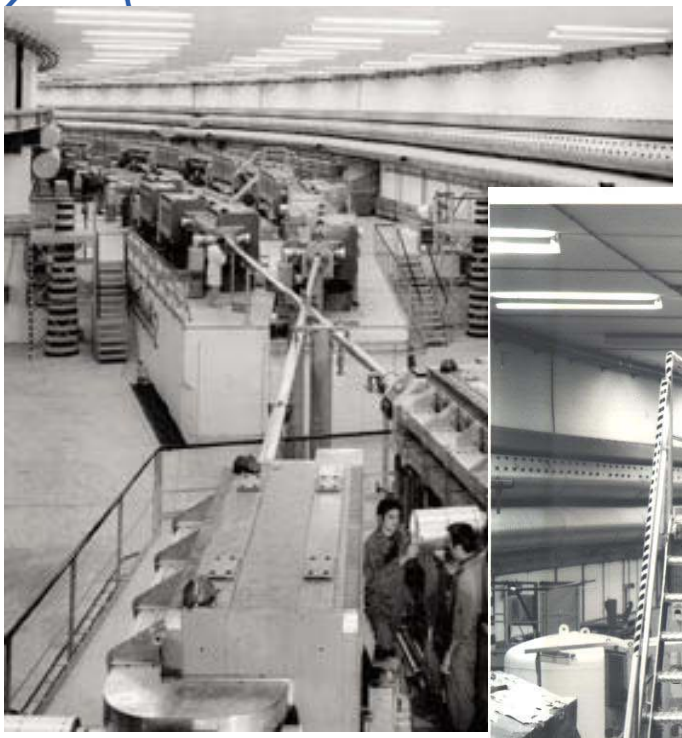

First superconducting magnets routinely operated in an accelerator

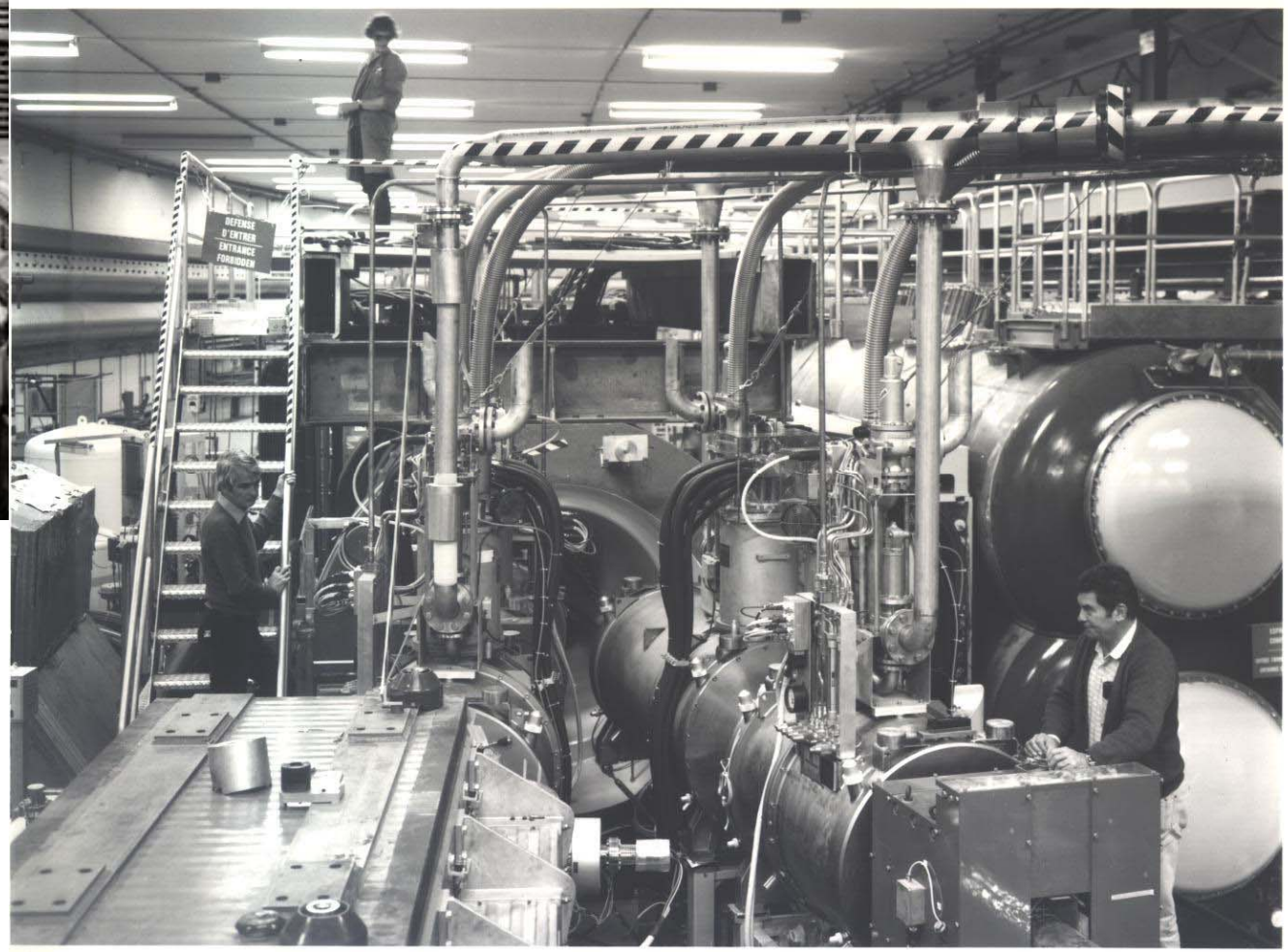

The Tevatron at Fermilab, USA (1983)

HERA proton ring at DESY, Germany (1992)

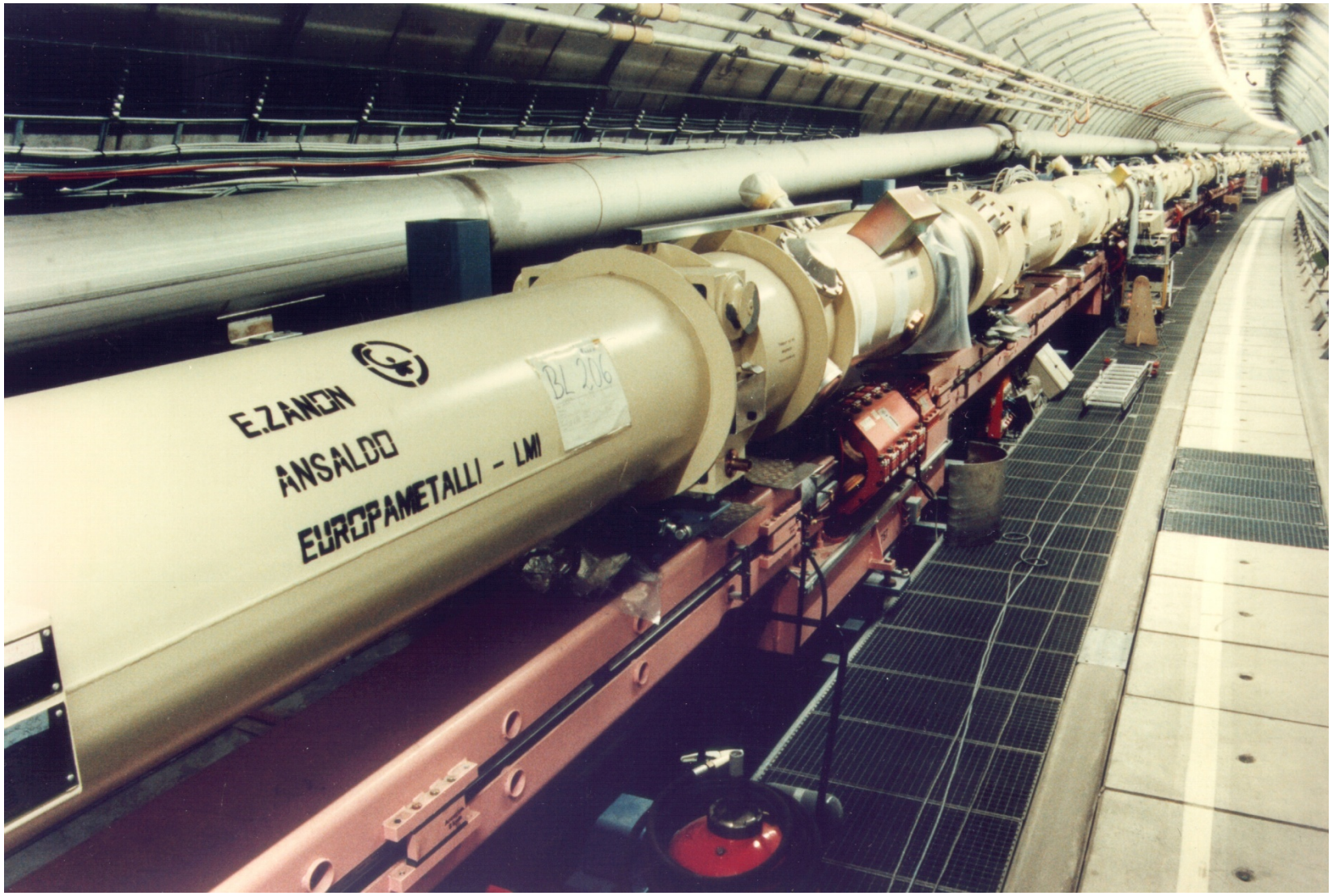

RHIC at Brookhaven National Lab, USA (2000)

Circumference & bending field of hadron colliders

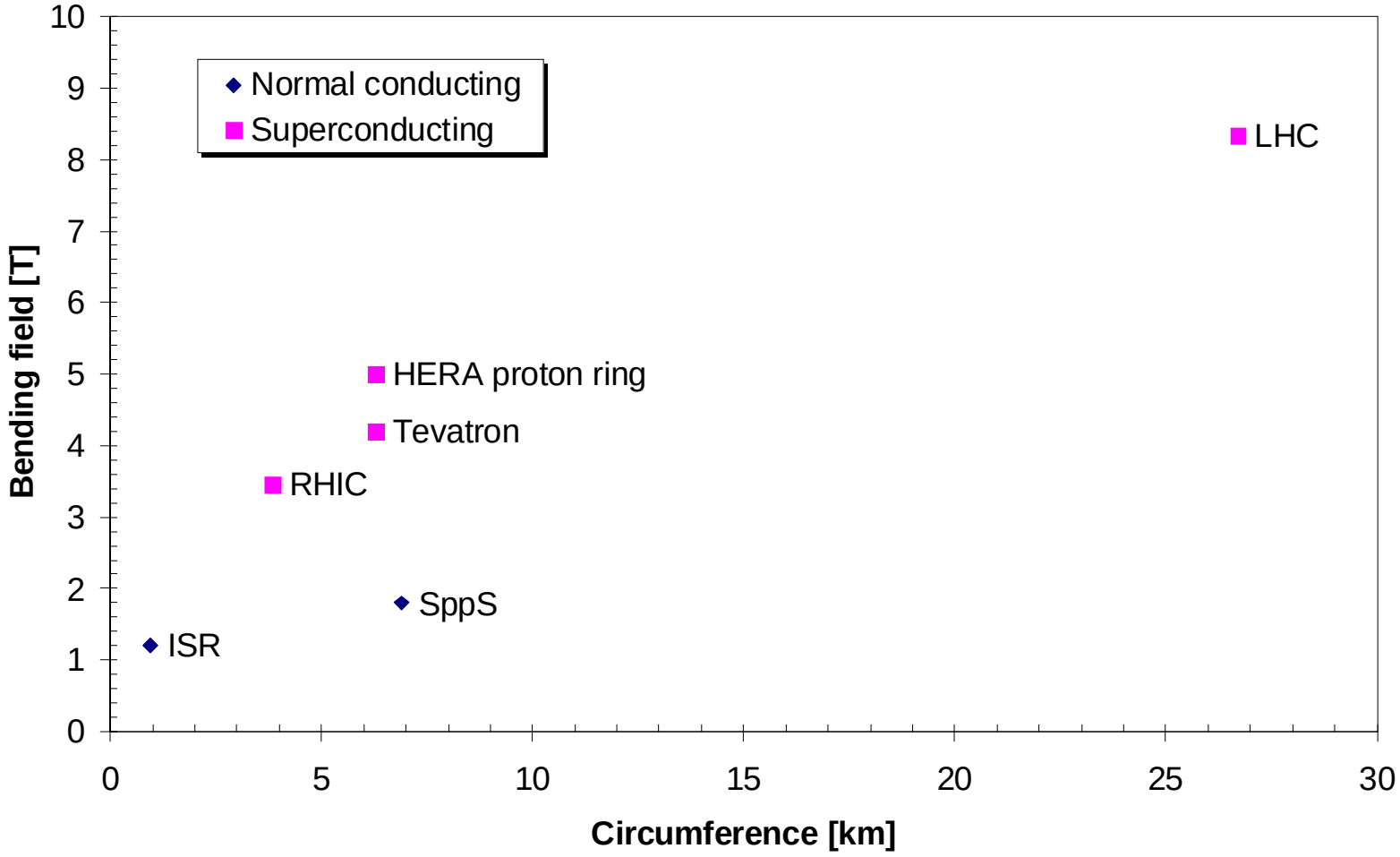

Size & cost of CERN hadron colliders

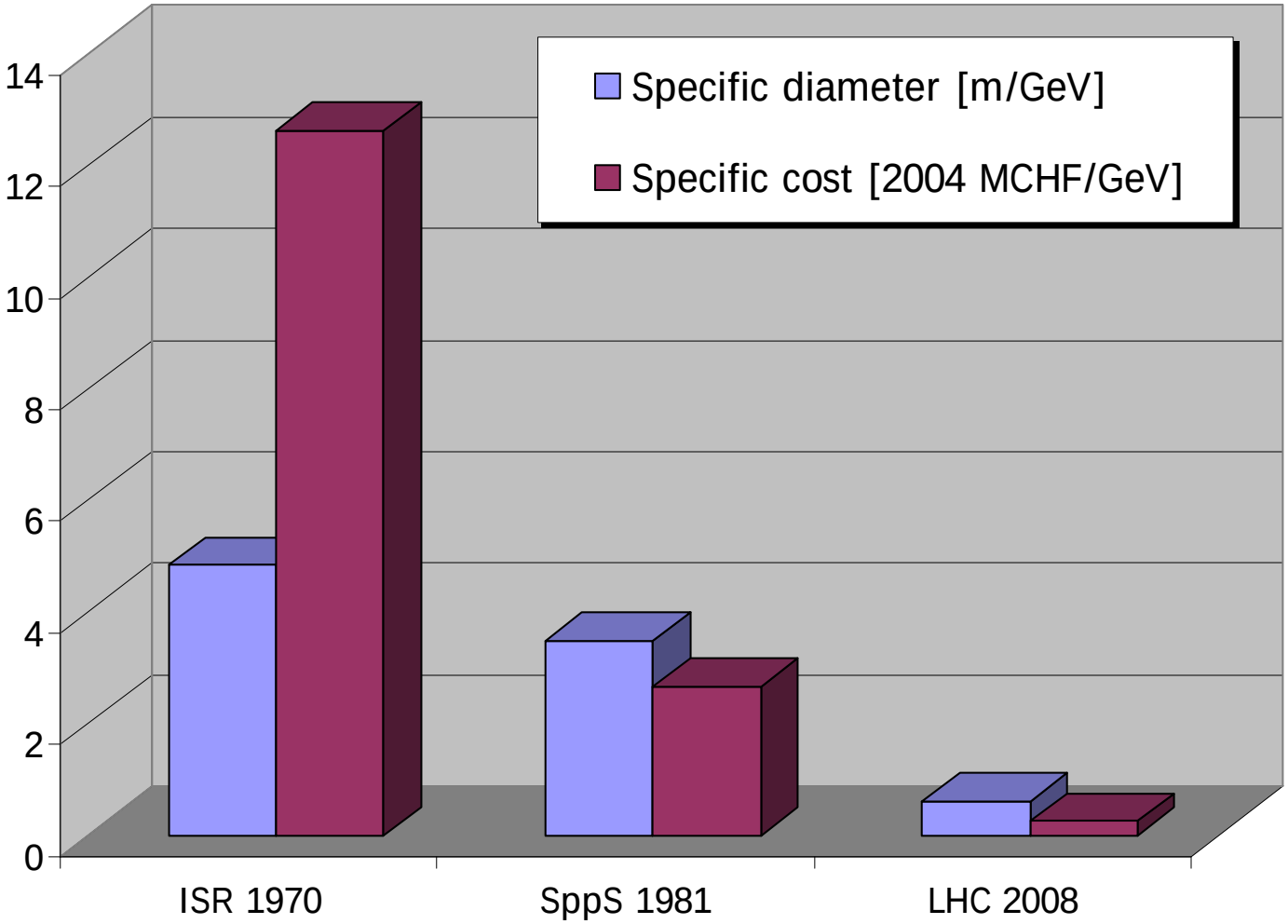

Electrical power consumption

- Superconducting magnets enable to contain electrical power consumption through two independent effects
  - Higher magnetic field ⇒ smaller circumference
  - No dissipation ⇒ lower power (refrigeration) per unit length

	Normal conducting	**Superconducting (LHC)**
Magnetic field	1.8 T (iron saturation)	8.3 T (NbTi critical surface)
Field geometry	Defined by magnetic circuit	Defined by coils
Current density in windings	10 A/mm^2	400 A/mm^2
Electromagnetic forces	20 kN/m	3400 kN/m
Electrical consumption	10 kW/m	2 kW/m

Joule heating

Refrigeration

Operating temperature of superconductors

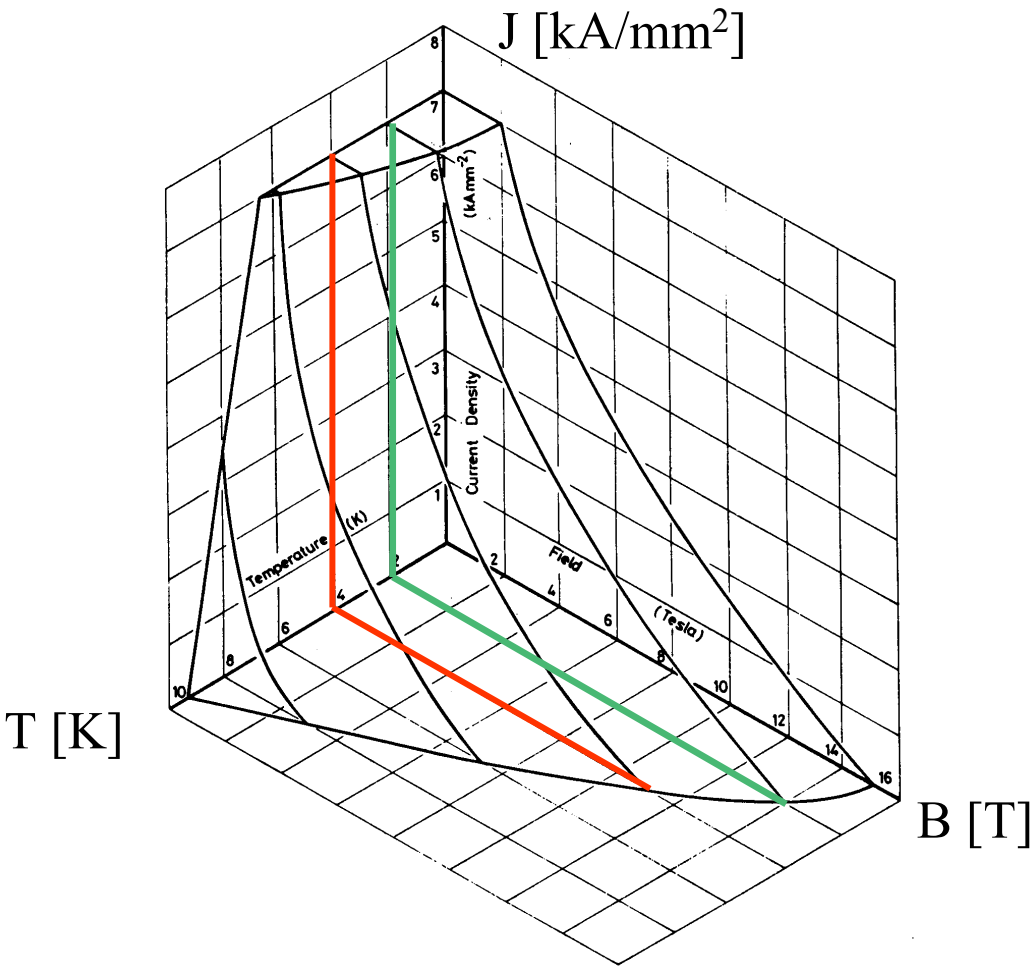

- The superconducting state only occurs in a limited domain of temperature, magnetic field and transport current density
- Superconducting magnets produce high field with high current density
- Lowering the temperature enables better usage of the superconductor, by broadening its working range

Critical current density of superconductors

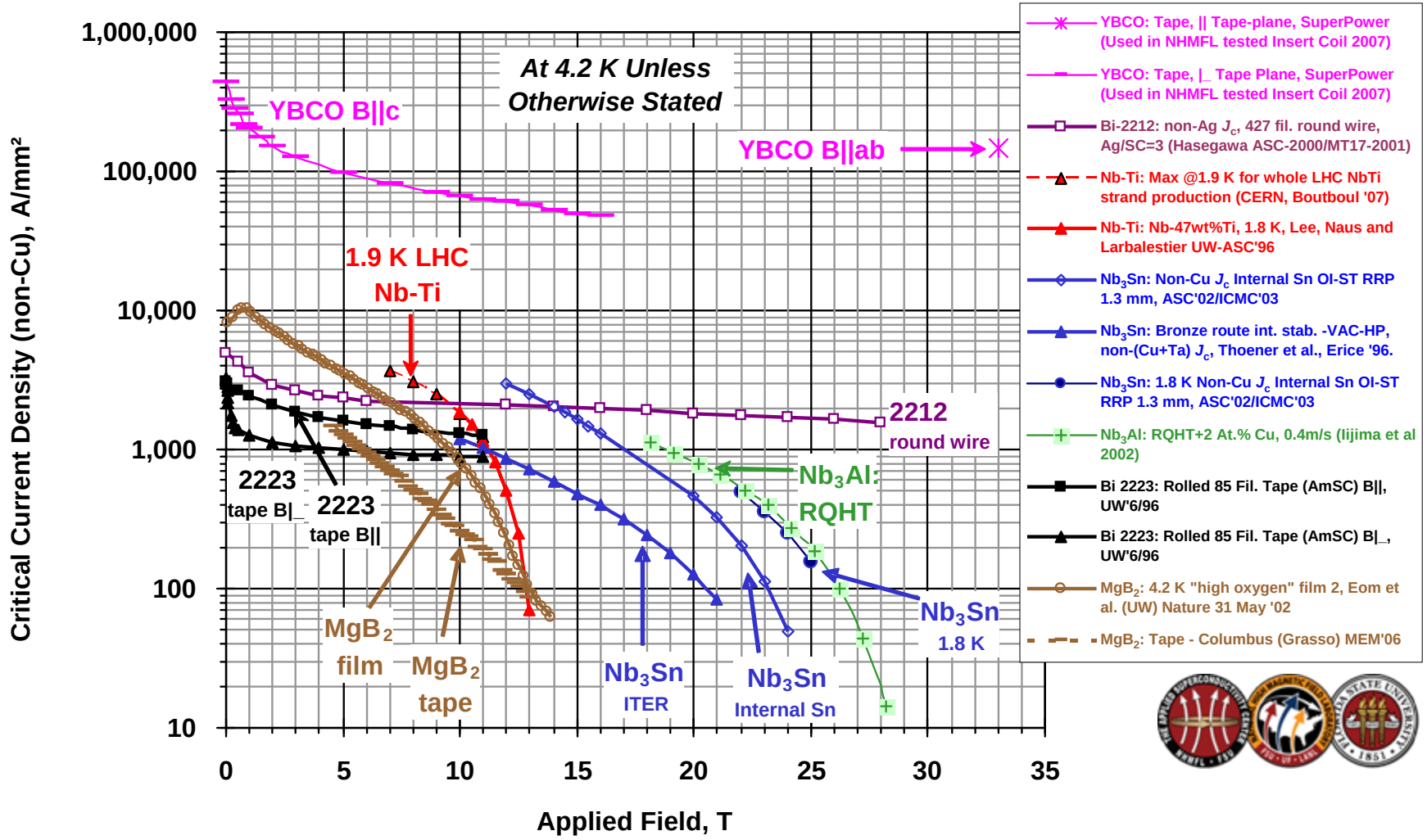

Critical current density of technical superconductors

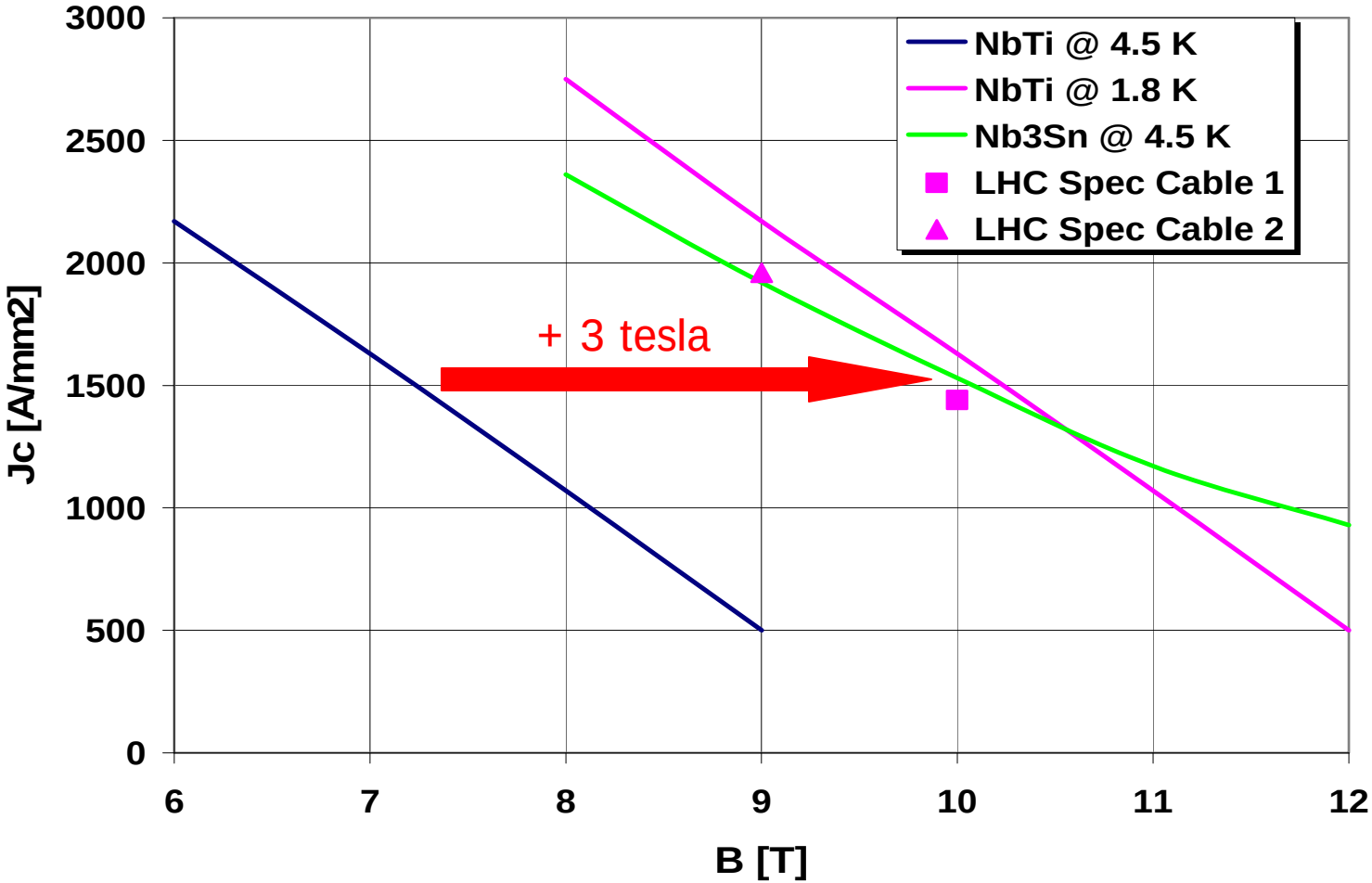

Rationale for superconductivity & cryogenics in particle accelerators

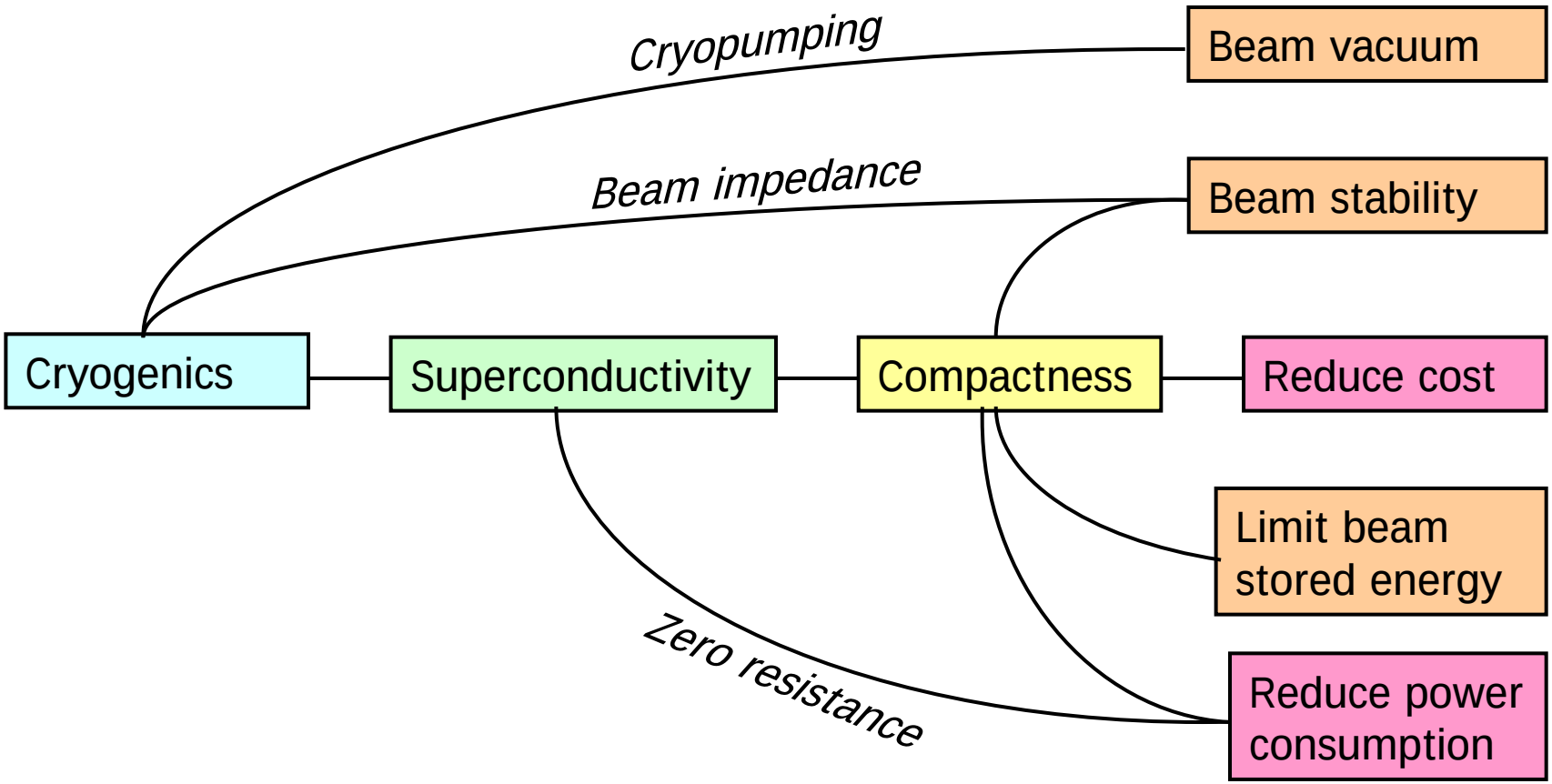

Contents

- The LHC in a nutshell
- Performance
  - Energy
  - Luminosity
  - Collective effects
  - Dynamic aperture
- Technology
  - Superconducting magnets
  - Powering and protection
  - Cryogenics
  - Vacuum
- Project management

Event rate and luminosity

$$R = L\ \sigma$$

Event rate — Luminosity — Cross-section

σ_{TOT} ~ 100 mbarn = 10^{-25} cm^2

$\sigma_{inelastic}$ ~ 60 mbarn = 6 10^{-26} cm^2

C. Amsler *et al.*, Physics Letters **B667**, 1 (2008)

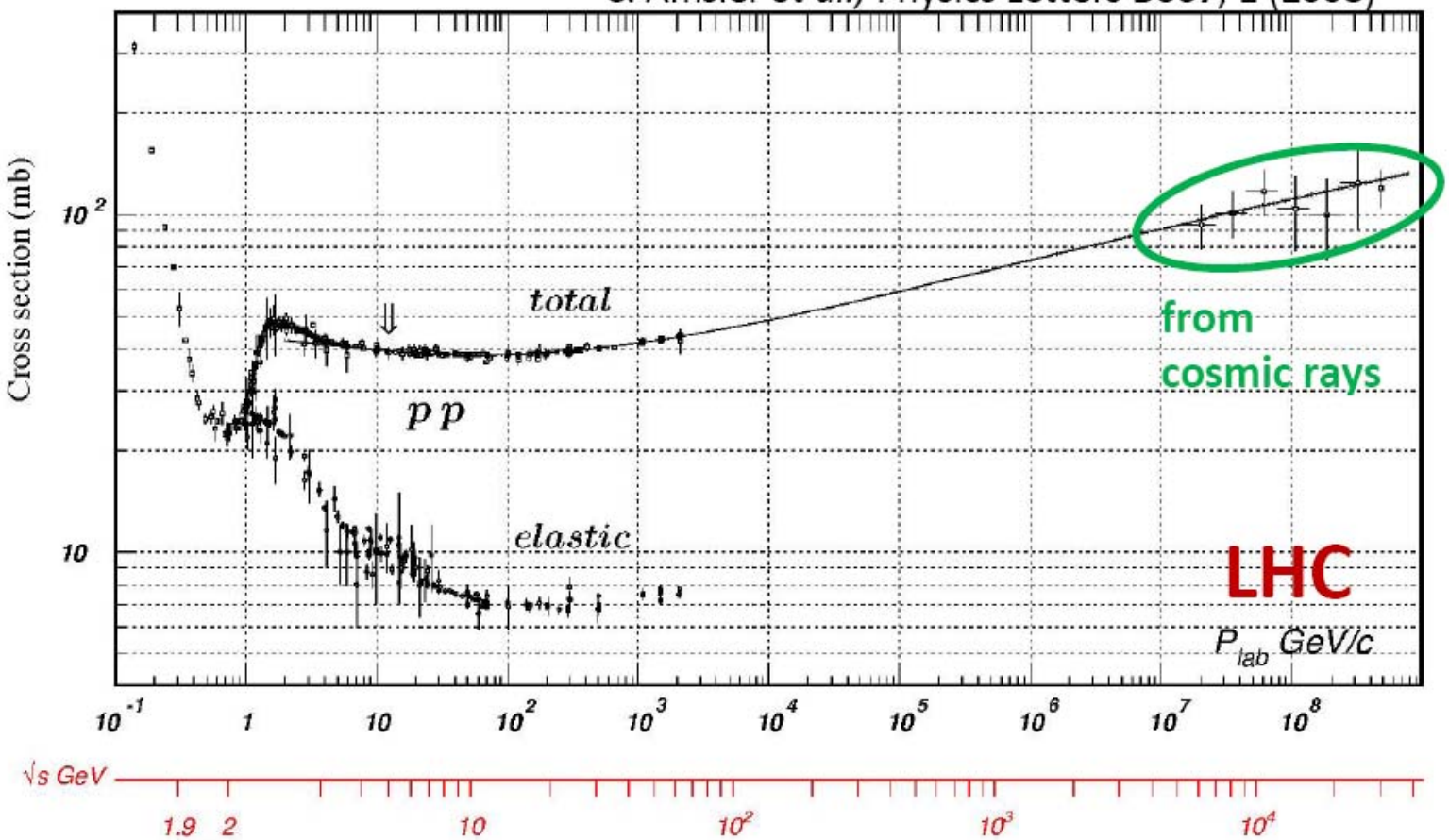

Luminosity

Number of bunches

Number of particles per bunch

Revolution frequency

Relativistic factor

$$L = \frac{N_b^2 \; n_b \; f_{rev} \; \gamma}{4 \, \pi \, \varepsilon_n \, \beta^*} F$$

Geometric factor linked to crossing angle

Normalized emittance

Beta function at collision point

- To maximize luminosity
  - increase bunch number, bunch population
  - reduce emittance, beta function at collision point
  - cross at small angle

limits?

Beam stored energy

- Energy stored in circulating beam

$$E_{beam} = m_0 \, c^2 \, \gamma \, N_b \, n_b$$

With 2808 bunches of 1.1 10^{11} protons at 7 TeV, E_{beam} = 362 MJ, equivalent to 80 kg TNT!

Set by injector chain

Set by collision optics

$$L = \frac{N_b \, f_{rev}}{4 \, \pi \, m_0 \, c^2 \varepsilon_n \, \beta^*} \, F \, E_{beam} = \frac{1}{4 \, \pi \, m_0 \, c^2} \, f_{rev} \, \frac{N_b}{\varepsilon_n} \, \frac{F}{\beta^*} \, E_{beam}$$

Set by machine circumference

Beam-beam effects

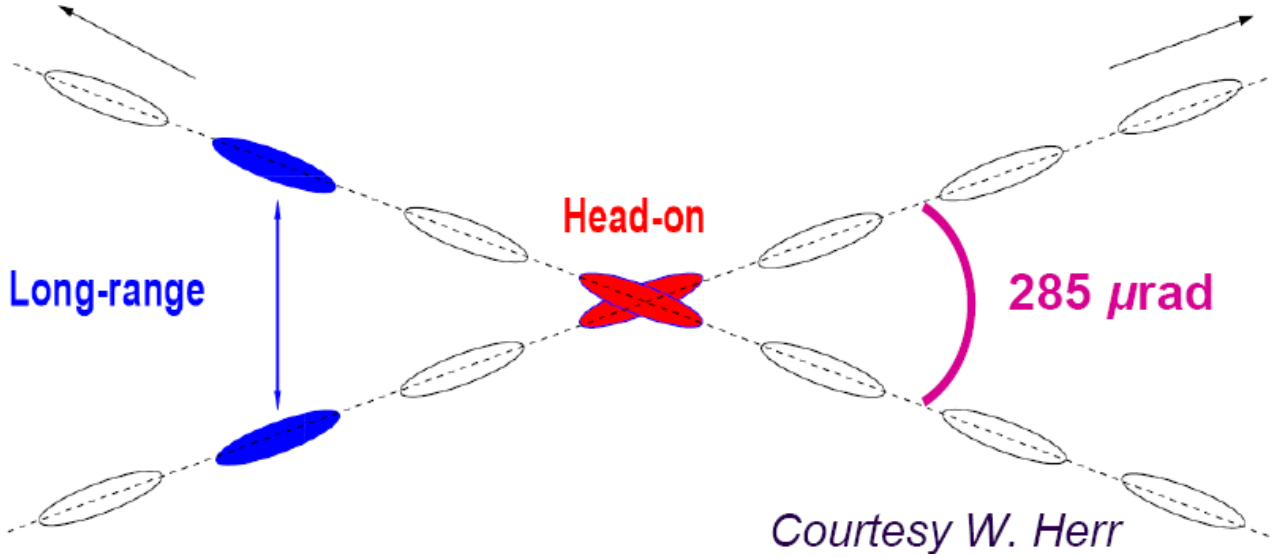

- Particle trajectories in one beam perturbed by e-m field of the other
- Head-on crossing
  - Excites betatron resonances
  - Generates tune spread
- Long-range
  - Additional non-linear tune spread
  - Minimum crossing angle > beam divergence at collision point

tune footprint must not cross low-order resonances

Head-on beam-beam tune shift

Number of collision points

Should not exceed 0.015 (empirical limit)

~ 0.01

$$\xi_{total} = \frac{k\ N_b\ r_p}{4\ \pi\ \varepsilon_n} F < \xi_{\max}$$

- Strategy to maximize luminosity
  - Operate at beam-beam limit
  - Maximize number of bunches, bunch population
  - Decrease beta at collision point

$$L = \frac{\xi_{total}\ N_b\ n_b\ f_{rev}\ \gamma}{k\ r_p\ \beta^*}$$

Beam-beam tune footprint

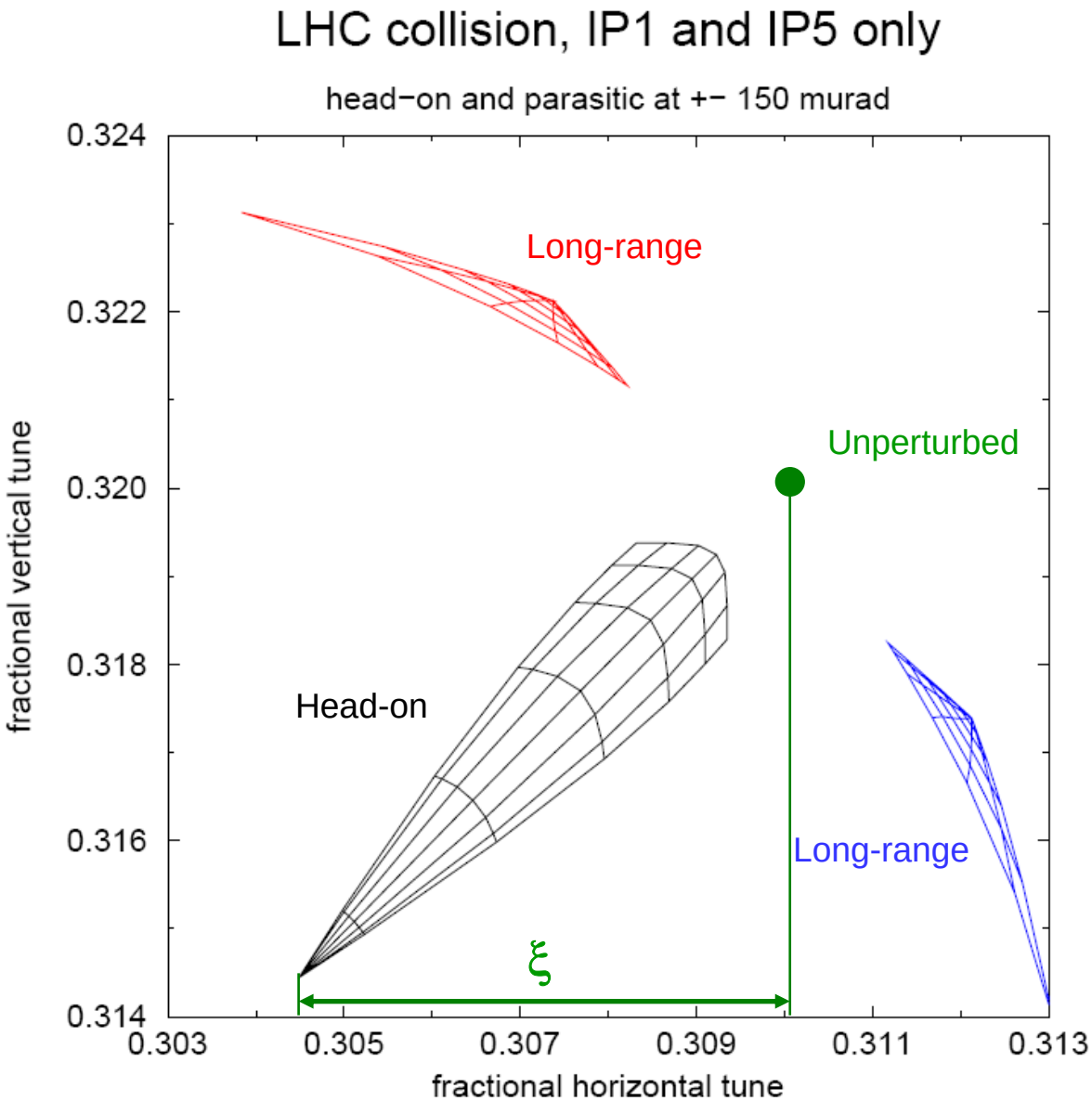

Beam-beam tune footprint

Head-on & long-range, 4 interaction points

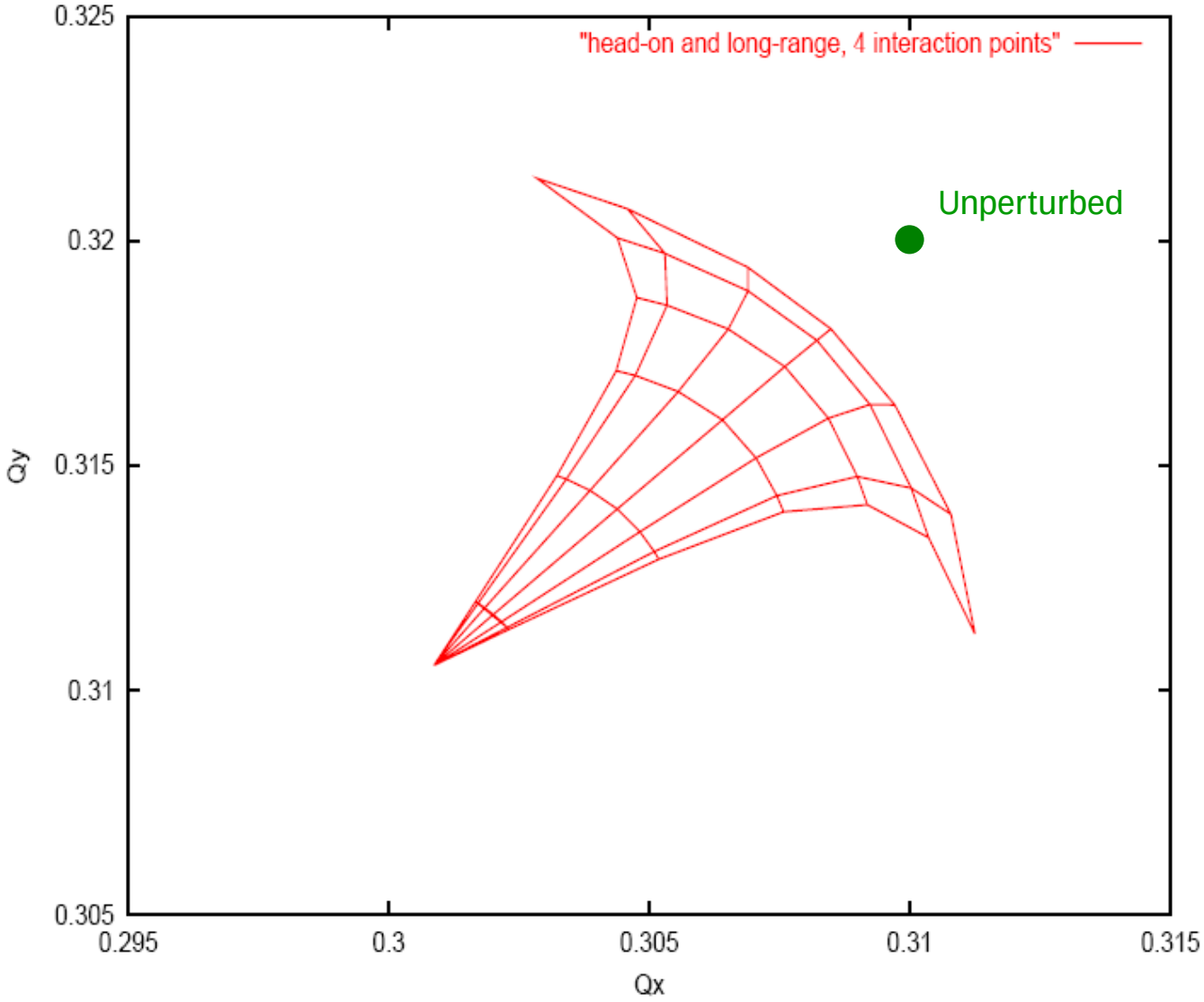

Layout of high-luminosity collision region

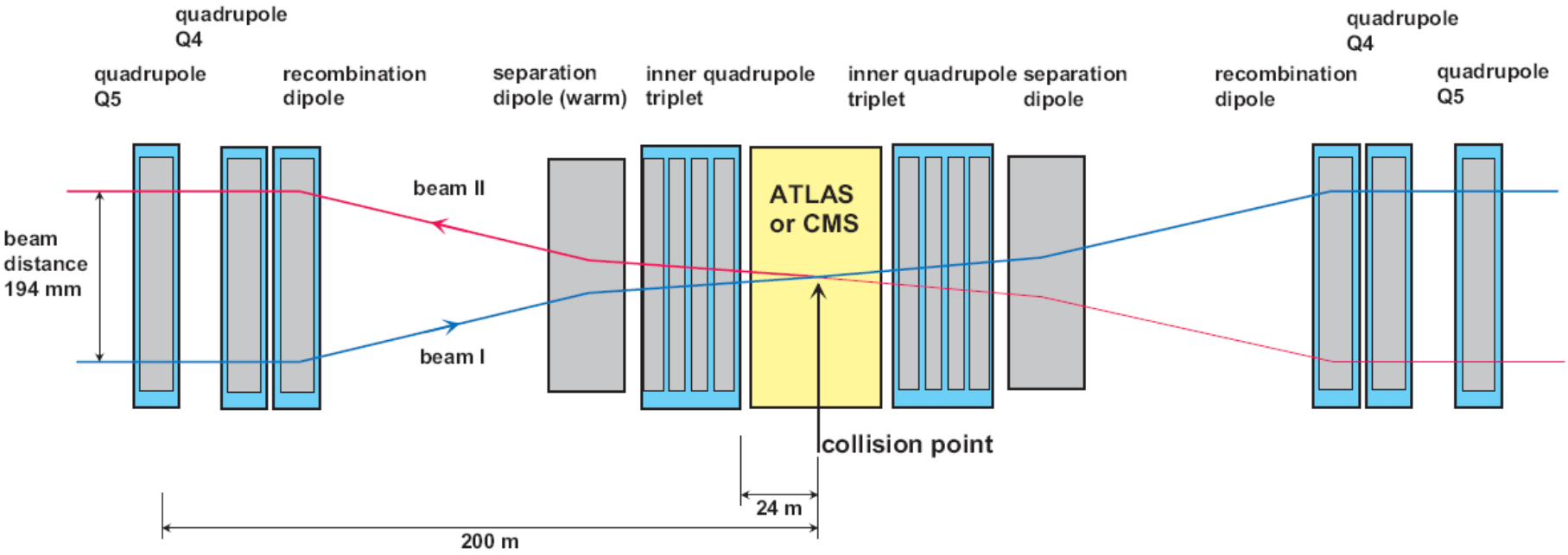

High-luminosity insertion optics

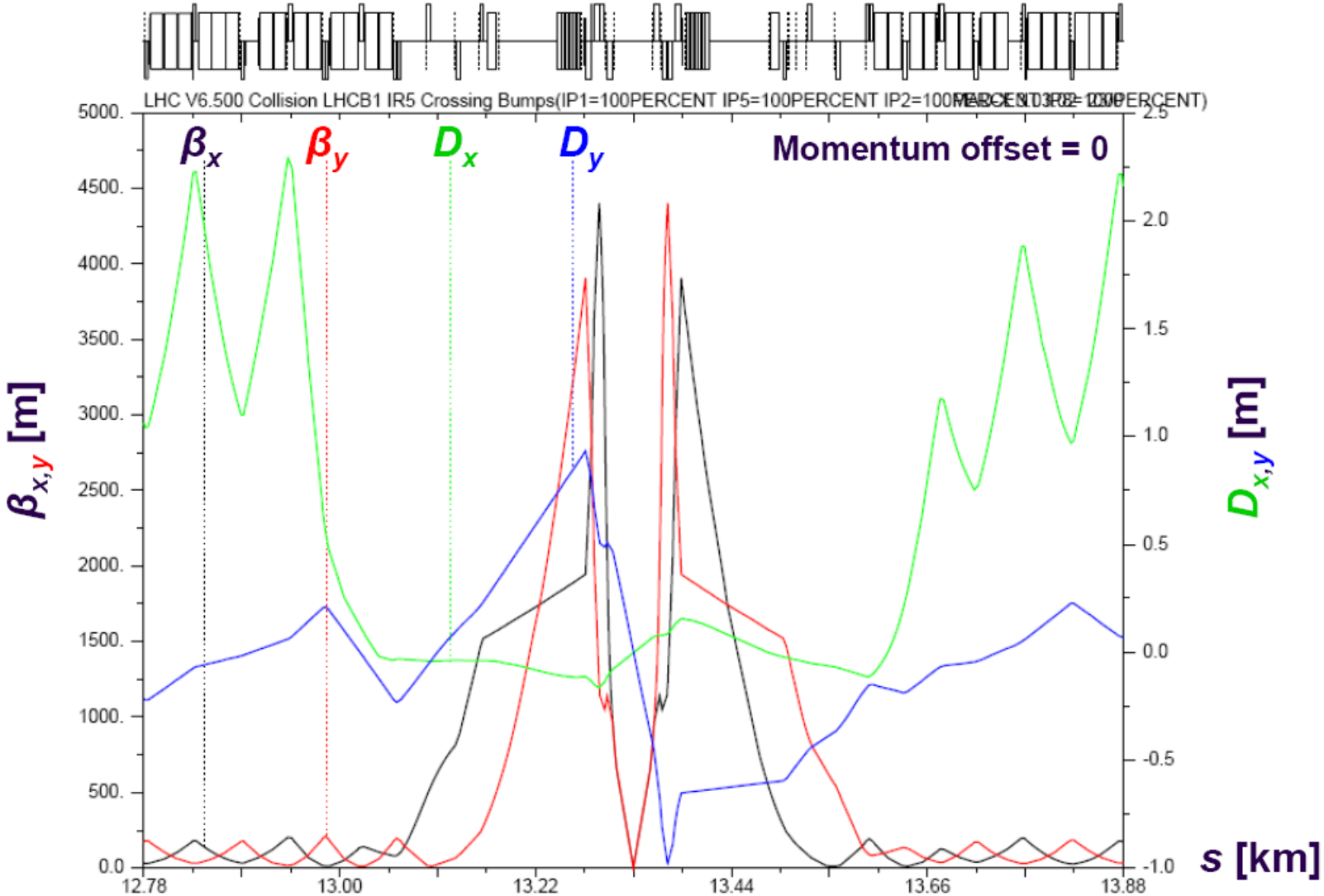

High-luminosity insertion

Preassembly of inner triplet

High-luminosity insertion
Inner triplet installed at LHC point 5

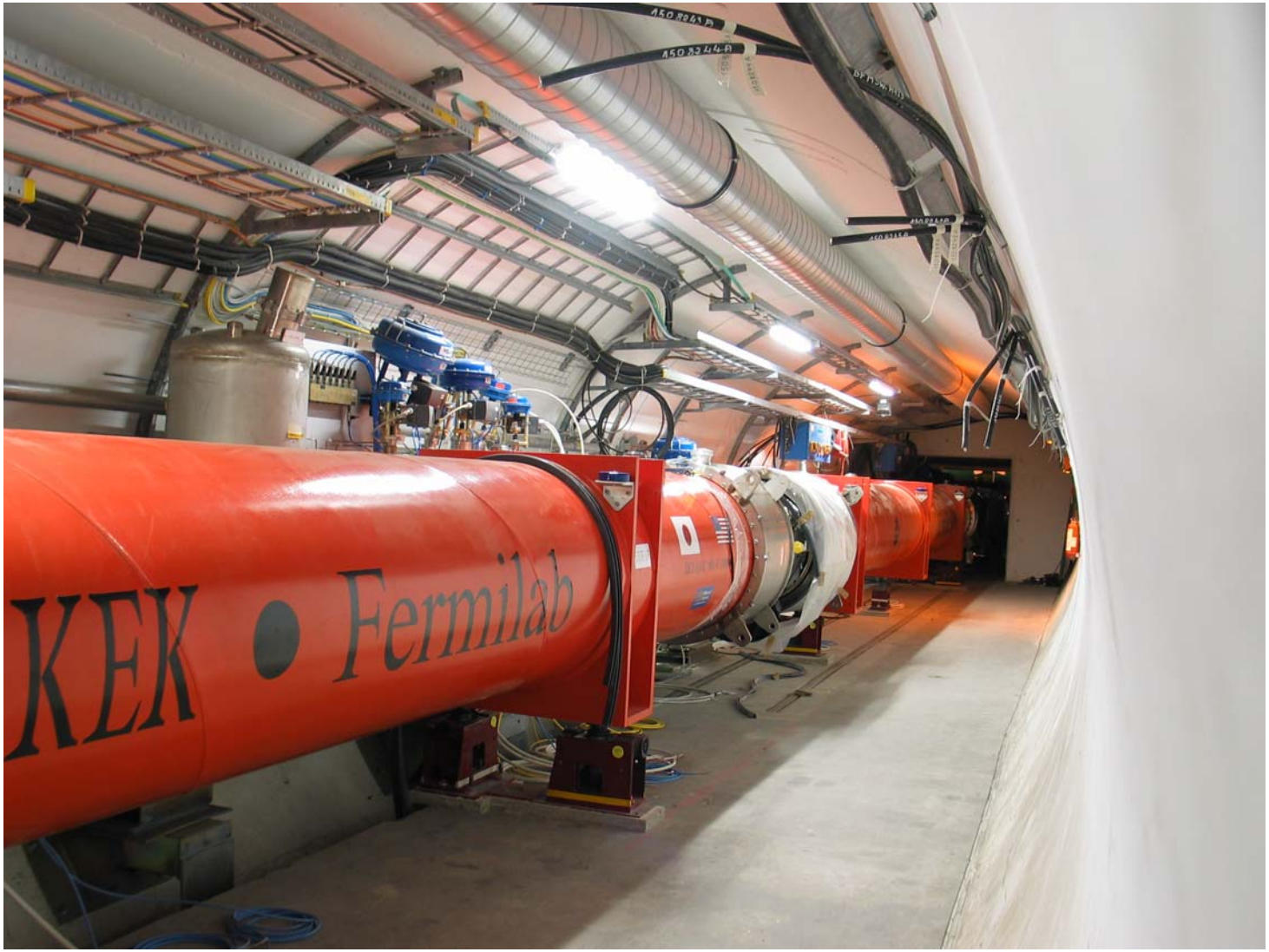

Luminosity lifetime

- Luminosity will decay with time due to degradation of beam intensity and emittance, by several processes
  - intra-beam scattering, i.e. multiple Coulomb scattering between particles in the same bunch
  - nuclear scattering of particles by residual gas molecules
  - the collisions themselves

~ 45 hours initially,
29 h as N_{total} and L decay

$$\tau_{nuclear} = \frac{N_{total}}{k\, L\, \sigma_{total}}$$

- Overall

$$\frac{1}{\tau_L} = \frac{1}{\tau_{IBS}} + \frac{2}{\tau_{gas}} + \frac{1}{\tau_{nuclear}}$$

~ 15 h, at least one fill per day

~ 80 h

~ 100 h, must be large w.r. to other processes

~ 29 h

Contents

- The LHC in a nutshell
- Performance
  - Energy
  - Luminosity
  - Collective effects
  - Dynamic aperture
- Technology
  - Superconducting magnets
  - Powering and protection
  - Cryogenics
  - Vacuum
- Project management

Beam impedance

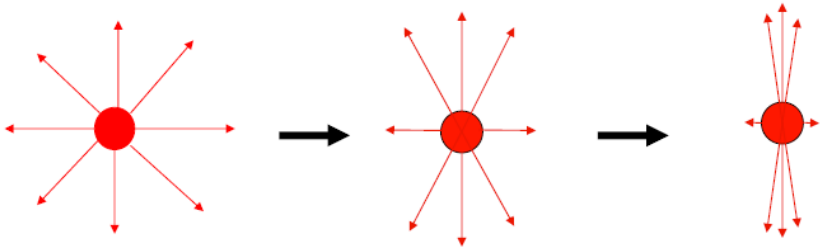

Perfect conductor

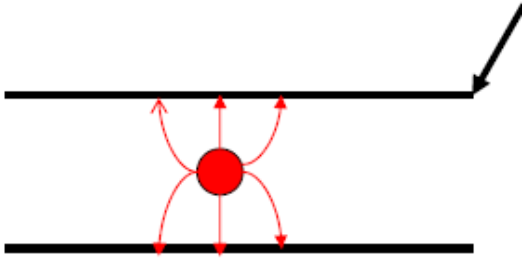

In case of resistive wall or change of cross-section, there is an interaction between the (charged) beam and the wall

$\Rightarrow$ energy dissipation (heating)

$\Rightarrow$ beam instabilities

This interaction can be described by an impedance $Z(\omega)$

Resistive wall or change of cross-section

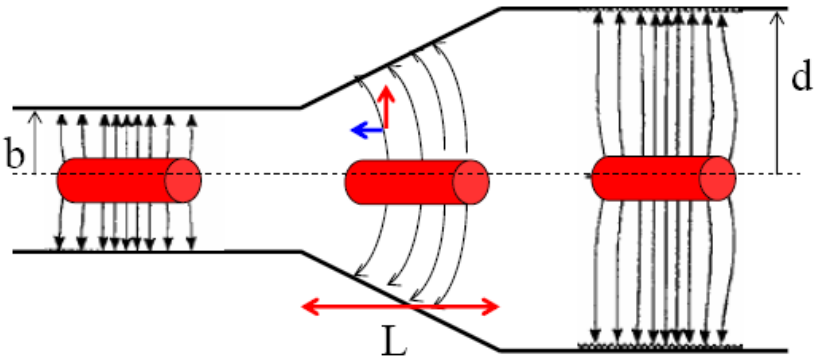

Instability driven by the chamber wall

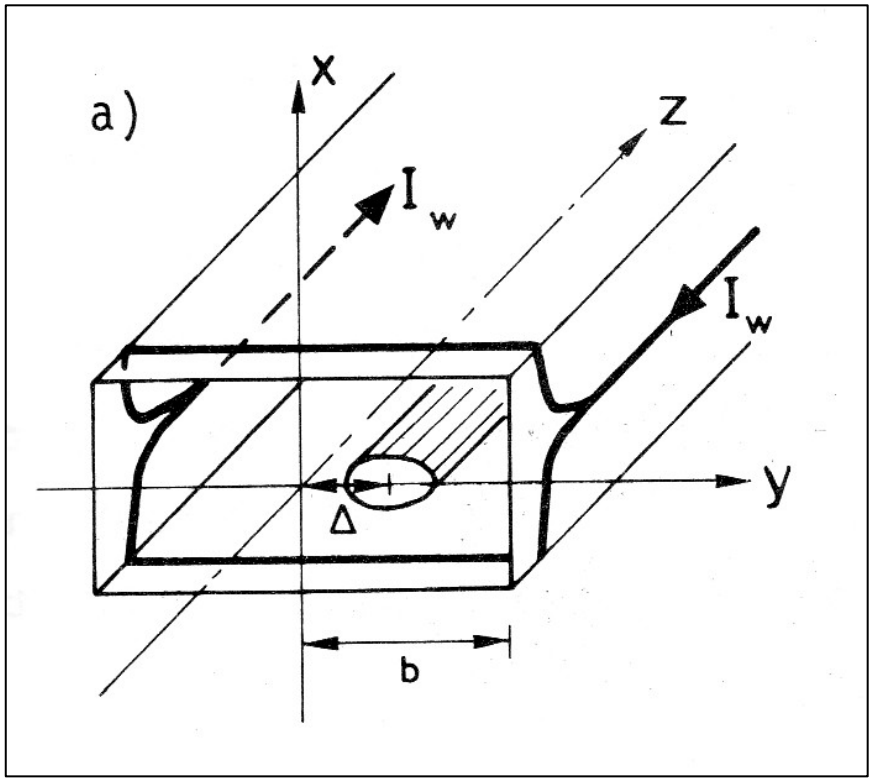

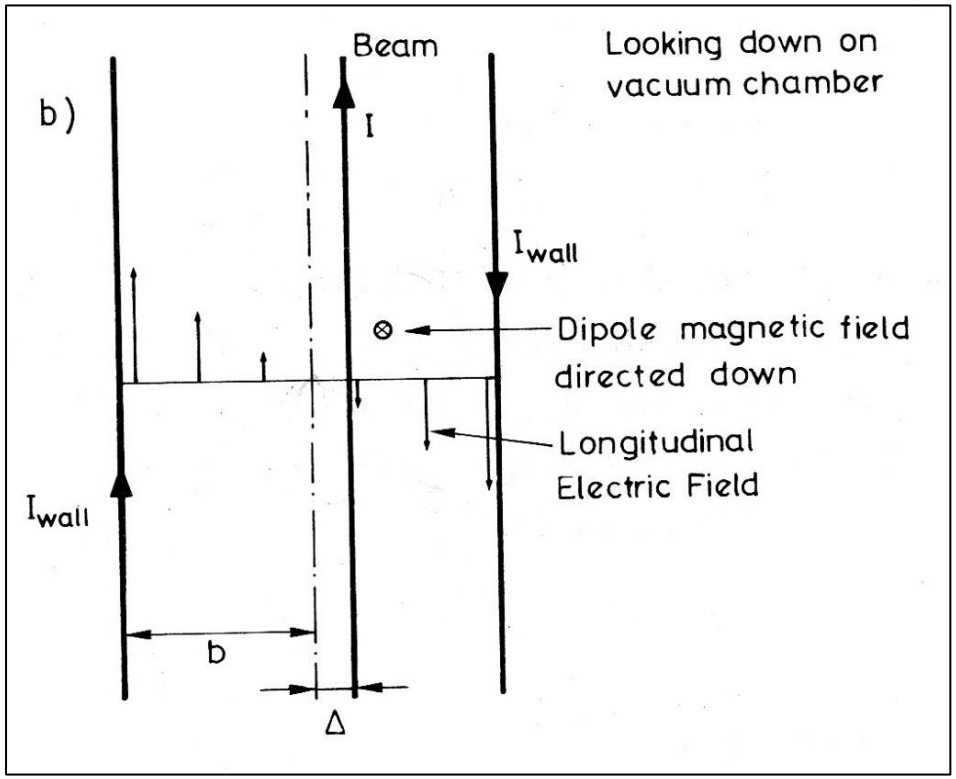

Low transverse impedance for beam stability

- Transverse impedance

  $Z_T(\omega) \sim \rho\, r / \omega\, b^3$

  ρ wall electrical resistivity

  r average machine radius

  b half-aperture of beam pipe

- Transverse resistive-wall instability
  - dominant in large machines
  - must be compensated by beam feedback, provided growth of instability is slow enough (~ 100 turns)
  - maximize growth time $\tau \sim 1/Z_T(\omega)$ i.e. reduce $Z_T(\omega)$

  $\Rightarrow$ *for a large machine with small aperture, low transverse impedance is achieved through low ρ, i.e. low-temperature wall coated with >0.05 mm copper*

Copper-coated beam screens

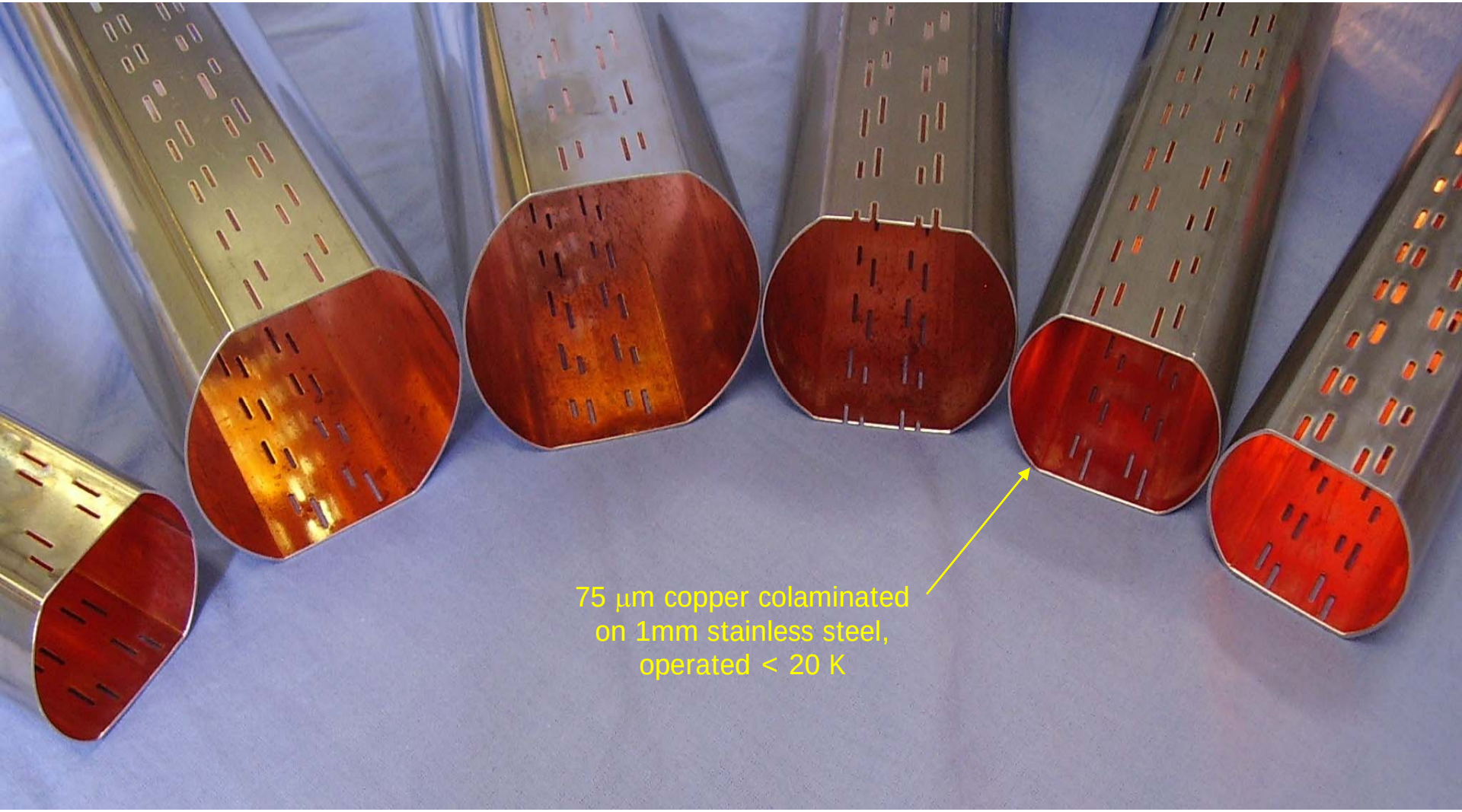

« Plug-in modules » for electrical continuity of beam pipe

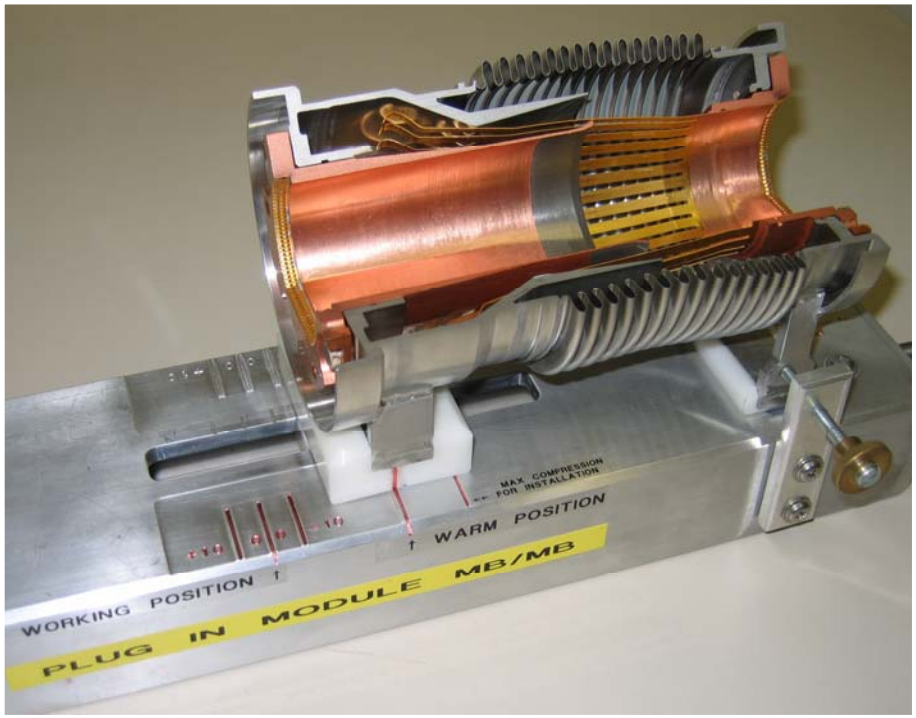

At room temperature

At cryogenic temperature

Synchrotron radiation

- Charged particle beams bent in a magnetic field undergo centripetal acceleration and emit e-m radiation
- When beams are relativistic, radiation is emitted in a narrow cone

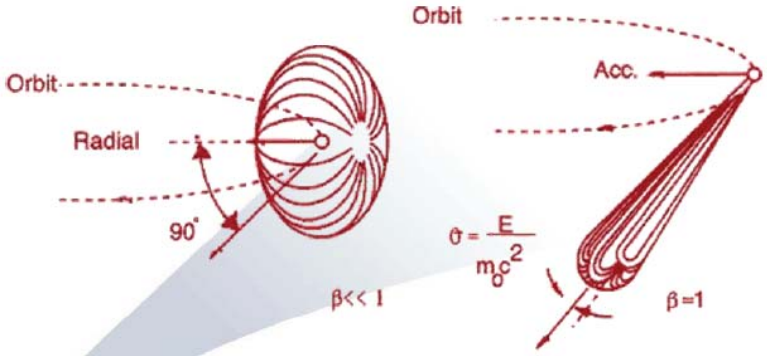

- Radiated power

Free space impedance

$$P_{syn} = \frac{Z_0 \, e^2 \, c \, \gamma^4}{3 \, R} N_b \, n_b \, f_{rev}$$

~ beam current

Bending radius

- Critical photon energy

$$u_c = \frac{3}{2} \hbar \, c \, \frac{\gamma^3}{R}$$

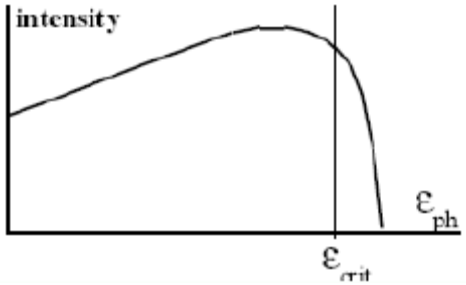

Synchrotron radiation

parameter	450 GeV	7 TeV
total power / beam	0.066 W	3886 W
energy loss per turn	0.11 eV	6.7 keV
average photon flux per metre and second	0.4×10^{16}	6.8×10^{16}
photon critical energy	0.01 eV	43.13 eV
longit. emittance damping time	5.5 yr	12.9 h
transv. emittance damping time	11 yr	26 h

large at low T

UV, easy to screen

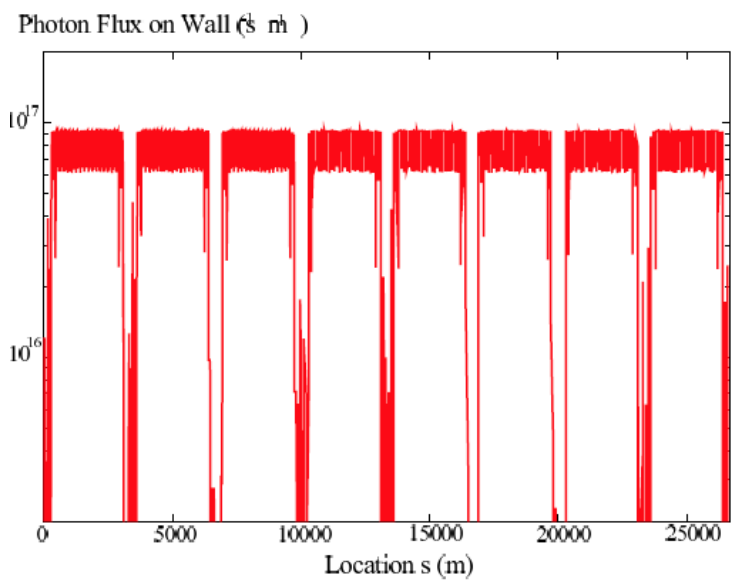

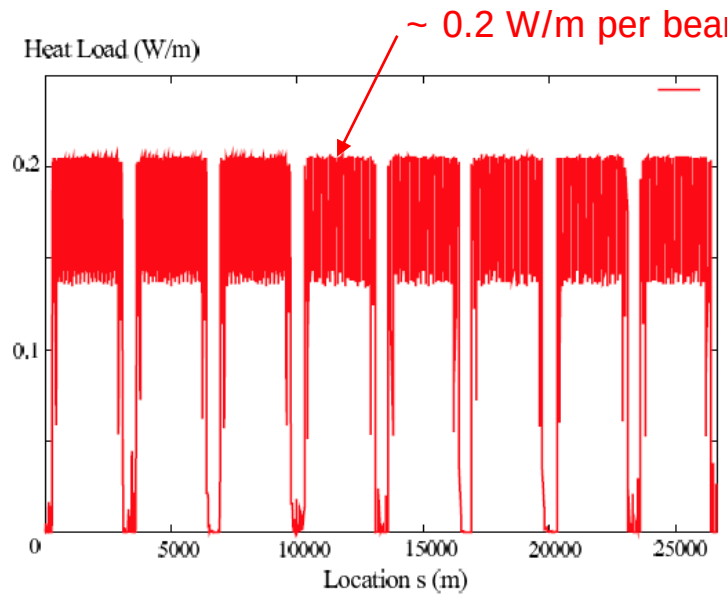

COP of cryogenic refrigeration & beam screen

Intercepting beam-induced heating at higher temperature

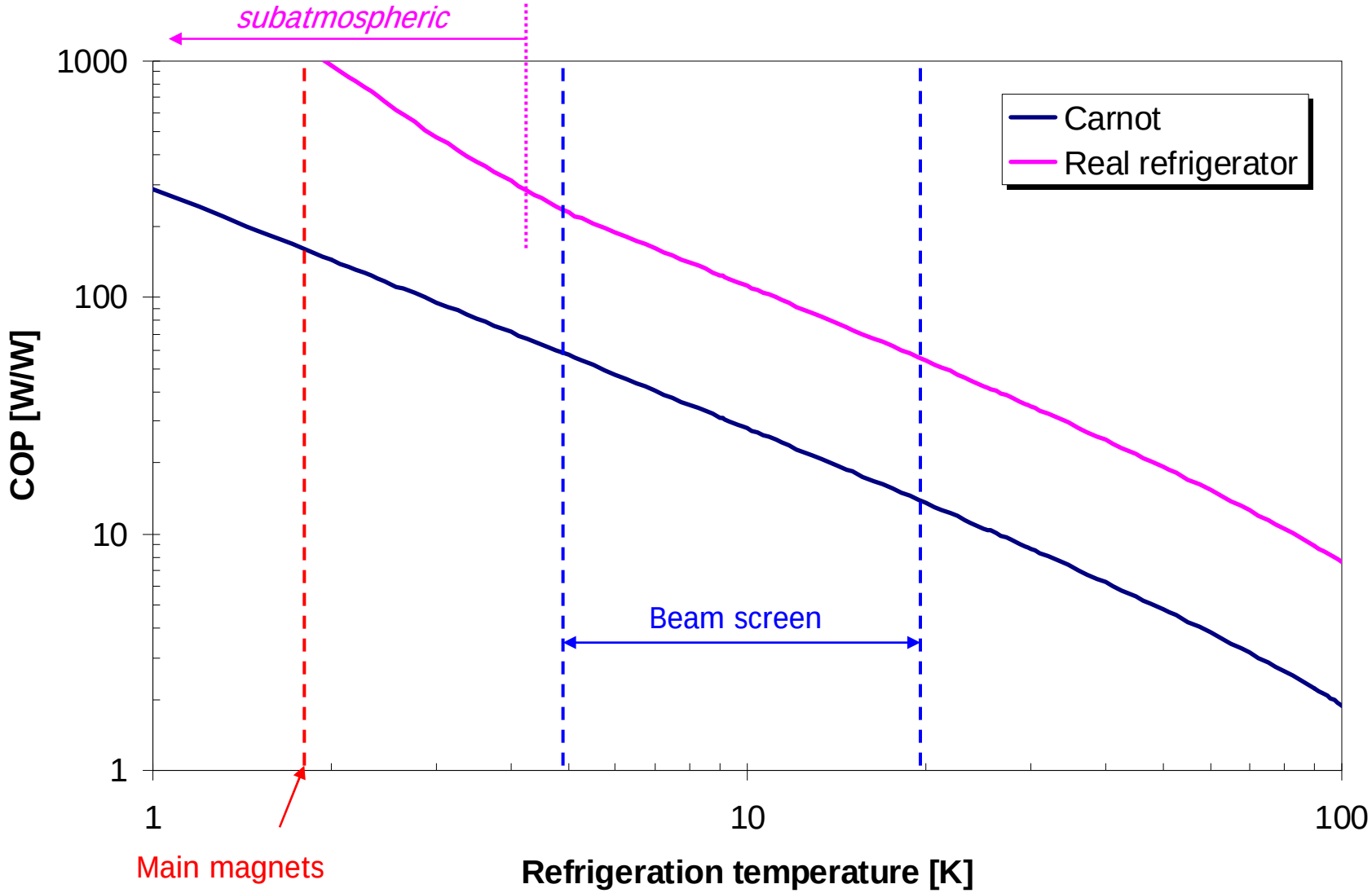

The electron cloud effect

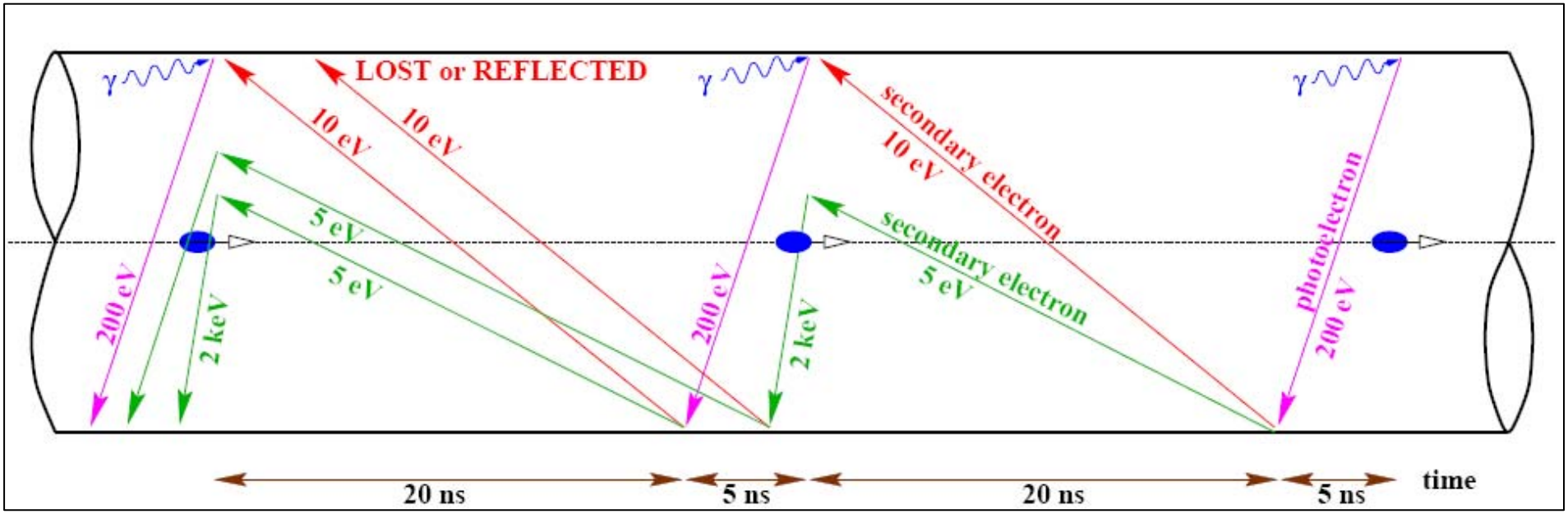

Simulated build-up of electron cloud

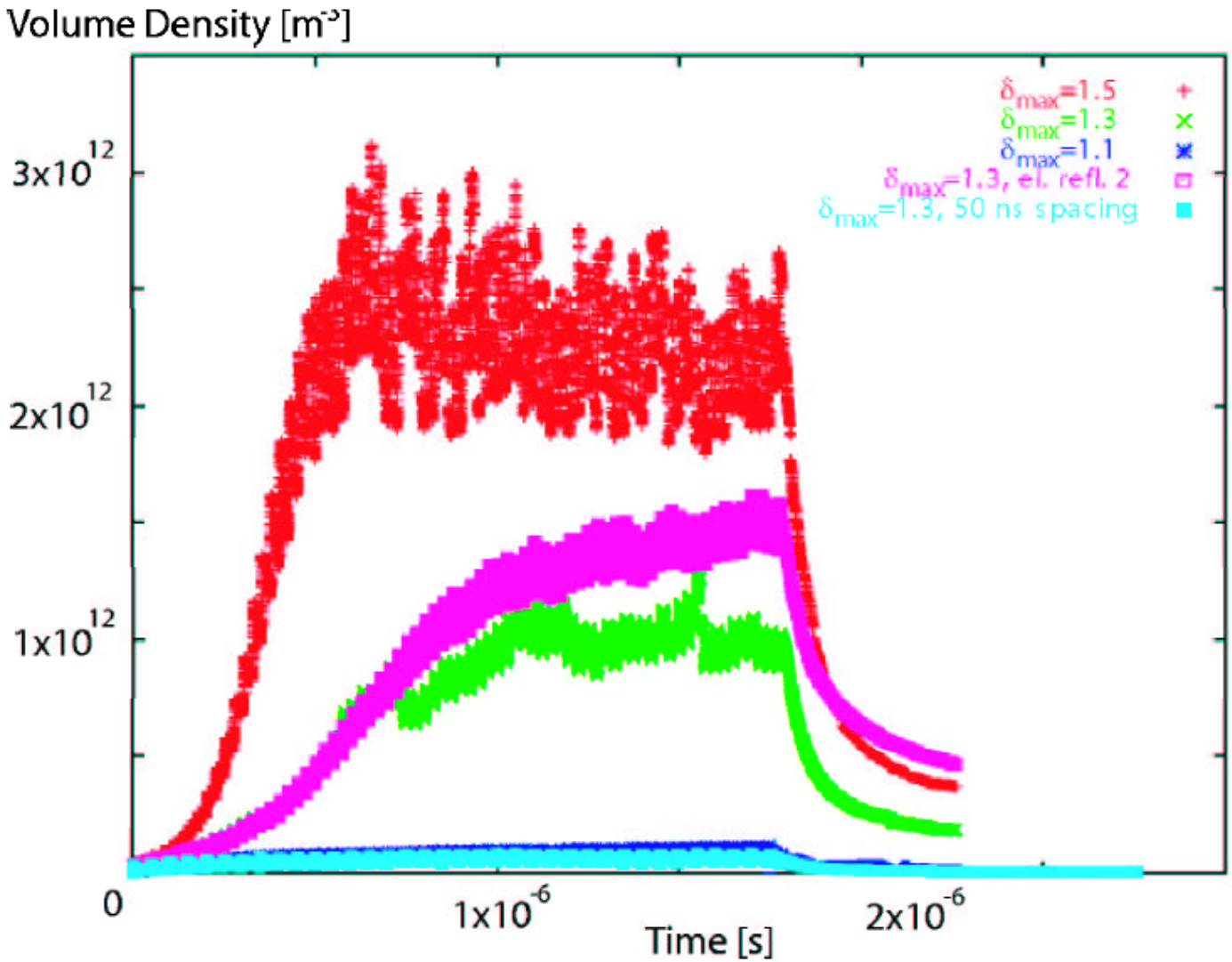

Heat load by electron cloud as a function of SEY

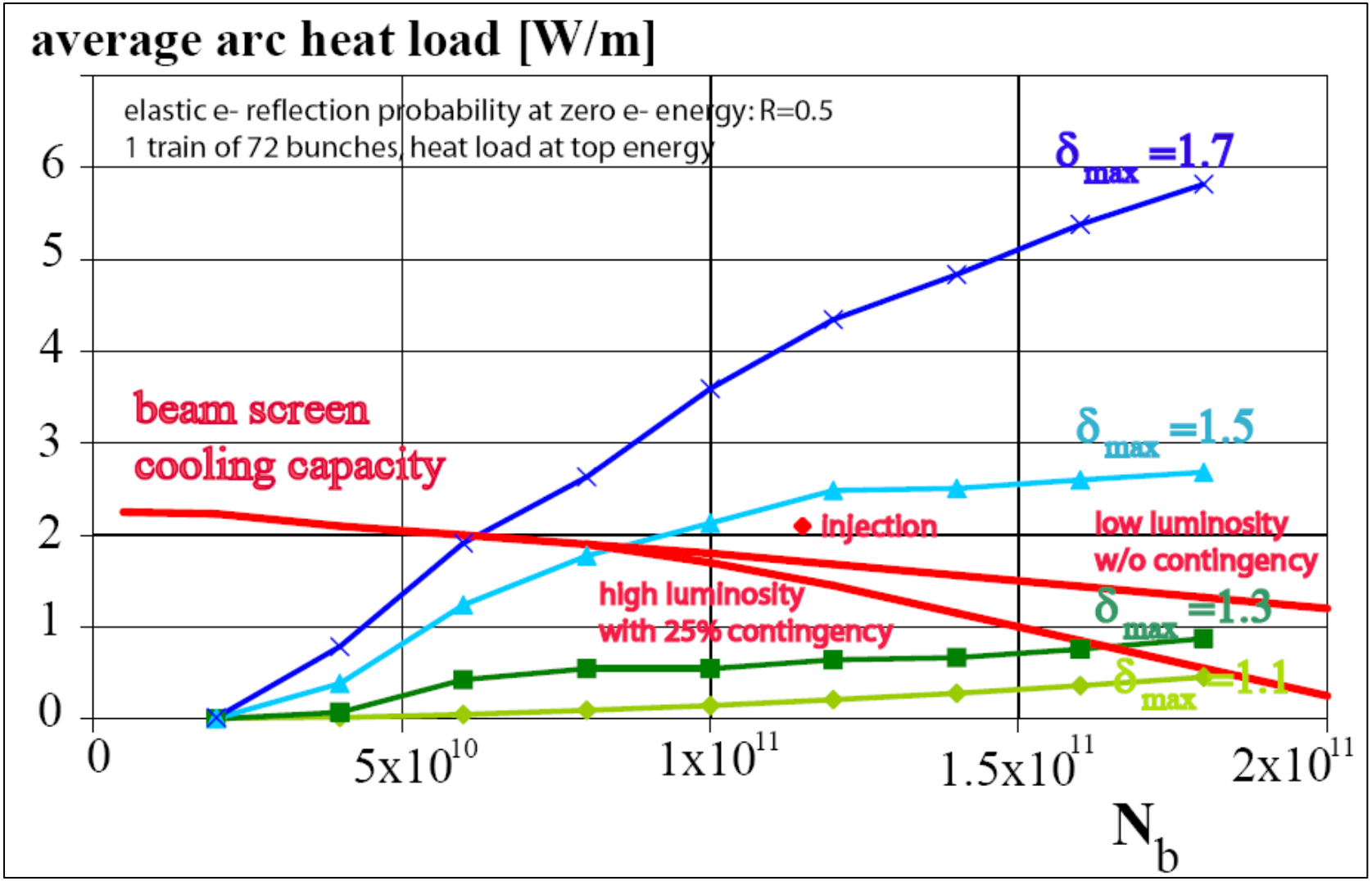

The beam screen

A multi-function component required by beam physics

- Interception of beam-induced heat loads at 5-20 K (supercritical helium)
- Shielding of the 1.9 K cryopumping surface from synchrotron radiation (pumping holes)
- High-conductivity copper lining for low beam impedance
- Low-reflectivity sawtooth surface at equator to reduce photoemission and electron cloud

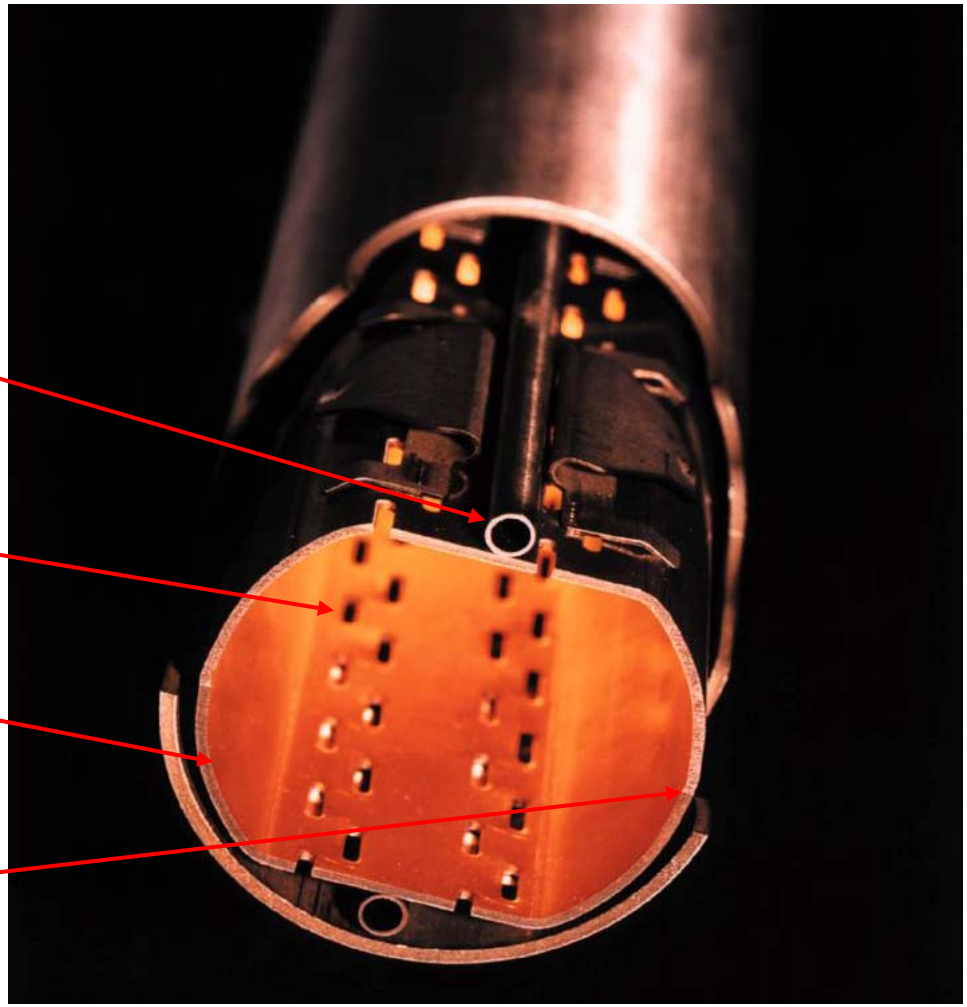

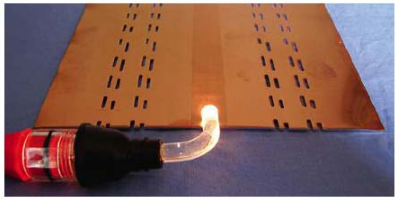

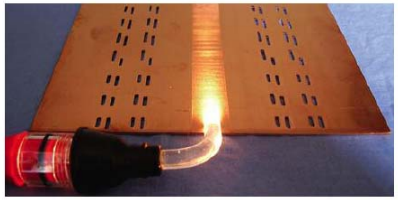

Contents

- The LHC in a nutshell
- Performance
  - Energy
  - Luminosity
  - Collective effects
  - Dynamic aperture
- Technology
  - Superconducting magnets
  - Powering and protection
  - Cryogenics
  - Vacuum
- Project management

Field quality in superconducting magnets

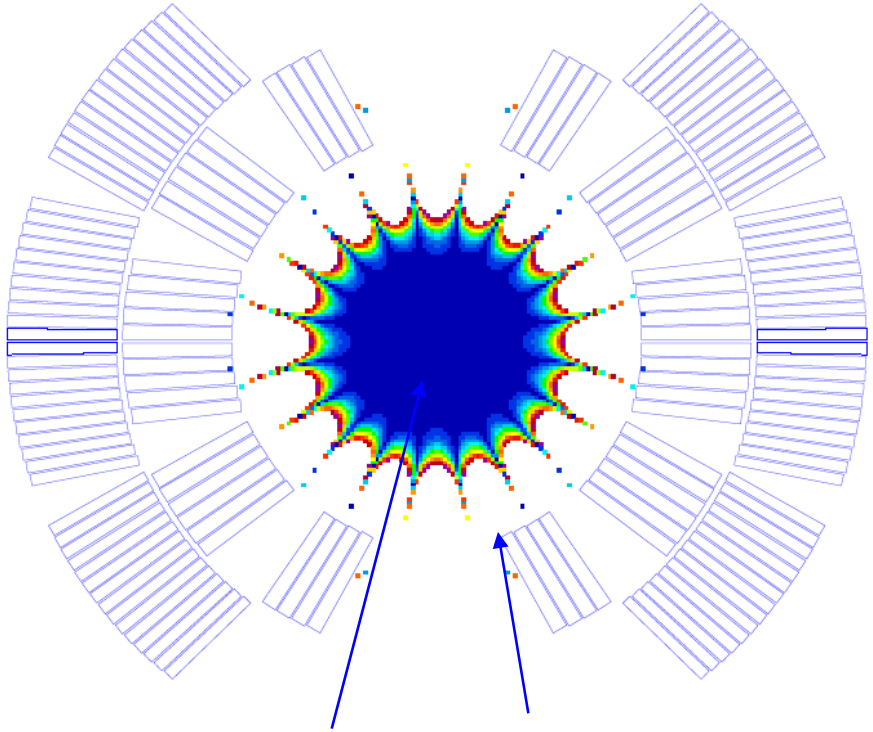

« Good field » region
$\Delta B/B < 10^{-4}$

Magnet
« aperture »

$$B_y + iB_x = B_1 \sum_{n=1}^{\infty} (b_n + ia_n) \left(\frac{x+iy}{r_{ref}} \right)^{n-1}$$

- In superconducting magnets, the field quality is determined by the positioning precision of a finite number of conductors and not by the geometry of the iron yoke, so it can never be as good as in conventional "iron-dominated" magnets
- As a consequence, the « good field » region is substantially smaller than the magnet aperture
- Dynamic aperture = aperture inside which particle orbits are stable
- Dynamic aperture estimated by computer « tracking » of particle orbits around virtual machines with distributed random and systematic imperfections
- Tracking results are used to define maximum systematic and random deviations of each field multipole

Dynamic aperture from tracking simulations

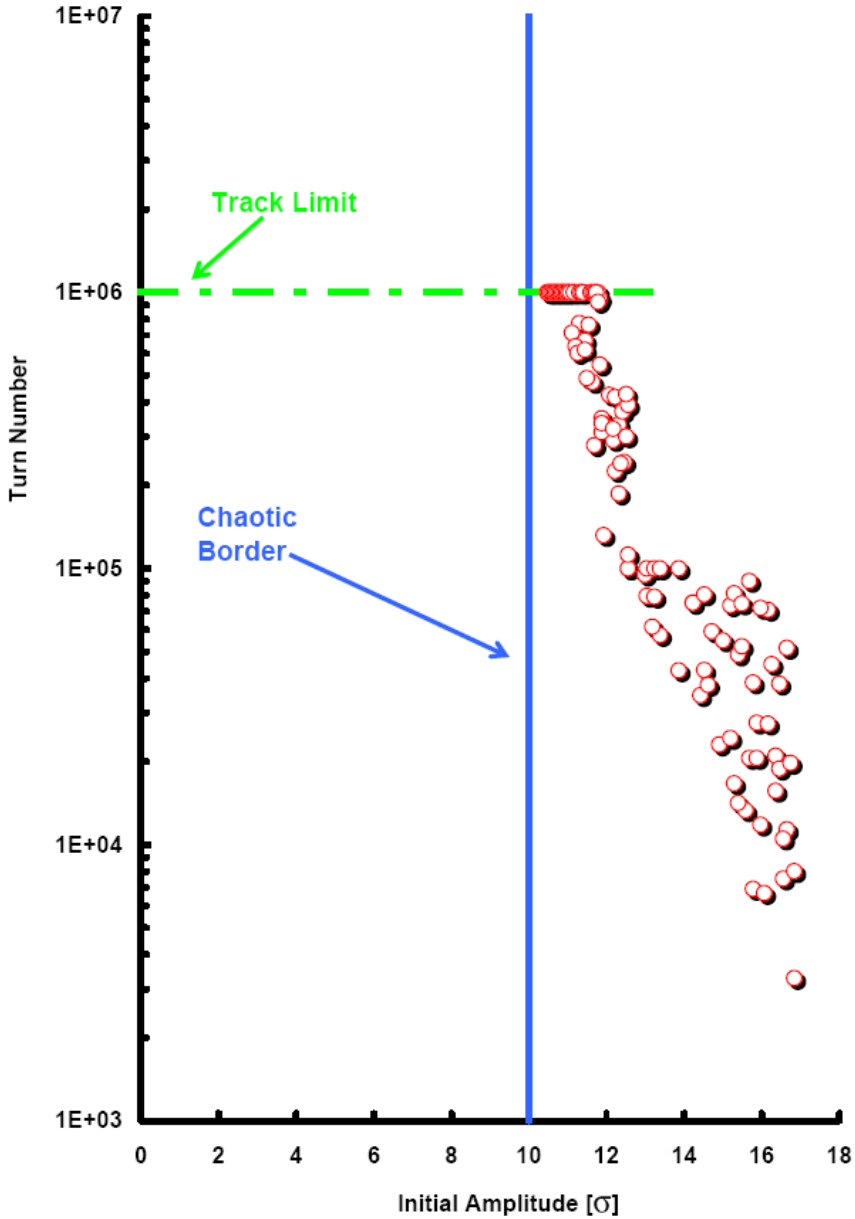

From tracking simulations to real d.a.

Source or Uncertainty	Impact	D.A. in σ
Target for tracking 10^5 turns		12
Finite mesh size	-5%	
Linear Imperfections[a]	-5%	
Amplitude ratio x_i/y_i plane	-5%	
Extrapolation to 4 10^7 turns	-7%	9.4
Time dependent multipoles	-10%	
Ripple	-10%	7.5
safety margin	-20%	6.0

Schematic layout of one LHC cell (23 periods per arc)

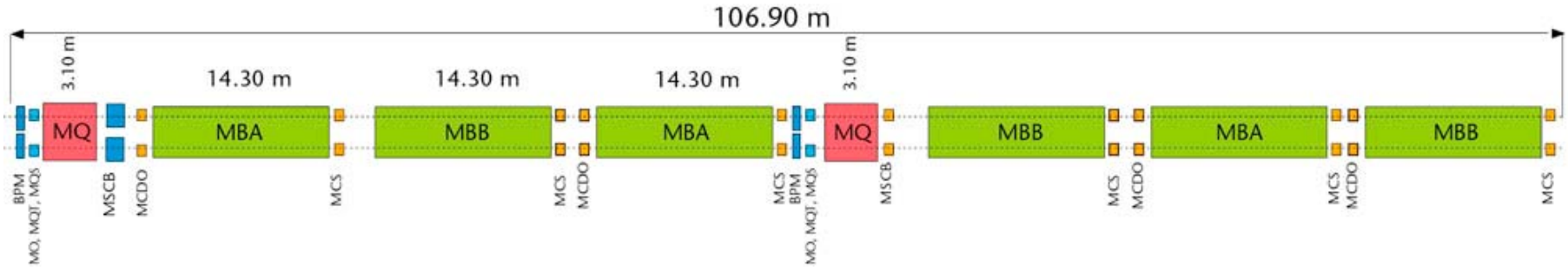

MQ: Lattice Quadrupole
MO: Landau Octupole
MQT: Tuning Quadrupole
MQS: Skew Quadrupole
MSCB: Combined Lattice Sextupole (MS) or skew sextupole (MSS) and Orbit Corrector (MCB)
BPM: Beam position monitor
MBA: Dipole magnet Type A
MBB: Dipole magnet Type B
MCS: Local Sextupole corrector
MCDO: Local combined decapole and octupole corrector

The LHC magnet zoo

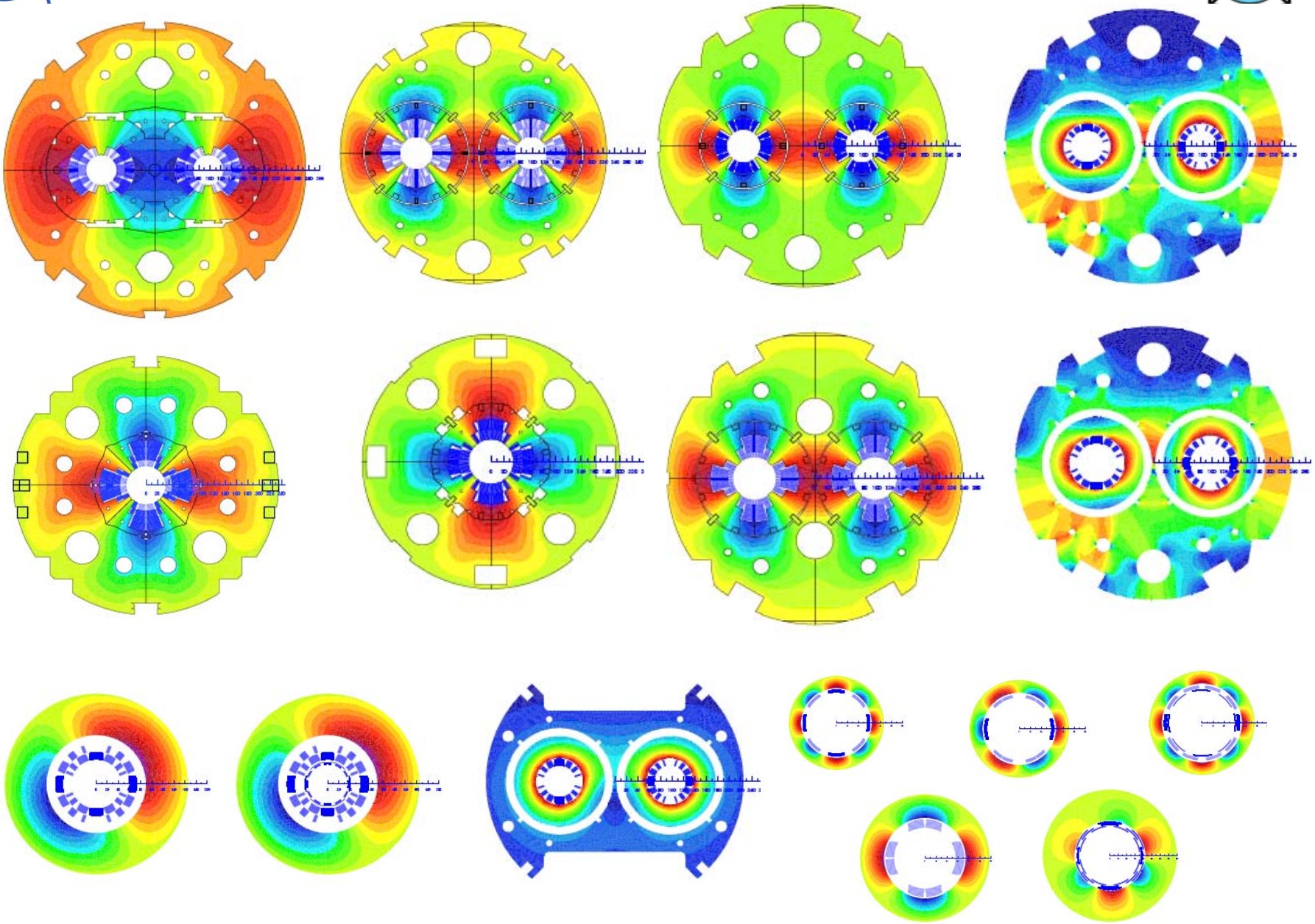

Contents

- The LHC in a nutshell
- Performance
  - Energy
  - Luminosity
  - Collective effects
  - Dynamic aperture
- Technology
  - Superconducting magnets
  - Powering and protection
  - Cryogenics
  - Vacuum
- Project management

Superconducting accelerator magnets

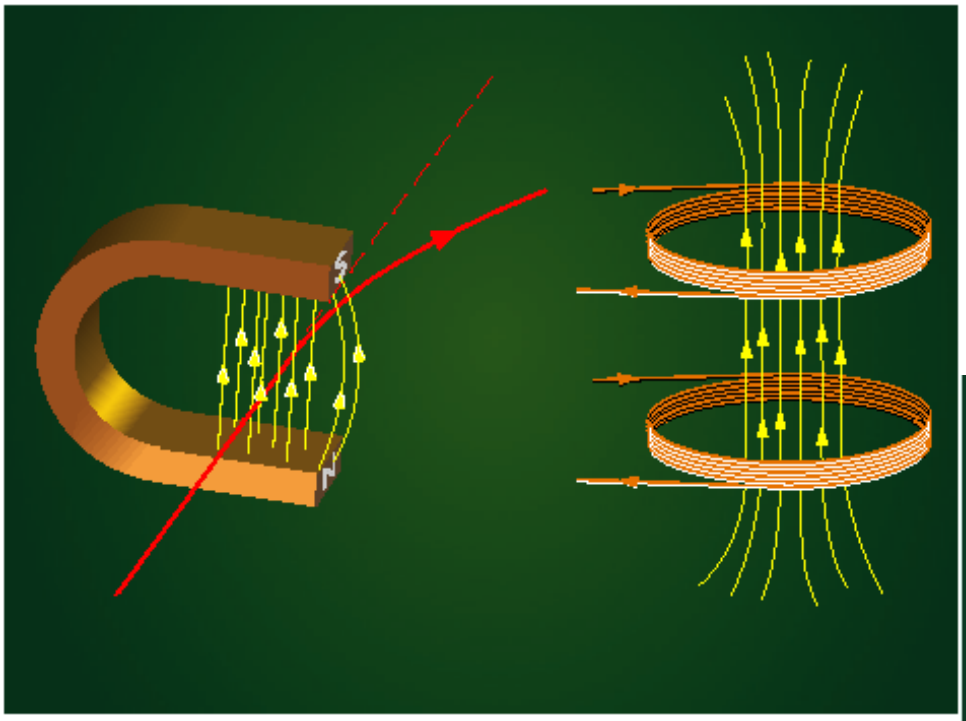

In a superconducting magnet, the field level and geometry is basically given by the current distribution in the coils

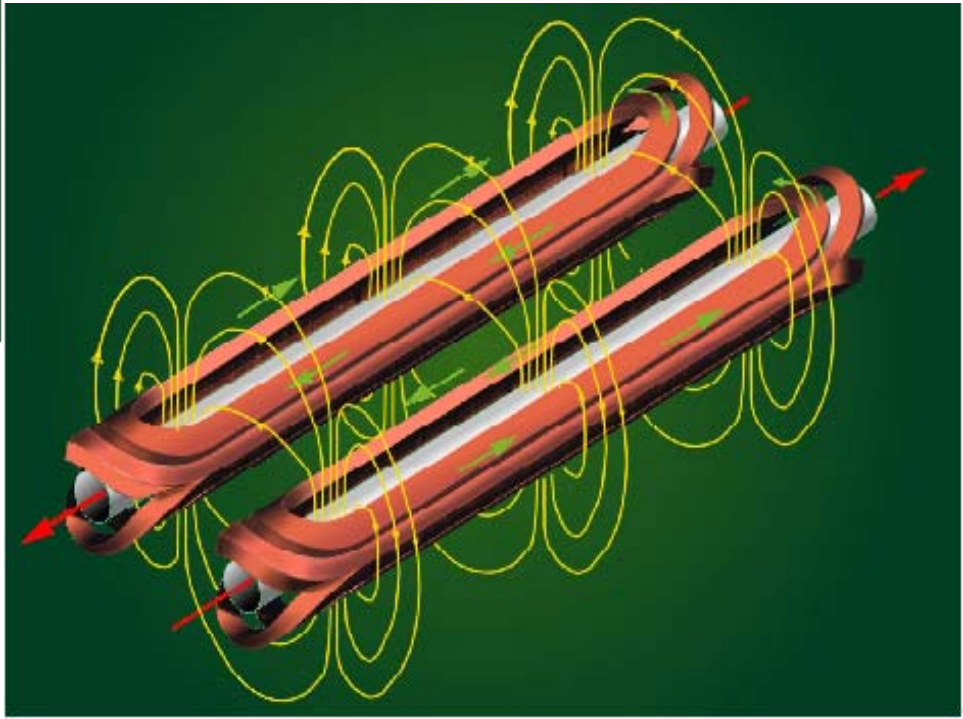

To match the geometry of the beam tubes, the coils are saddle-shaped & elongated

In the LHC, two sets of coils create opposite fields in the neighbouring apertures

Magnetic field inside conducting cylinder

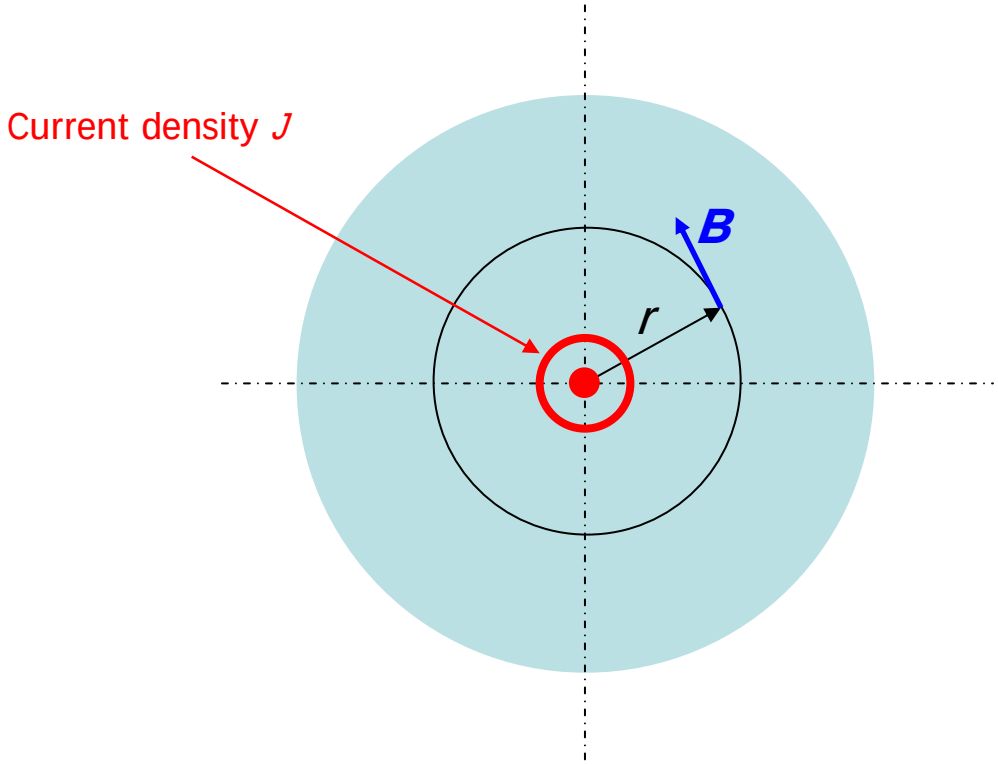

From Ampere's theorem

$$\oint B(r)\, ds = \mu_0\, I(r)$$

Field inside conductor

$$B(r) = \mu_0\, J\, r/2$$

Current distribution for producing dipole field

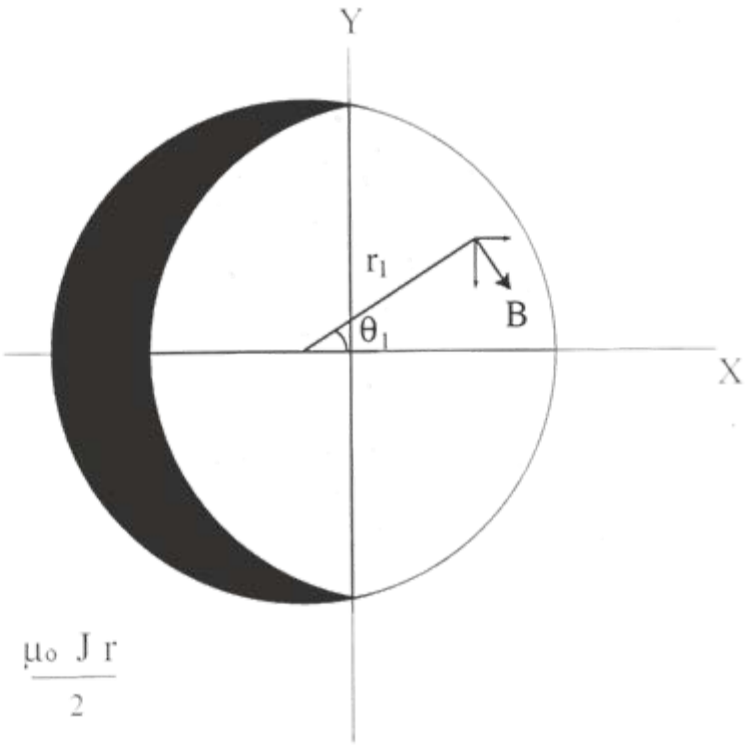

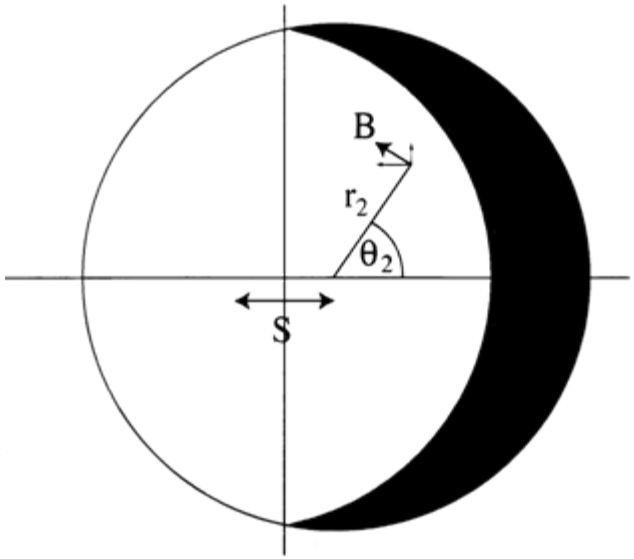

$$B = \frac{\mu_0 J r}{2}$$

$$B_Y = \frac{\mu_0 J}{2} \left\{ - r_1 \cos \theta_1 + r_2 \cos \theta_2 \right\} = - \frac{\mu_0 J s}{2}$$

$$B_X = \frac{\mu_0 J}{2} \left\{ r_1 \sin \theta_1 - r_2 \sin \theta_2 \right\} = 0$$

Current distributions

Two intersecting ellipses with uniform current density generate uniform dipole and quadrupole fields ⇒ "**cos θ**" geometry

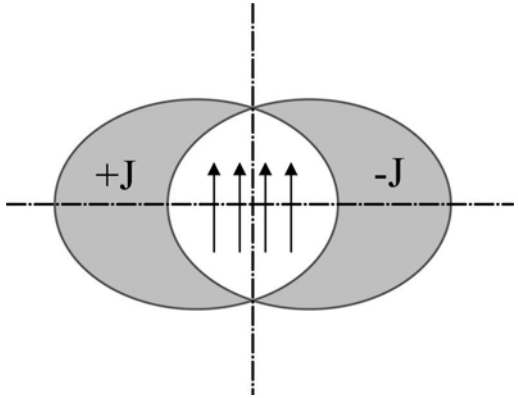

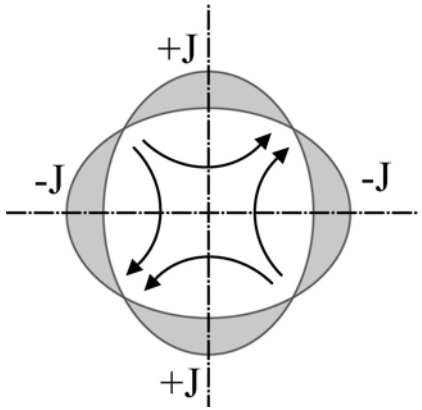

In practice, this can be approximated by current sheets, leading to "**block**" or "**layer**" coil designs

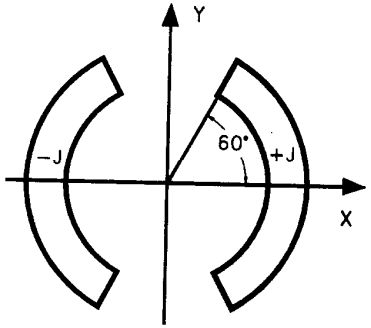

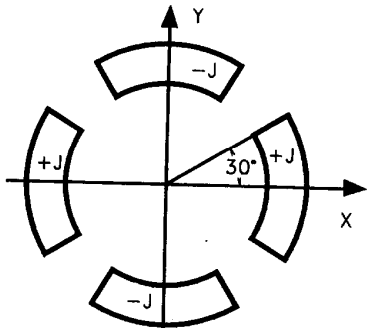

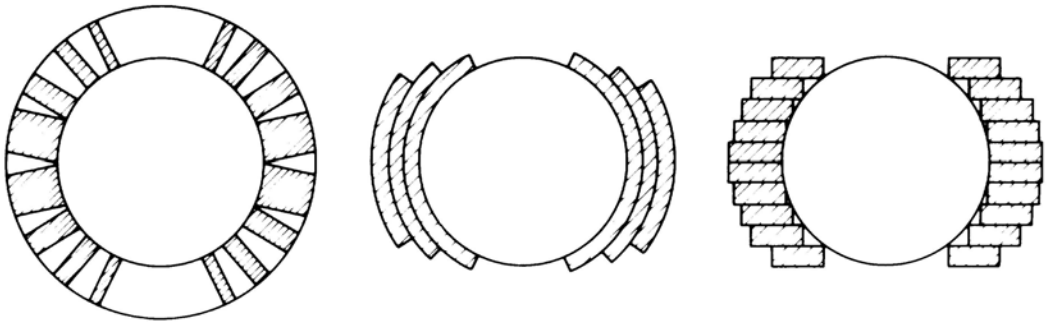

Field of single-layer dipole coil

Average current density in coil

$$B = \frac{\mu_0 \sqrt{3}}{\pi} \, j_{tech} \, w$$

Coil width

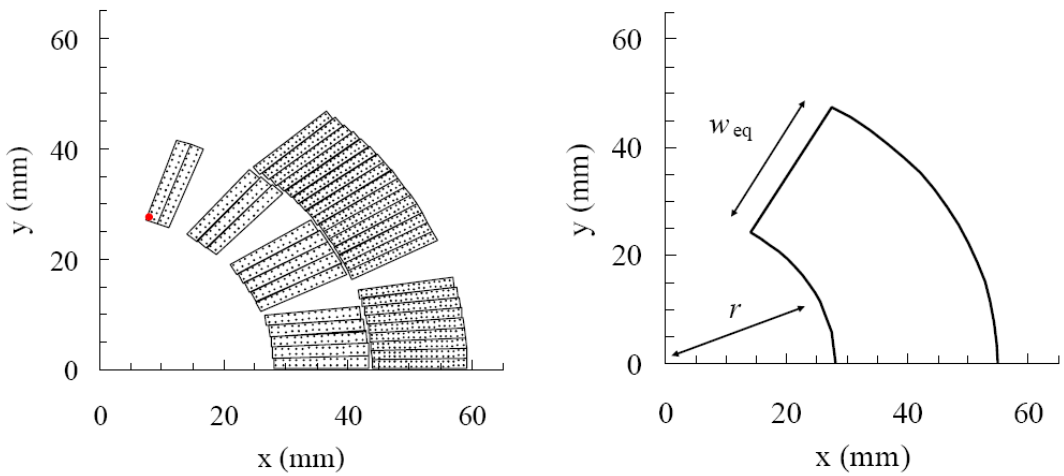

Typical critical lines of Nb-Ti superconductor

$$j_{Nb-Ti} \approx c\left(b - B\right)$$

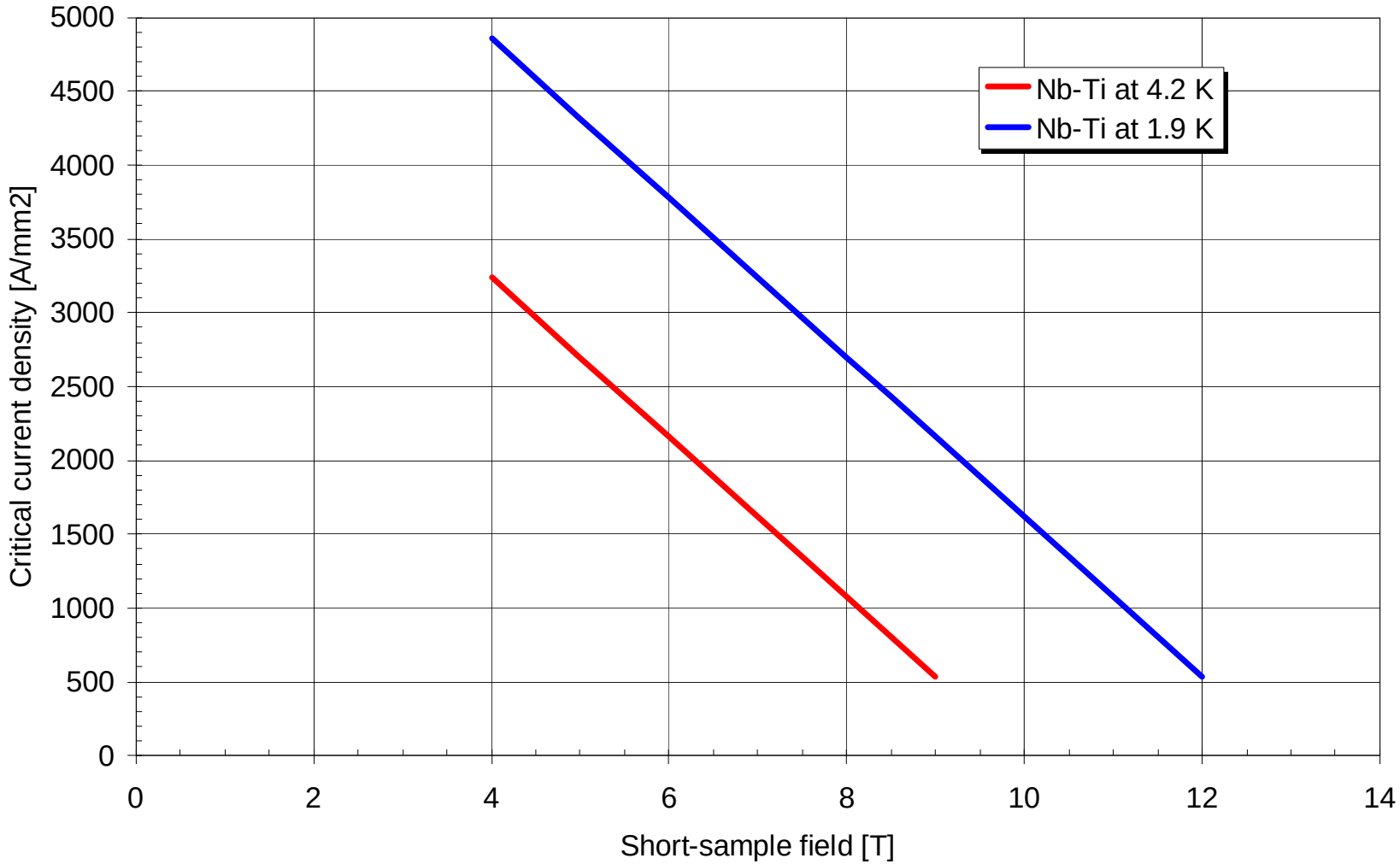

Superconducting cos θ dipoles in Nb-Ti
Coil width vs field

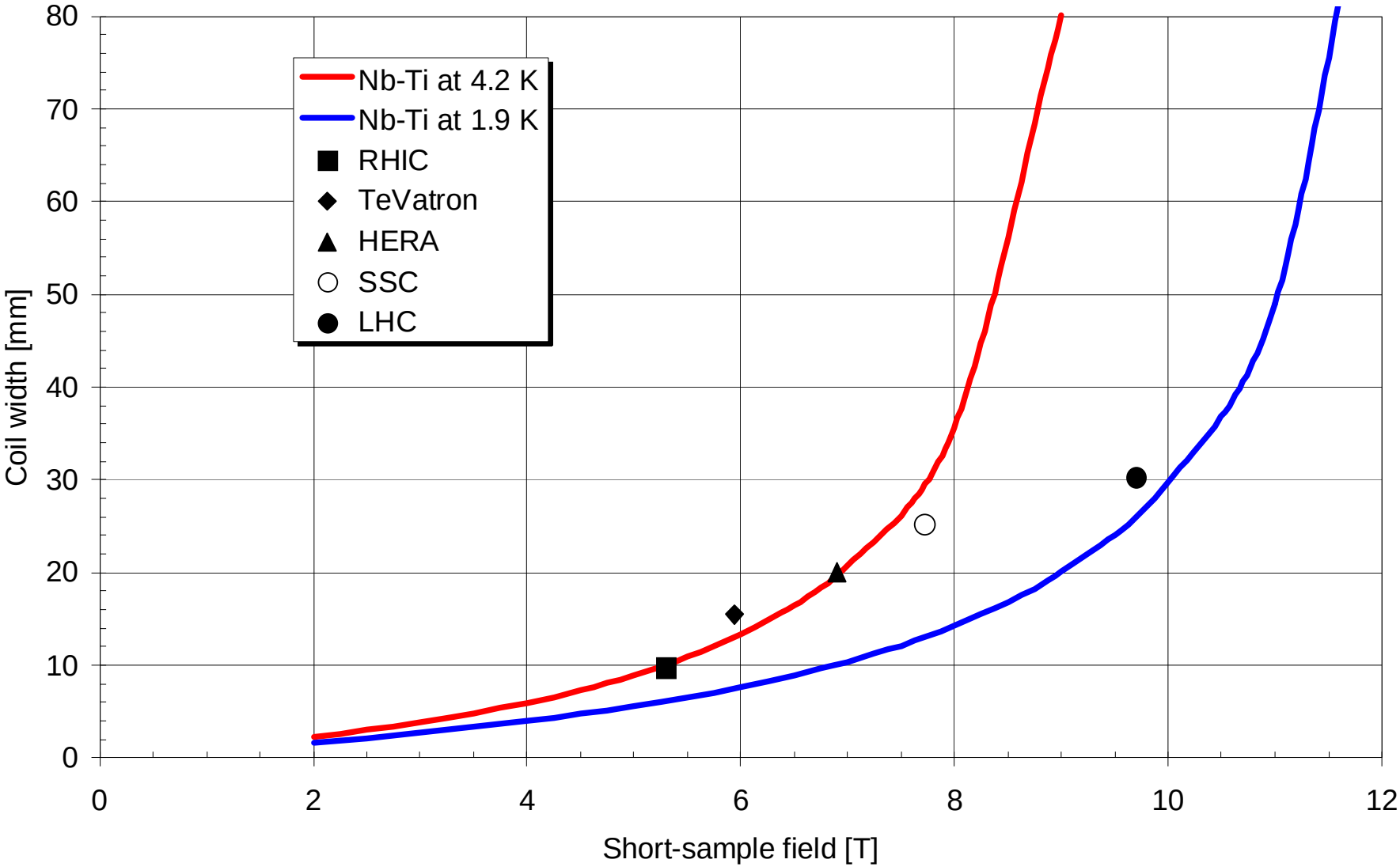

Superconducting cos θ dipoles in Nb-Ti
Coil cross-section vs field

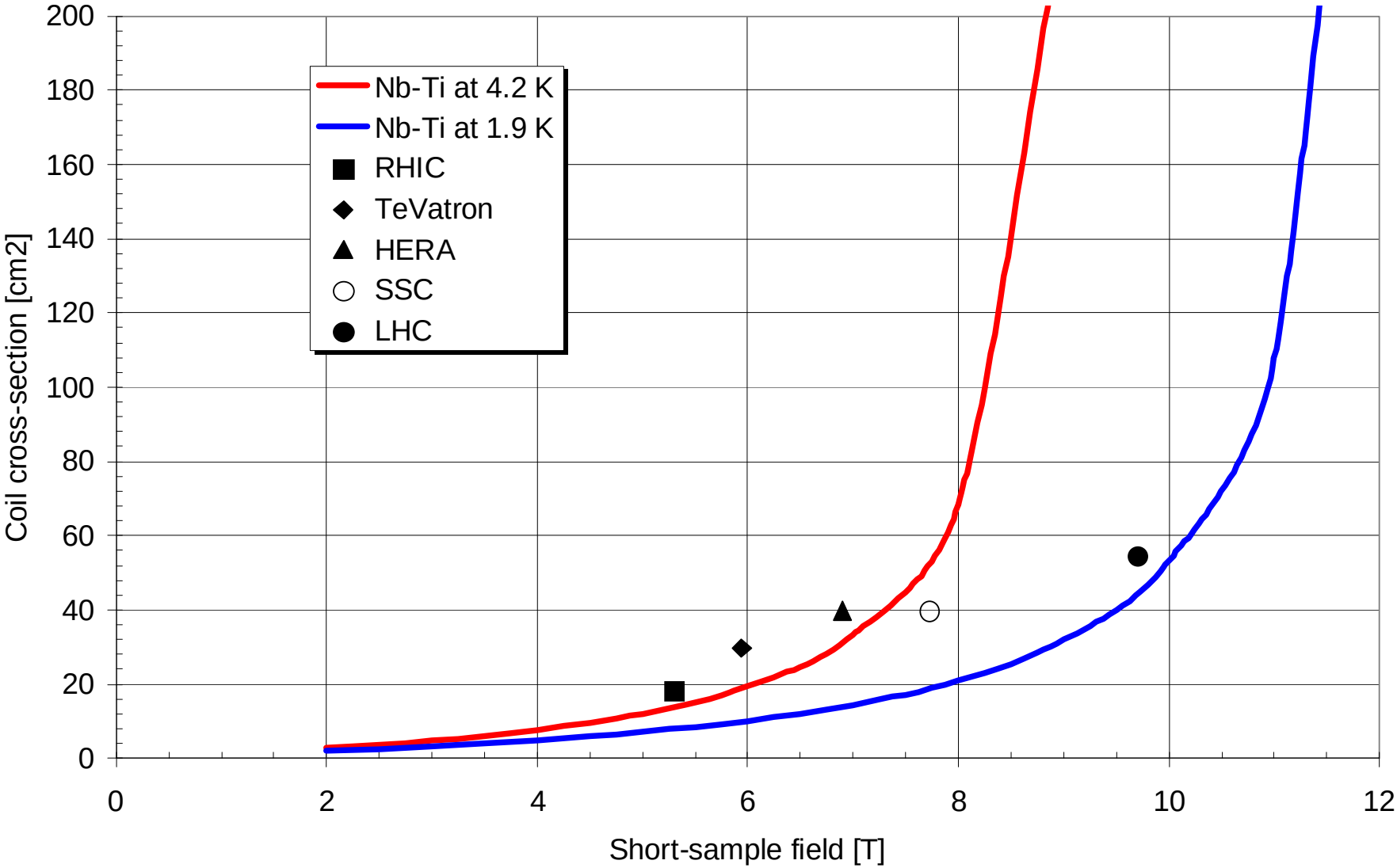

Load lines of LHC main dipole

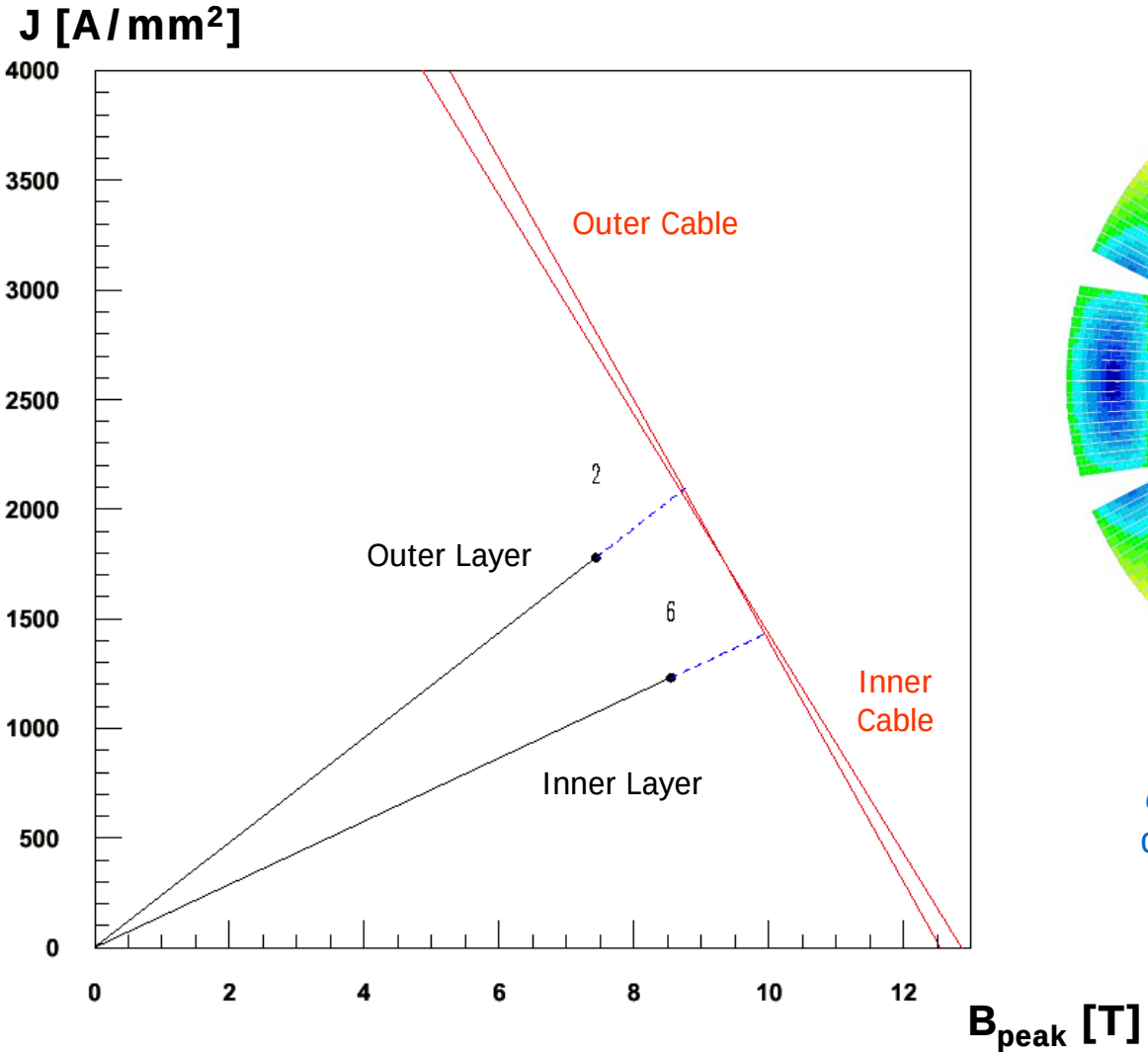

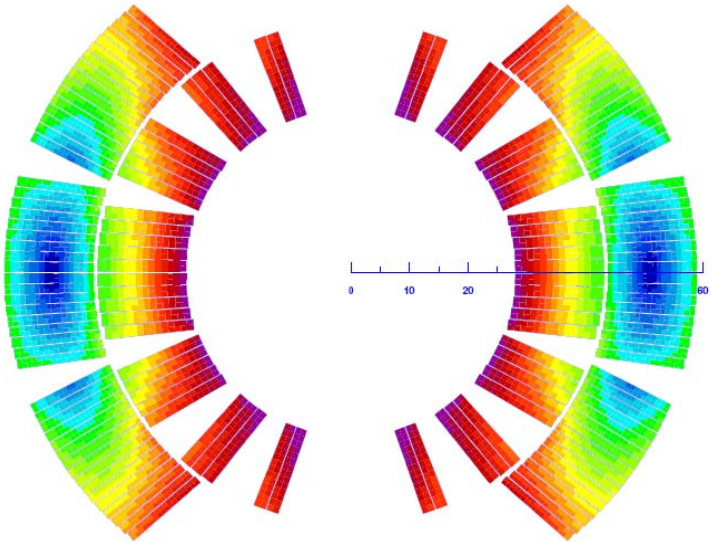

Current grading permits the outer cable, which sees a lower field, to operate at higher current density

Inter-layer splice in graded coil

Superconducting cable with etched strands showing Nb-Ti filaments

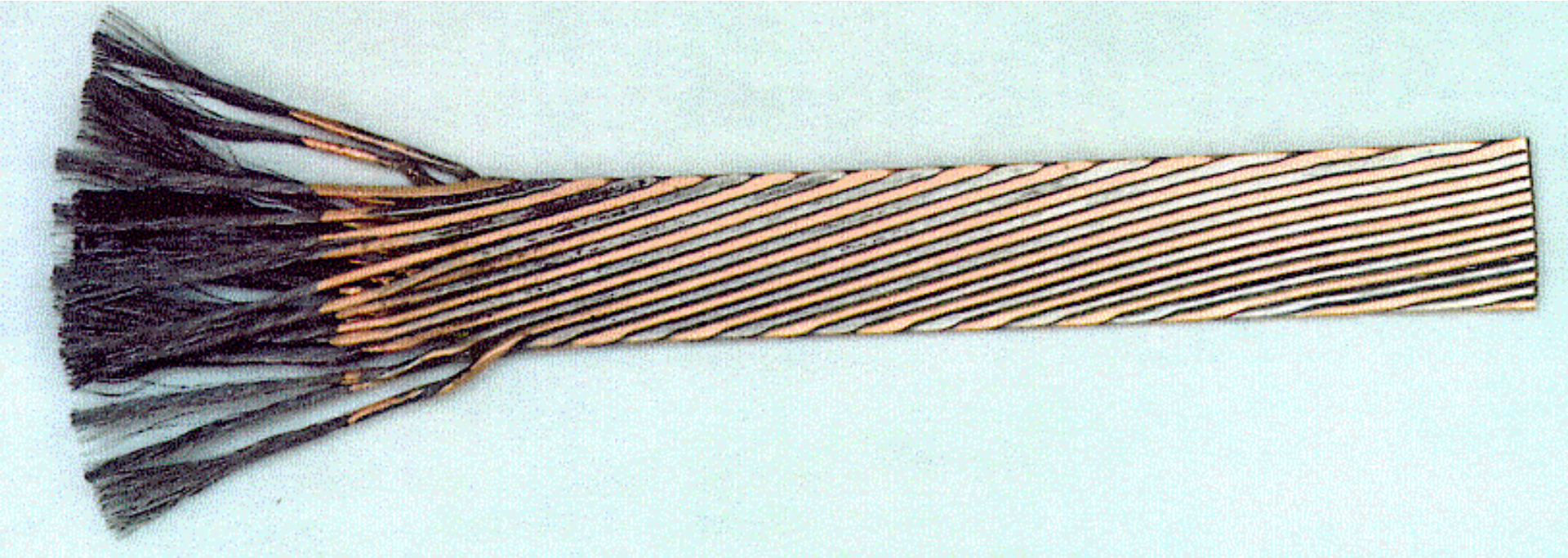

7500 km of superconducting cables with tightly controlled properties

	Inner Cable	Outer Cable
Number of strands	28	36
Strand diameter	1.065 mm	0.825 mm
Filament diameter	7 µm	6 µm
Number of filaments	~ 8900	~ 6520
Cable width	15.1 mm	15.1 mm
Mid-thickness	1.900 mm	1.480 mm
Keystone angle	1.25 °	0.90 °
Transposition length	115 mm	100 mm
Ratio Cu/Sc	≥ 1.6	≥ 1.9

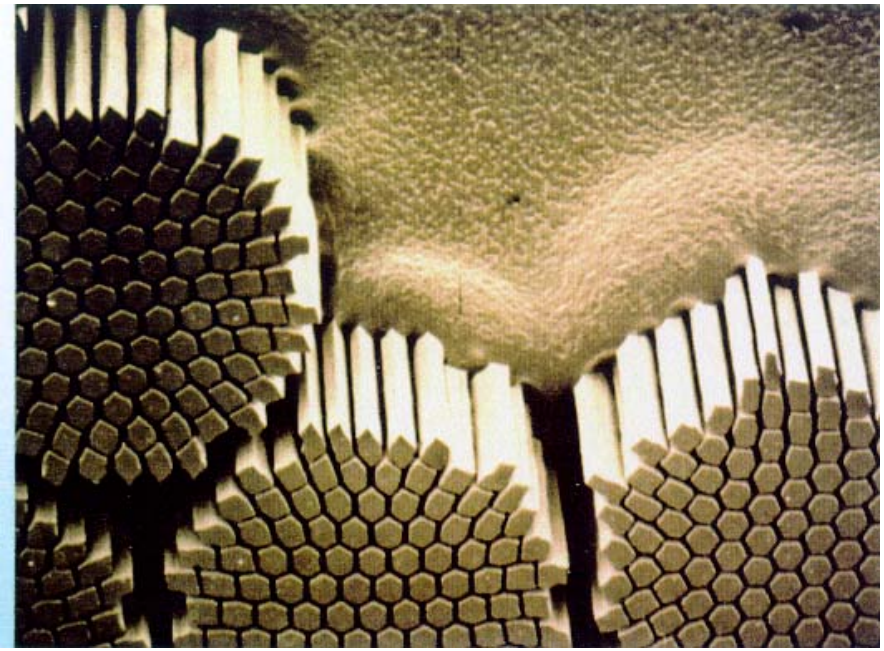

Persistent currents in superconductors

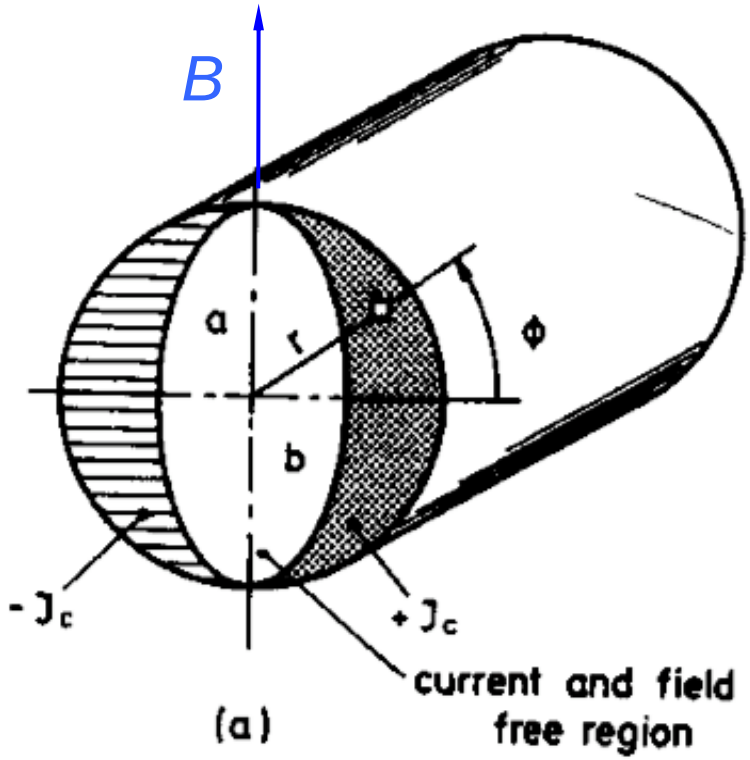

H. Brück, et al., Z. Phys. C, Particles and Fields, 44, pp. 385-392, 1989

- (Quasi) persistent currents flow in the superconducting filaments to shield the interior from outer field variations
- The pattern of persistent current depends mostly on:
  - history of field variation,
  - filament geometry,
  - Jc(B)
- The result is complex, and in the majority of relevant situations, not amenable to analytical solution

Strand magnetization in an LHC dipole coil

For a round filament in a resistive matrix and assuming full penetration ($\lambda = A_{SC}/A_{tot}$)

$$M = \pm \frac{2}{3\pi} \mu_0 J_c D \lambda$$

Opposed to background field

Filament diameter

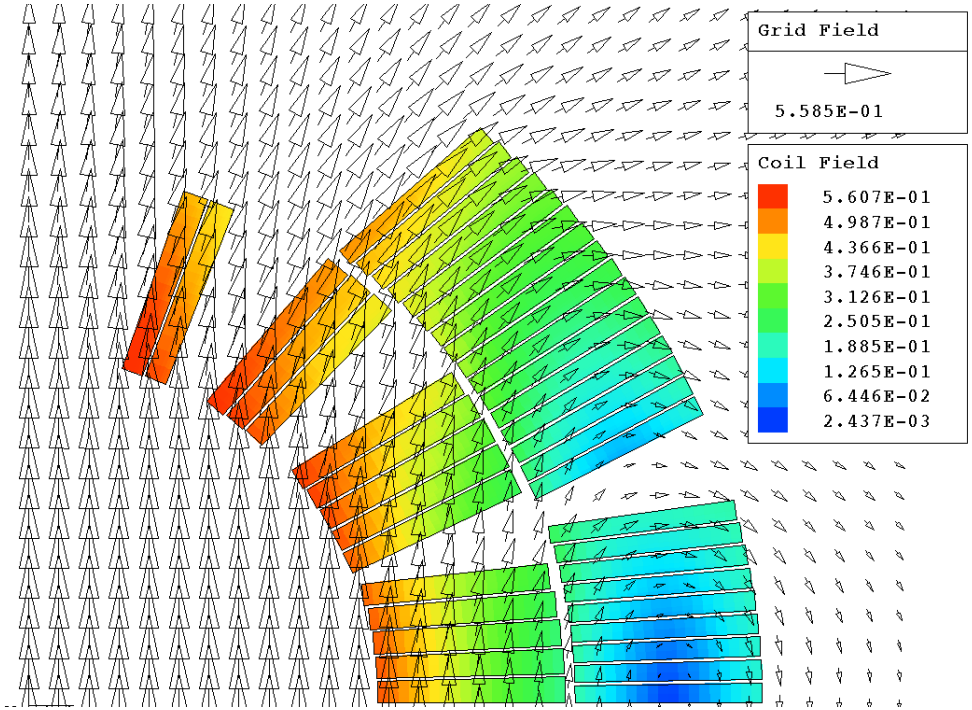

Field at injection (760 A)

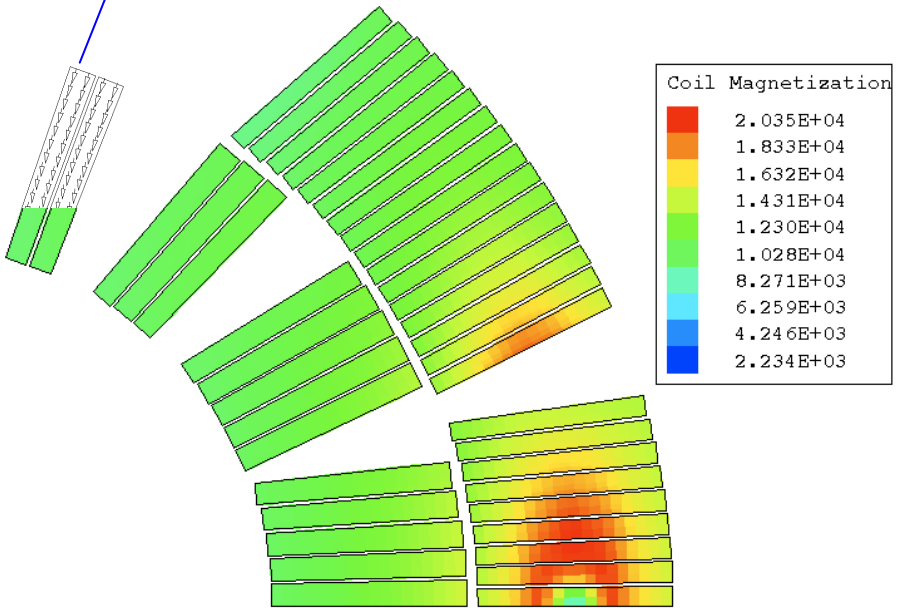

Magnetization at injection (760 A)

Locally the filaments are not fully penetrated by the flux change

Multipole field errors from persistent currents

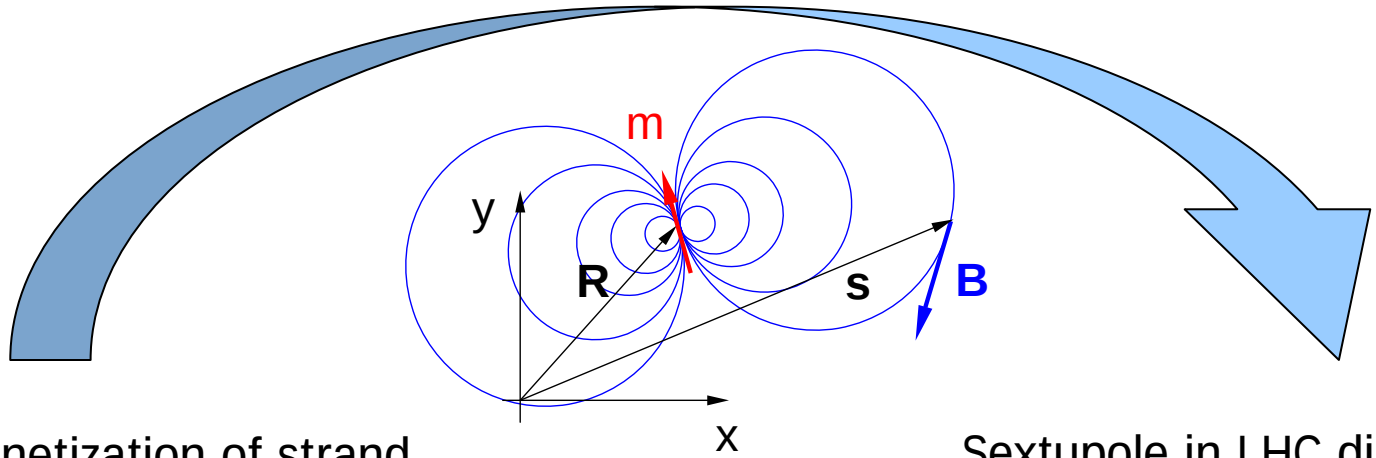

Magnetization of strand

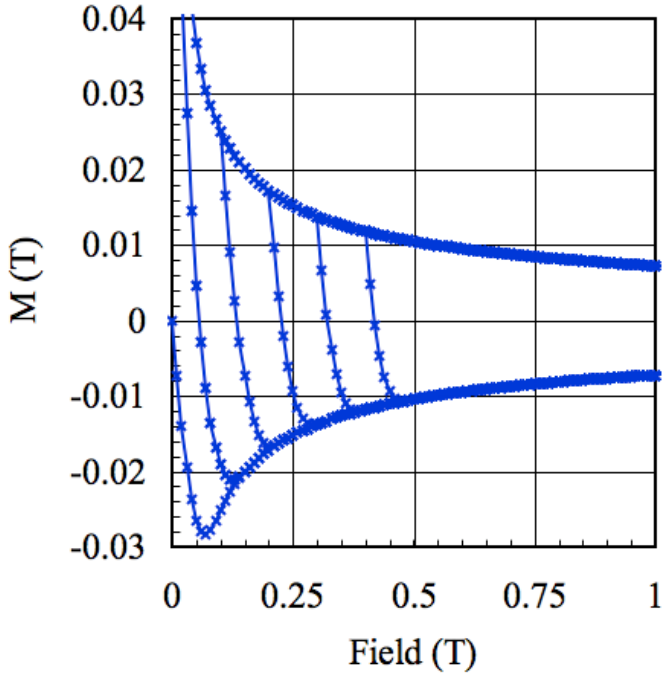

Sextupole in LHC dipole

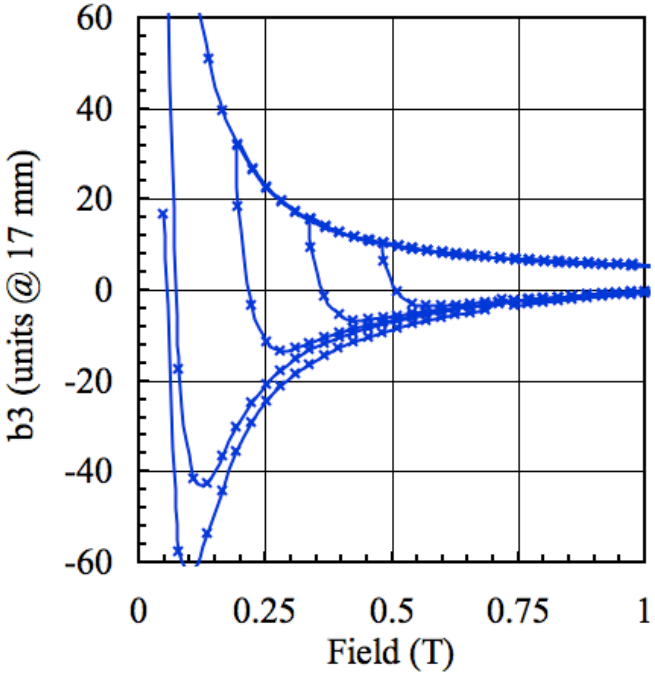

Production of superconducting wires & cables

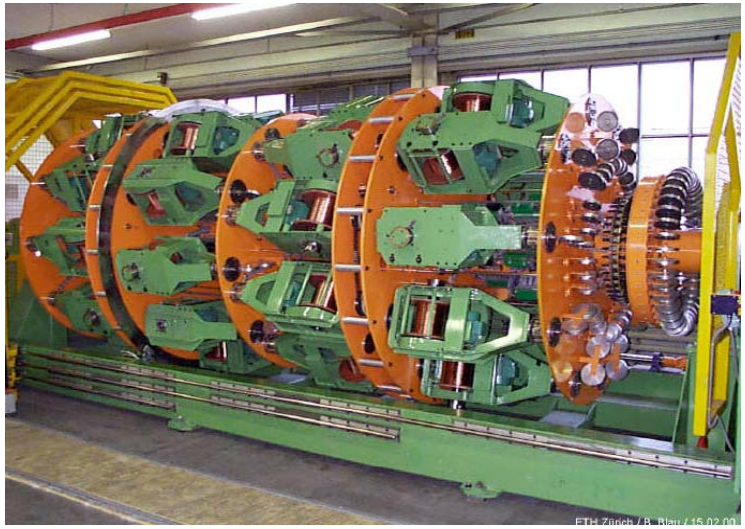

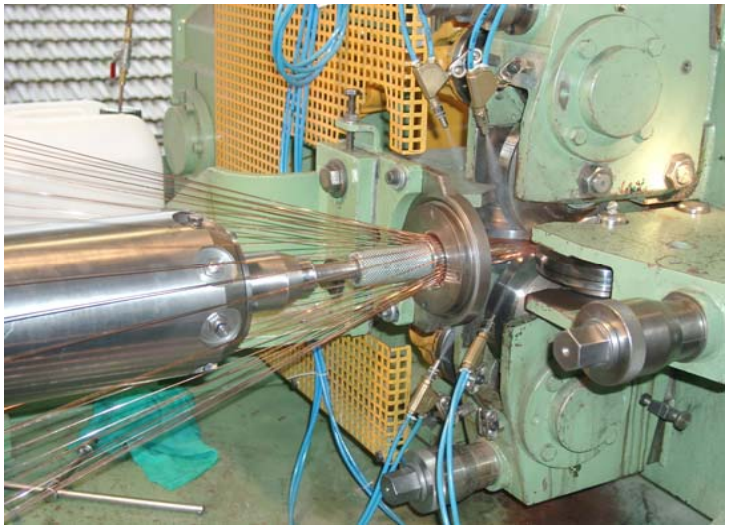

Superconducting cable production statistics

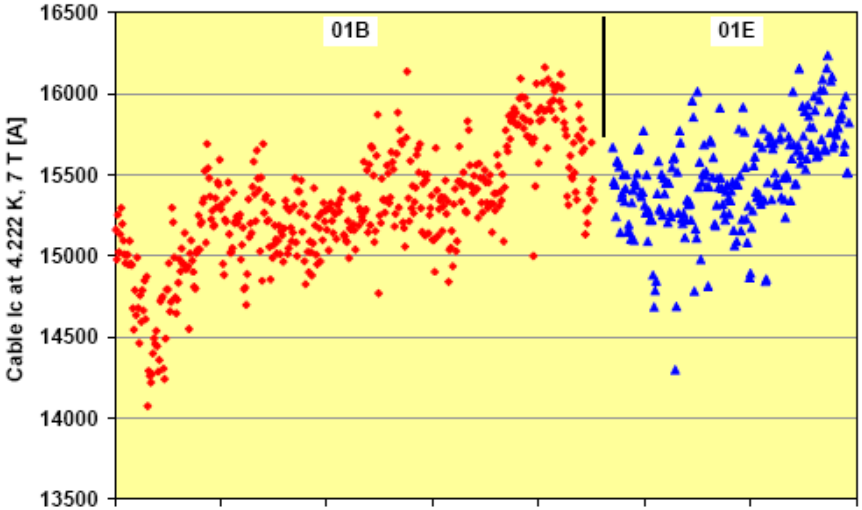

Specified 14140 A at 4.2 K, 7 T

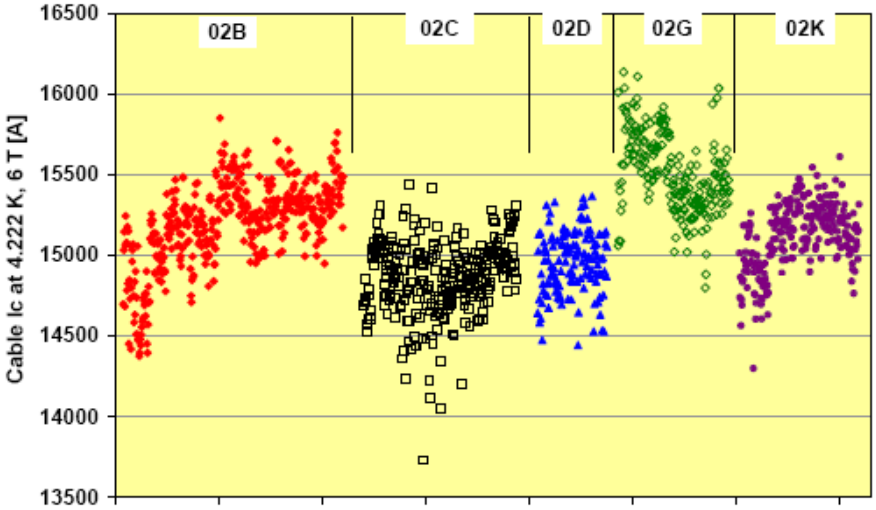

Specified 13236 A at 4.2 K, 6 T

- Critical current ~10% above specified value
- Magnetization and inter-strand resistance under control
- Cables within tight dimensional tolerances
- Rejection/declassification rate < 1%

Cable insulation by double polyimide wrap

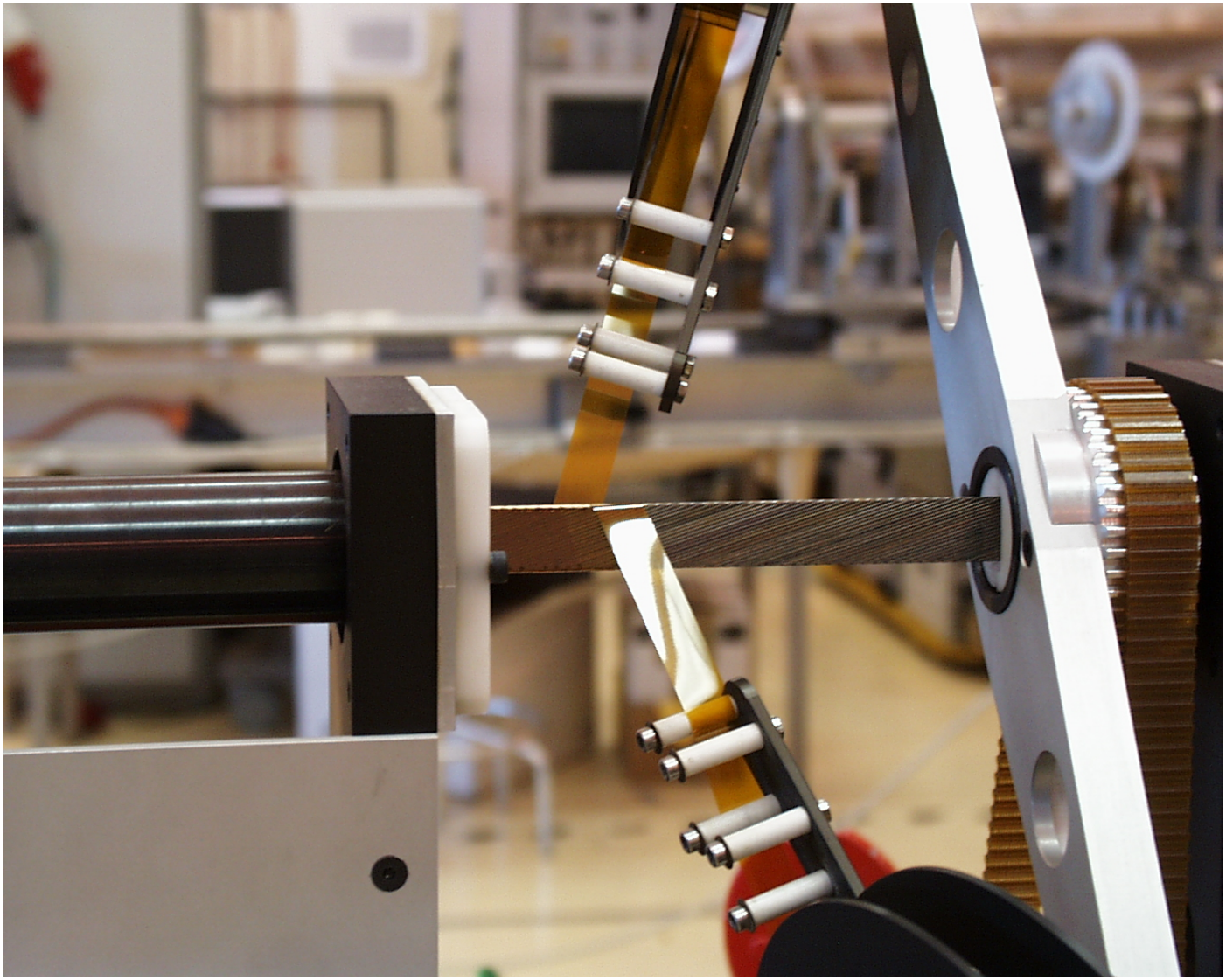

Coil cross-section showing inter-turn and ground insulation

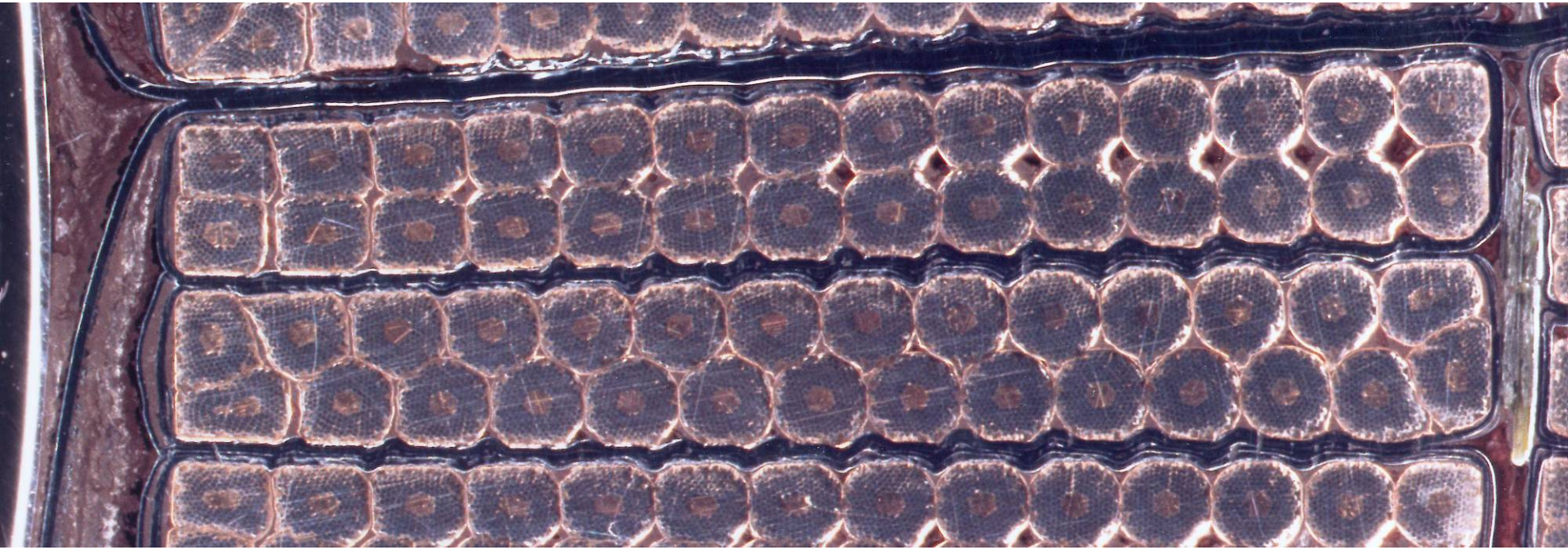

Manufacturing of superconducting coils

Sueprconducting coils extracted from mould

Electromagnetic forces

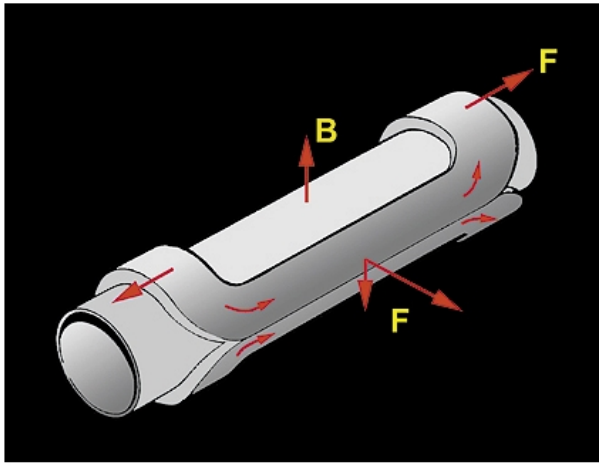

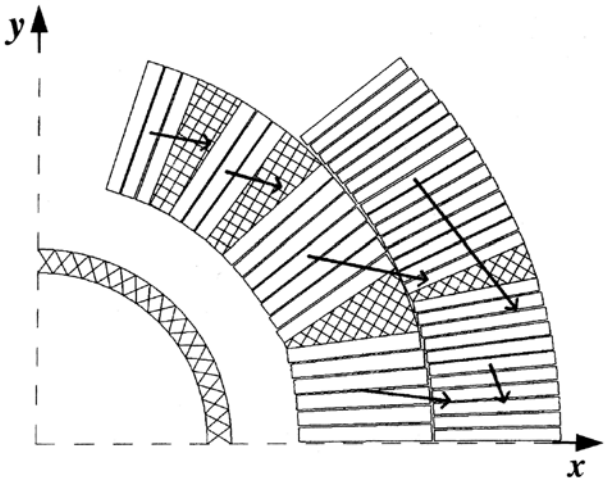

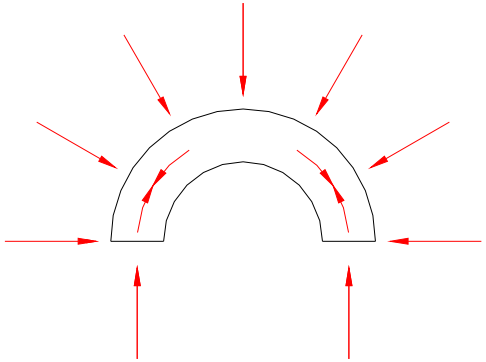

High magnetic field acting on high current generates large **electromagnetic forces** at right angle, which cannot be resisted by the mechanical strength of the conductor: saddle-shaped coils of accelerator magnets are not self-supporting

B = 10 T, I = 10 kA ⇒ 10^5 N/m per turn !

⇒ "**roman arch**" coil geometry to contain the azimuthal component

⇒ external **support structure** against the radial component

Coil-collar assembly

Twin-aperture dipole magnet

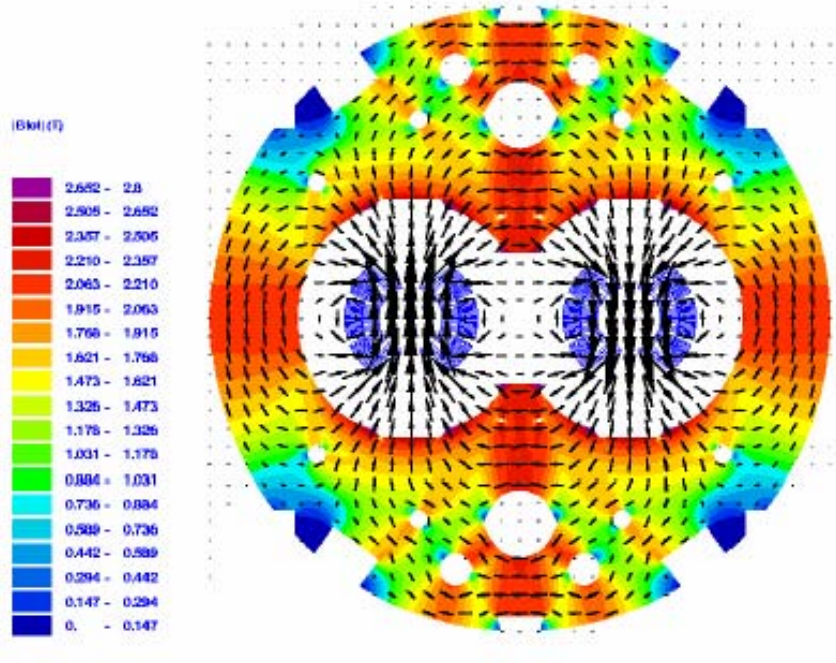

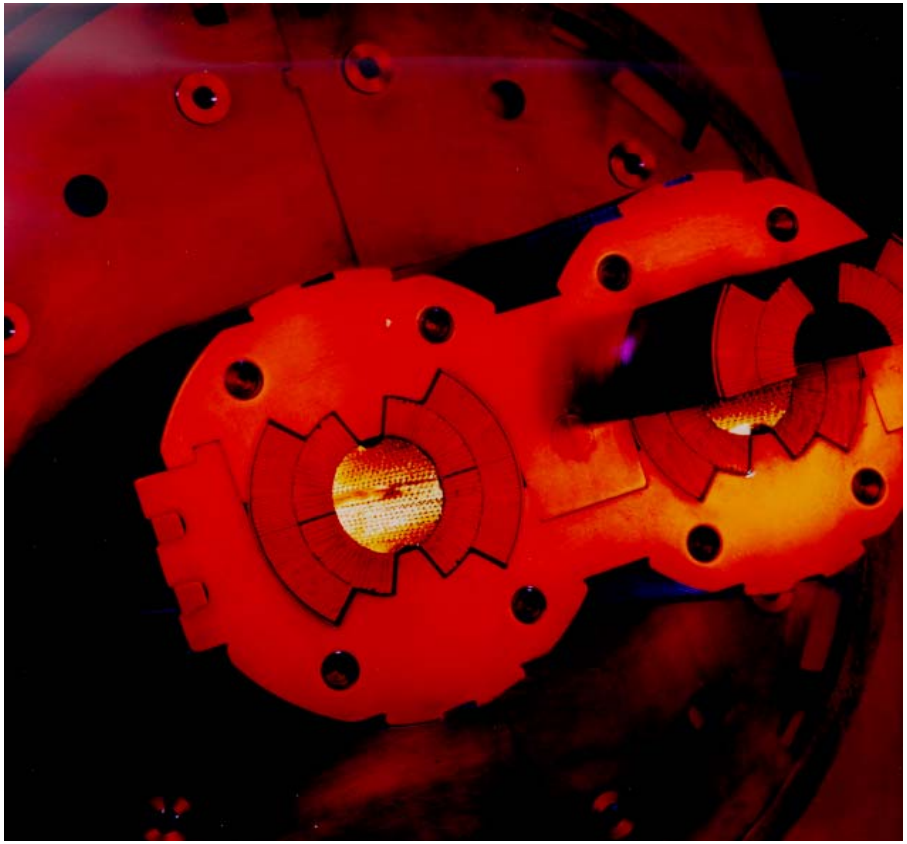

Field reproducibility/precision ~ 10^{-3}

Field homogeneity ~ 10^{-4}

$\Rightarrow$ Winding precision < 0.05 mm

Assembly of dipole cold masses

LHC DIPOLE
CROSS SECTION

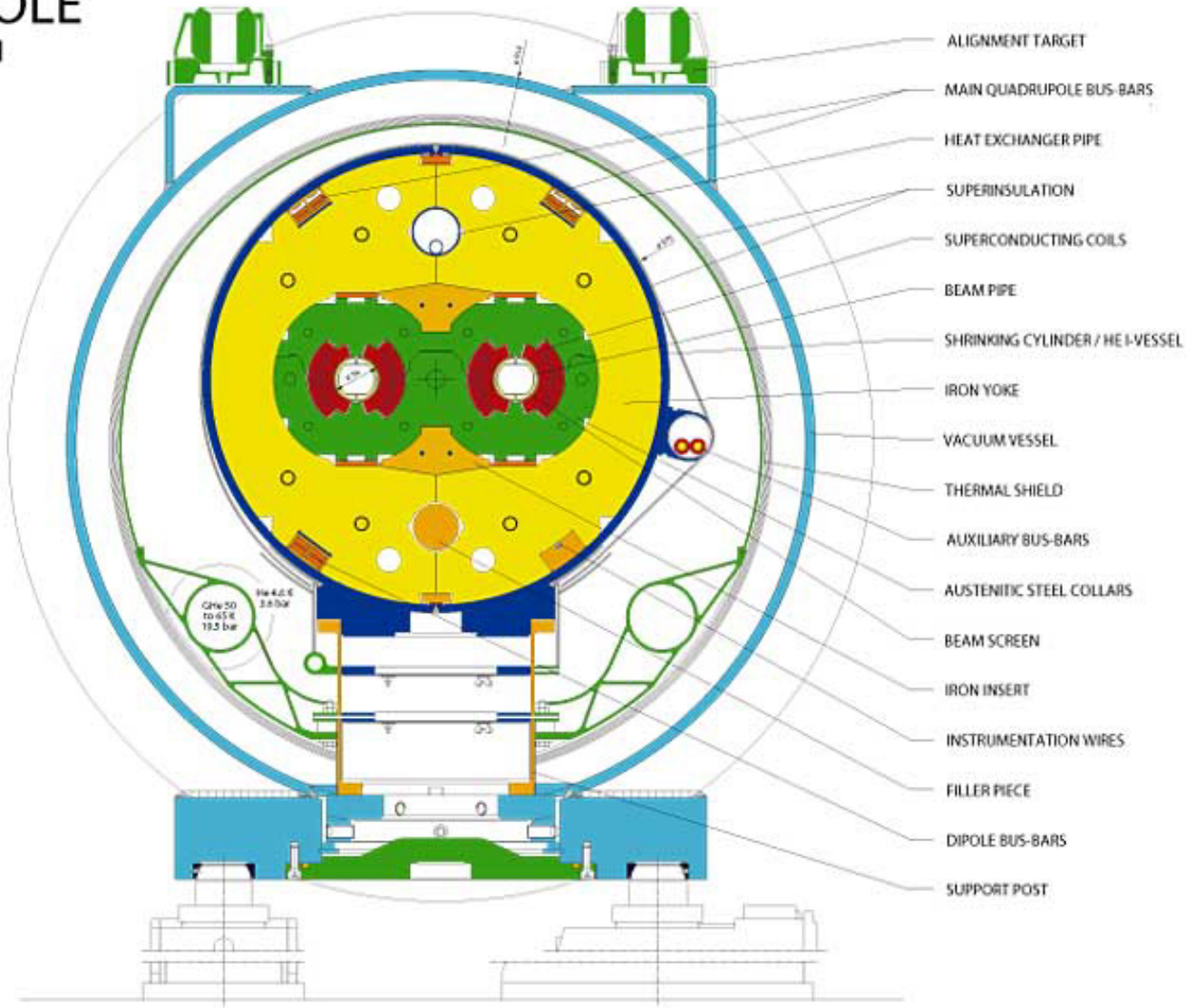

Final assembly of cryomagnets at CERN

Cryogenic tests of magnets

Training of superconducting magnets

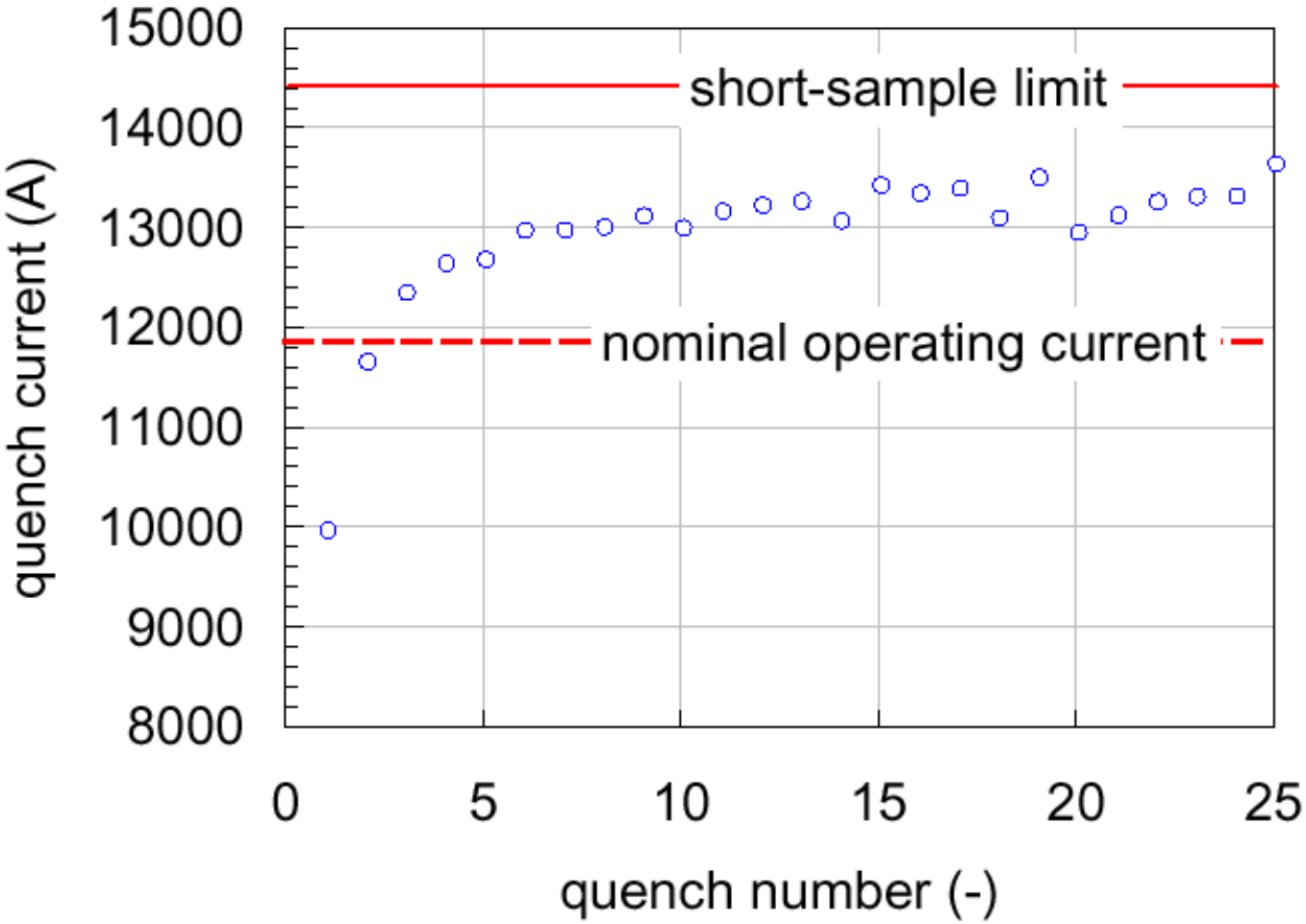

10 T in magnet bore

8.3 T in magnet bore

Quenches to reach 8.33 T on virgin dipoles

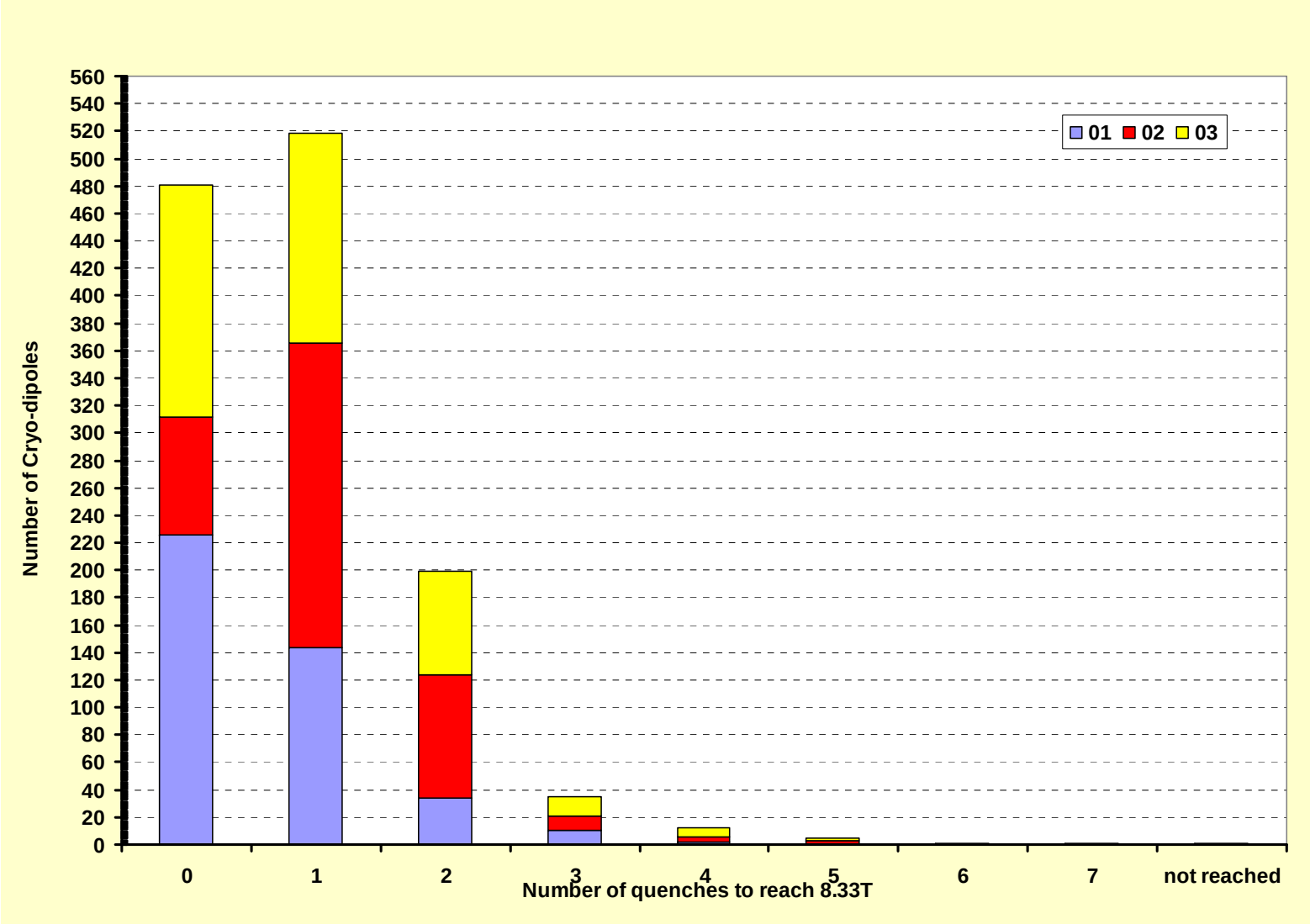

Quenches to reach 8.33 T after thermal cycle

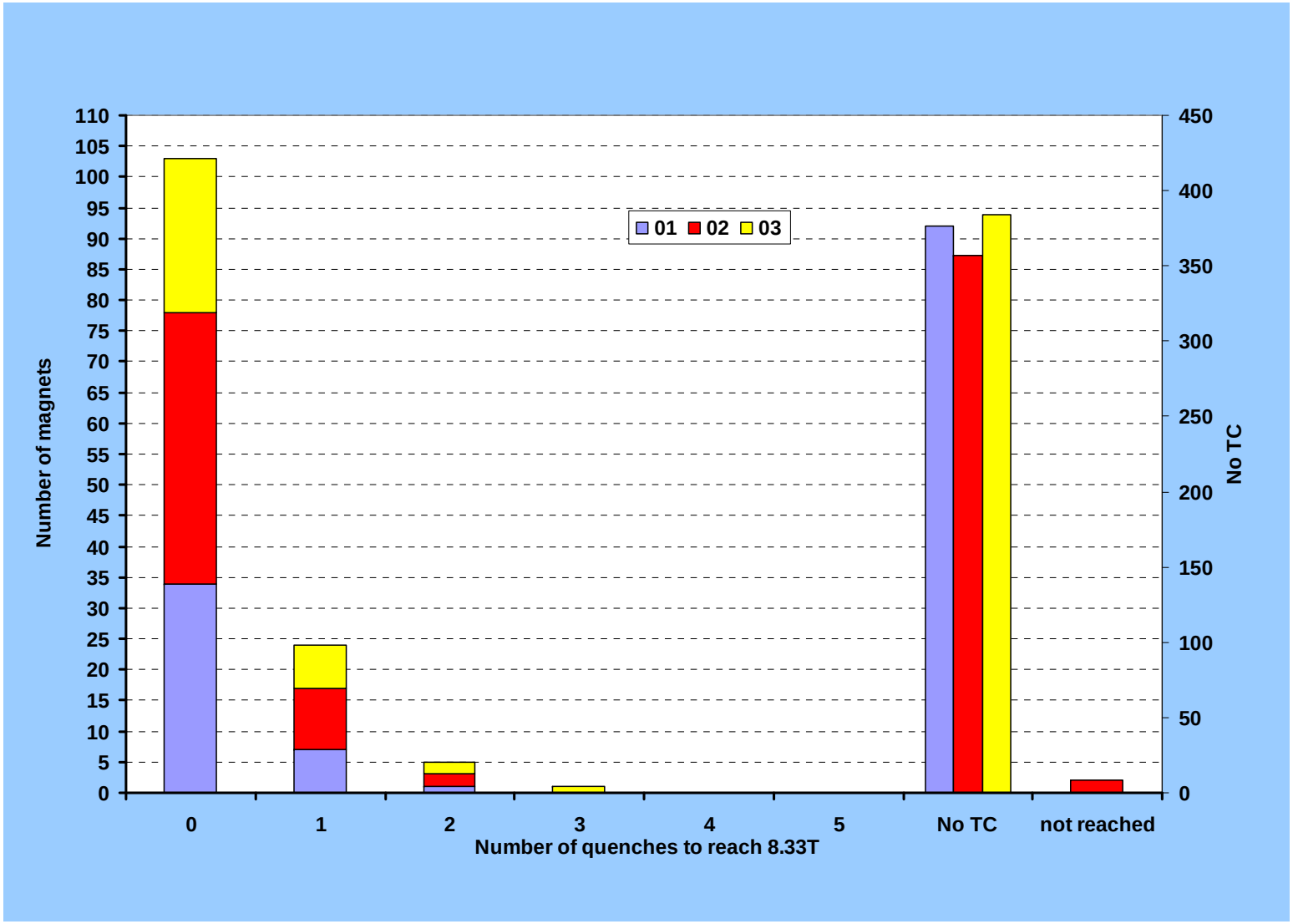

Dipole field quality in series production

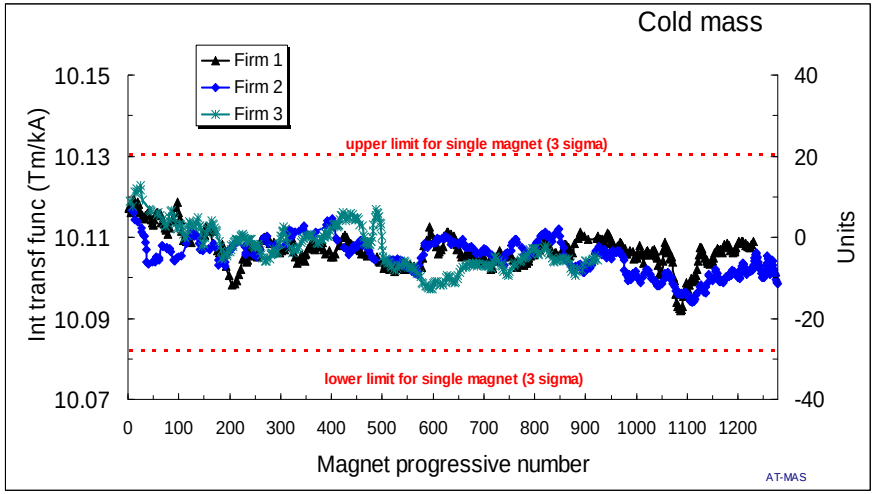

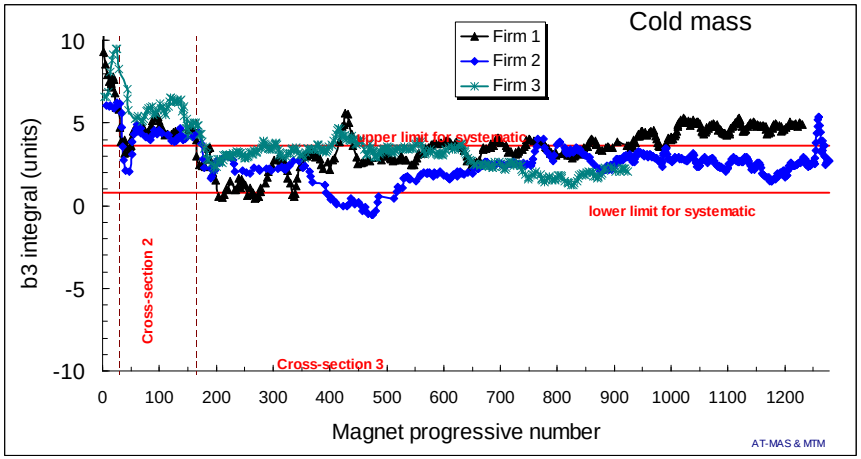

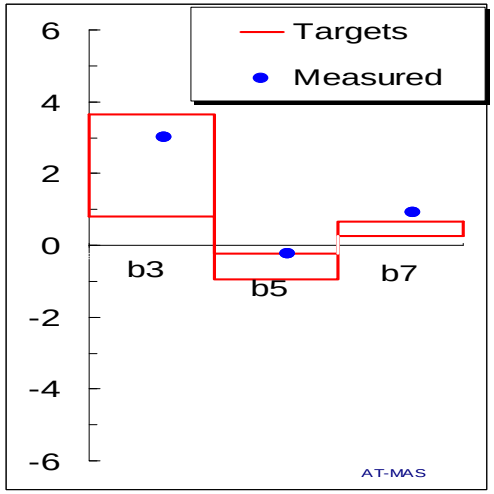

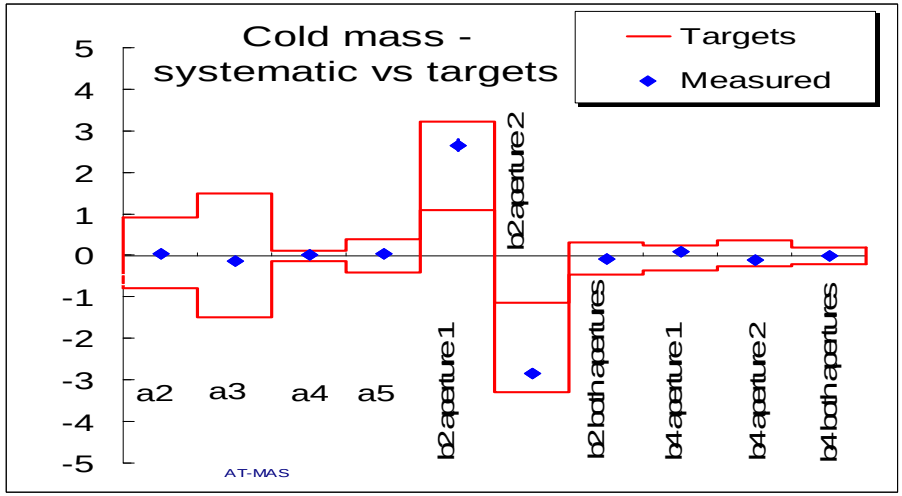

Magnet Evaluation Board
Clearance and sorting for installation

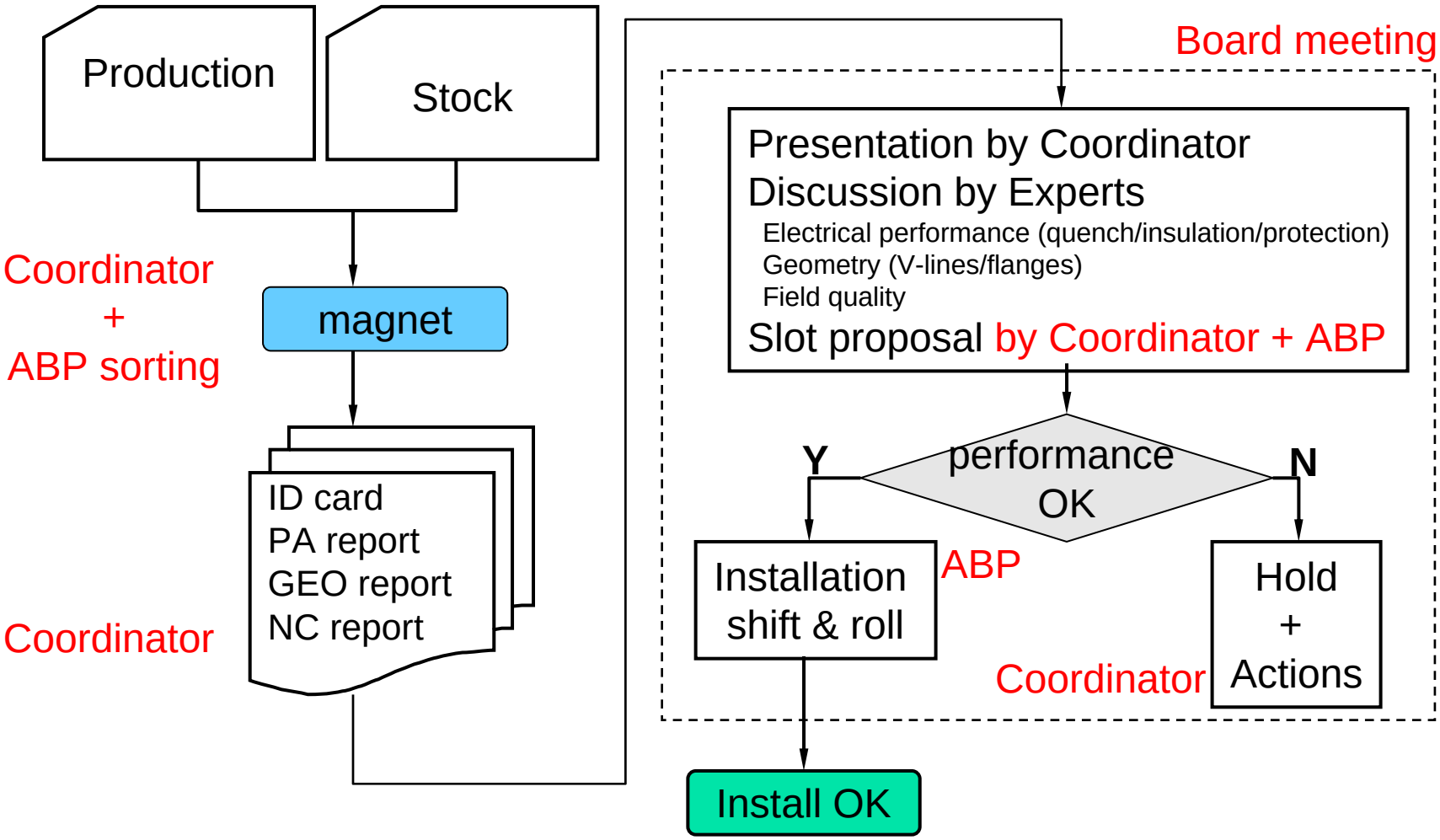

Sorting of dipoles by geometry

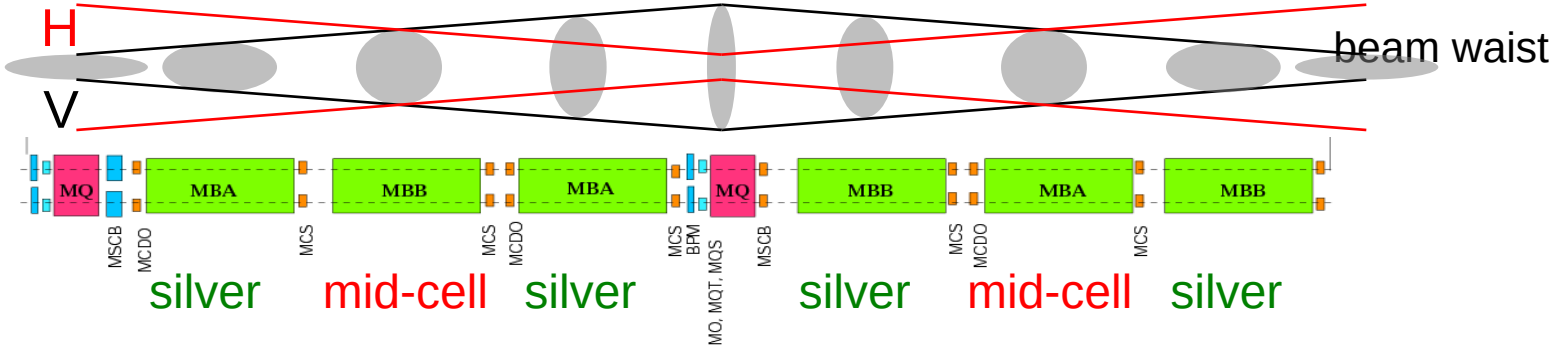

Definition of geometry classes

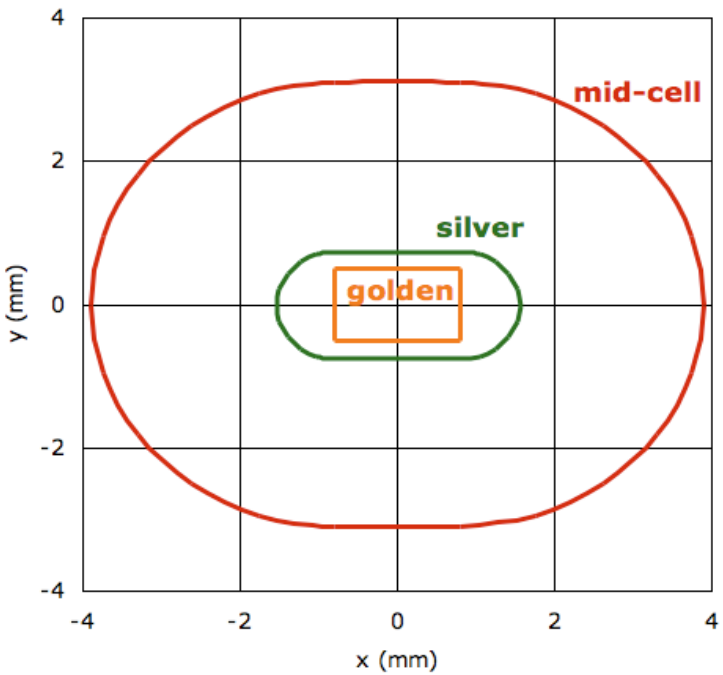

Distribution of *as-built* MB's

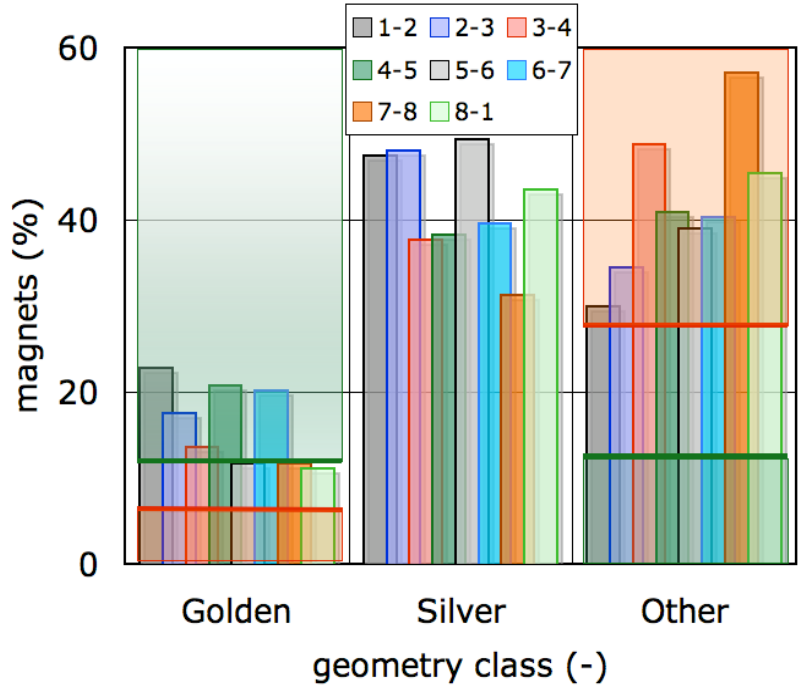

Local sorting of dipoles by sextupole error

b3 distribution in sector 7-8

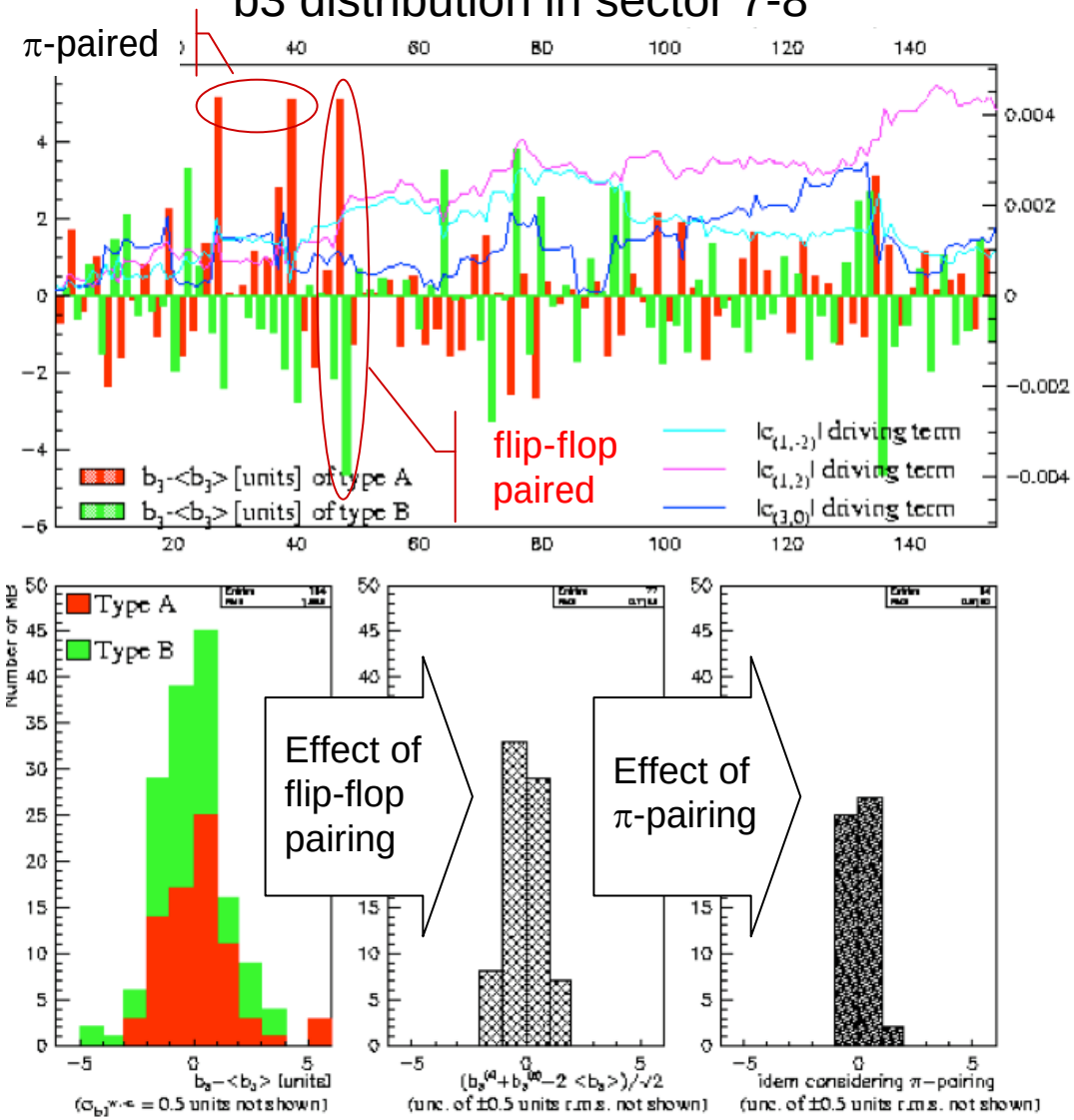

Buffer storage allows sorting, reduces dispersion

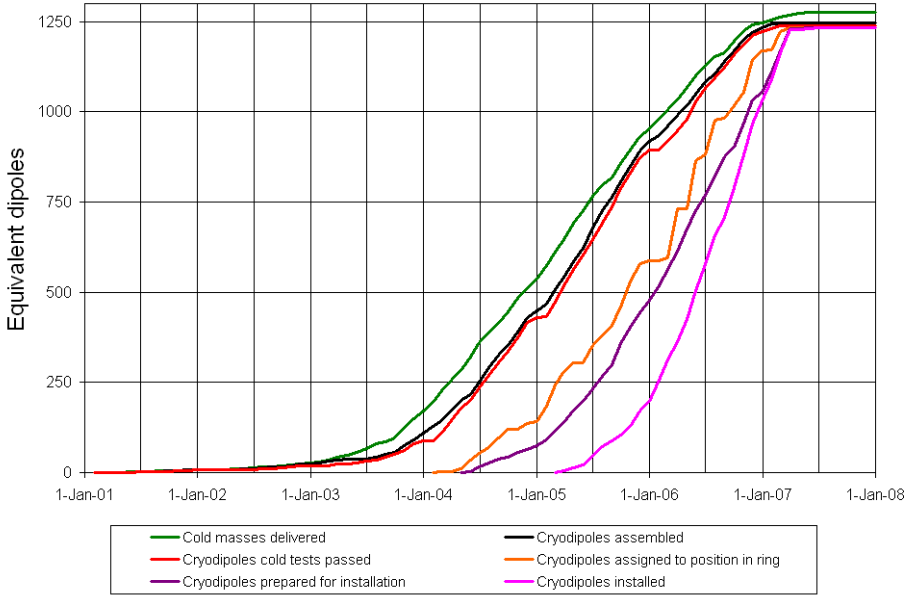

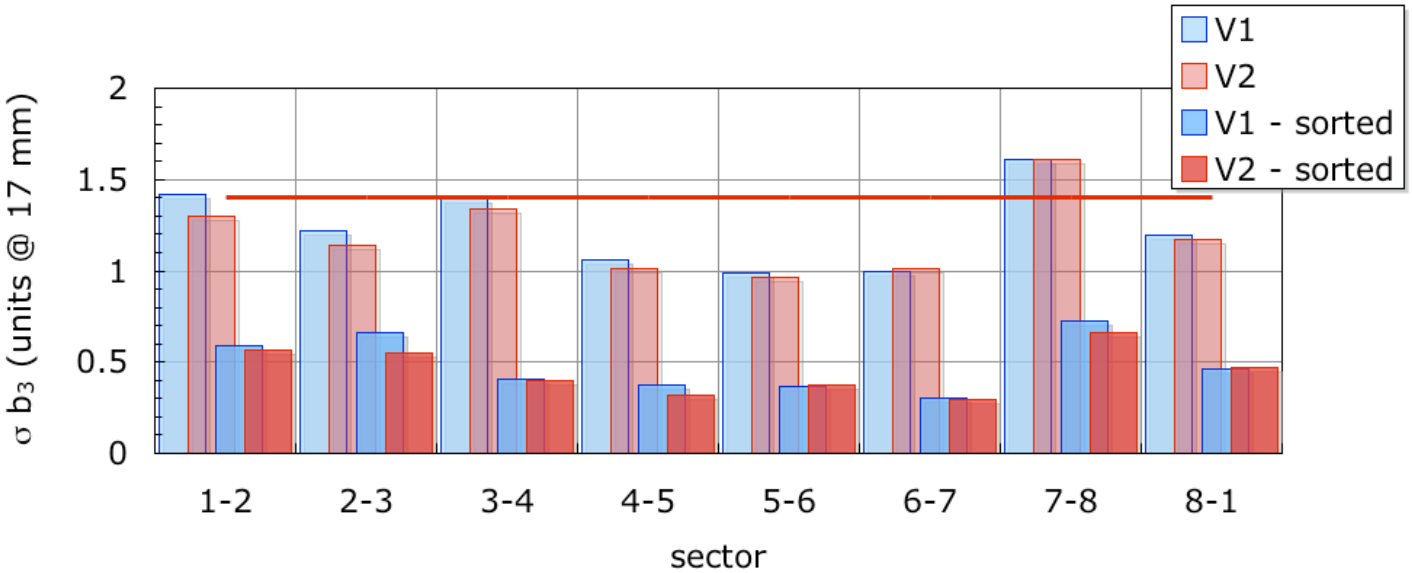

Lowering of magnets in tunnel

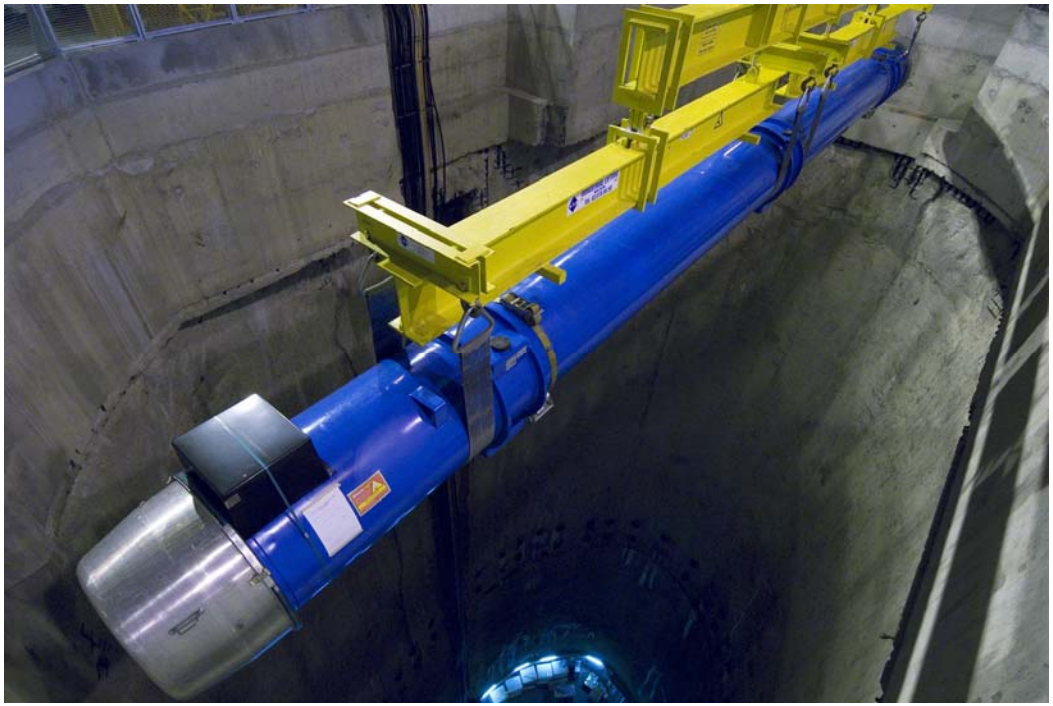

Cryomagnet installation in tunnel

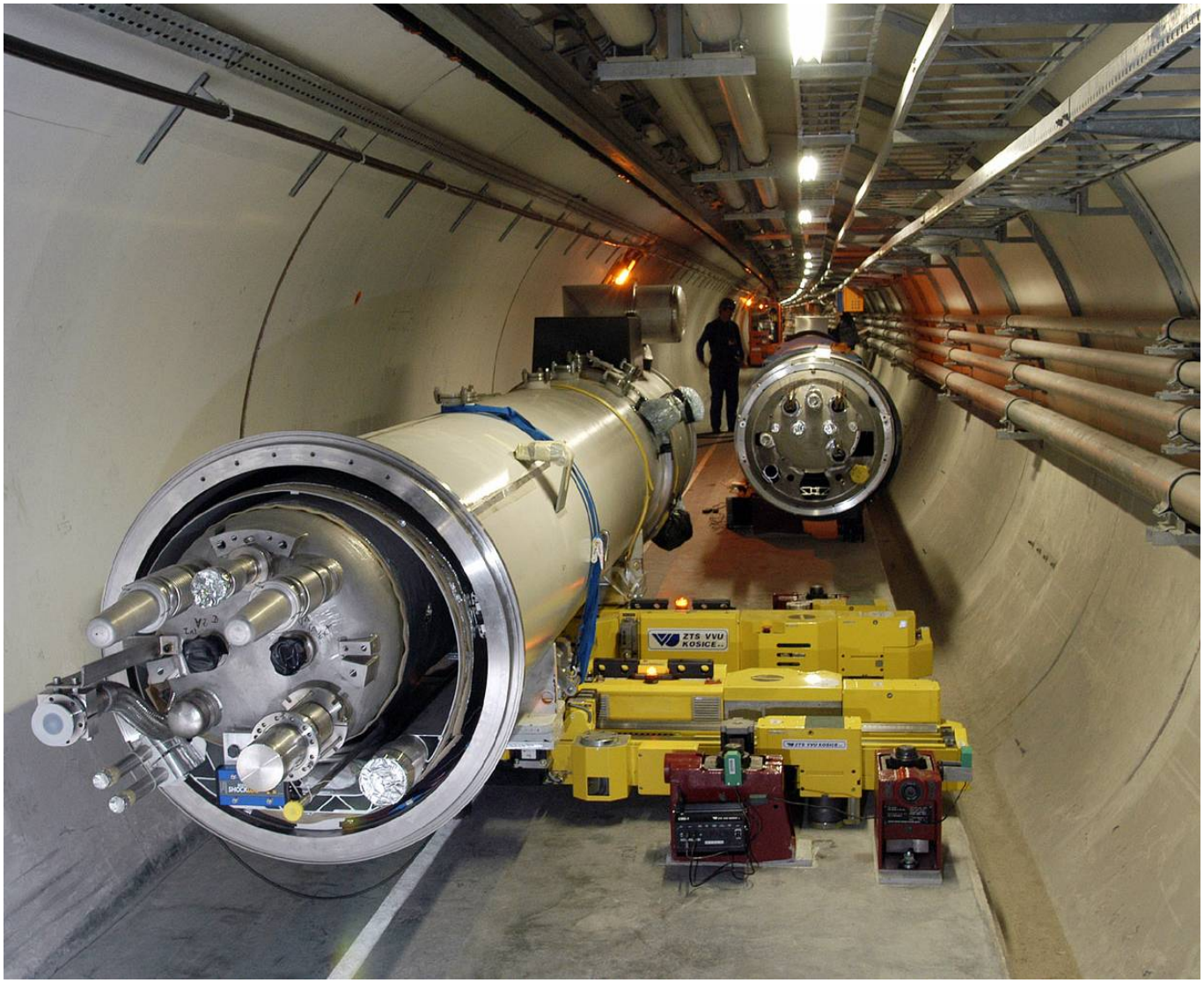

Interconnections in tunnel

65’000 electrical joints

Induction-heated soldering

Ultrasonic welding

Very low residual resistance

HV electrical insulation

40’000 cryogenic junctions

Orbital TIG welding

Weld quality

Helium leaktightness

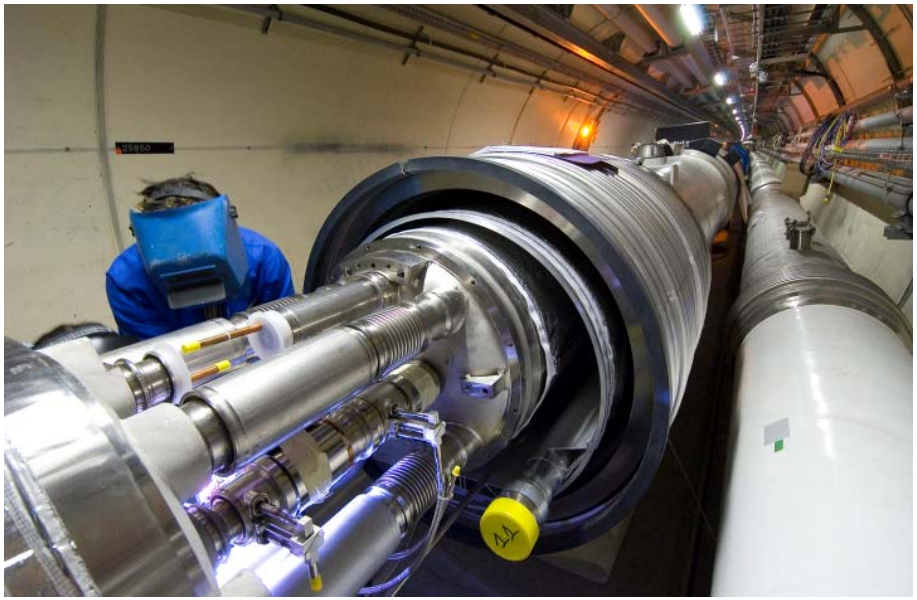

Contents

- The LHC in a nutshell
- Performance
  - Energy
  - Luminosity
  - Collective effects
  - Dynamic aperture
- Technology
  - Superconducting magnets
  - Powering and protection
  - Cryogenics
  - Vacuum
- Project management

Arc electrical feedbox

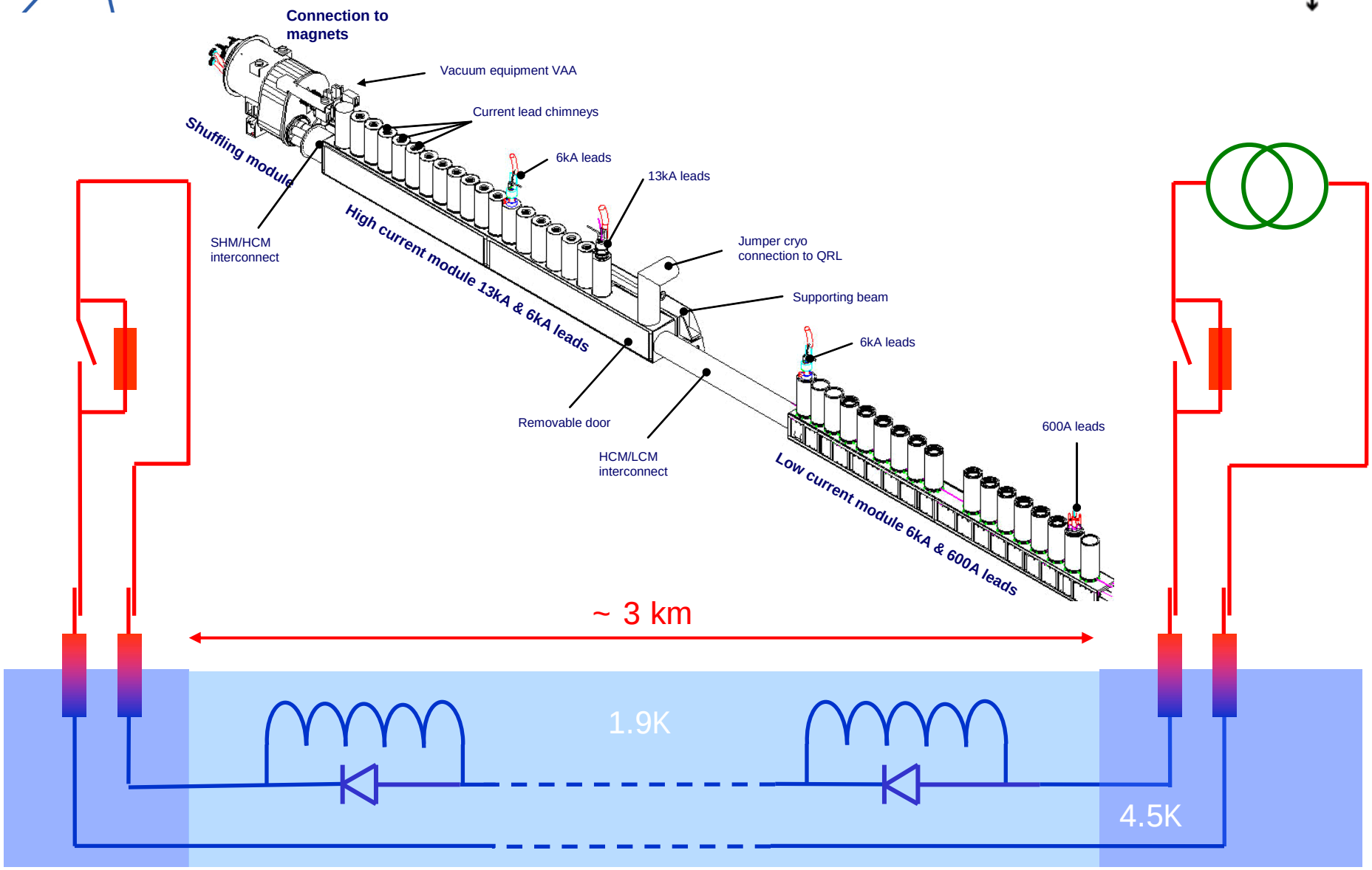

Cryogenic current leads

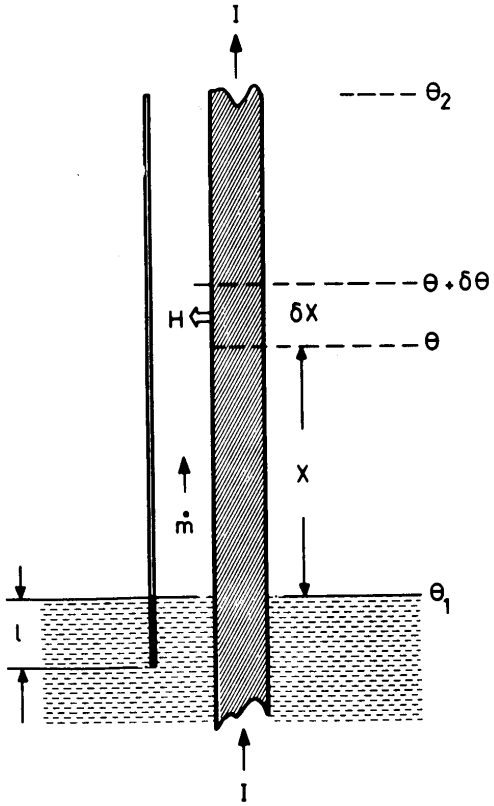

Heat transfer processes at work

- Solid conduction
- Joule heating
- Convective cooling by He vapor

Metals are good electrical AND thermal conductors (Wiedemann-Franz-Lorentz law)

Optimal sizing of current lead results from compromise between heat conduction and Joule heating

Superconductors do not follow WFL law

They are perfect electrical conductors with low thermal conductivity

They can make excellent current leads... up to their transition temperature!

⇒ niche application for "high-temperature" superconductors

Discovery of high-temperature superconductors (1986)

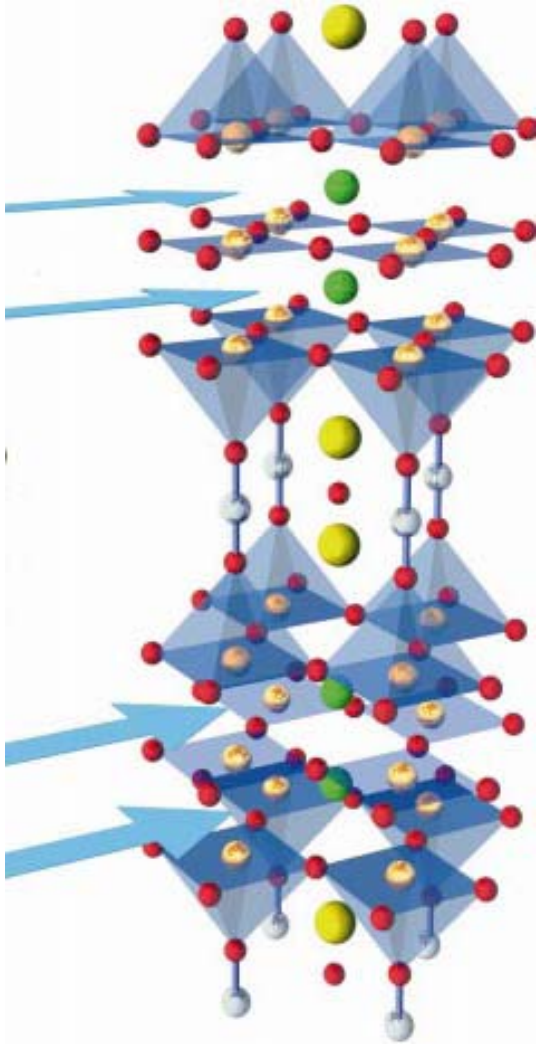

J. Georg Bednorz

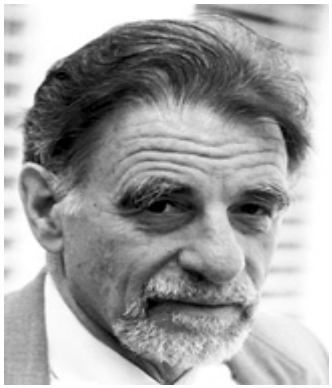

K. Alexander Müller

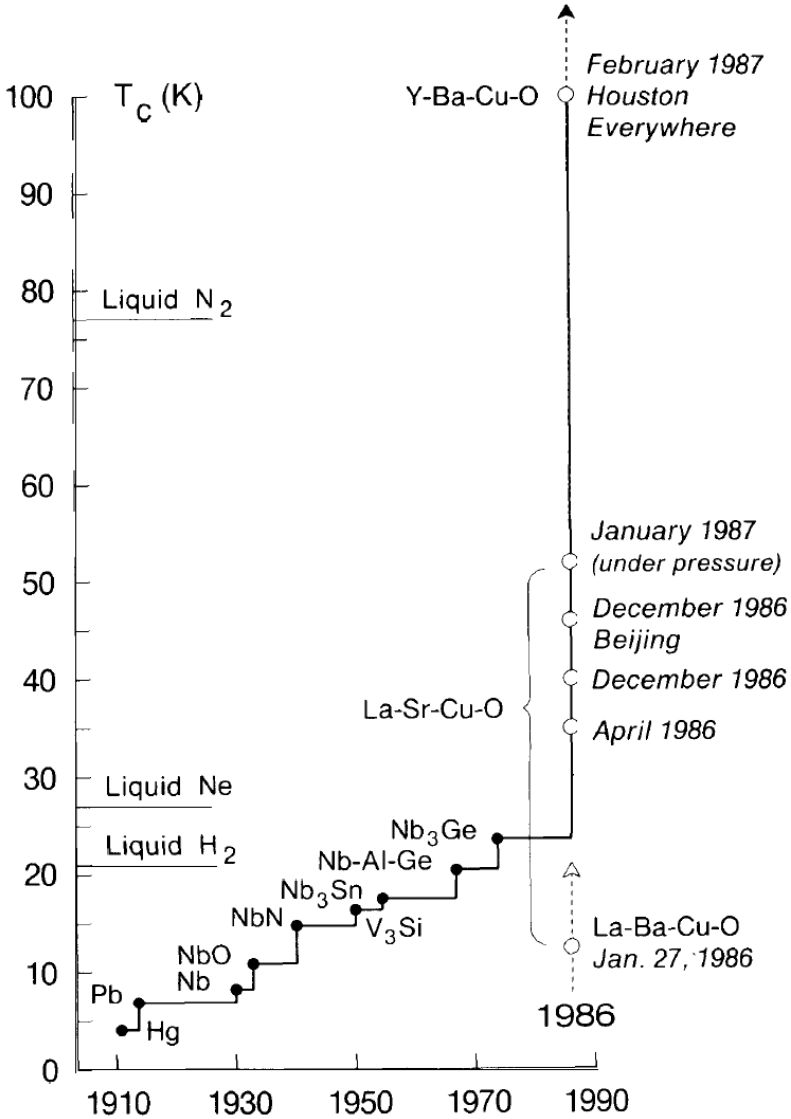

Current leads using HTS superconductor

	Resistive (WFL)	HTS (4 to 50 K) Resistive (> 50 K)
Heat inleak to liquid helium	1.1 W/kA	0.1 W/kA
Exergy loss	430 W/kA	150 W/kA
Electrical power of refrigerator	1430 W/kA	500 W/kA

13 kA HTS current lead for LHC

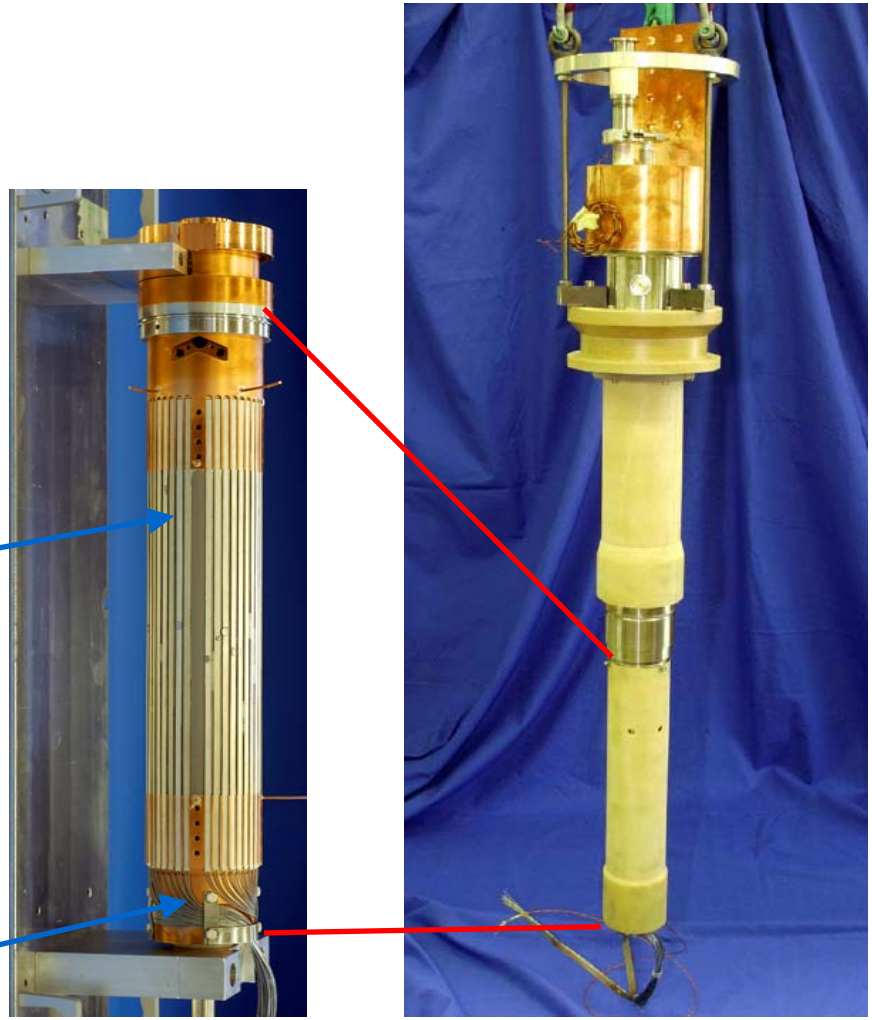

Sum of currents into LHC ~ 1.7 MA, i.e. need current leads for 3.4 MA total rating (in and out)

Economy ~ 3400 W in liquid helium ~ 5000 l/h liquid helium

⇒ *capital: save extra cryoplant*

⇒ *operation: save ~ 3.2 MW*

HTS current leads in the LHC tunnel

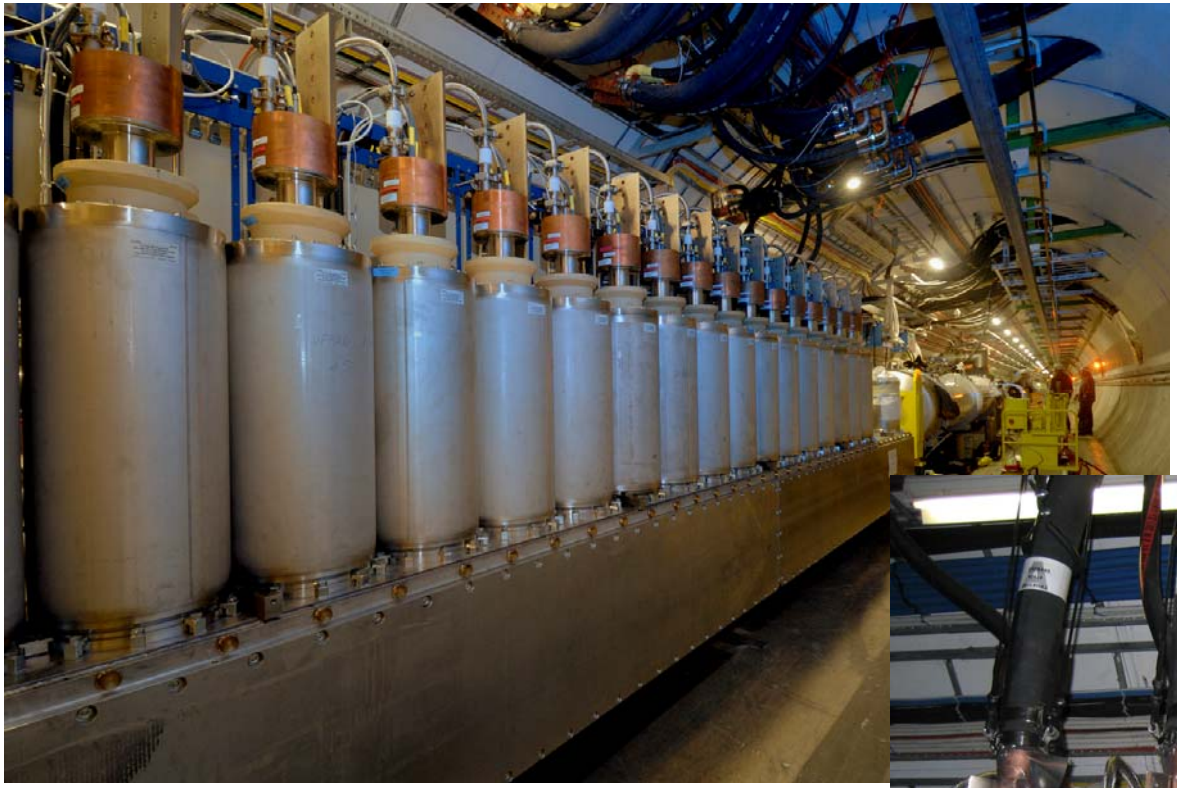

6 & 13 kA leads on electrical feed-box

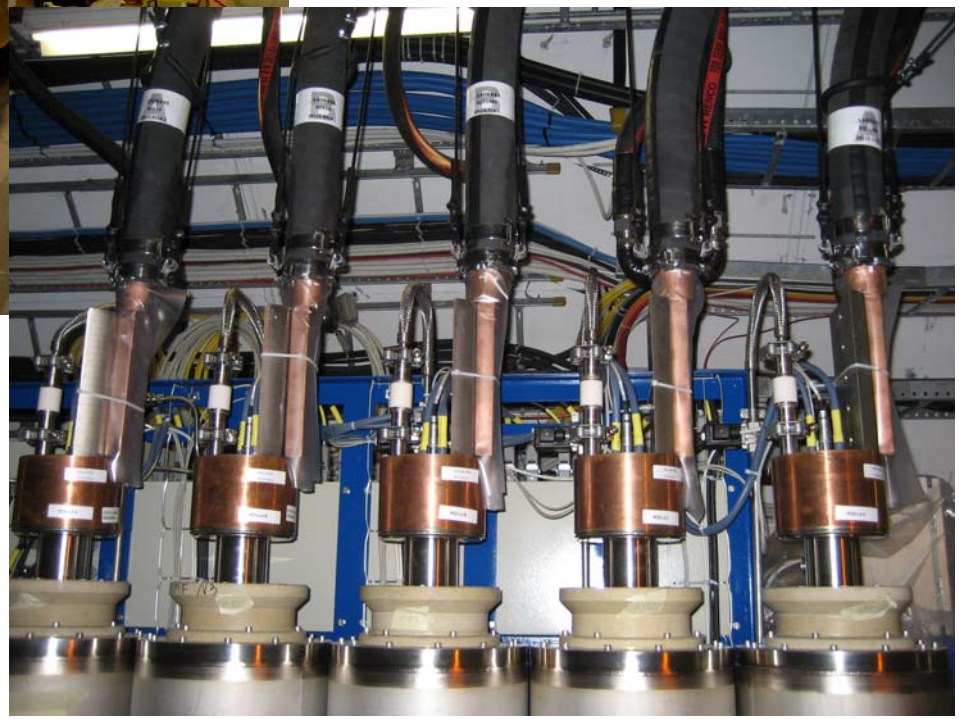

Water-cooled cables on current lead lugs

High-precision, modular switched-mode power converters

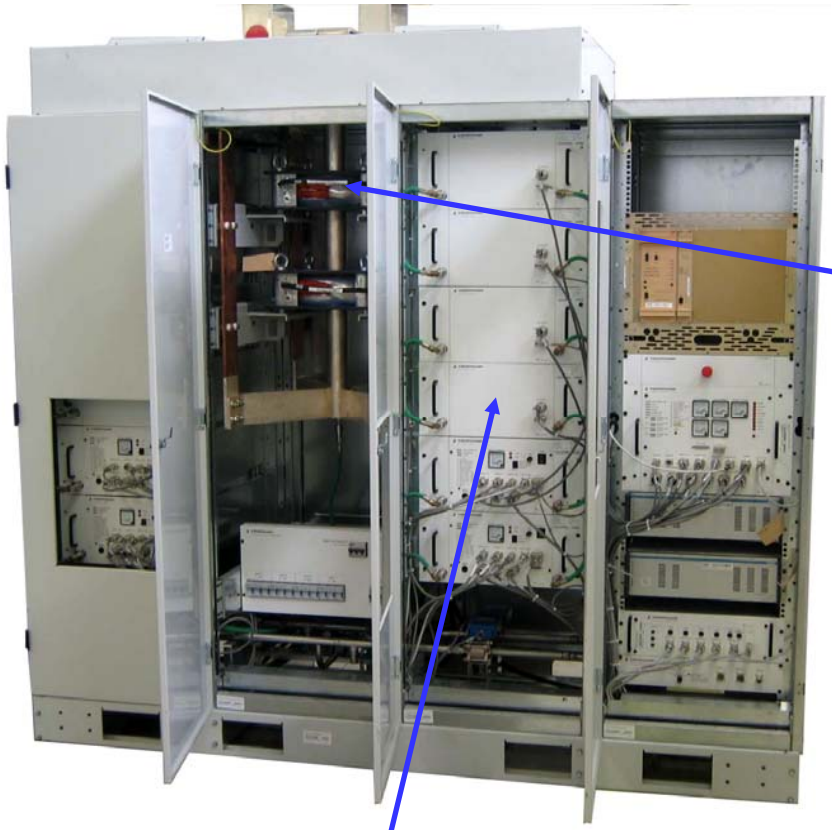

[2kA,8V] converters

High-precision DCCT

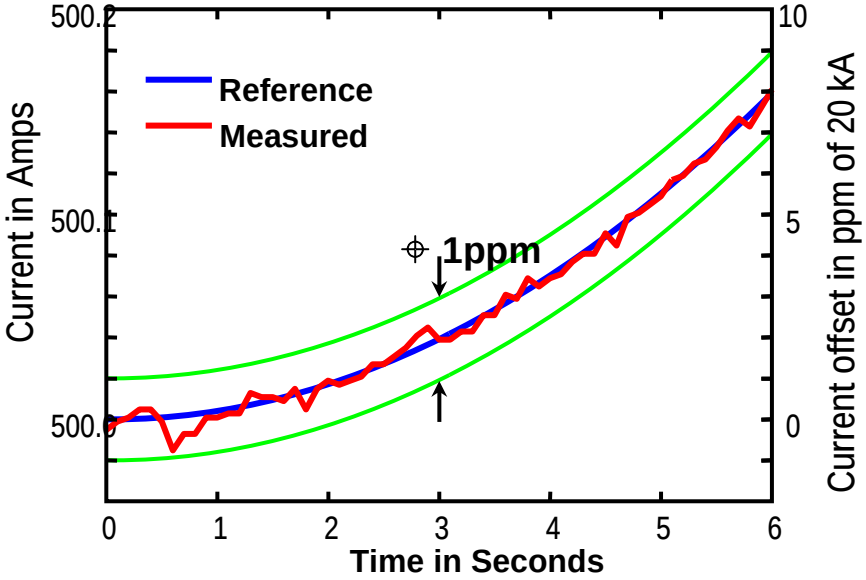

Ramp and squeeze of the main circuits

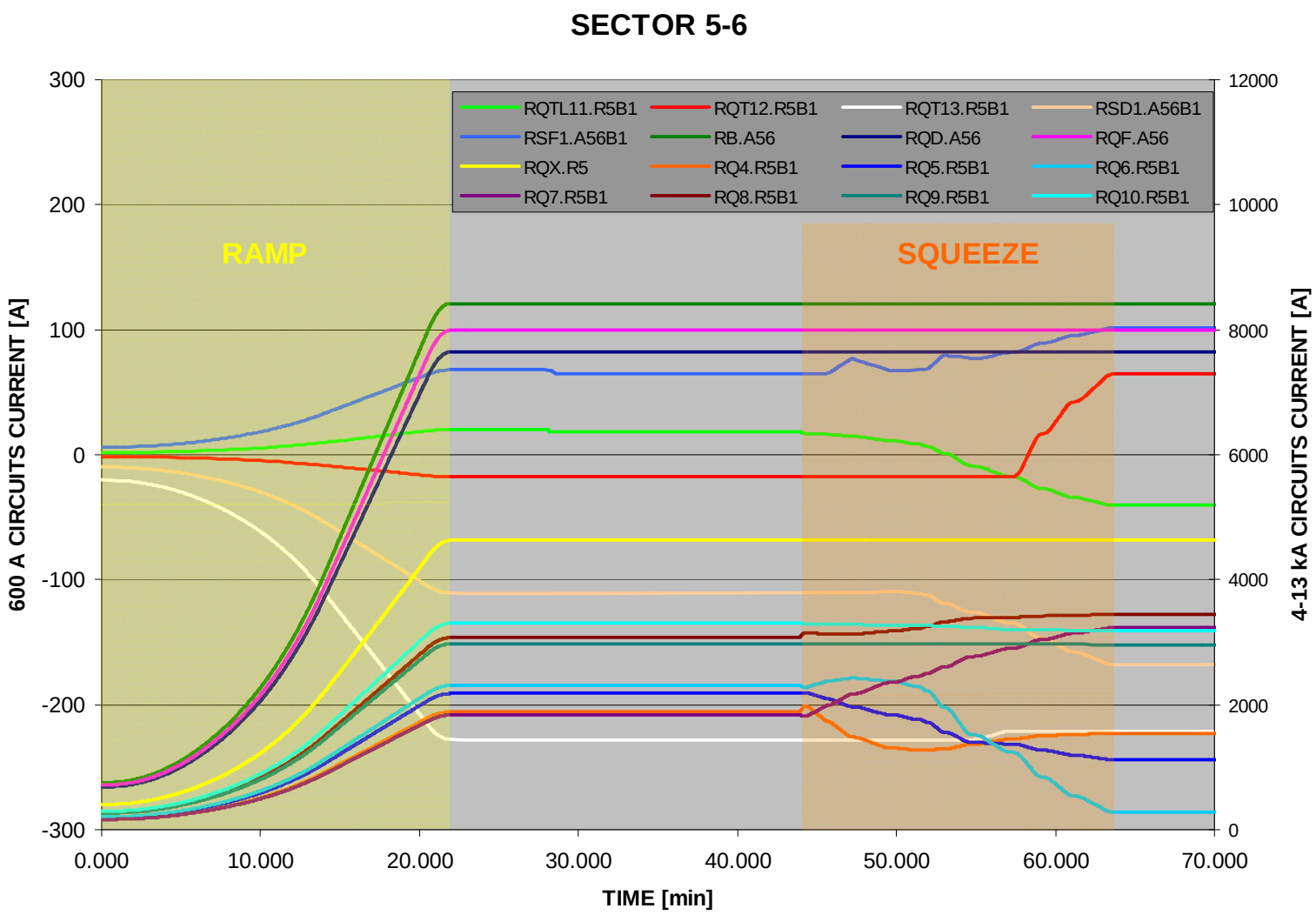

Superconductors are basically unstable!

Heat capacity of materials drops at low temperatures

$\Delta T = \Delta E/\gamma C$

ΔE of few μJ on a superconducting strand in the cable generates ΔT pushing the operating point beyond the critical surface $\Rightarrow$ *resistive transition ("quench")*

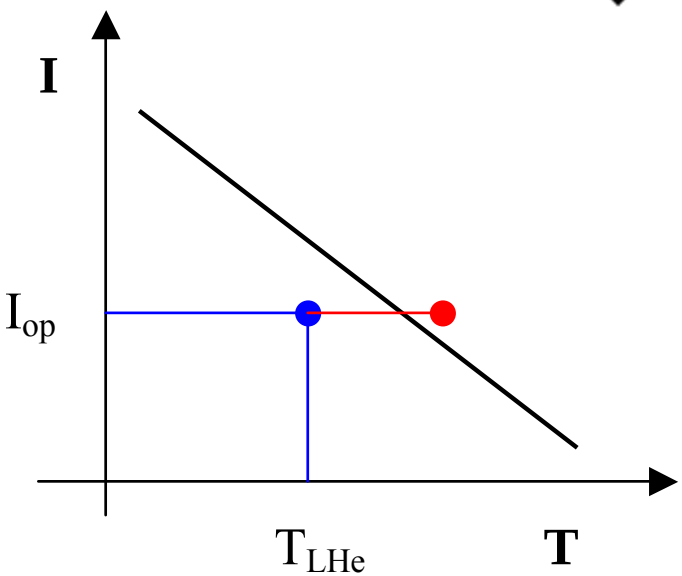

Temperature margin of superconductor	~ 1.5 K
Specific quench energy	~ 10 mJ/cm^3
Energy stored inductively in magnet	6.9 MJ
Energy stored in beam	360 MJ

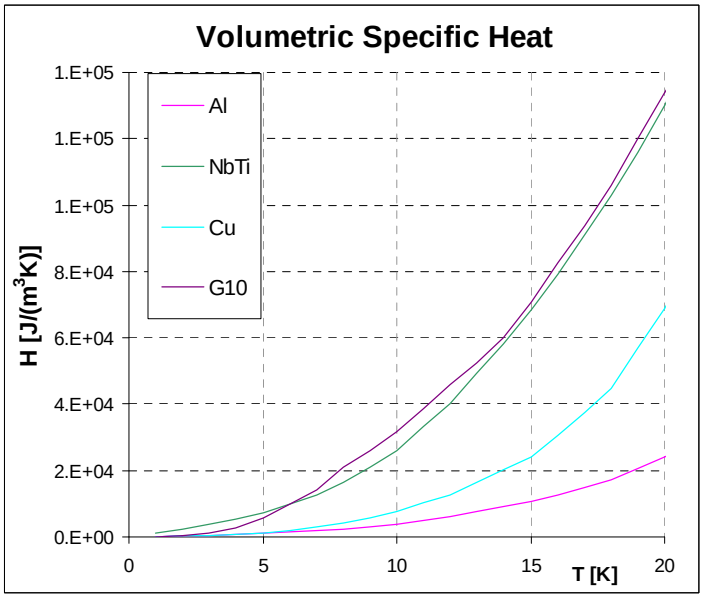

Stabilization of superconductors

Electrodynamic stabilization:

intimate contact between the superconductor and a good conductivity material (Cu or Al) with sufficient cross-section

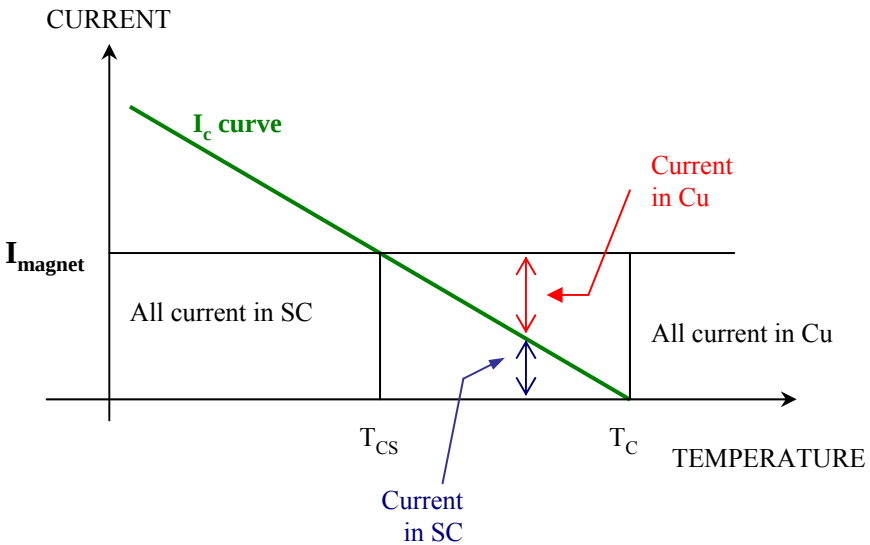

Cryogenic stabilization:

specific heat of LHe is 10-100 times that of conductor, which provides stability if good thermal contact is ensured (across electrical insulation)

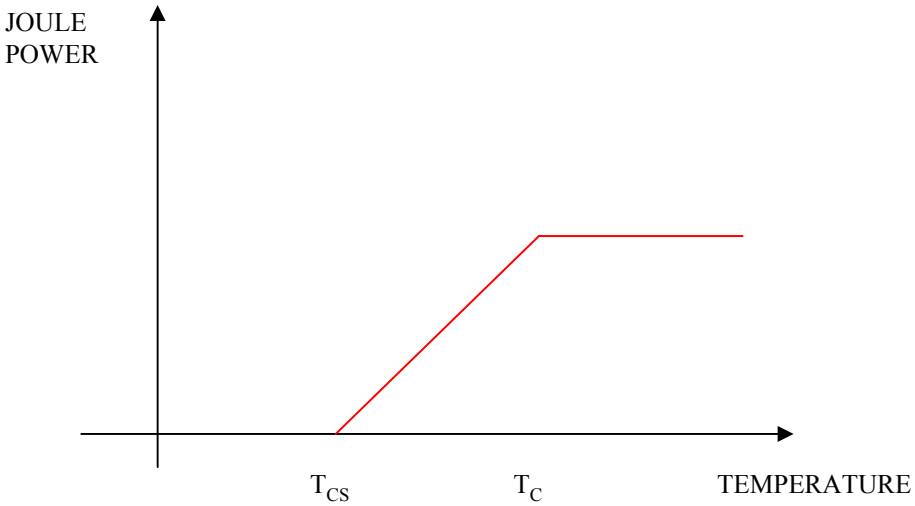

Stability of superconducting cable

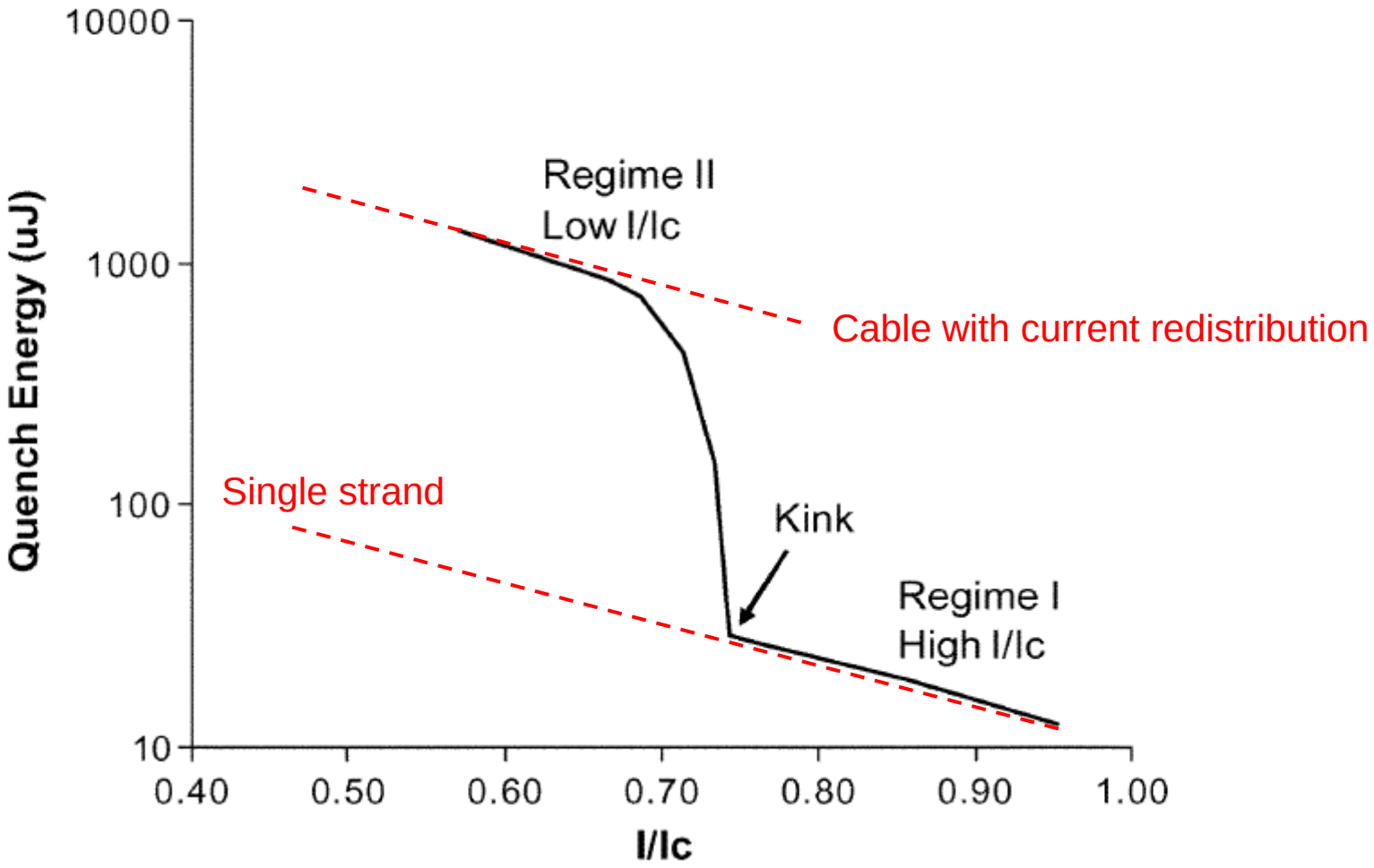

Perturbation spectrum of superconductor

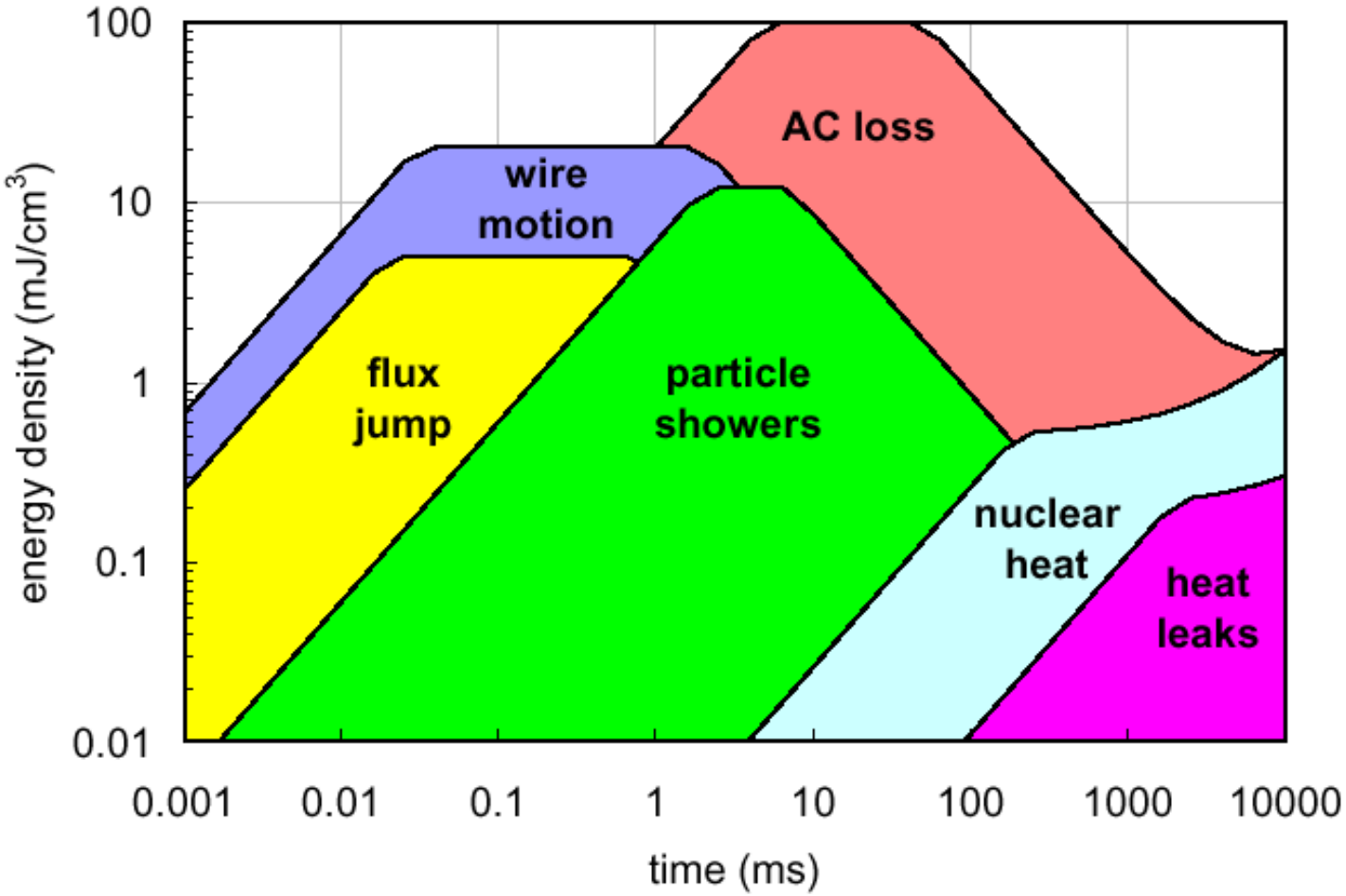

Network model of superconducting cable

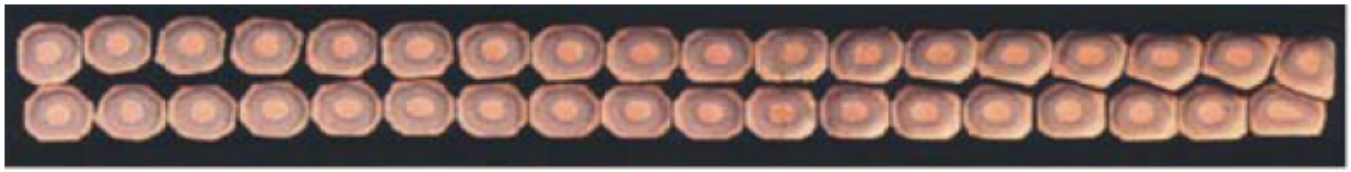

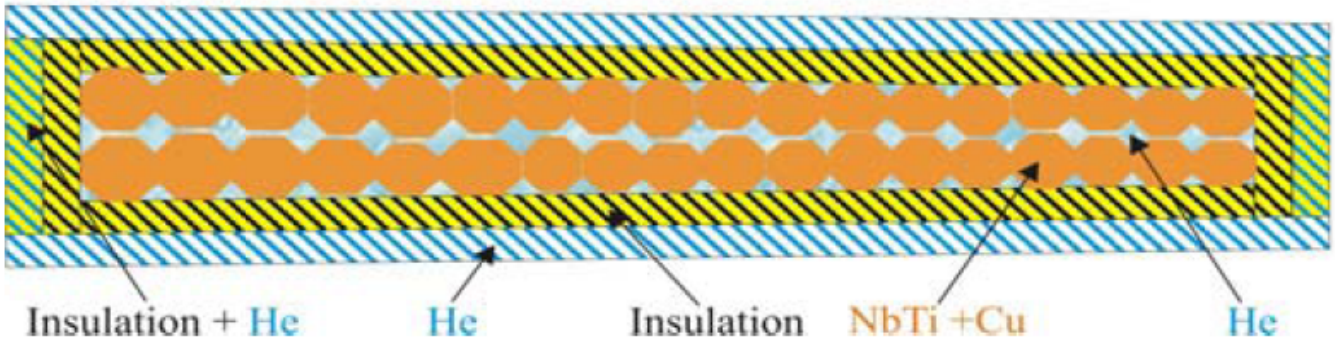

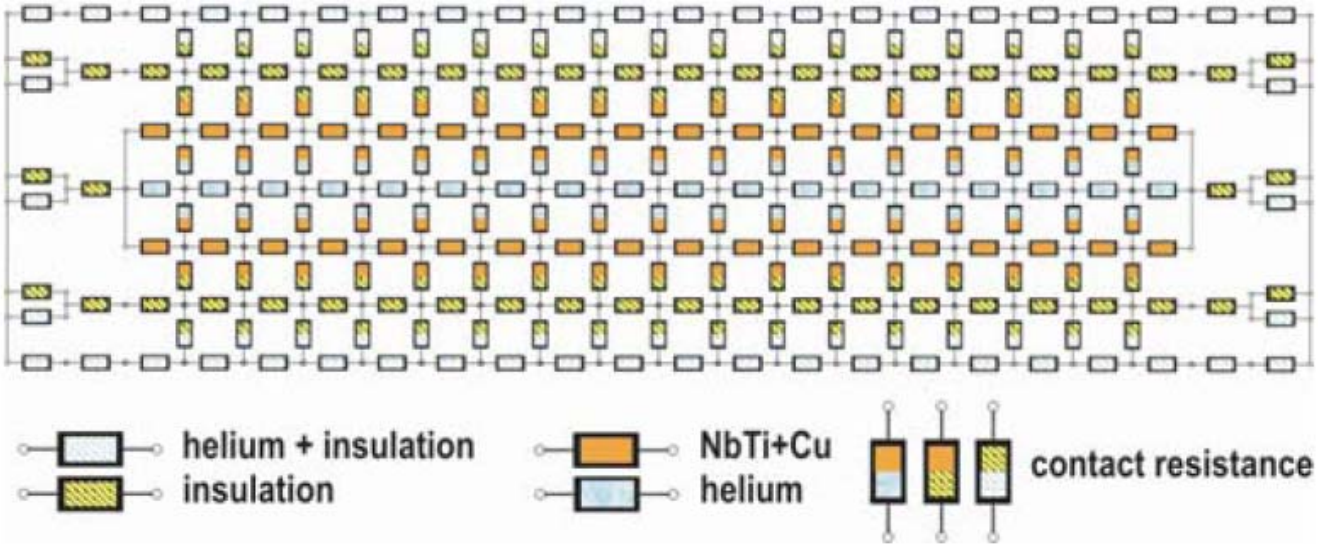

Transient stability of superconducting cable

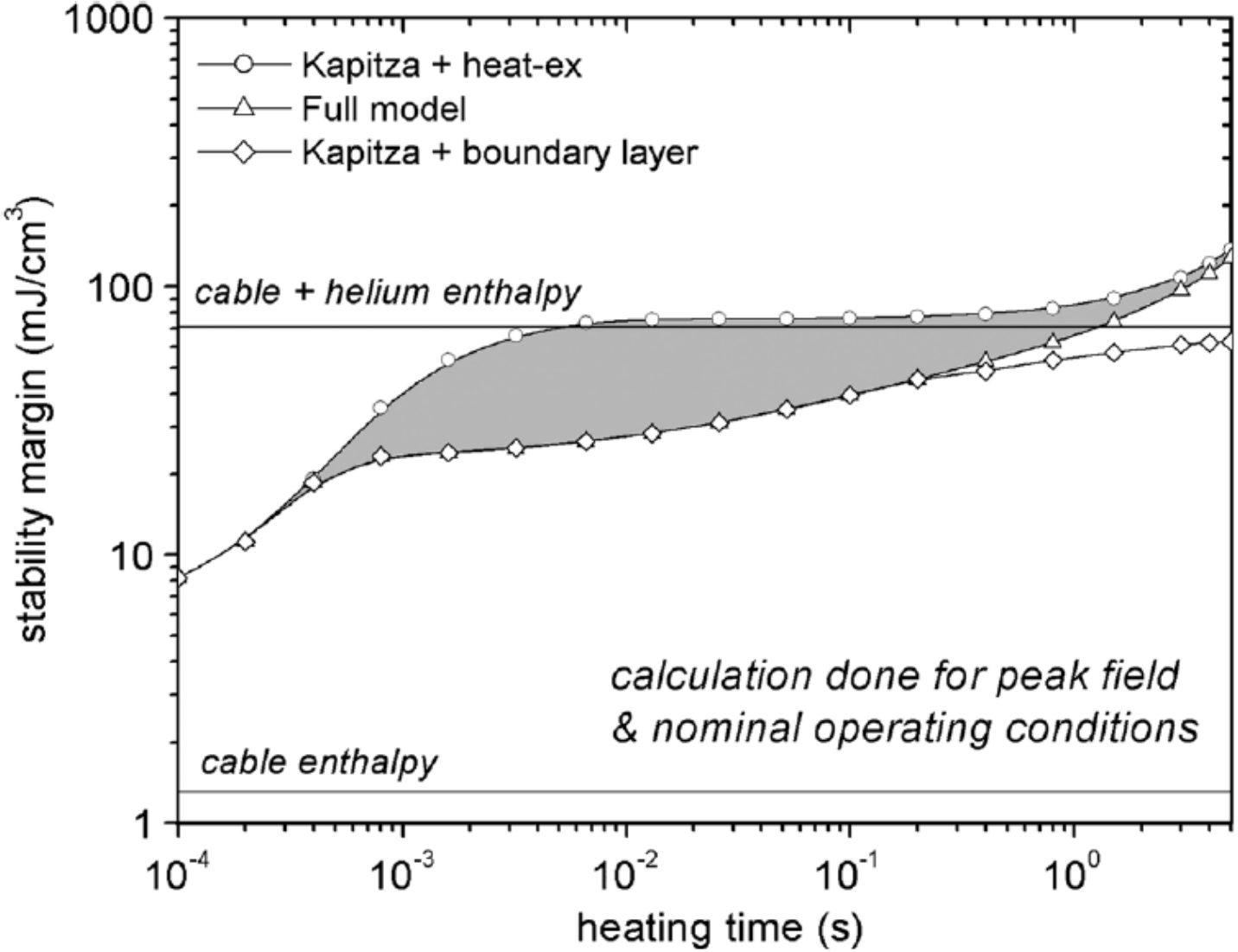

Hot spot temperature after a quench

Assume that quenched section is heated only by Joule effect and adiabatic (no conduction)

$$J^2(t)\rho(T)dt = \gamma C(T)dT \qquad \int_0^{\infty} J^2(t)dt = \int_{T_{op}}^{T_m} \frac{\gamma C(T)}{\rho(T)} dT \qquad J_0^2 T_d = U(T_m)$$

MIITs

To avoid too high hot spot temperature, speed up the quench propagation by any means

1) **Heater**: must be activated fast and reliably (20 ms)

2) "**Quench-back**" inductively propagated

This goes against having LHe in good contact with the conductor (i.e. against stability)!

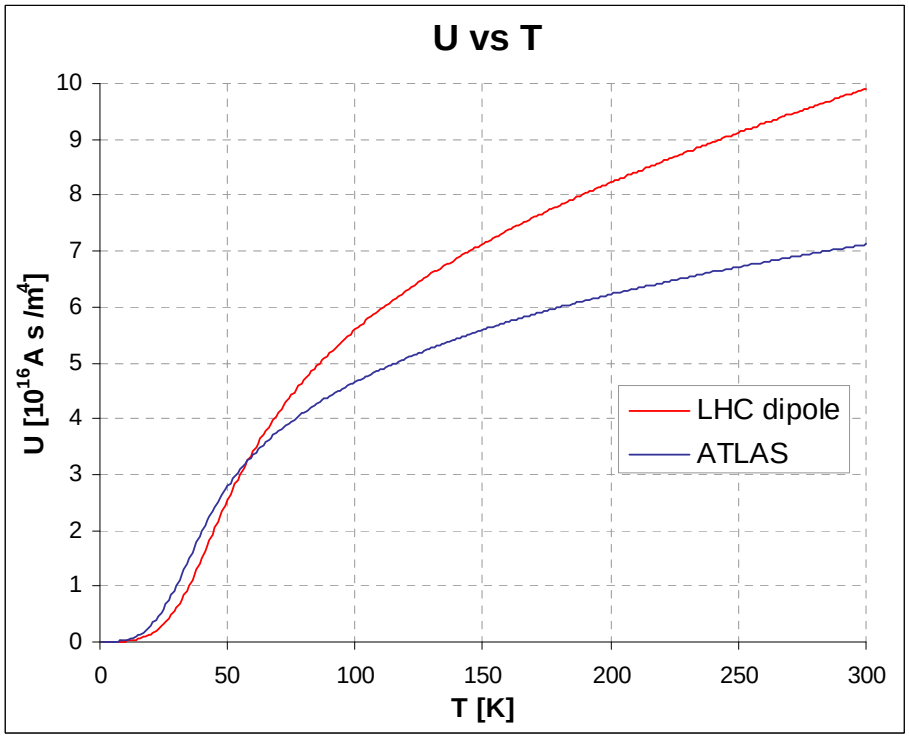

LHC magnet circuit protection scheme

Dissipate energy of magnet string by inserting discharge resistor in circuit

Fire heater to spread the quench over maximum coil volume and limit temperature

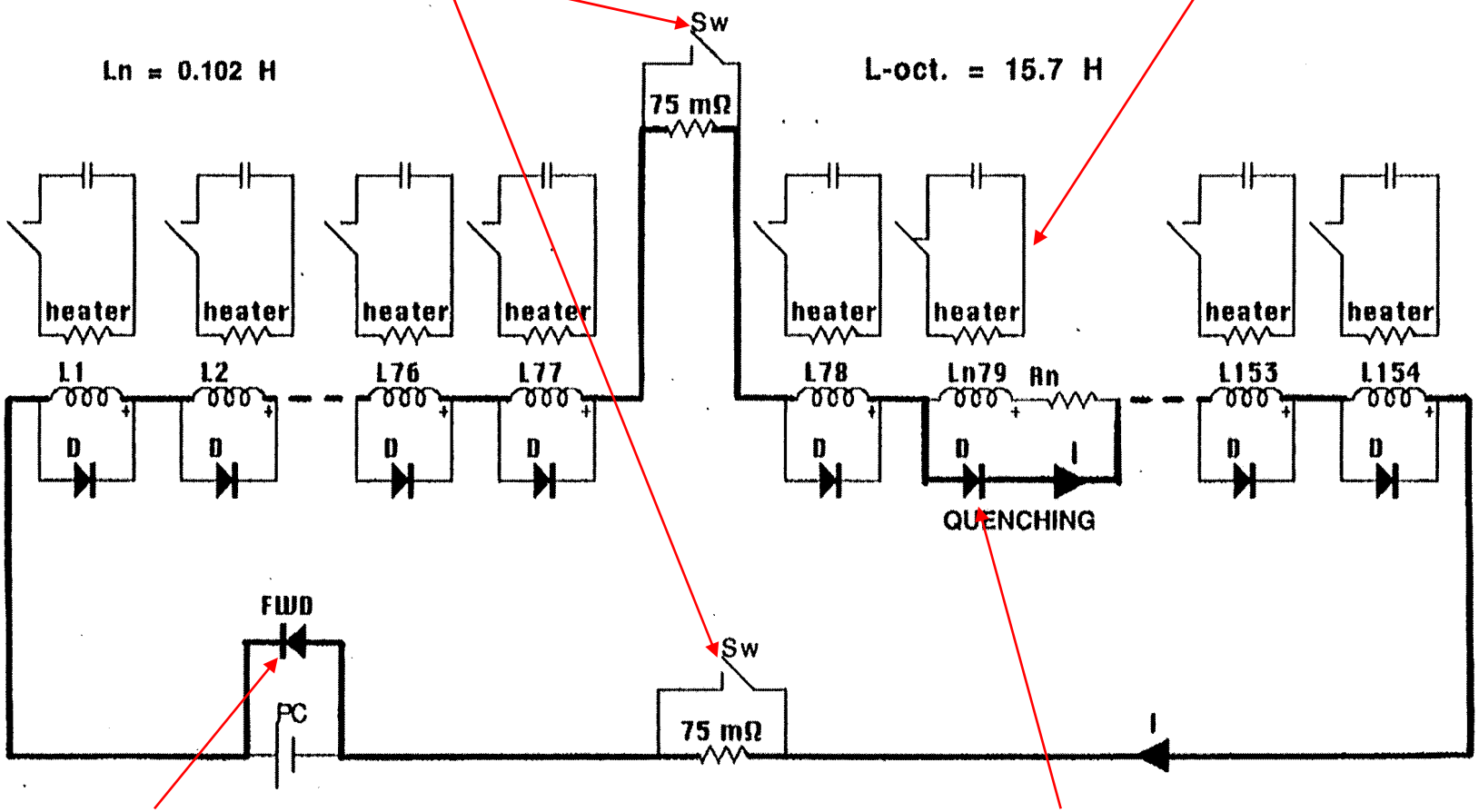

Free-wheeling diode across power converter

Diode bypasses quenched magnet during current discharge in string

Magnet bypass diodes

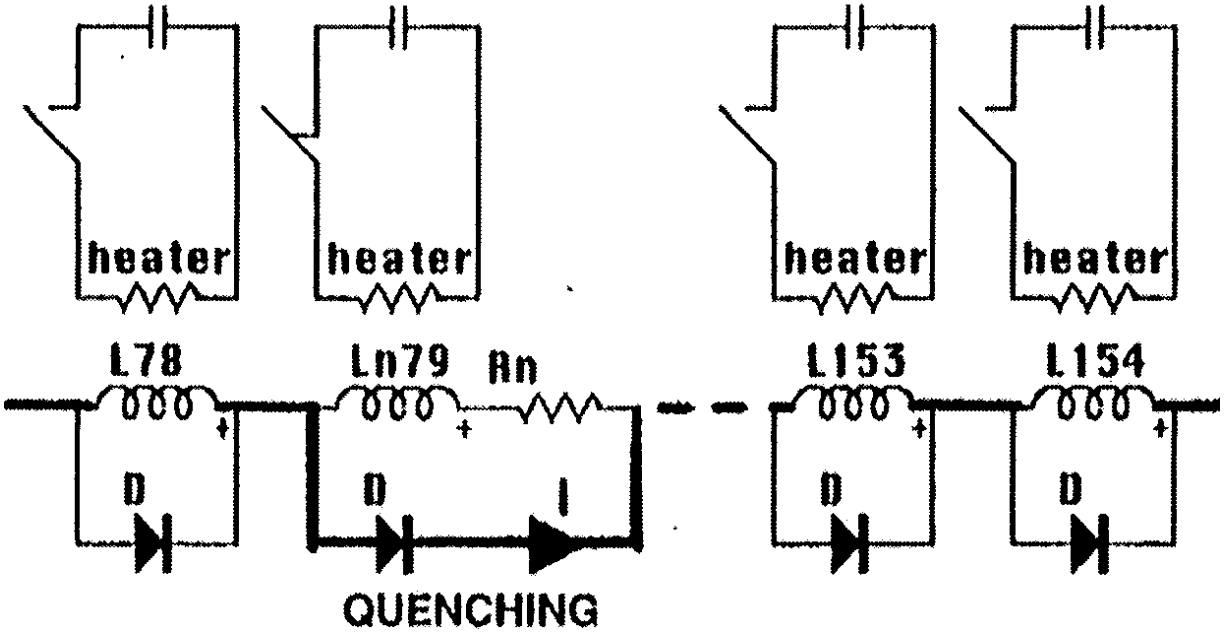

Io = 12 kA

Current discharge time constant ~ 100 s

12 kA DC switchgear & discharge resistors

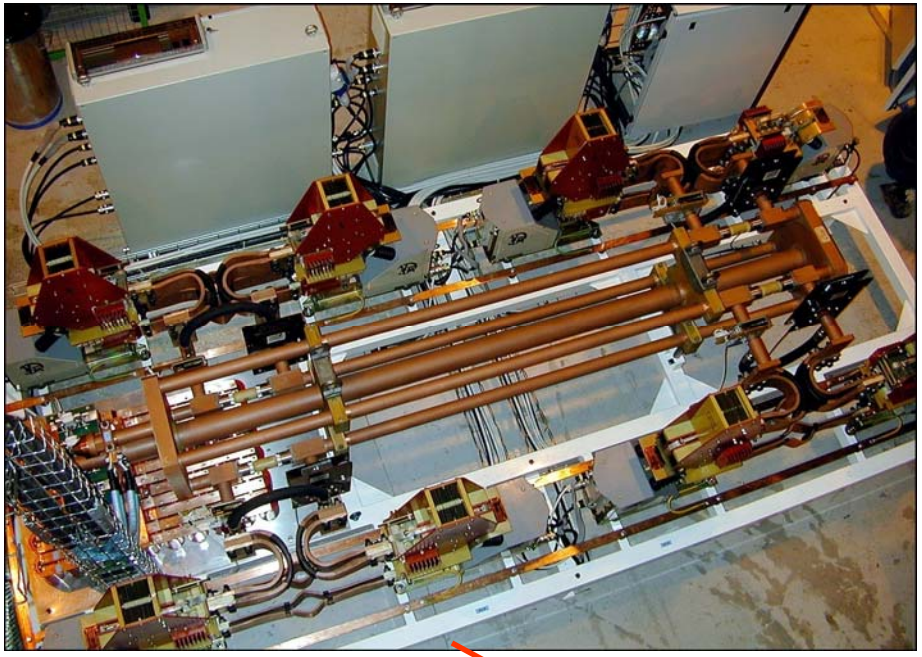

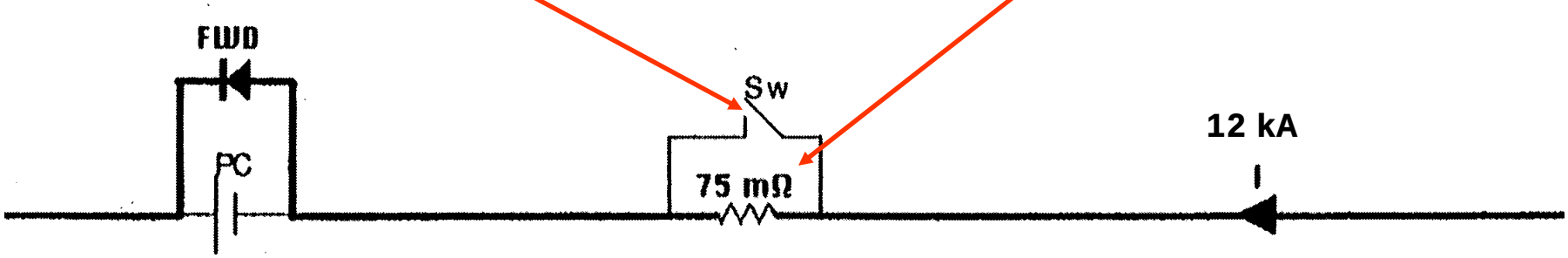

Contents

- The LHC in a nutshell
- Performance
  - Energy
  - Luminosity
  - Collective effects
  - Dynamic aperture
- Technology
  - Superconducting magnets
  - Powering and protection
  - Cryogenics
  - Vacuum
- Project management

General layout of LHC cryogenic system

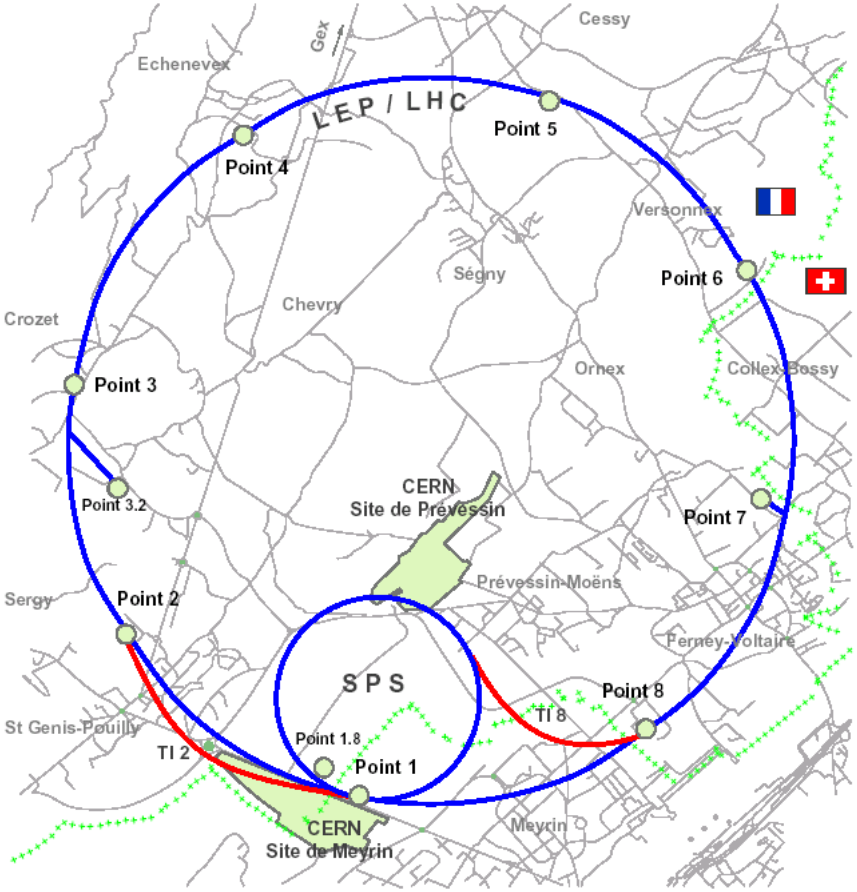

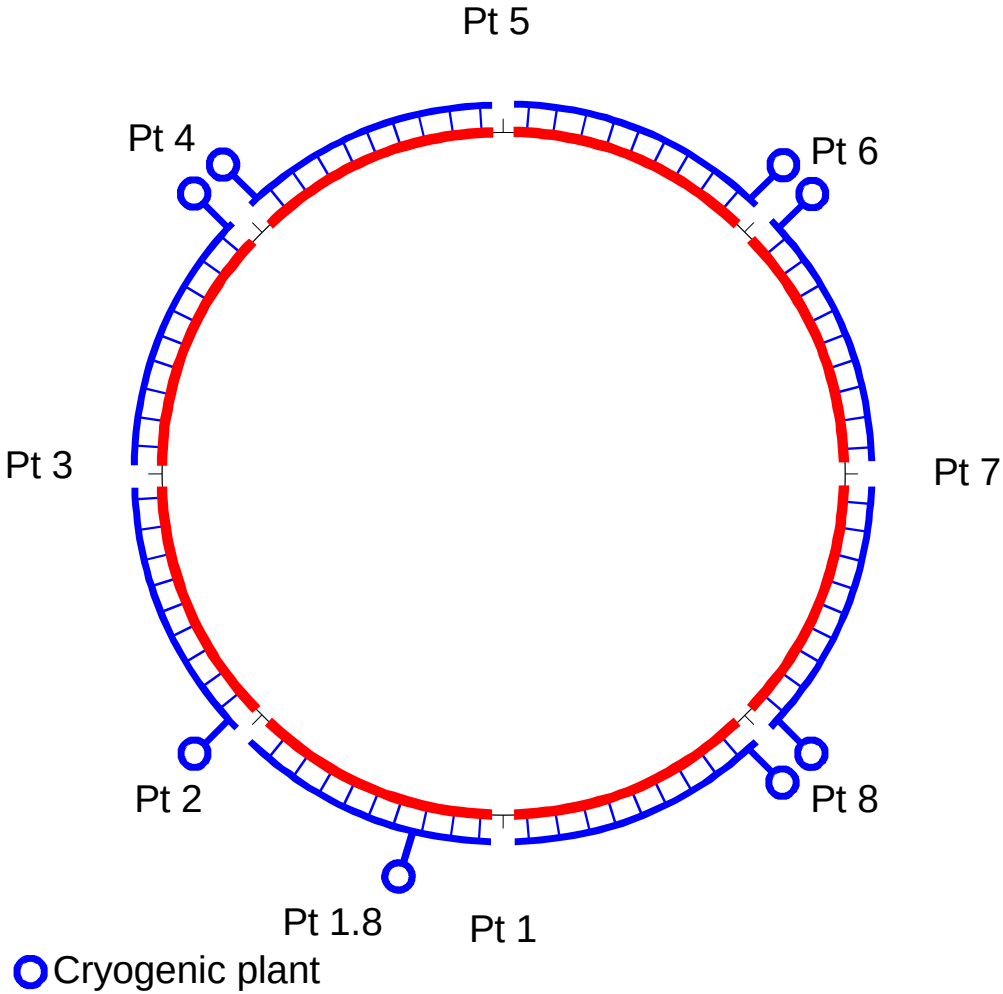

Transport of refrigeration in large distributed cryogenic systems

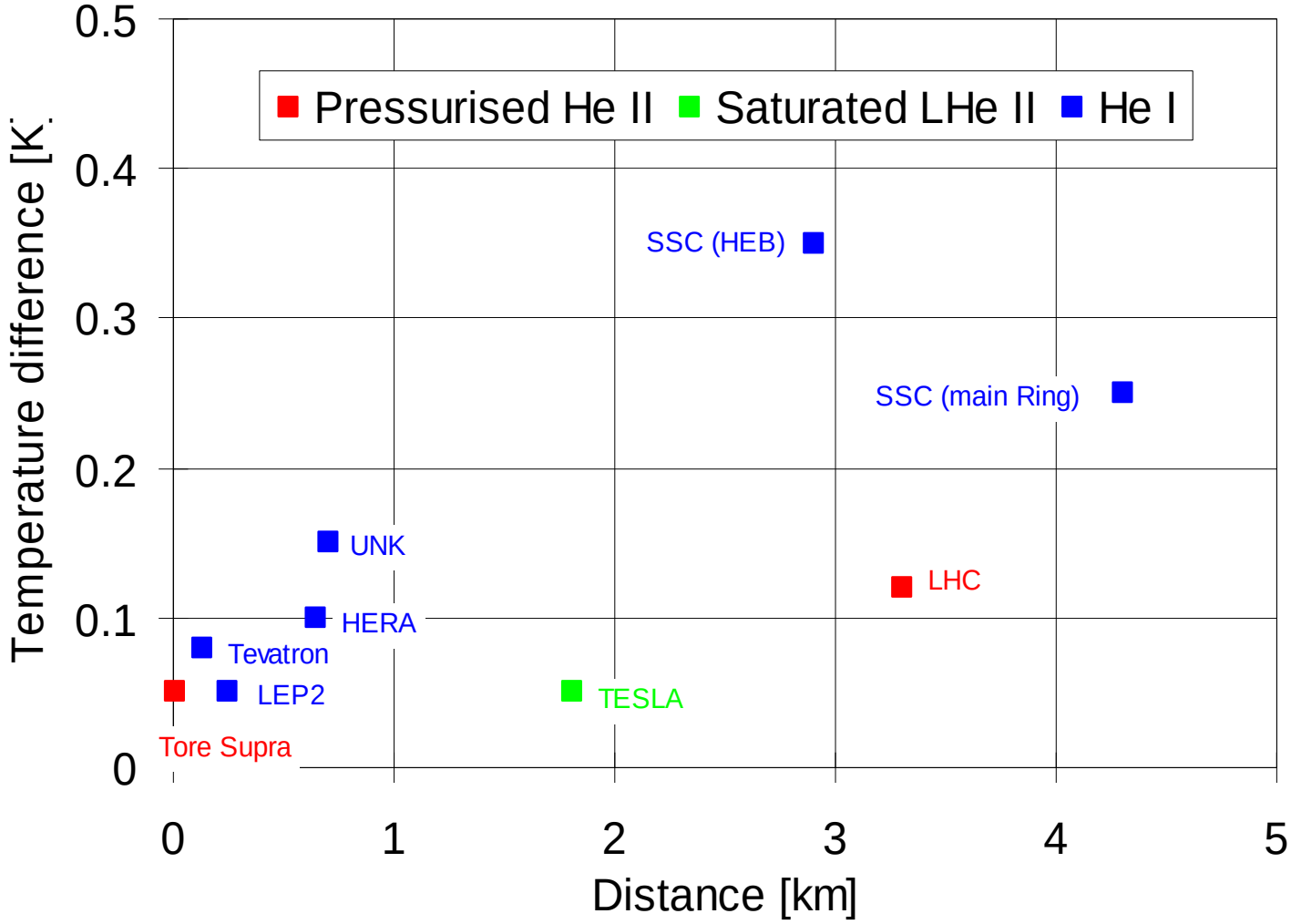

Cooling with superfluid helium

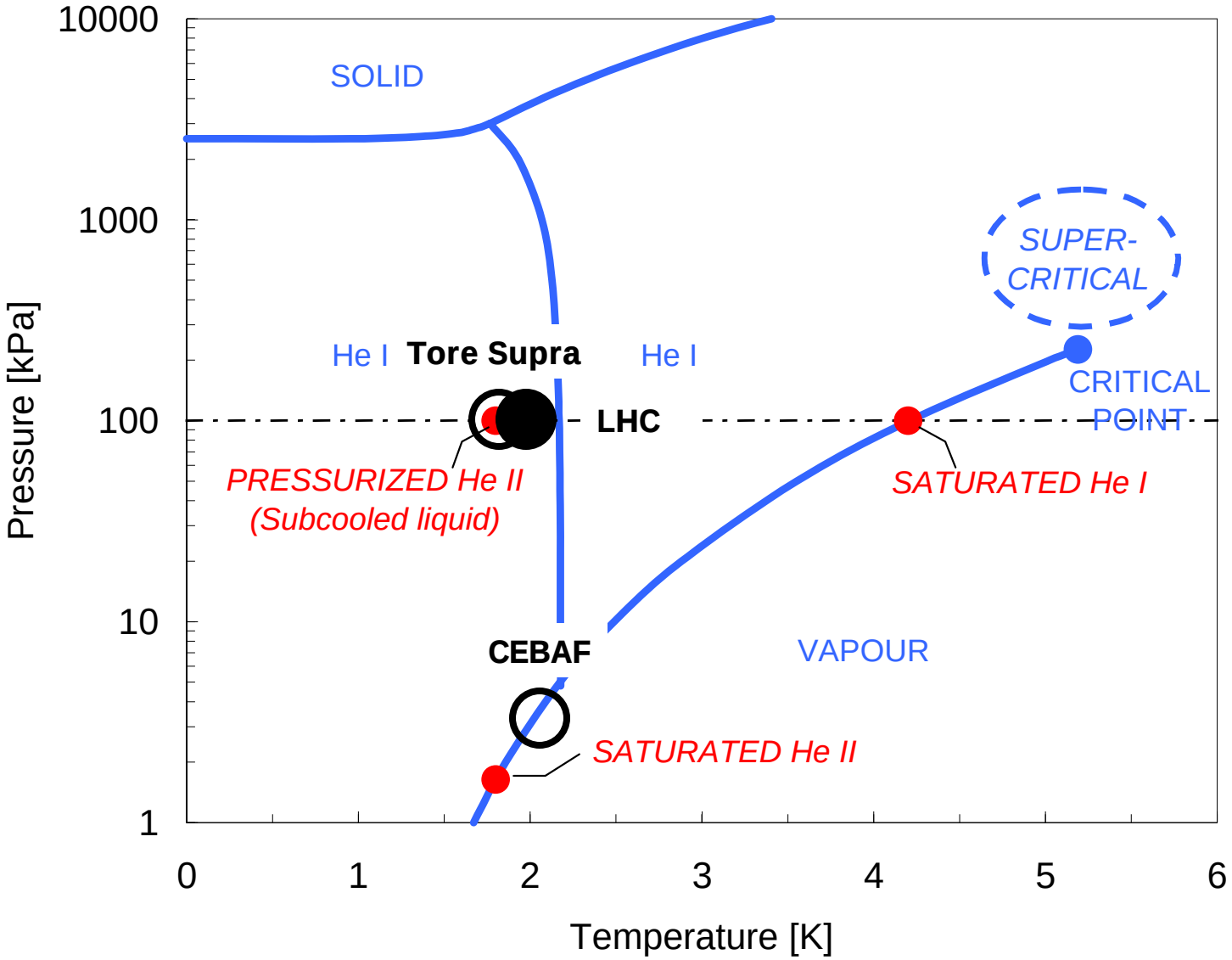

Large projects cooled by superfluid helium

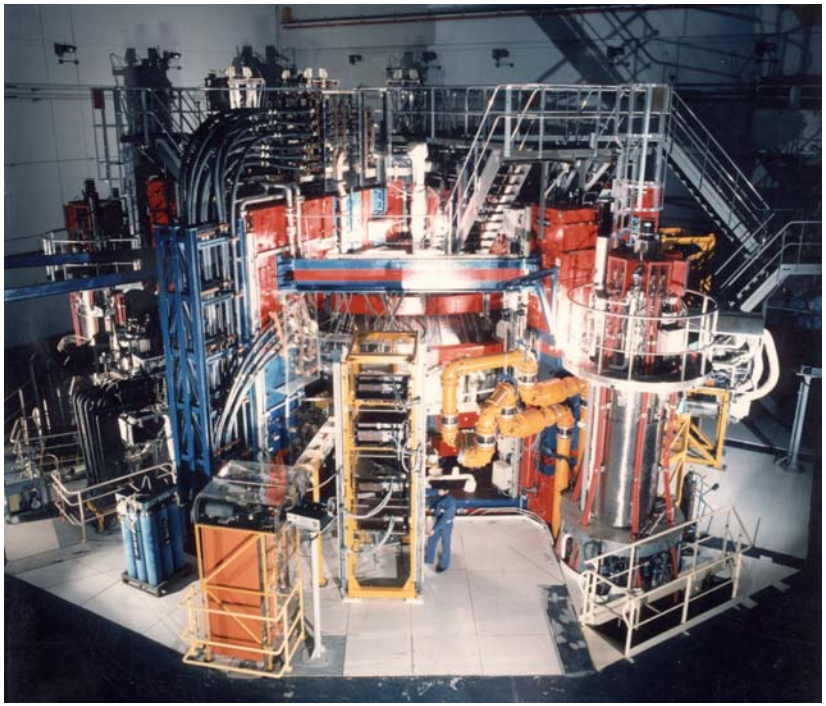

Tore Supra tokamak,
Cadarache (France)

CEBAF accelerator,
Newport News (USA)

Large-scale superfluid helium systems

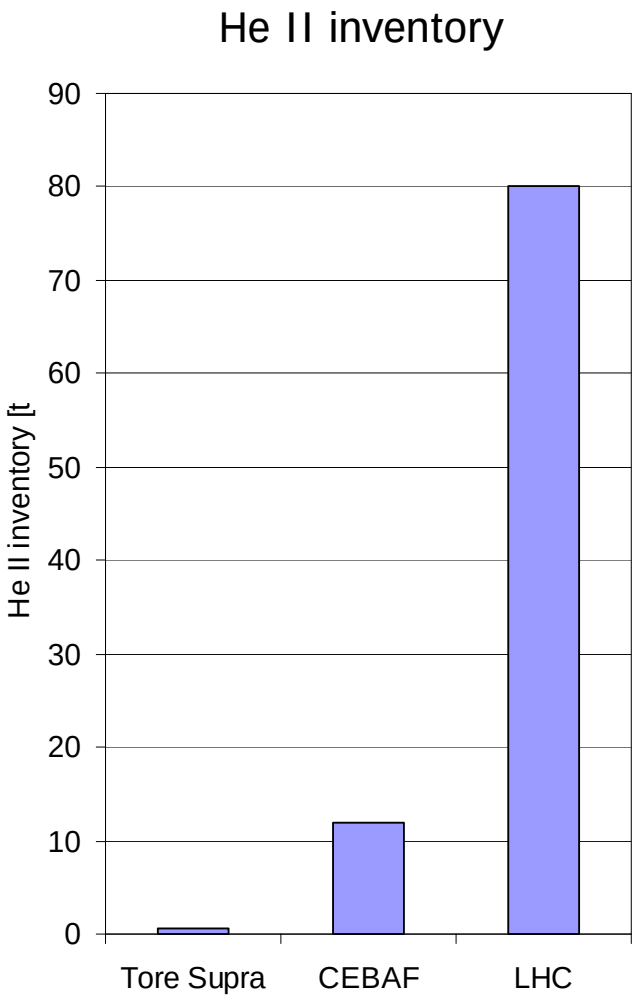

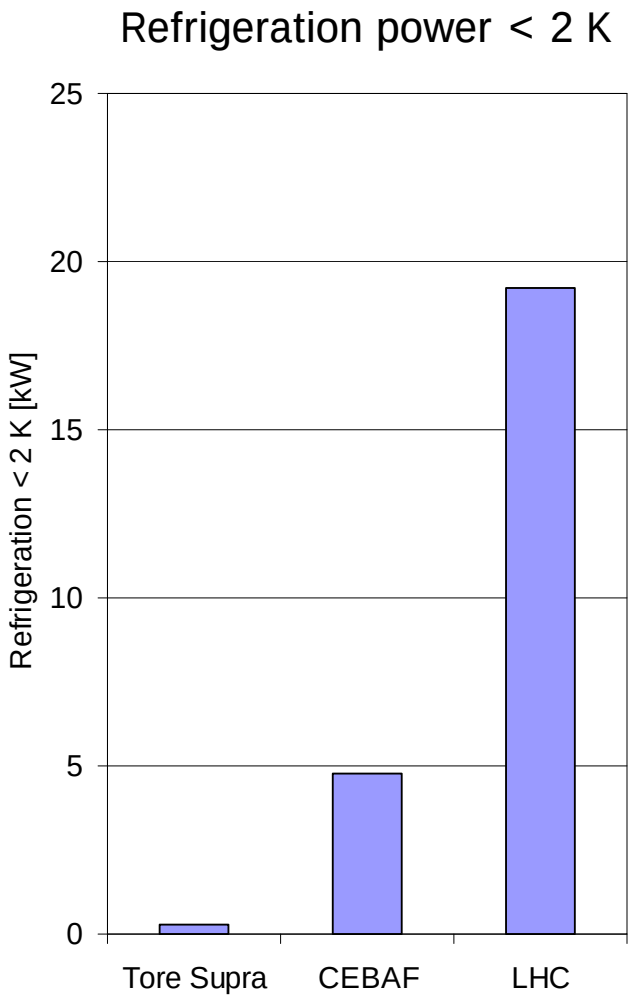

Discovery of superfluidity in He II (1938)

J.F. Allen & A.D. Misener (Cambridge)
P.L. Kapitsa (Moscow)

Vaporization of liquid helium above and below the transition

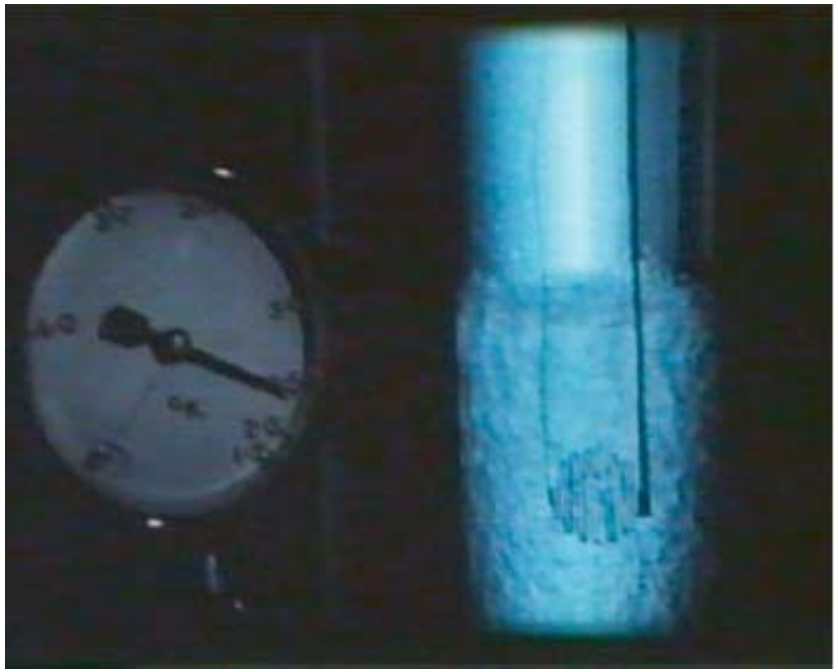

He I (T=2.4 K)

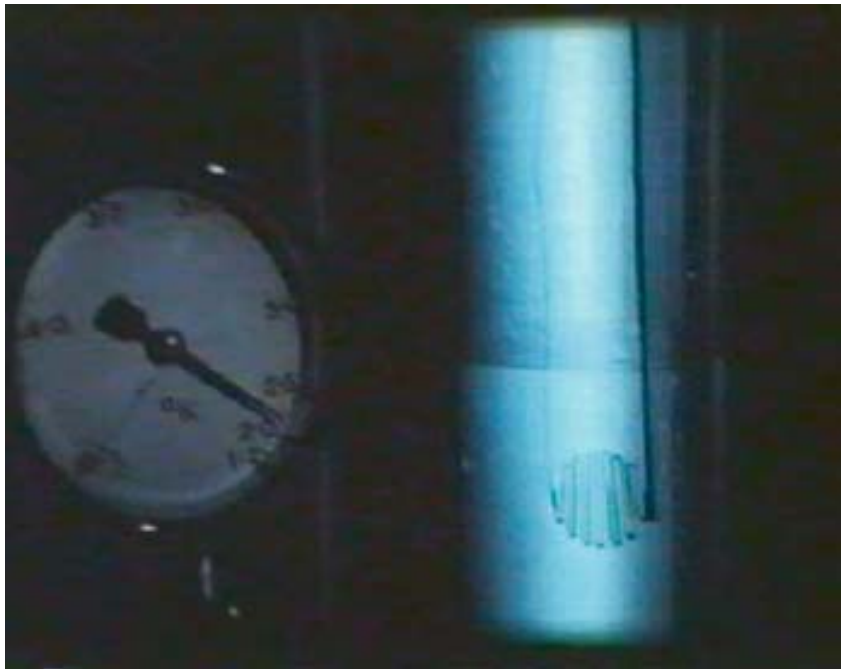

He II (T=2.1 K)

Theoretical approaches to superfluid helium

Fritz London

Laszlo Tisza

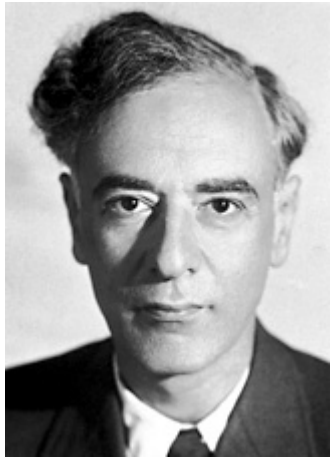

Lev Davidovich Landau

$$T_{\mathrm{BEC}} = \left(\frac{2\pi\hbar^2}{1.897 m k_B} \right) n^{2/3}$$

Bose-Einstein condensation

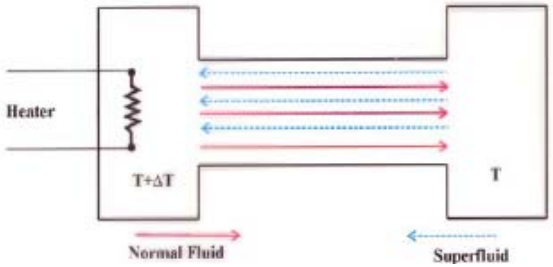

Two-fluid model

$$\epsilon = \hbar\omega = \Delta + \frac{(p - p_0)^2}{2\mu}$$

Quasi-particle description

Thermophysical properties of He II

- Temperature < 2.17 K
- Low effective viscosity
  - 100 times lower than water at normal boiling point
- Very high specific heat
  - 10^5 times that of the conductor by unit mass
  - 2×10^3 times that of conductor by unit volume
- Very high thermal conductivity
  - 10^3 times that of OFHC copper, cryogenic grade
  - Peaking at 1.9 K
  - Still, insufficient for transporting heat over large distances across small temperature gradients

Specific heat of liquid helium and copper

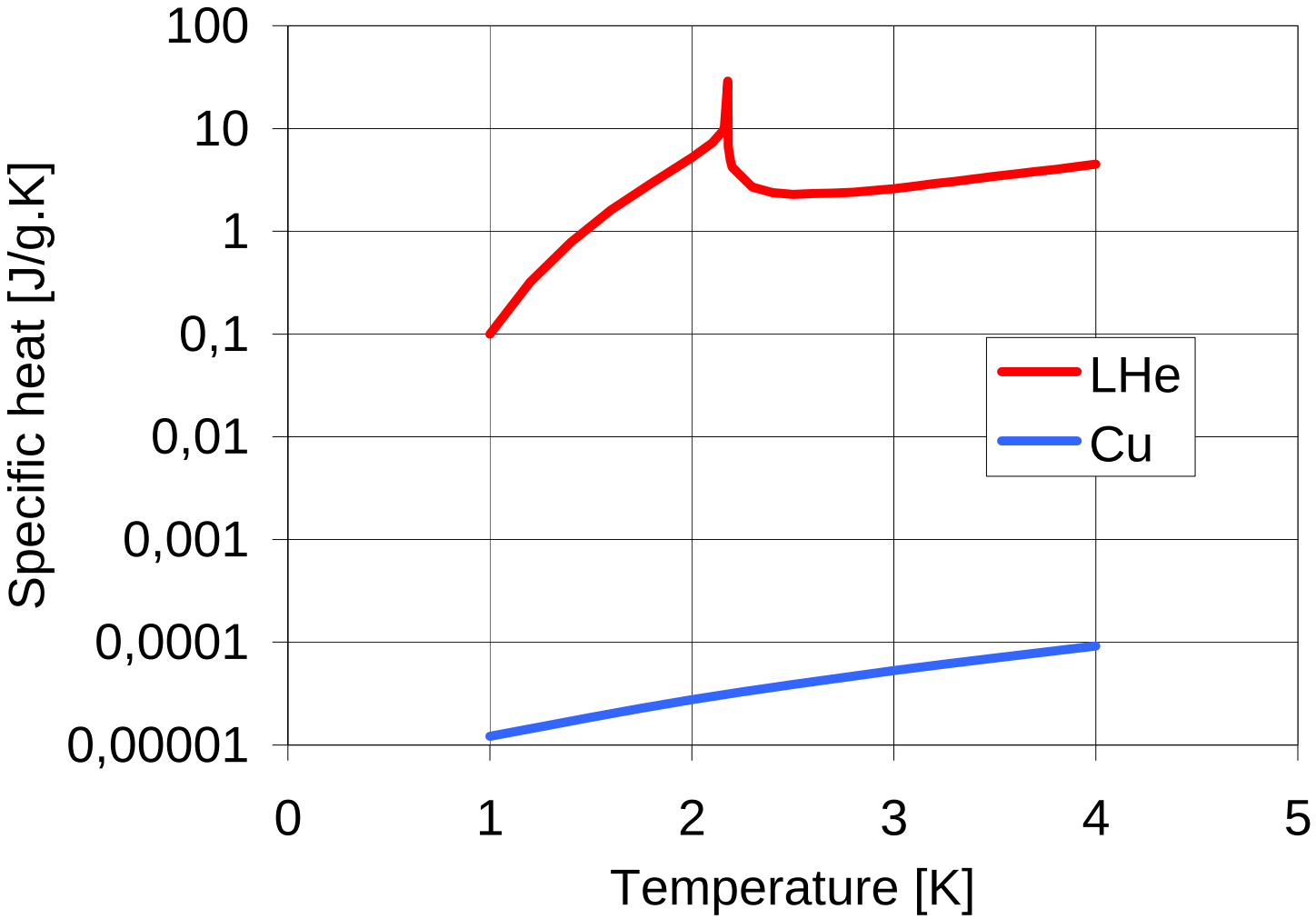

Thermal conduction in He II: two-fluid model

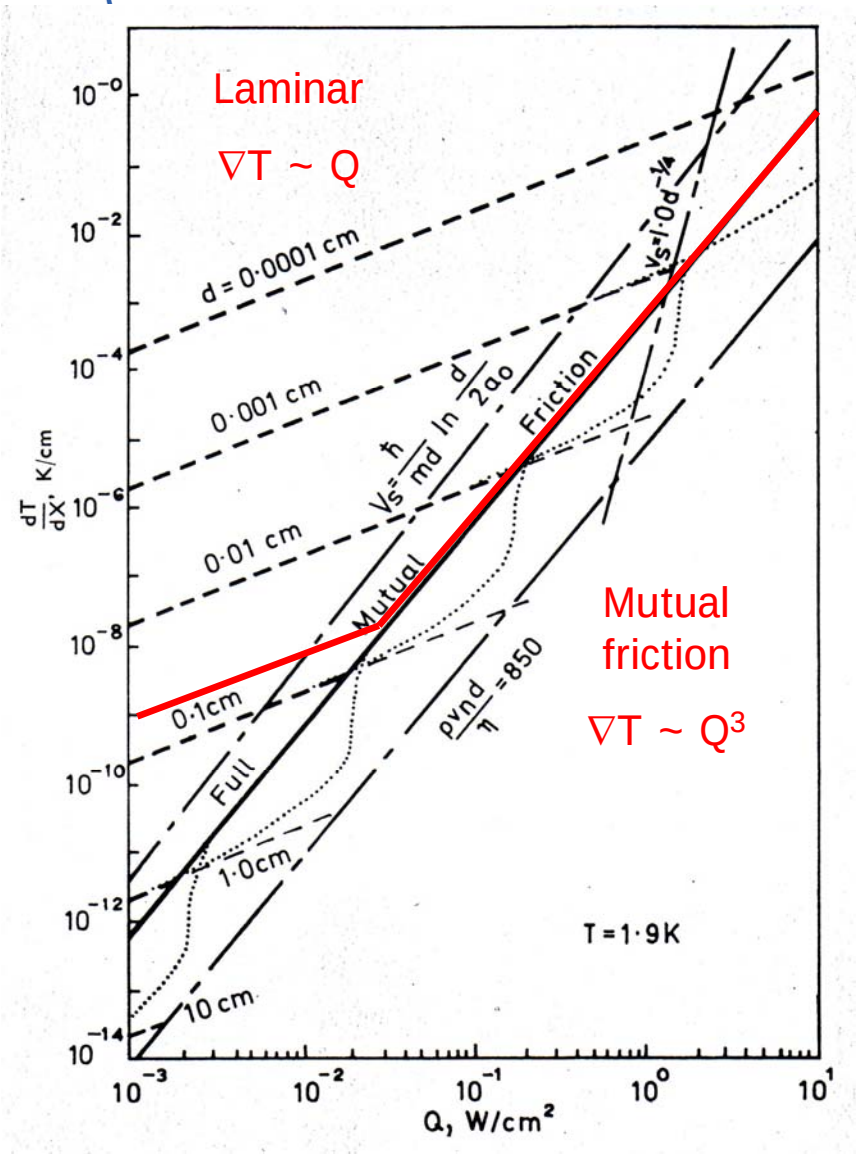

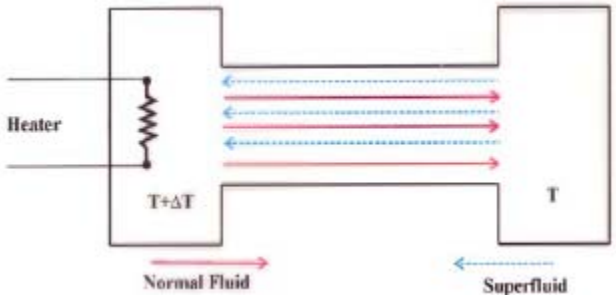

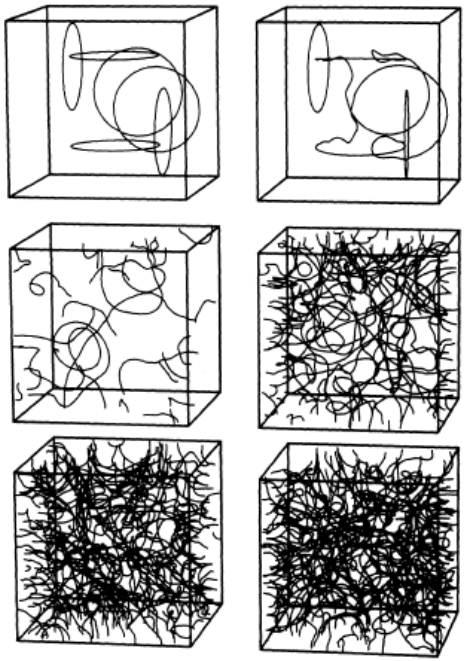

V. Arp

K.W. Schwartz

Thermal conduction in He II: practical results

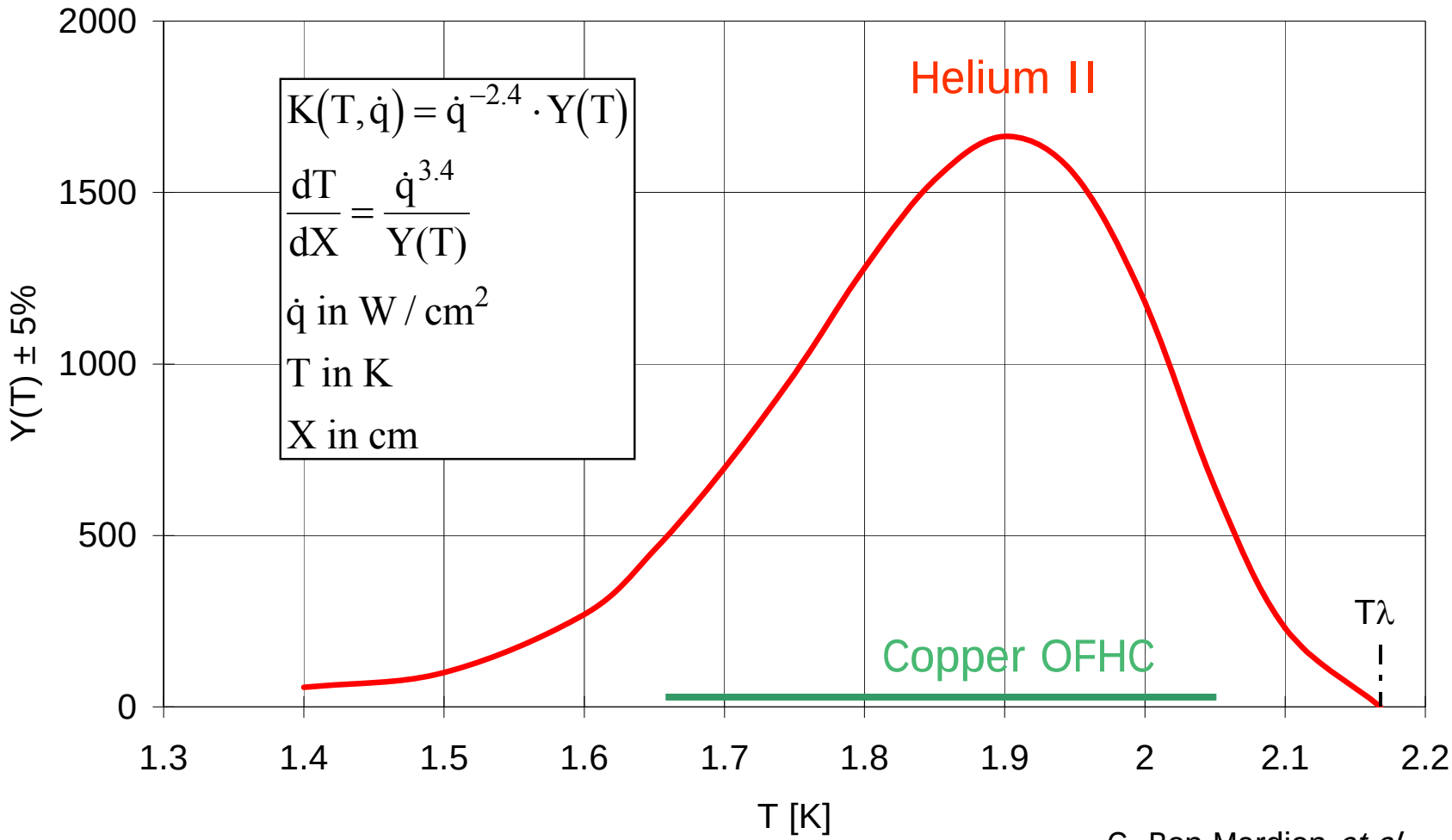

G. Bon Mardion *et al.*

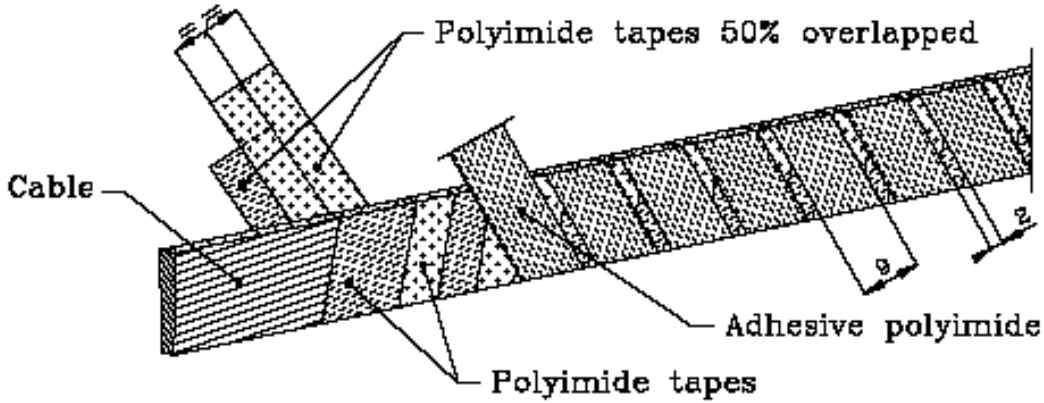

Heat transfer across electrical insulation of superconducting cable

Conduction in polyimide

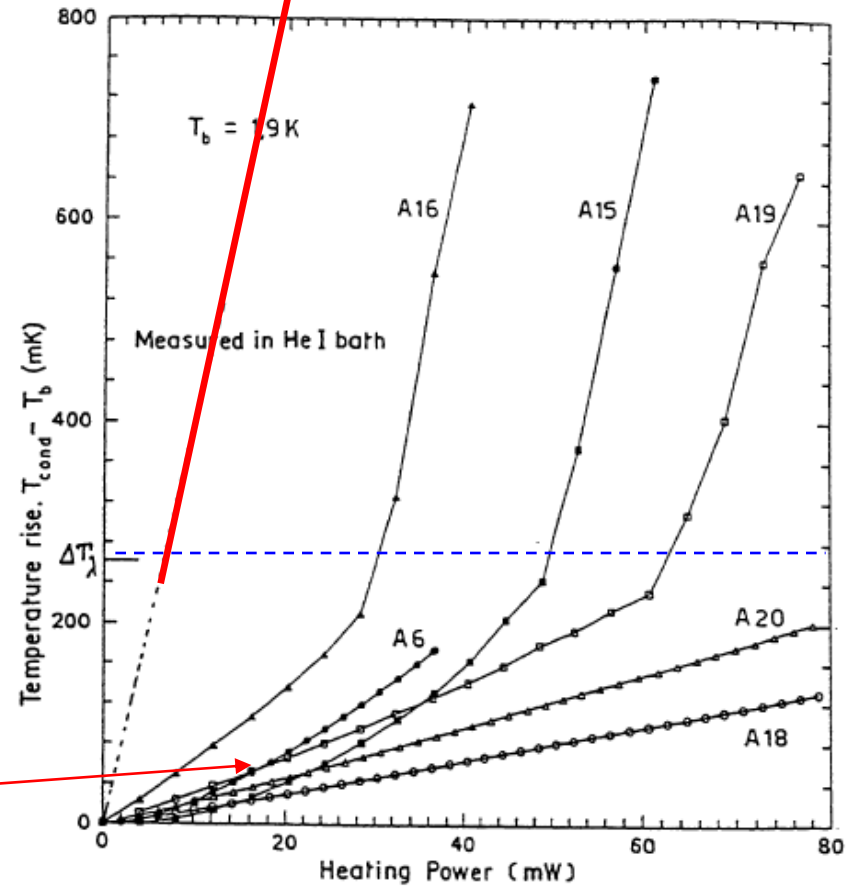

Conduction in polyimide short-circuited by He II

C. Meuris *et al.*

LHC magnet string cooling scheme

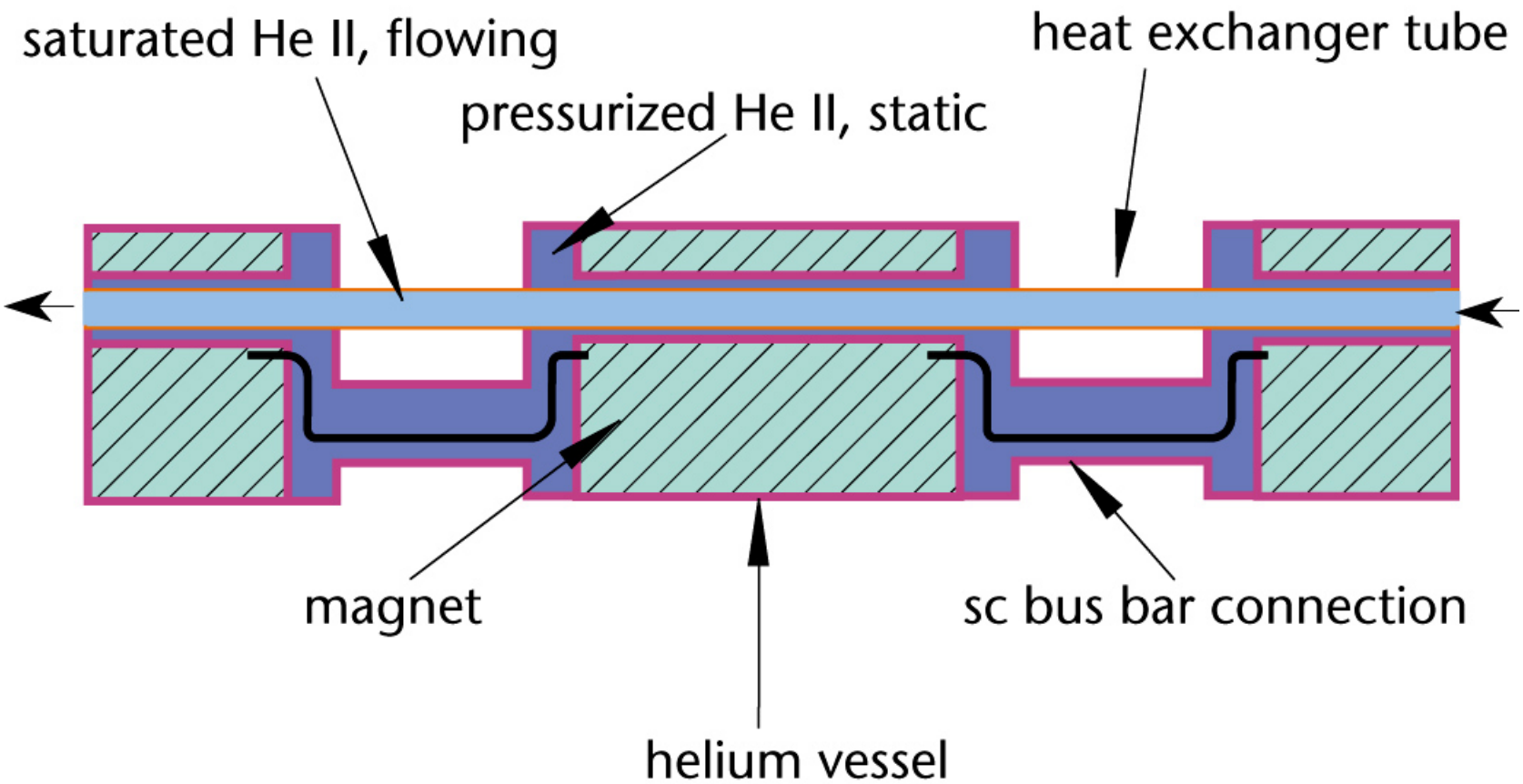

Cryogenic operation of LHC sector

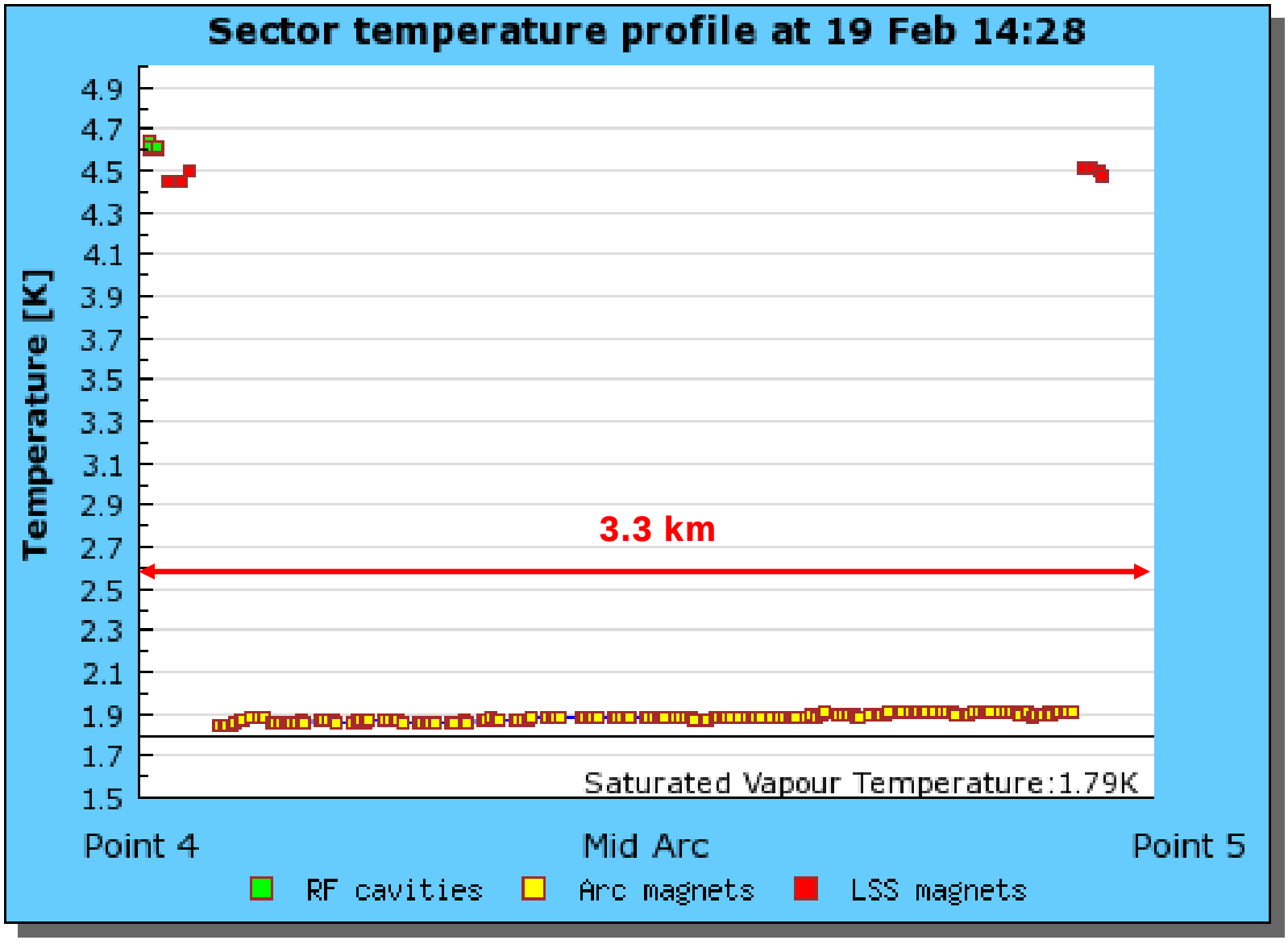

18 kW @ 4.5 K helium refrigerators

Compressor station

18 kW @ 4.5 K helium refrigerators

Coldboxes

33 kW @ 50 K to 75 K
23 kW @ 4.6 K to 20 K
41 g/s liquefaction

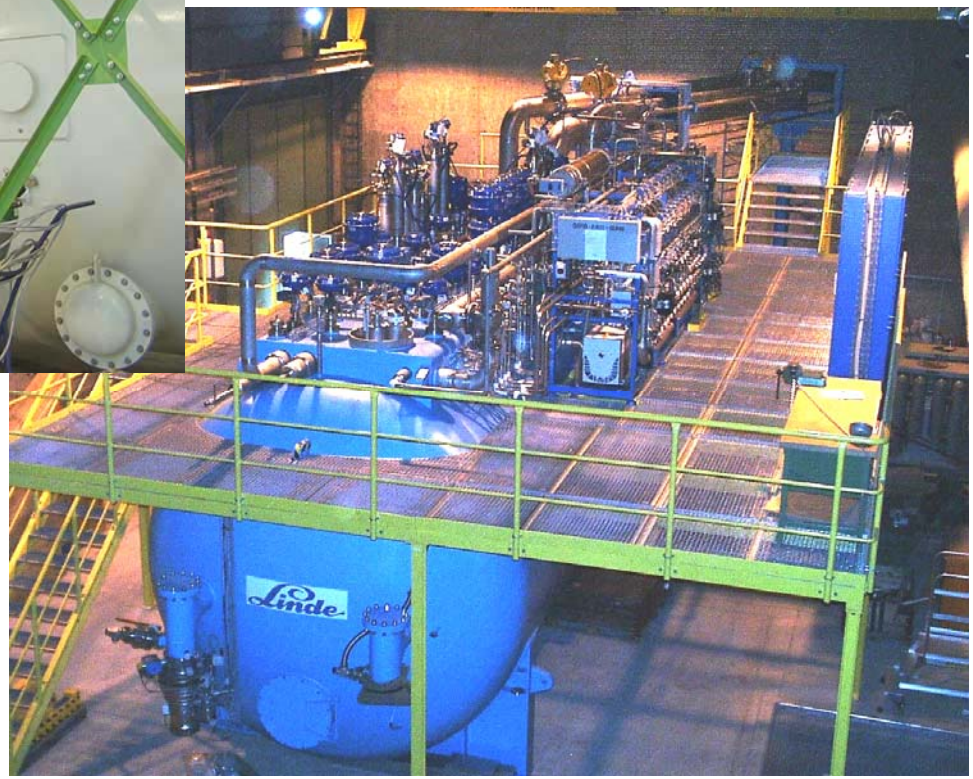

Process cycle & T-S diagram of 18 kW @ 4.5 K cryoplant

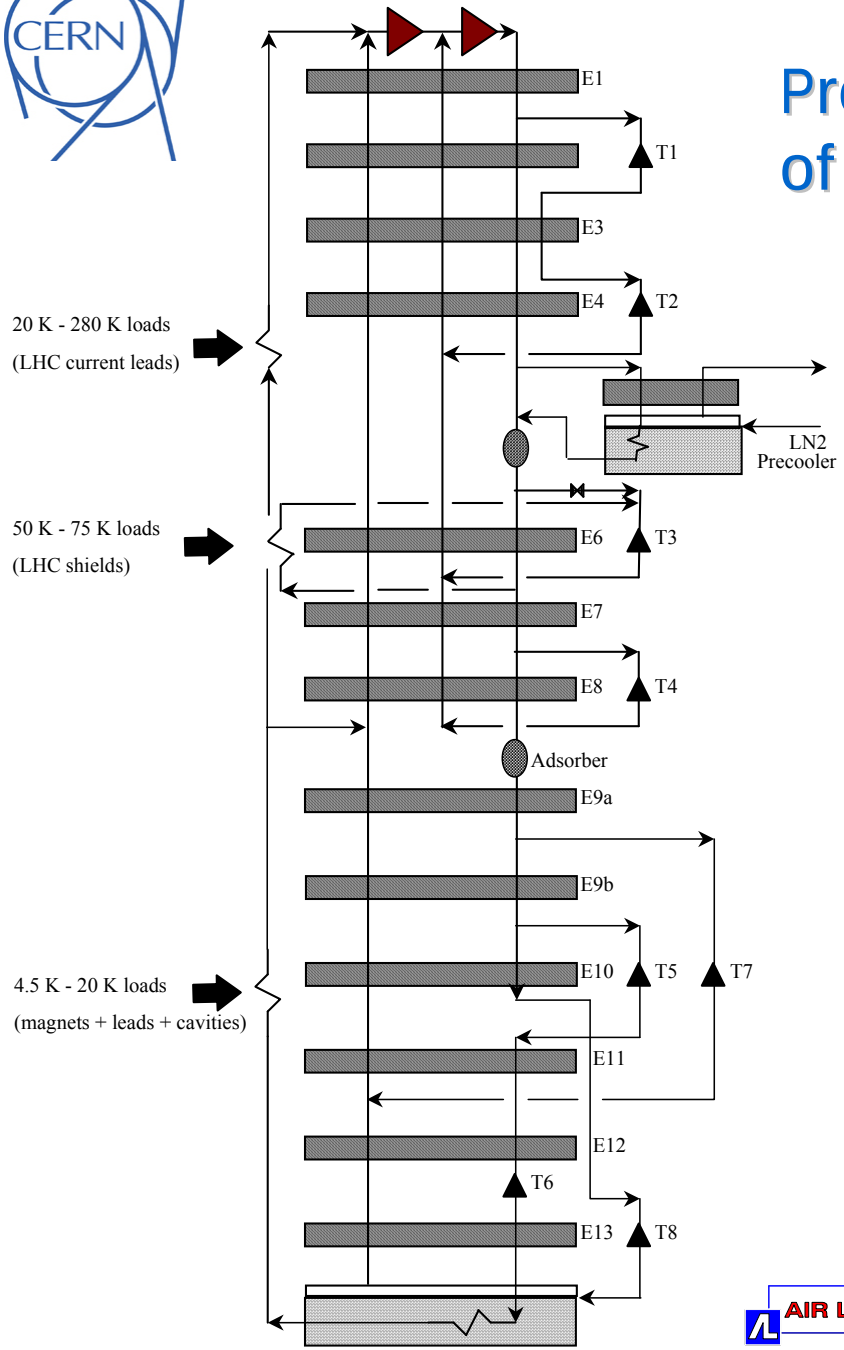

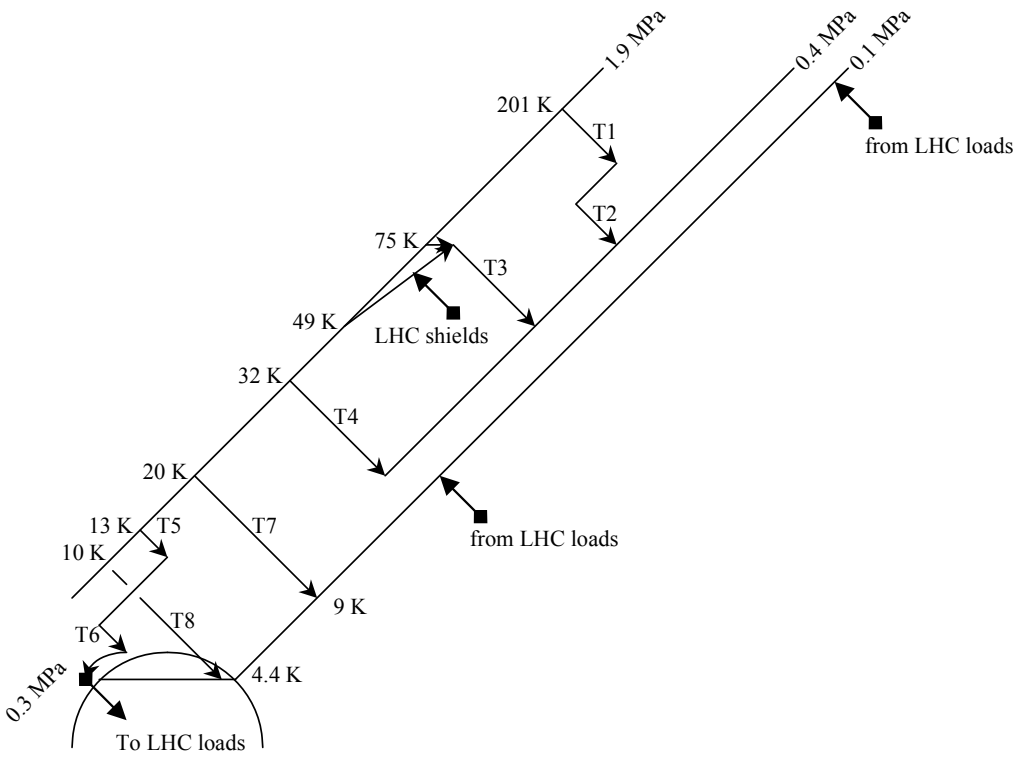

C.O.P. of large cryogenic helium refrigerators at 4.5 K

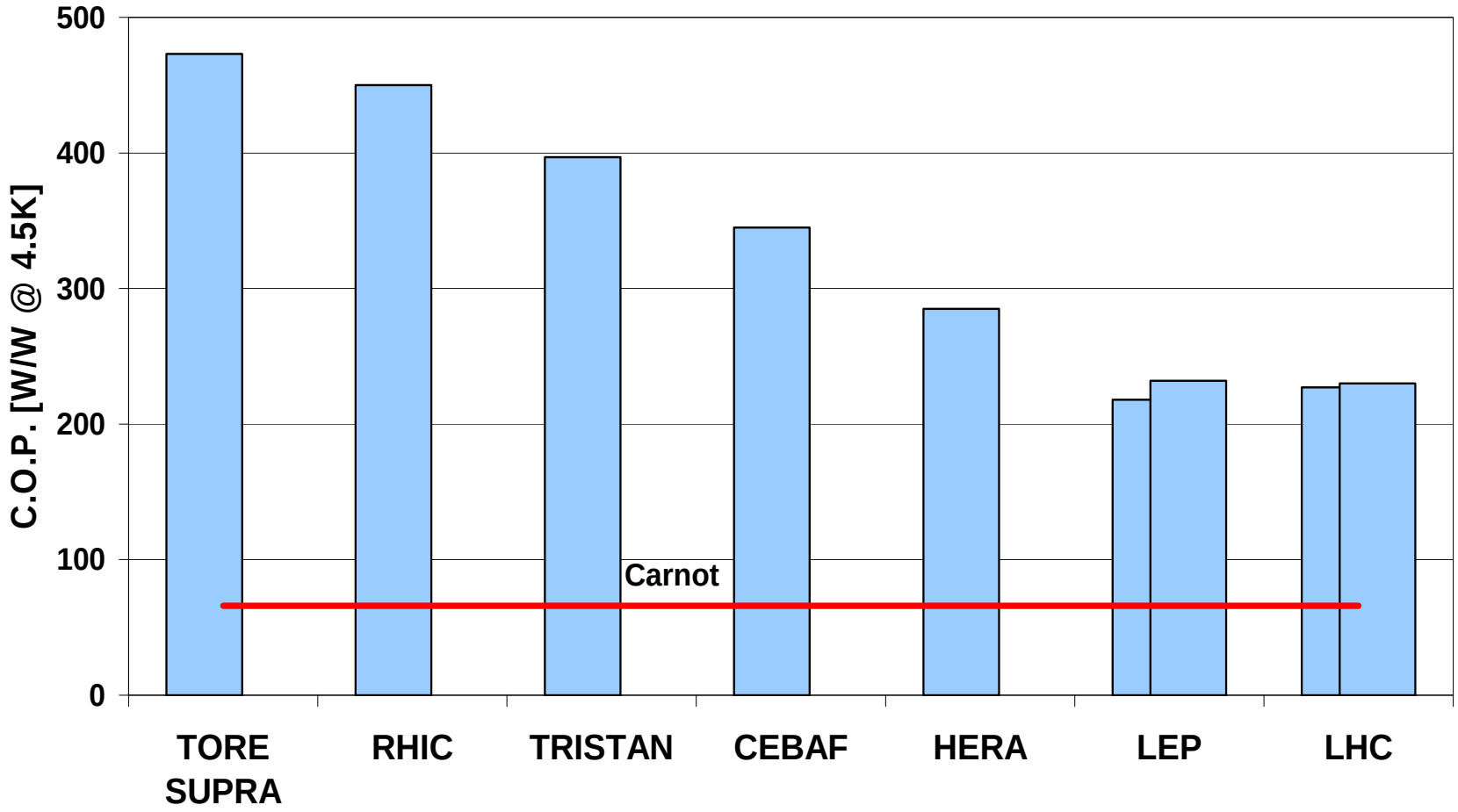

Challenges of high-power 1.8 K refrigeration

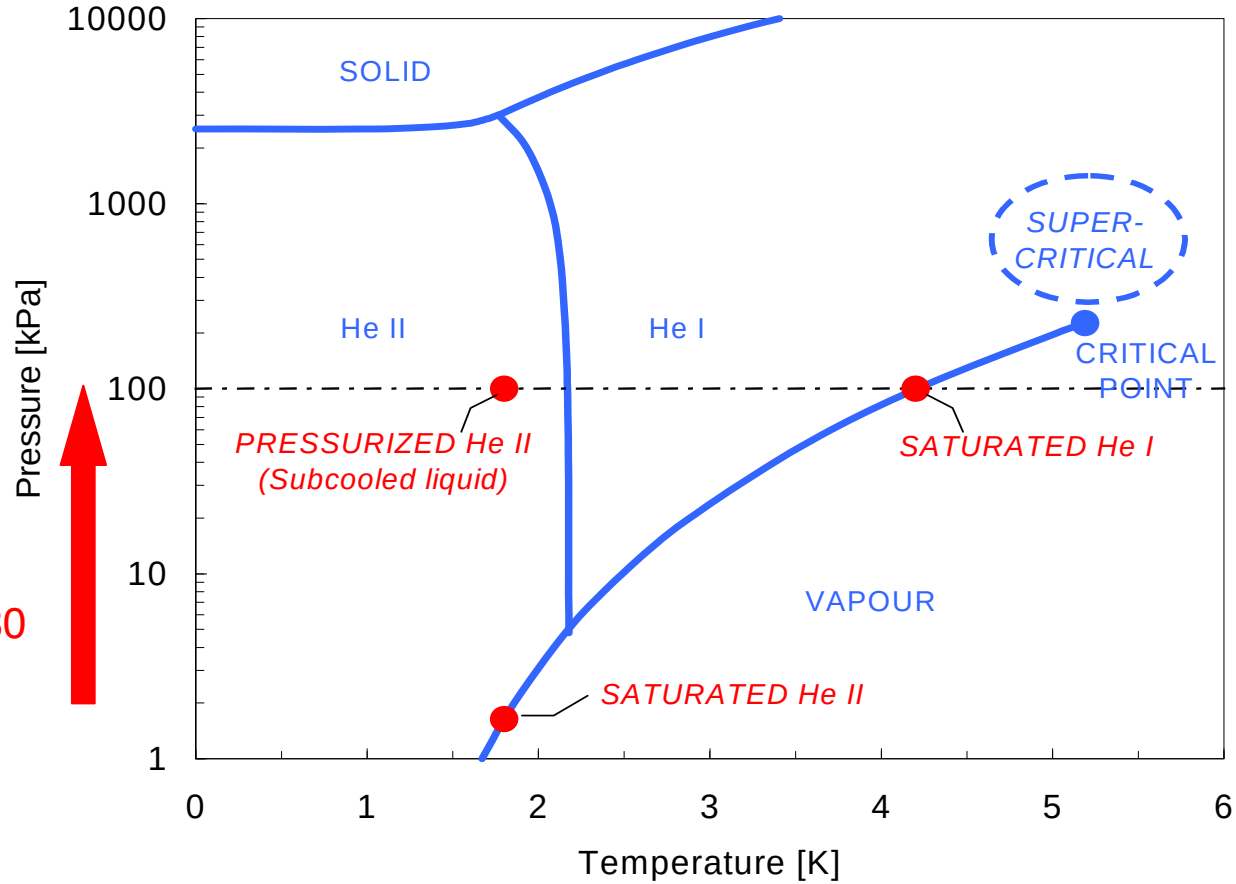

Pressure ratio > 80

- Compression of large mass flow-rate of He vapor across high pressure ratio

⇒ intake He at maximum density, i.e. cold

- Need contact-less, vane-less machine ⇒ hydrodynamic compressor
- Compression heat rejected at low temperature ⇒ thermodynamic efficiency

Cold compressors for 1.8 K refrigeration

Axial-centrifugal impeller

Cartridge 1st stage

4 cold compressor stages

Cooldown of LHC sector (4625 t over 3.3 km)

Unloading of LHe & LN2

600 kW precooling to 80 K with LN2 (up to ~5 tons/h)

First cool-down of LHC sectors

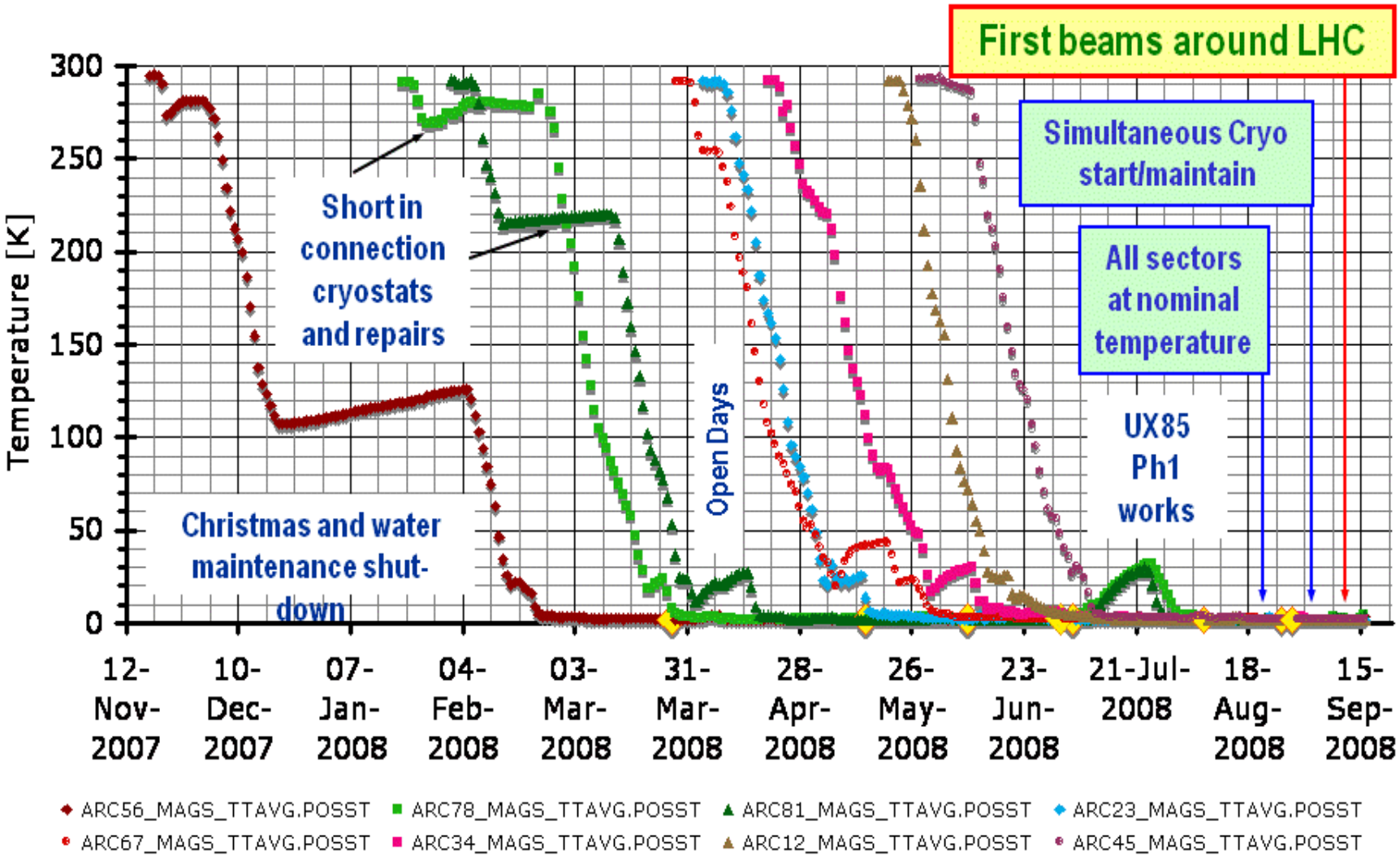

Thermal insulation techniques
Multi-layer reflective insulation

10 layers around cold mass at 1.9 K

30 layers around thermal shield at 50-75 K

Cold surface area in LHC ~ 9 hectares!

Thermal radiation from 290 K (black-body) ~ 400 W/m^2 = 4 MW/ha

Heat flux from 290 K across 30 layers MLI ~ 1 W/m^2 = 10 kW/ha

Thermal insulation techniques

Low-conduction non-metallic support posts

LHC cold mass to be supported = 37'500 tons

Conduction length = support height ~ 0.2 m

At a compressive stress of 50 N/mm^2, this requires a total support cross-section of 7.5 m^2, representing a large thermal conduction path

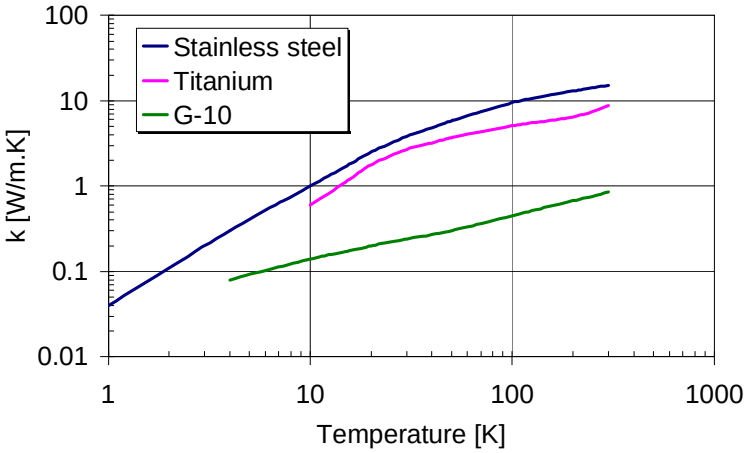

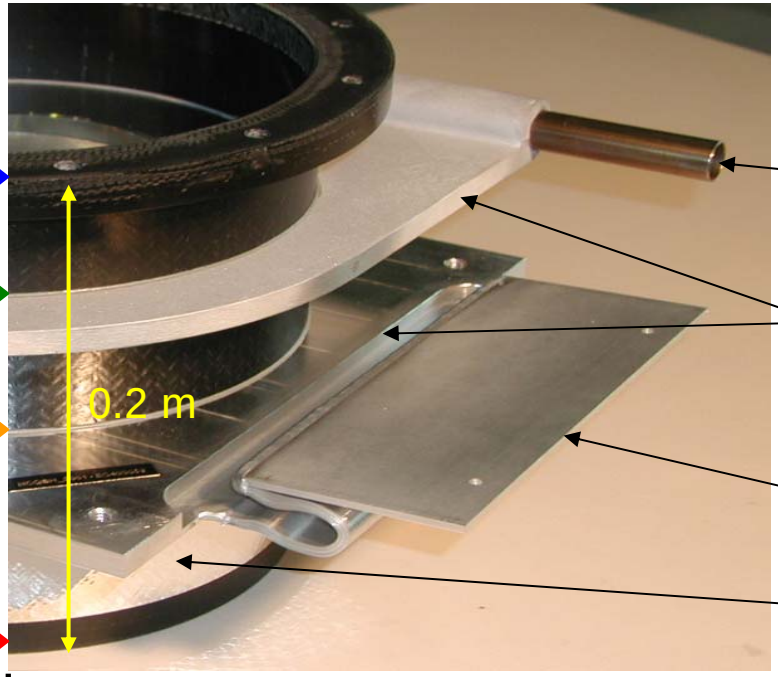

1.9 K

5 K

~ 70 K

290 K

100 kN

5 K cooling line (SC He)

Aluminium intercept plates glued to G-10 column

Aluminium strips to thermal shield at 50-75 K

Reflecting layer on section exposed to 300 K radiation

Heat inleak measurements on full sectors confirm thermal budget

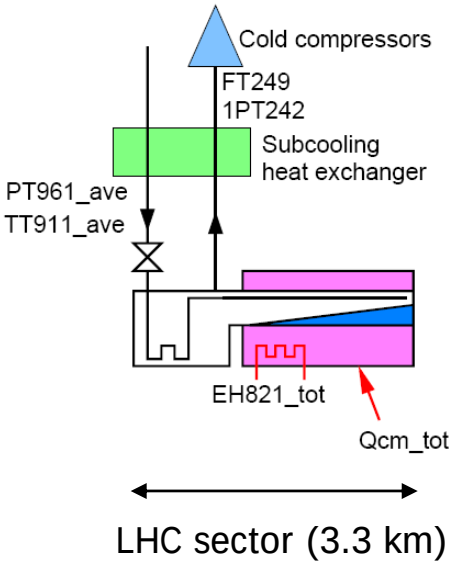

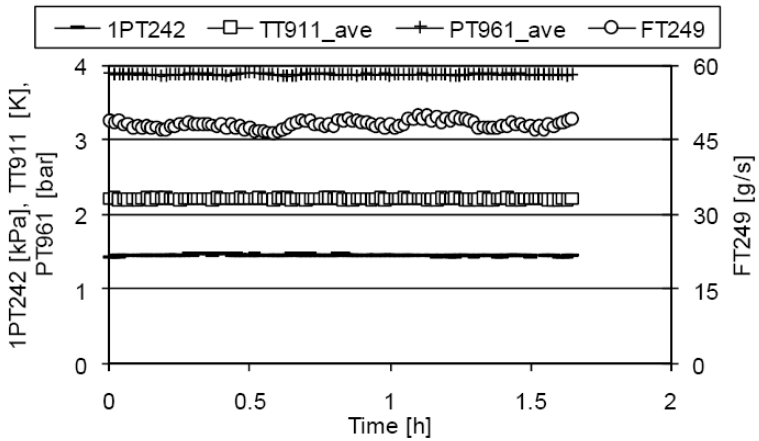

Temperatures and pressures stabilized, flow-rate integrated

Measured

$$\dot{Q} = \dot{m}\,\Delta h(P,T)$$

He property tables

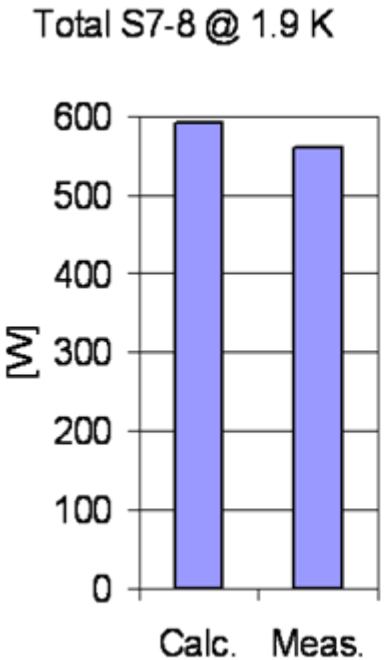

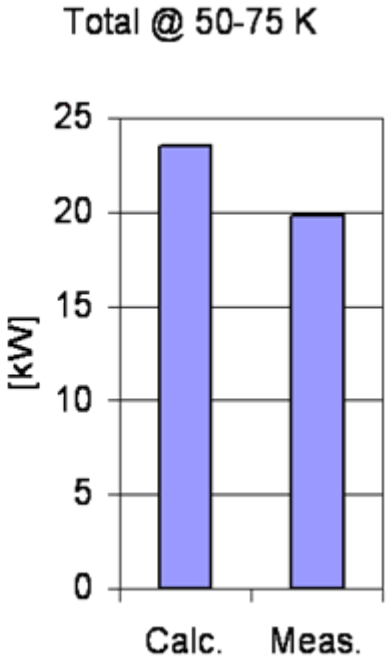

On line at http://lhc.web.cern.ch/lhc/

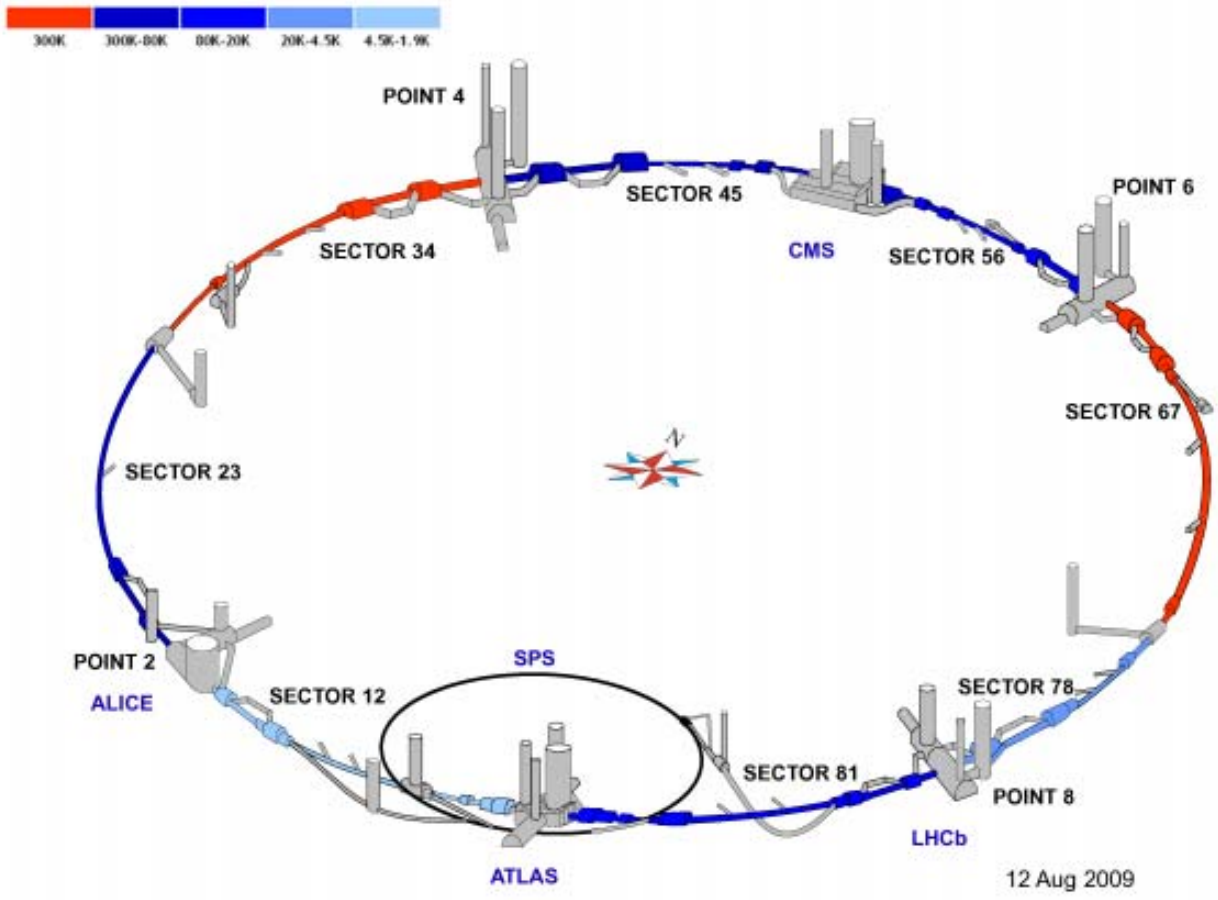

Contents

- The LHC in a nutshell
- Performance
  - Energy
  - Luminosity
  - Collective effects
  - Dynamic aperture
- Technology
  - Superconducting magnets
  - Powering and protection
  - Cryogenics
  - Vacuum
- Project management

Beam vacuum lifetime

- Dominated by nuclear scattering of protons on residual gas
- Lifetime of 100 h required to
  - Limit decay of beam intensity
  - Reduce energy deposited by scattered protons to ~ 30 mW/m

Scattering cross-section

$$\frac{1}{\tau_{gas}} = -\frac{1}{N}\frac{dN}{dt} = v \sum_i \sigma_i \, n_i$$

Gas density

Proton velocity

Sum over gas species

- Partial pressure

$$P_i = n_i \, k_B \, T$$

Proportional to temperature for given gas density

Beam vacuum lifetime

Gas species	Nuclear scattering cross-section [mbarn]	Gas density for 100 h lifetime [m^{-3}]	Pressure at 5 K for 100 h lifetime [Pa]
H_2	95	9.8 E14	6.7 E-8
He	126	7.4 E14	5.1 E-8
CH_4	566	1.6 E14	1.1 E-8
H_2O	565	1.6 E14	1.1 E-8
CO	854	1.1 E14	7.5 E-9
CO_2	1320	0.7 E14	4.9 E-9

Vacuum in presence of beam

- Without beam

Outgassing rate

$$P = \frac{Q}{S}$$

Dynamic pressure

Pumping speed

- With beam

Photon/electron/ion desorption yield

Photon/electron/ion flux

$$P = \frac{Q + \eta \dot{\Gamma}}{S}$$

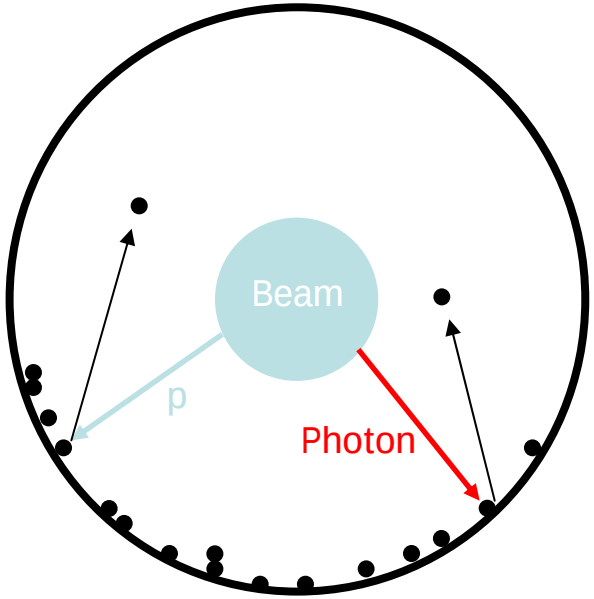

Condensed gas molecules

Cryopumping of beam vacuum at 1.9 K

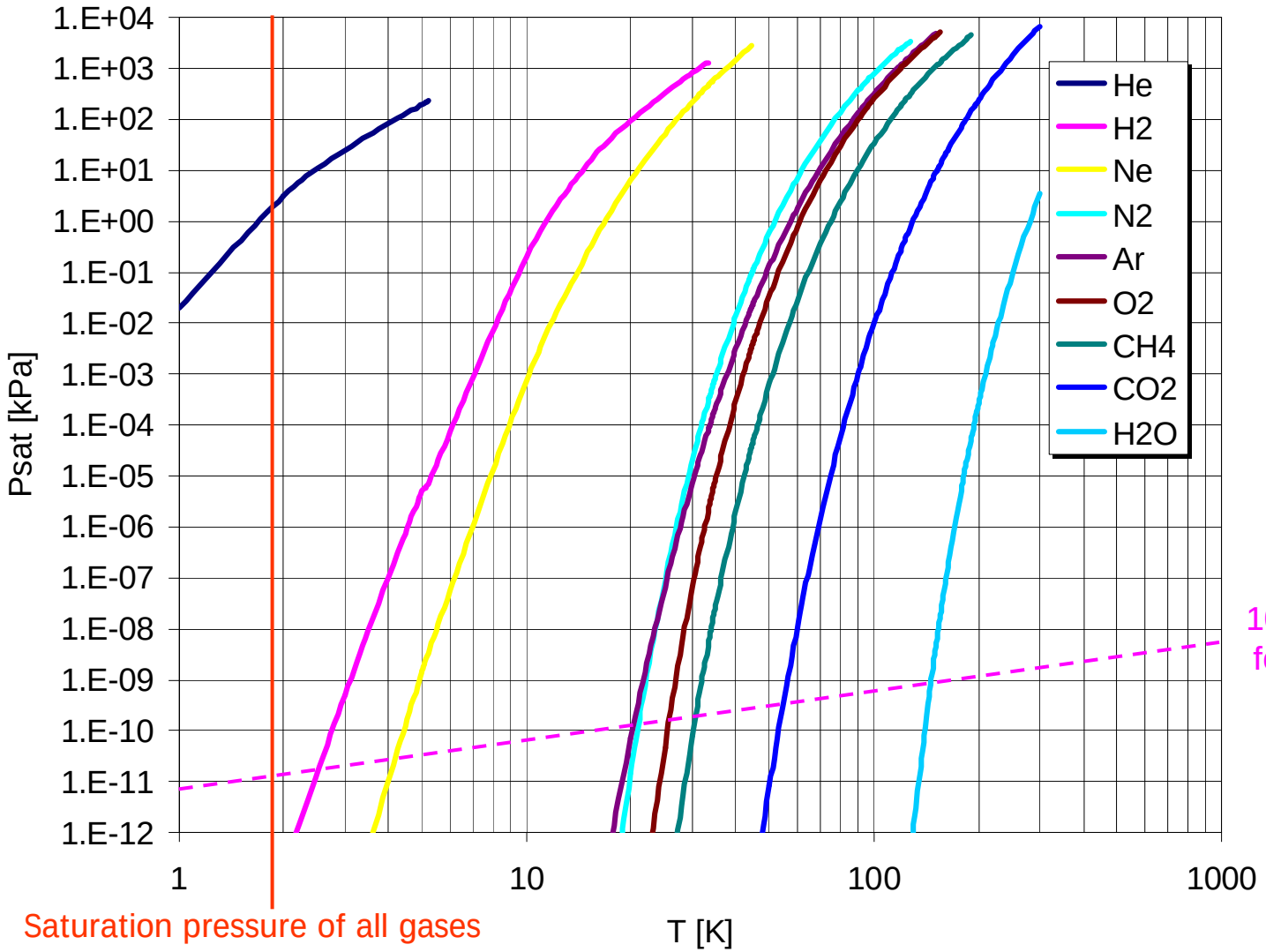

100 h lifetime for hydrogen

Saturation pressure of all gases except helium vanish at 1.9 K

Pumping desorbed gas through the beam screen

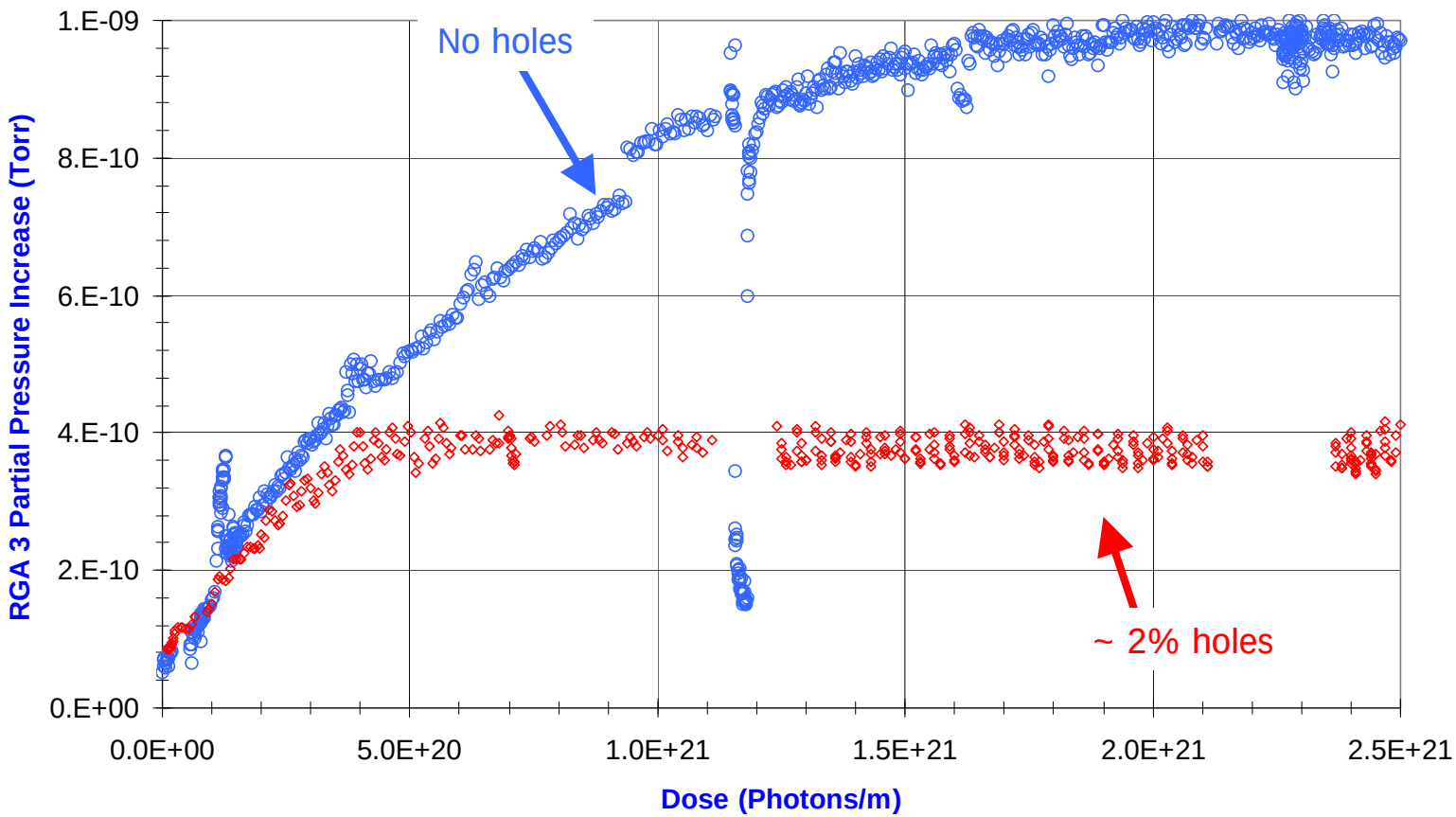

Cryosorption of beam vacuum at 4.5 K

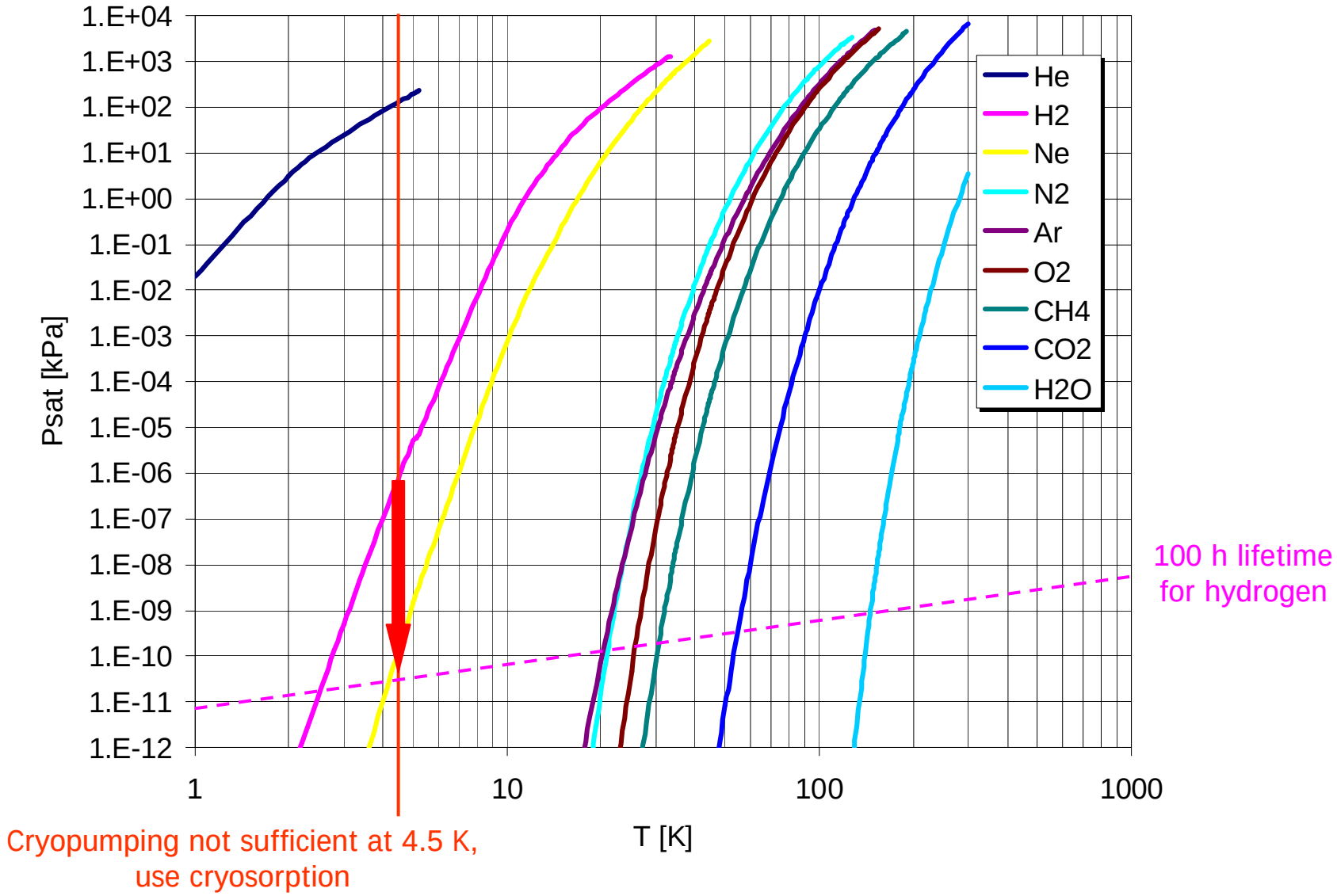

Cryosorber

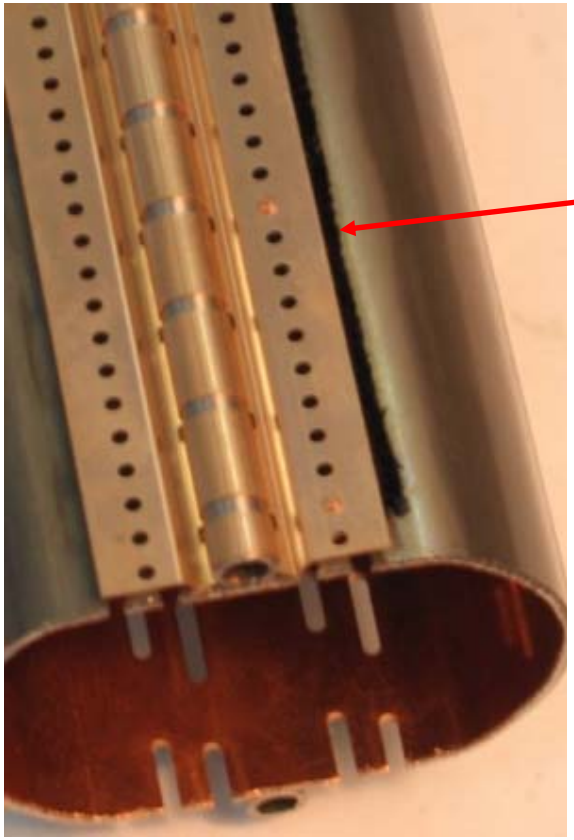

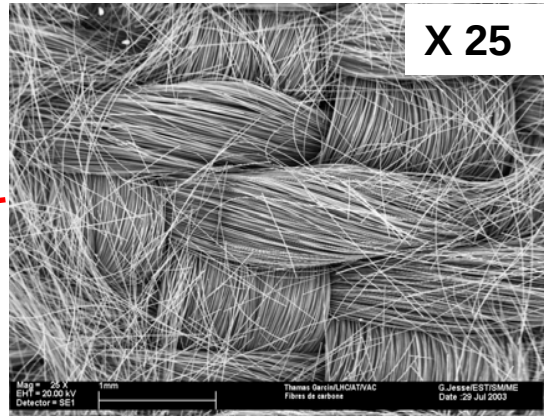

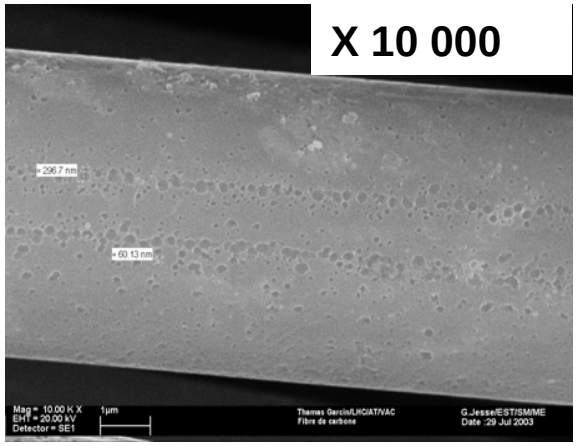

Carbon fiber mesh on the beam screen, to pump hydrogen
Capacity sufficient for regeneration only during annual shutdown

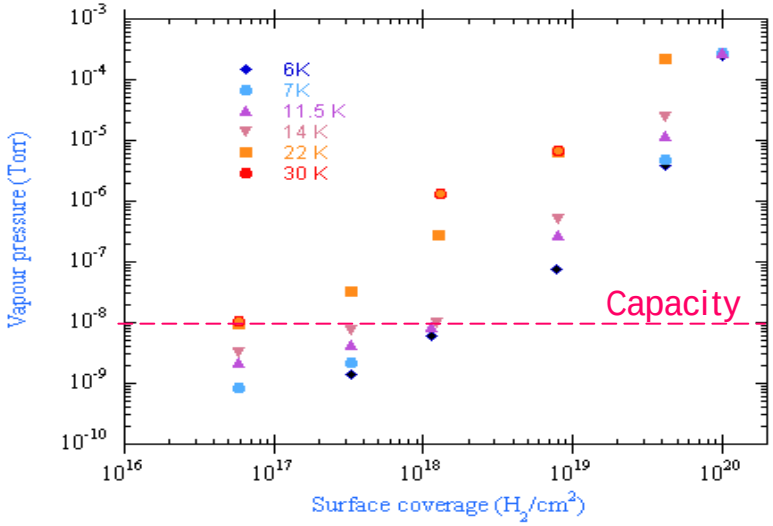

Non-evaporable getter coated vacuum chambers

Distributed pumping integrated into beam pipe

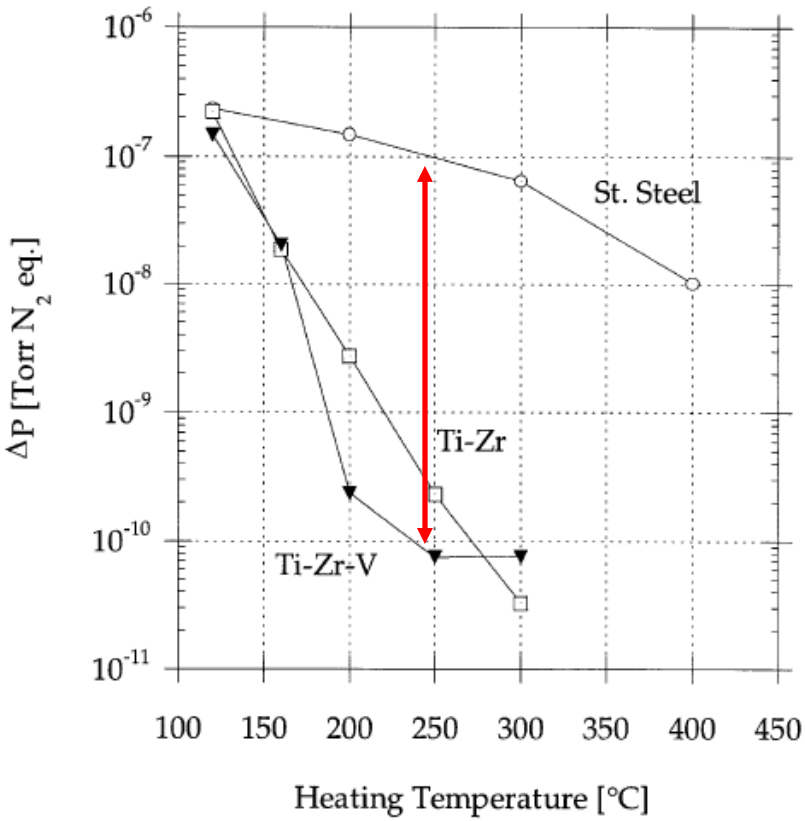

Pressure increase by 500 eV electron bombardment of surface at 20° C, after heating for 2 hours

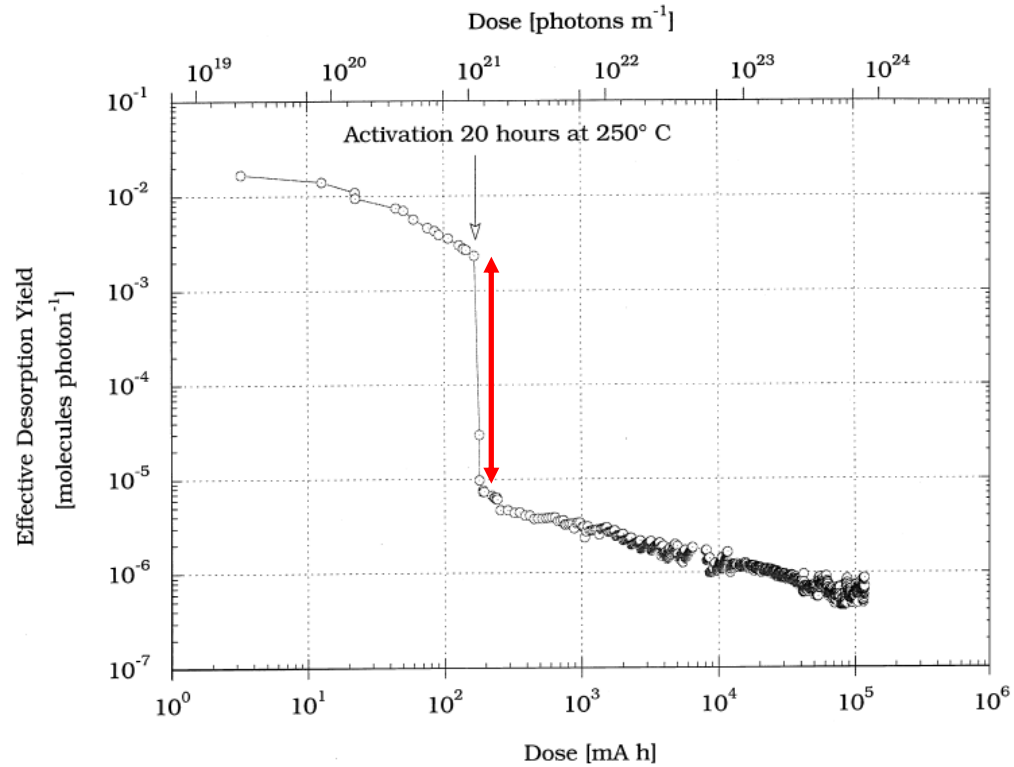

Effective molecular desorption yield as a function of photon dose, on TiZrV NEG coating of stailess steel chamber

NEG-coated vacuum chambers

Beam vacuum in long straight sections

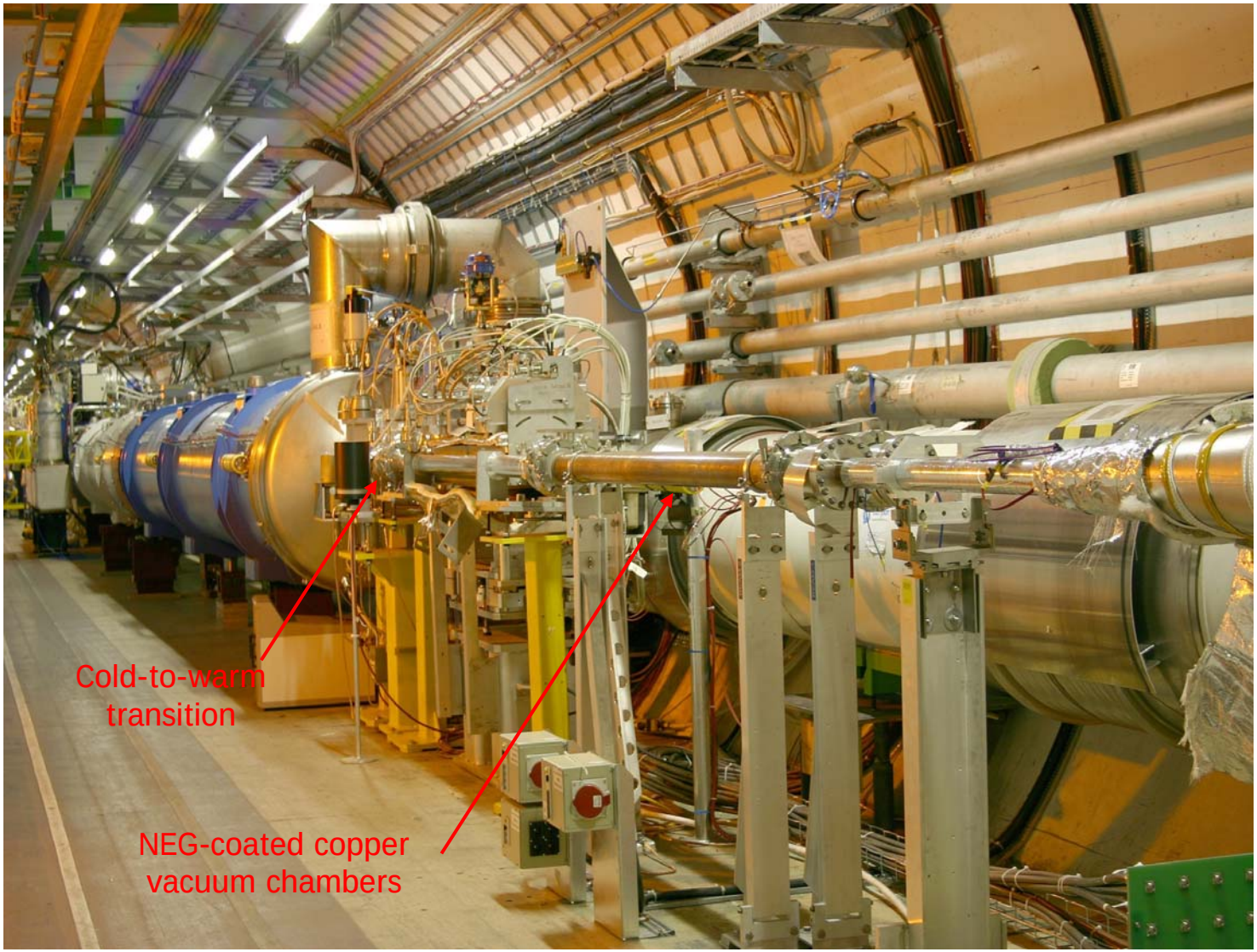

Beam vacuum in long straight sections

Separate beam pipes

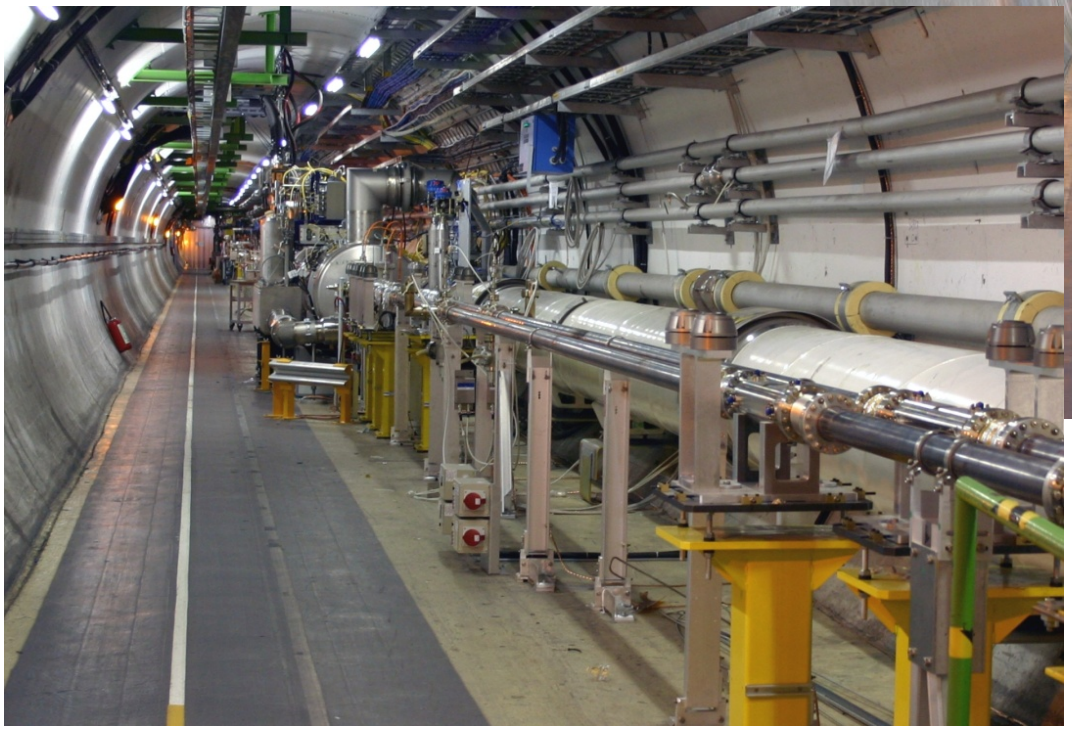

Common beam pipe

Contents

- The LHC in a nutshell
- Performance
  - Energy
  - Luminosity
  - Collective effects
  - Dynamic aperture
- Technology
  - Superconducting magnets
  - Powering and protection
  - Cryogenics
  - Vacuum
- Project management

Cost structure of the LHC accelerator

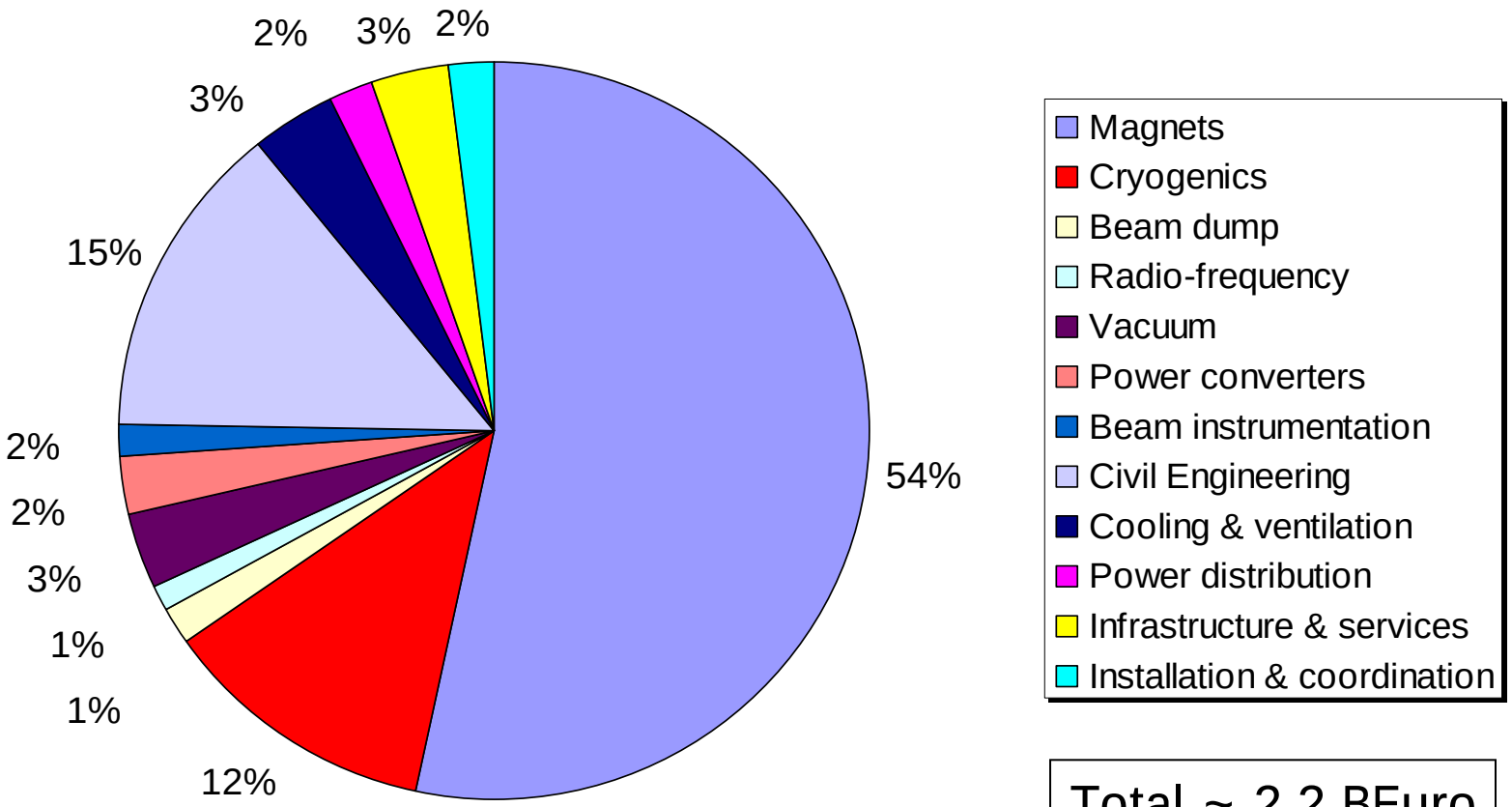

Total ~ 2.2 BEuro

90 main industrial contracts in the world

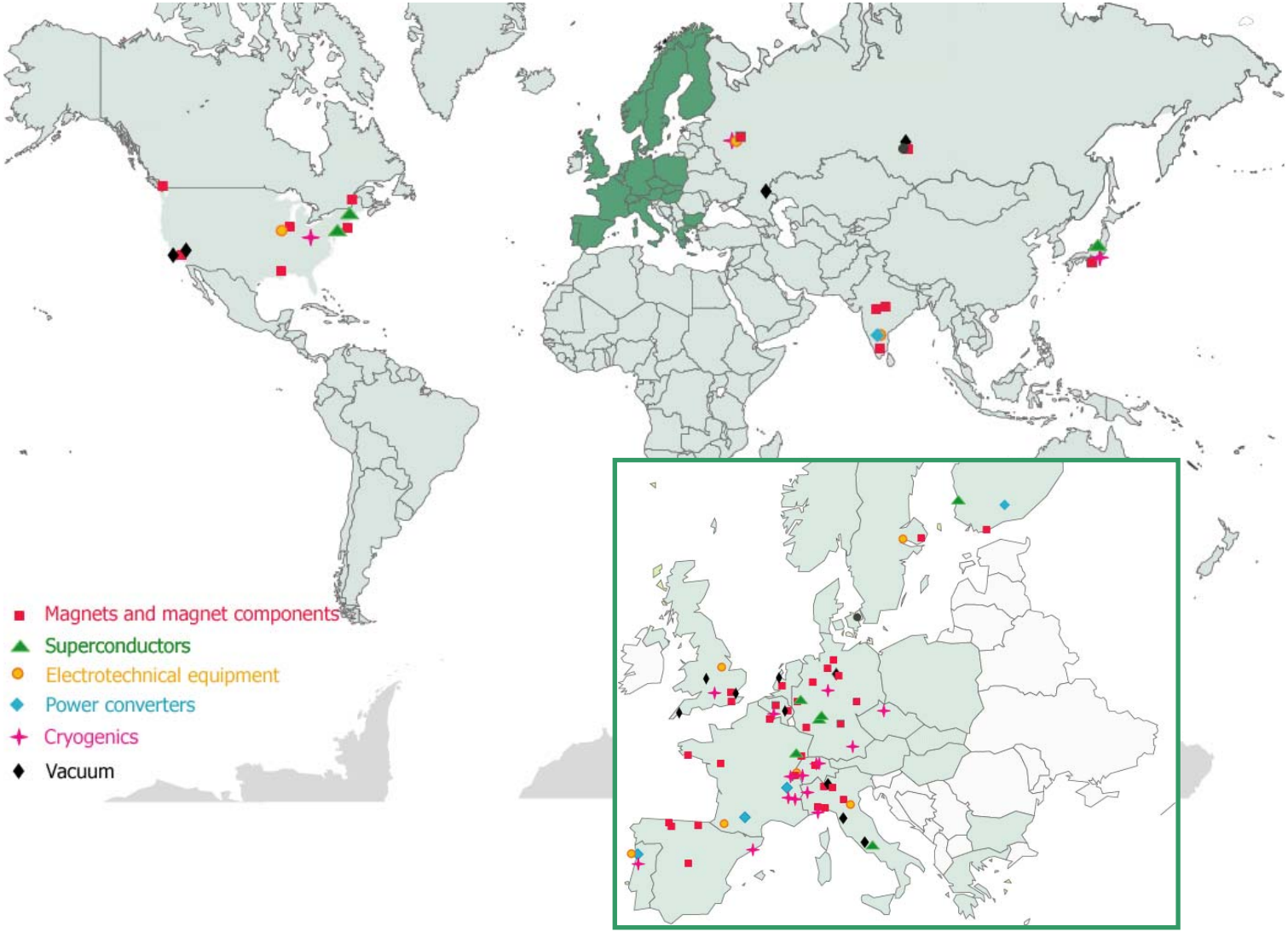

A global project spanning space...

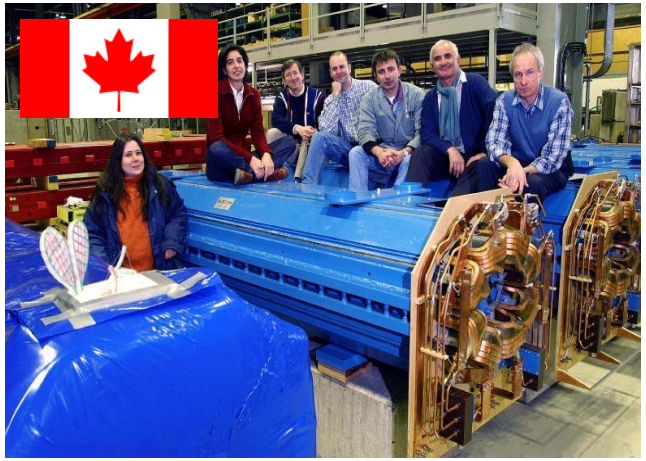

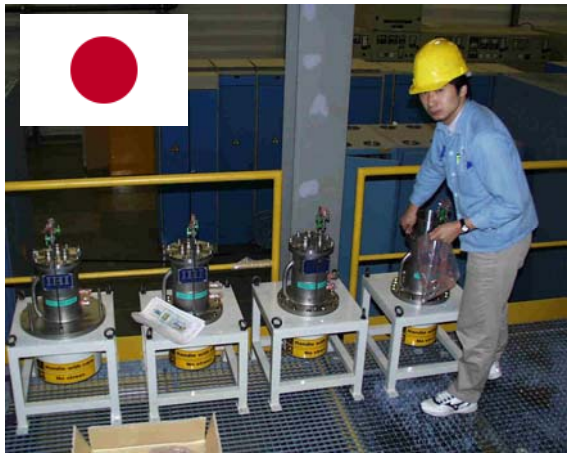

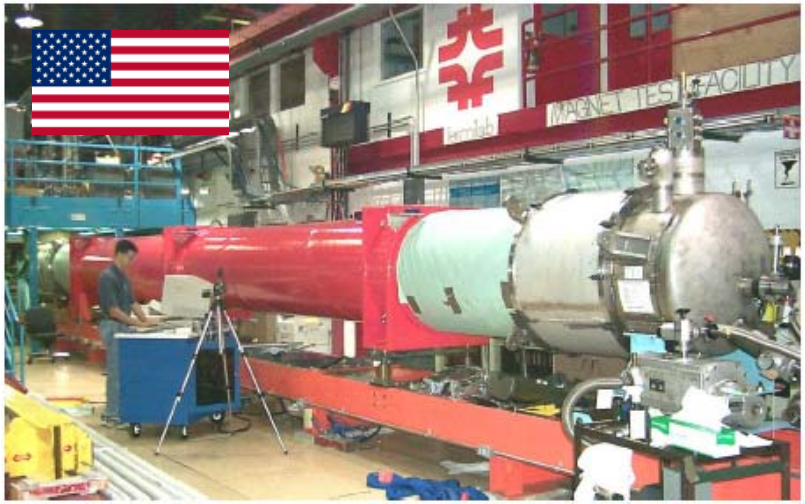

...and time

• Preliminary conceptual studies	1984
• First magnet models	1988
• Start structured R&D program	1990
• Approval by CERN Council	1994
• Industrialization of series production	1996-1999
• DUP & start civil works	1998
• Adjudication of main procurement contracts	1998-2001
• Start installation in tunnel	2003
• Cryomagnet installation in tunnel	2005-2007
• Functional test of first sector	2007
• Commissioning with beam	2008
• Operation for physics	2009-2030

Engineering data management system

Single data repository, access via WWW

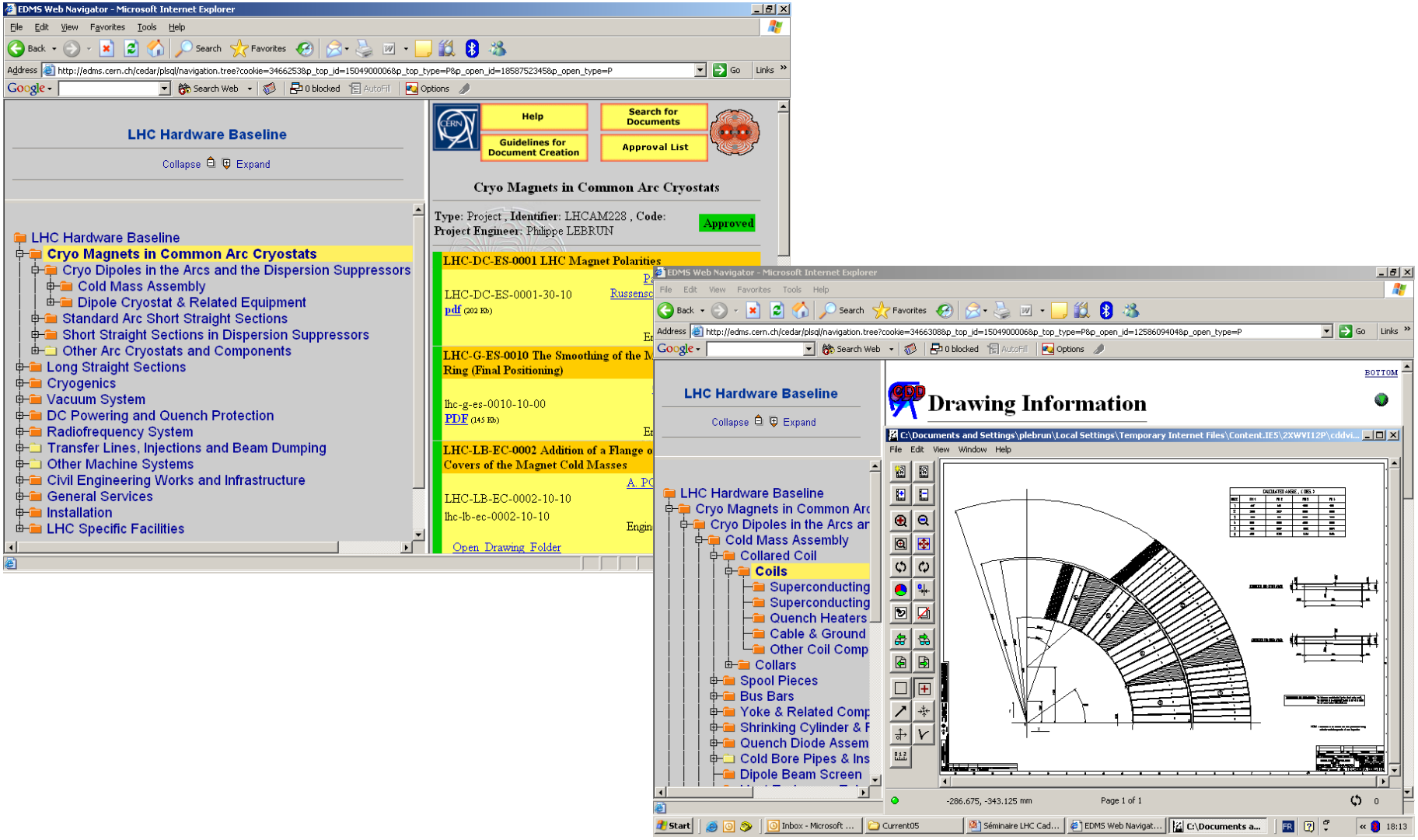

Specification & procurement strategy

- Regulatory framework & international status
  - CERN purchasing rules (essentially « lowest bidder »)
  - Seeking « fair return » among CERN Member States
  - Handling special « in-kind» contributions
- Call for tenders
  - Selecting the right companies
  - Building know-how & maintaining interest through prototyping, preseries and series
  - Technical specification: functional & interface vs. build-to-print
- Contract
  - Split: security of supply & balanced return vs. additional follow-up
  - Intermediate supply & logistics
  - MTF and inspection
  - Just-in-time vs. production buffer & sorting

Procurement & installation logistics

Quality & quantity at the right time in the right place

Installed in LHC tunnel: 50 000 t

Transported throughout Europe: ~150 000 t

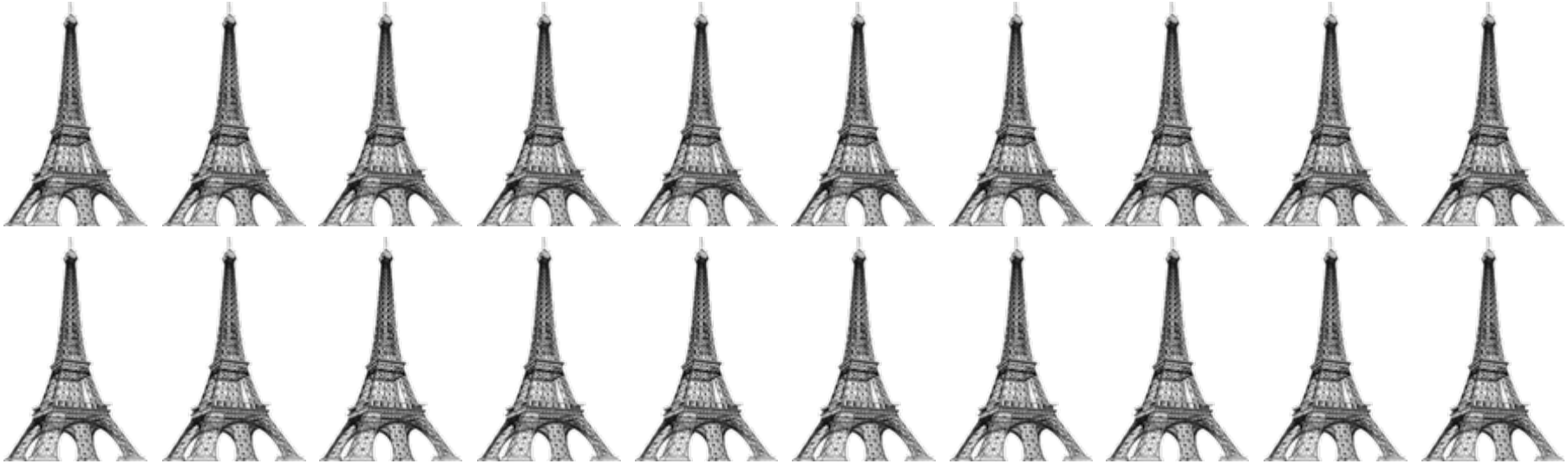

The Manufacturing & Test Folder (MTF), key to quality assurance in production

CERN
CH-1211 Geneva 23
Switzerland

the **Large Hadron Collider** project

LHC Project Document No.
LHC-PM-QA-309.00 rev 1.0

CERN Div./Group or Supplier/Contractor Document No.

EDMS Document No.
103562

Date:1999-06-16

Quality Assurance Procedure

MANUFACTURING AND INSPECTION OF EQUIPMENT

Abstract

This document describes the procedures and responsibilities involved in the manufacturing, the assembly and the inspection and test of LHC systems, sub-systems, assemblies, sub-assemblies and parts.

It establishes a policy for the control of all stages of manufacturing and assembly, from raw material procurement until final inspection and test, and it defines responsibilities and procedures to verify that all specified requirements are met.

The policy and guidelines apply to all materials, parts and equipment manufactured and/or assembled by Contractors, collaborating Institutes and CERN Divisions or Groups, that are to be installed in the LHC.

Prepared by :	*Checked by :*	*Approved by :*
P. Lienard LHC/MMS Patrick.Lienard@cern.ch **M. Mottier** EST/ISS Marcel.Mottier@cern.ch	**LHC Quality Assurance Working Group**	**Paul Faugeras** Deputy to LHC Project Leader for Quality Assurance

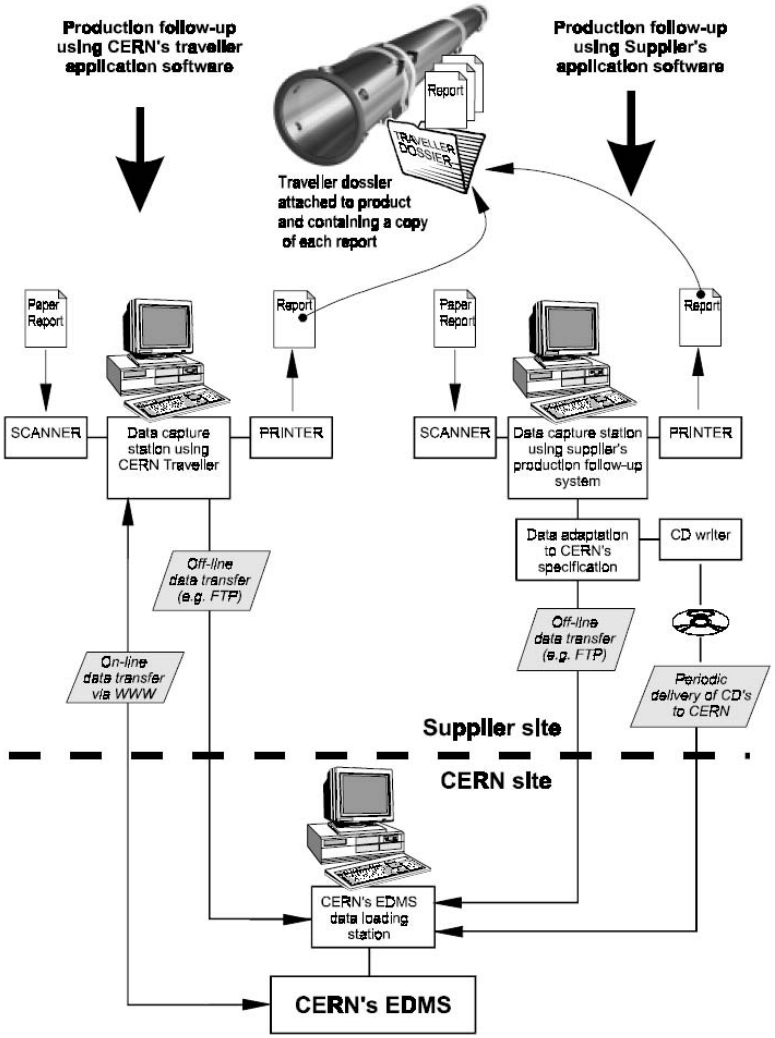

Partnership in commercial contracts

Steering magnet production for quality and homogeneity

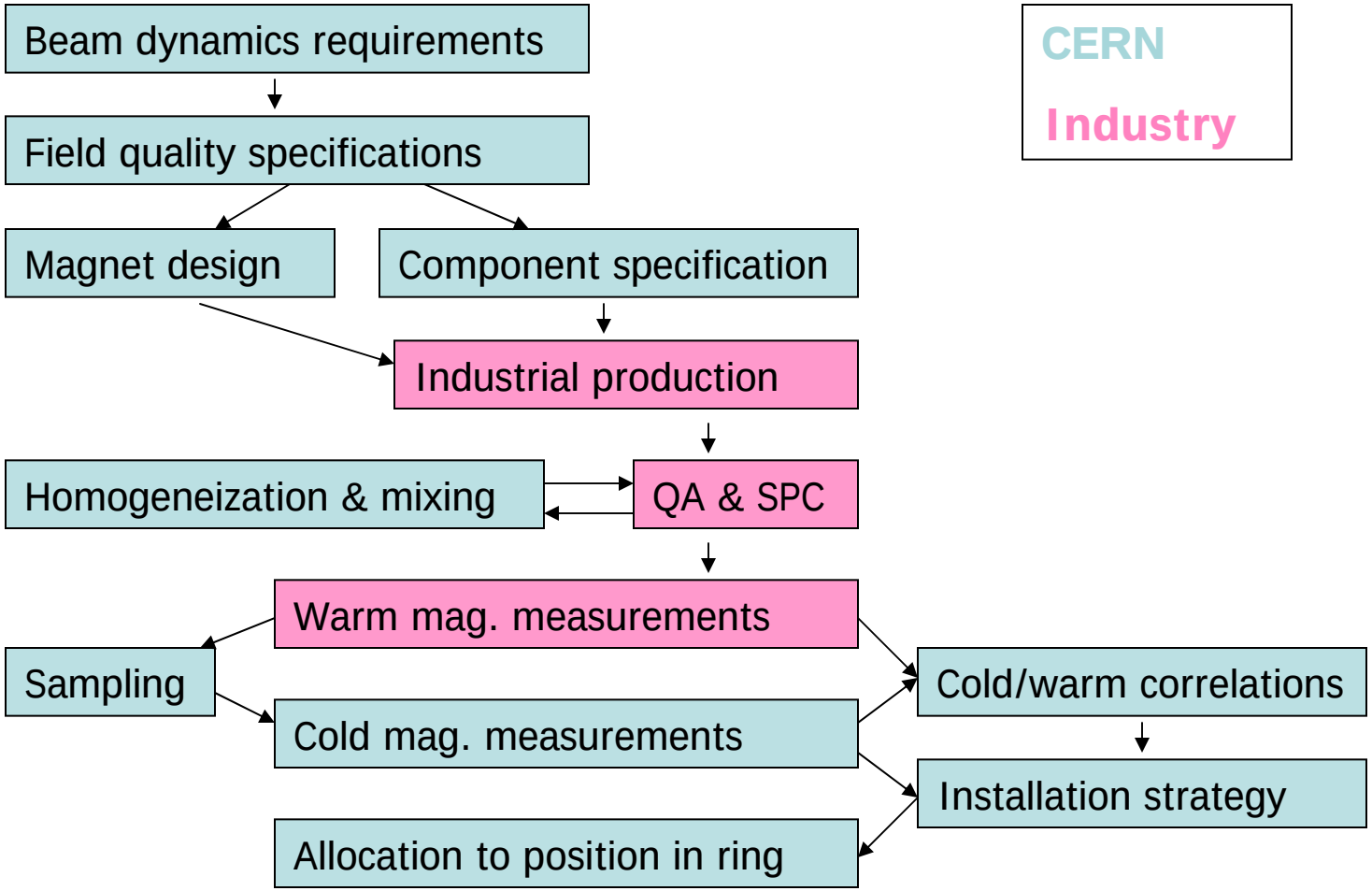

Statistical production control of components

Maintaining critical parameters within allowed range

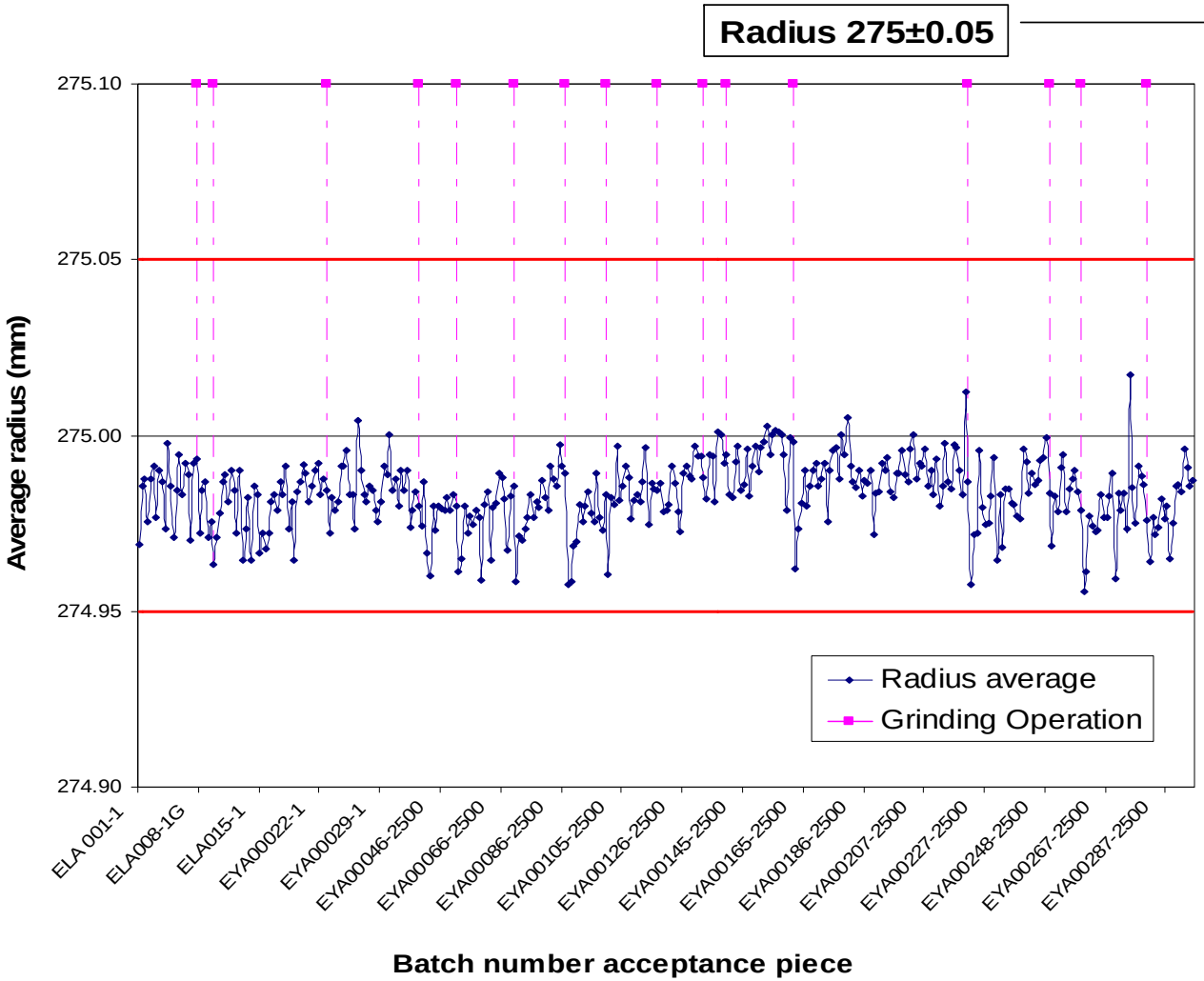

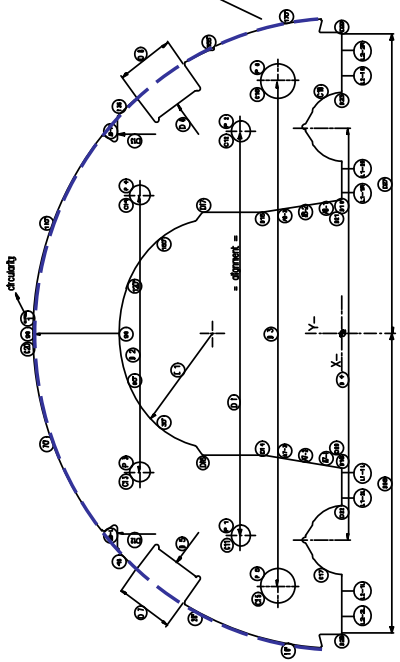

Industrial development of cold compressors

An exercise in cooperation/competition

- Preexisting state-of-the-art
- Preliminary studies
- Prototypes
- Preseries/series

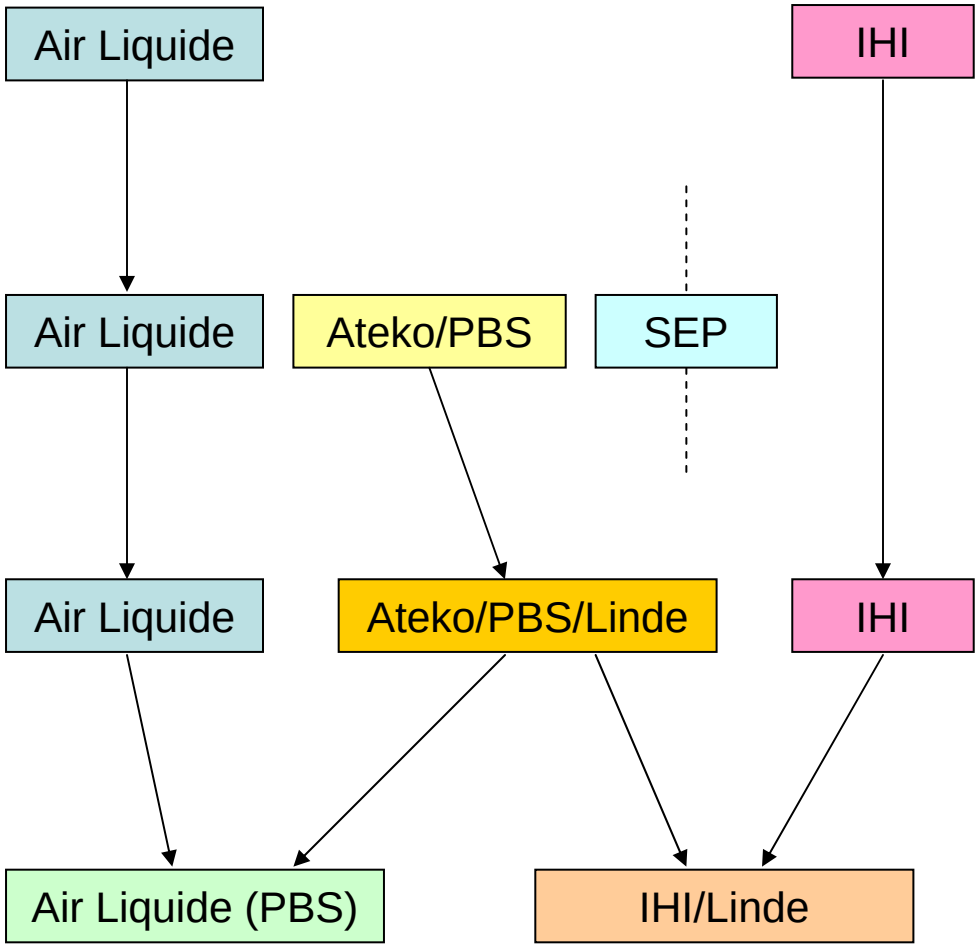

Industrialization & production ramp-up
Superconducting cable

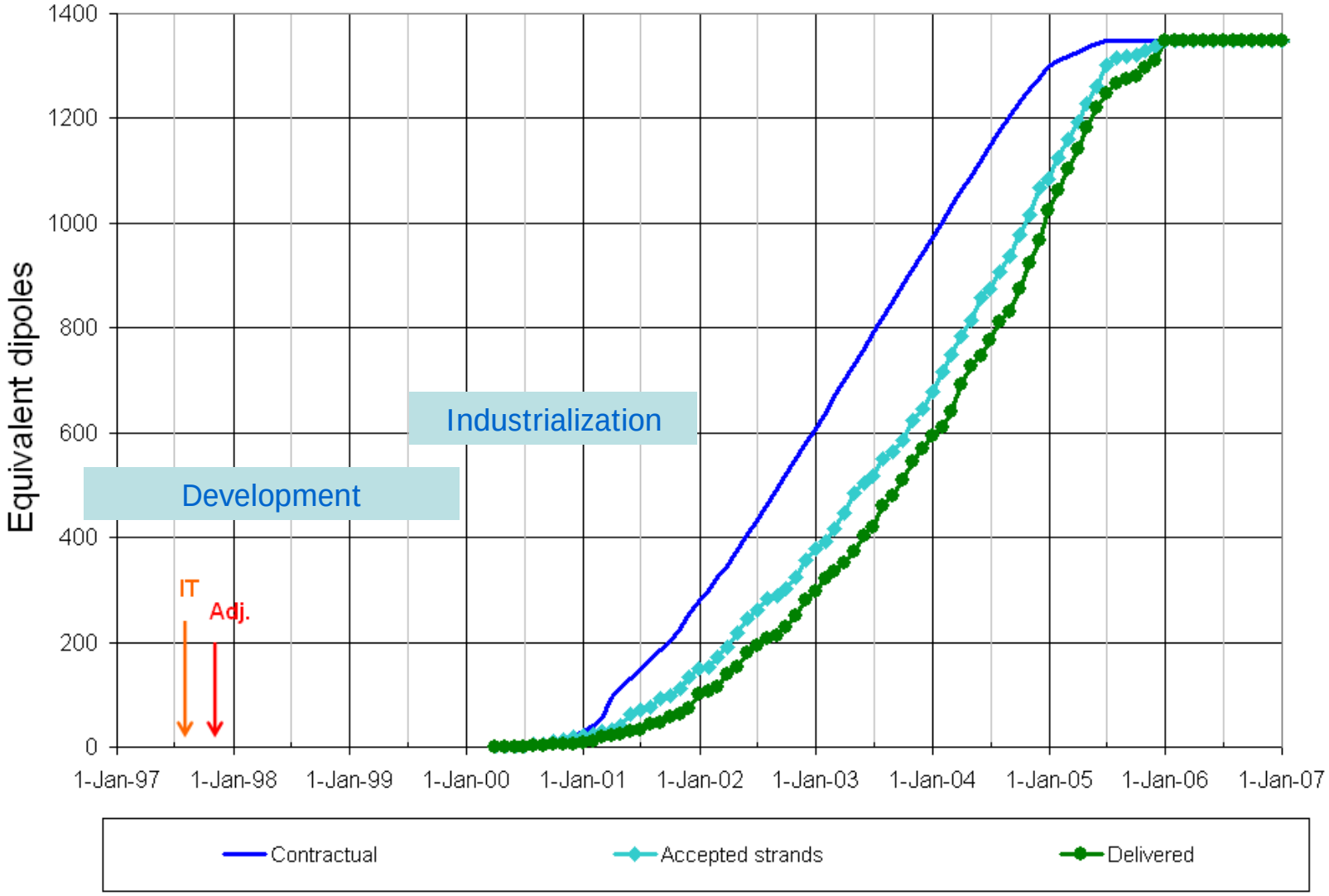

Industrialization & production ramp-up

Superconducting dipoles

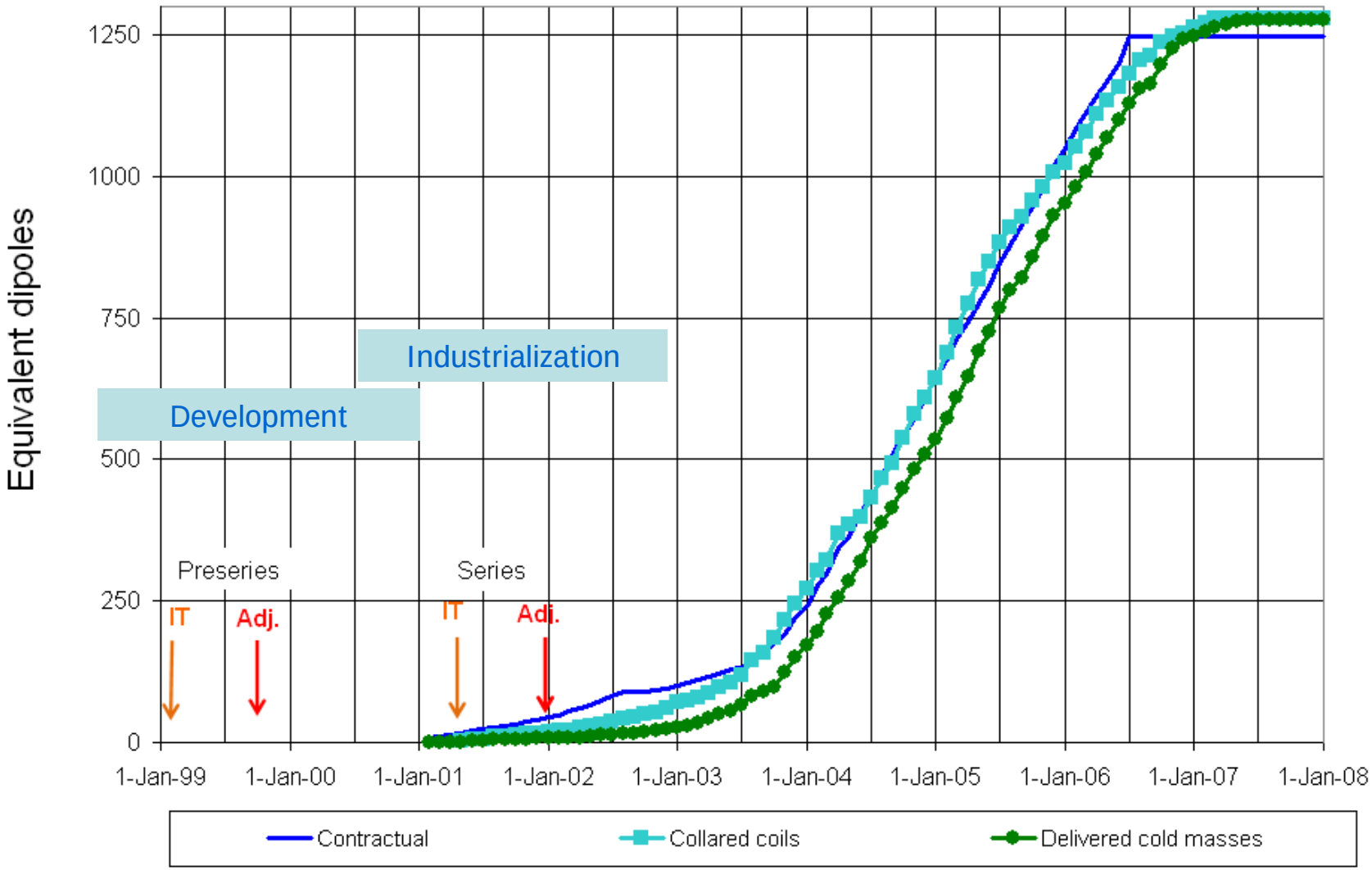

Earned-value management

Tracking progress and cost of project

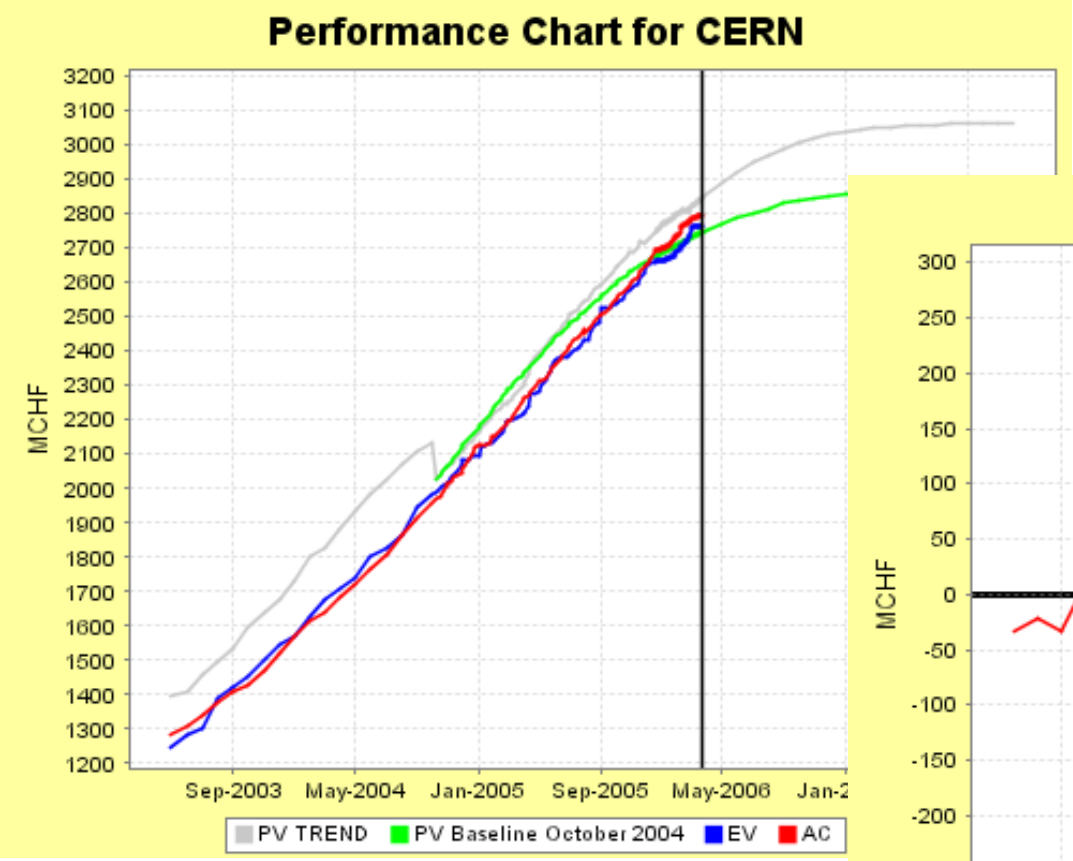

Earned value EV

Actual cost AC

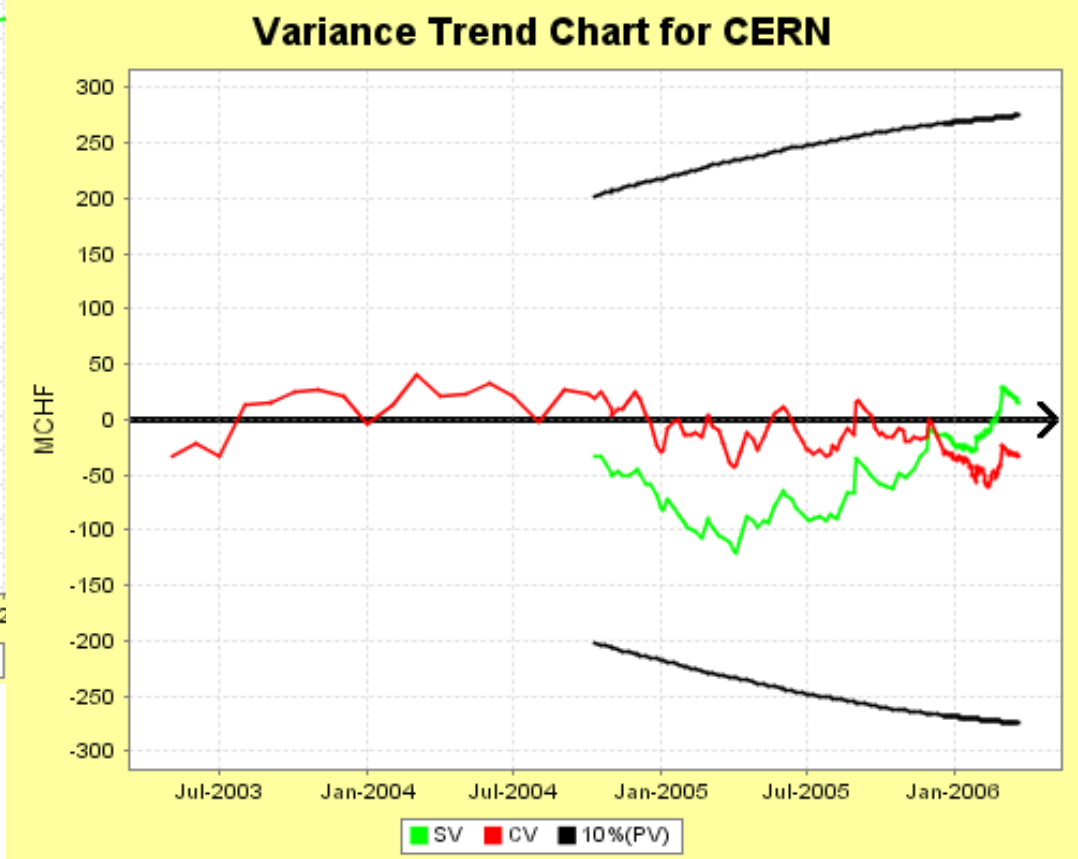

Schedule variance SV = EV – PV

Cost variance CV = EV - AC

Recovering from industrial difficulties

Internalization of SSS assembly after insolvency of contractor

Recovering from industrial difficulties

Repair & reinstallation by CERN of cryogenic ring line sectors following technical/managerial production errors

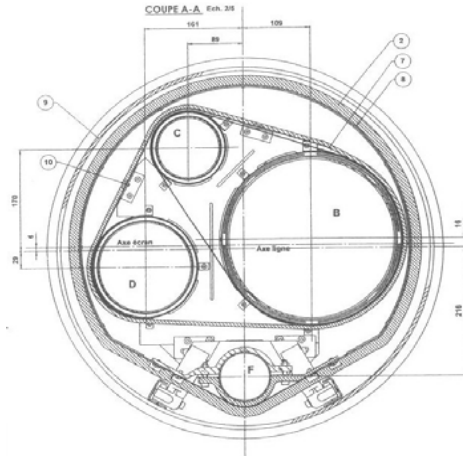

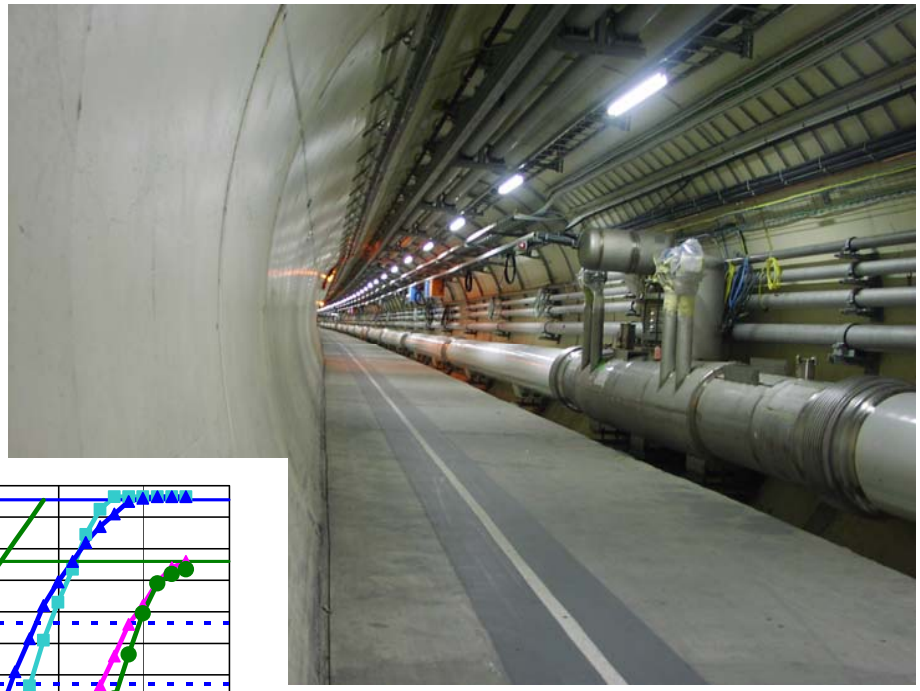

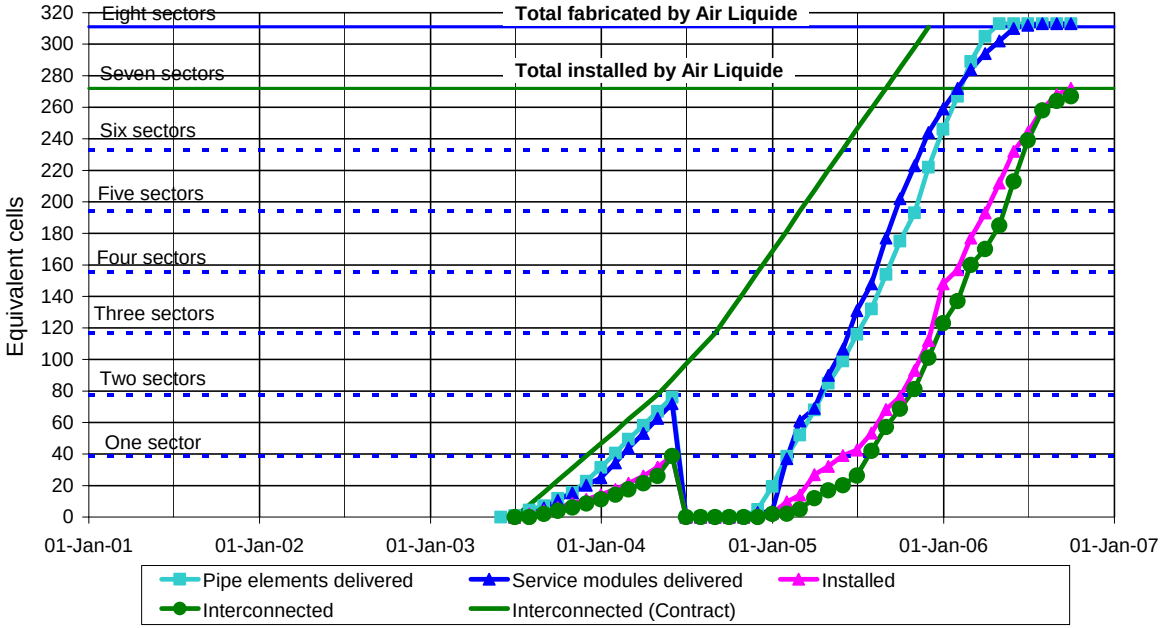

Thanks

- V. Baglin
- F. Bordry
- L. Bottura
- L. Evans
- S. Fartoukh
- J-M. Jimenez
- L. Rossi
- S. Russenschuck
- L. Tavian
- E. Todesco
- F. Zimmermann